Thesis Title

Mechanisms of plant cell proliferation control by light, during leaf initiation and acclimation to high light irradiance

Binish Mohammed

This thesis was submitted for the degree of Doctor of Philosophy at
Royal Holloway University of London, May 2017

Declaration

I, Binish Mohammed, hereby declare that the work in this thesis is my own (unless where acknowledgments have indicated otherwise) and that this work is original and has not been, or will be, submitted for any other degree in this or any other university (except where students have produced dissertations with my consent). This work is subject to copyright otherwise.

Signed: Date:

Abstract

Plant growth is continuously shaped by environmental and internal cues, pivotal among which are light and energy status. In plants such as *Arabidopsis thaliana,* light drives leaf initiation and development.

Control of proliferation is needed for leaf initiation and growth. Cessation of proliferation-dependent growth results in differentiation, growth that is accompanied by endoreduplication/cell expansion. To understand how the transcription factor E2FB controls proliferation I examined, at the cellular and gene expression level, lines with modified E2FB function. I show that E2FB has other developmental functions, apart from regulating the duration of proliferation.

Dissection of the shoot apex during leaf initiation upon dark to light transfer of seedlings (deetiolation) previously revealed key gene signatures involved in organ initiation. To understand how light regulates proliferation-dependent growth we first noted a close integration between expression of cell cycle genes, phosphorylation state of the core cell cycle RETINOBLASTOMA-RELATED protein, light signalling pathways and carbon availability. I then monitored growing leaf primordia upon transfer to dark and return to light. I observed growth arrest in the dark, its reversal by light being accompanied by similar gene expression signatures to those during light-driven *de novo* leaf initiation, namely a reversal of an "energy starvation" state, a transient shift of hormone responses from auxin to cytokinin, and coordinated build-up of ribosomes.

Leaves that acclimate to high light have a multi cell layered palisade but fail to show this anatomy in chloroplast-defective cells of variegated mutants. To understand a possible link between energy and proliferation-dependent growth I monitored mitotic growth and cell ploidy level. My findings suggest that high light causes leaf cell proliferation-dependent growth to intensify but terminate sooner.

Overall I have introduced an easily-tractable cell synchronisation assay, and provided evidence for the integration of light signals controlling proliferation.

Acknowledgements

I would like to thank my supervisor, Dr Enrique Lopez-Juez, and co-supervisor, Professor Laszlo Bogre, for the opportunity to do this PhD. This opportunity has provided me with a learning curve from which I have gained academically and personally. My experience at conferences and the retreat to Budapest are memories that I will cherish for a long time. I thank Royal Holloway University of London for funding my PhD (Reid Scholarship).

I would also like to thank all the project students that participated in this process. I value all of their input but to name my favourite would be Xenia: for me, a perfect student in every way and together we gained exceptional data. Many thanks to all other colleagues, visitors and collaborators, particularly Dr Zoltan Magyar, for their contributions.

Dr Safina Khan, at first you were a lab member/colleague, a mentor from whom I learned so much and then you became a good lunchtime companion. I cannot pin point the time when we became best of friends and now are nothing less than family. Some people just click and that is us. There are no thanks and goodbyes here, just lots of love, because the journey continues.

My family, immediate and extended, your encouragement and love has been everything I needed. I am aware you understood little of my work but you never failed to support me. I am thankful to God for such a caring family.

The submission of my thesis will be my greatest accomplishment so far but there is still so much more I want to achieve. I hope this is just the beginning.

Thank you Saud, Sulaiman, Serish and mum. You are my ‘WHY?’

Dedication

I dedicate my thesis to my parents (Mr Sher Mohammed and Mrs Bilqis Mohammed) and husband (Mr Saud Qasim). My parents have always encouraged me to gain knowledge and I would like to thank them for their patience and support for the many years I spent studying at Royal Holloway University of London. Equally, I could not have come this far without my husband. My family is always my strength that pushes me to achieve beyond my own expectations.

Table of contents

Table of figures

Table of tables

Abbreviations

°C	Degree celcius
%	Percent
35S	35S promoter (CaMV)
3dD	3 days dark
4E-BP1	4E binding protein 1
4hD	4 hours dark
4hL	4 hours light
Ab	Antibody
ABA	Abscisic acid
ABA2	Abcisic acid (ABA) deficient2
ABRC	Arabidopsis biological resource centre
AD	After dark
AKIN	SNF1 kinase homolog
AMP	Adenosine monophosphate
AMPK	AMP activated protein kinase
APB	Active phytochrome B
APC	Anaphase promoting complex/cyclosome
APS	Ammonium persulfate
ARF	Auxin response factor
ARP	Asymmetric leaf/rough sheath 2/phantastica
ARR	Arabidopsis type-A response regulator
AS1/2	Asymmetric leaf 1/2
At	Arabidopsis thaliana
atm	Atmospheric pressure
AUX	Auxin resistant
AXR	Auxin resistance gene
B	Border
BBX	B-box zinc finger
BD	Before dark
bHLH	basic-helix-loop-helix
bp	Base pairs
BPC	Biotechnology performance certified
BY2	Bright yellow 2
bZIP	basic region/leucine zipper motif
C	Carbon
CaMV	Cauliflower Mosaic Virus
CCA1	Circadian clock associated1
CCS52	Cell cycle switch protein52
CD	Continous dark

CDC	Cell division control
CDD	COP10/DDB1/DET1
CDK	Cyclin dependent kinase
cDNA	Complementary DNA
cFR	Continuous far red
CI	Curvature index
CK	Cytokinin
CKI	Cyclin dependent kinase inhibitor
CKS1	CDK-subunit1
CL	Continous light
CLV	Clavata
Col	Columbia
COP/DET/FUS	Constitutively-photomorphogenic/deetiolated/fusca
COP1	Constituitively photomorphogenic 1
CRF	Cytokinin response factors
CRN	Coryne
CRY	Cryptochromes
CSN	COP signalosome
CUC	Cup shaped cotyledon
CYC	Cyclin
CZ	Central zone
D	Dark
D-box	Destruction box
dag	days after germination
DAPI	4',6-diamidino-2-phenylindole
DAS	Days after stratification
DCMU	3-(3,4-dichlorophenyl)-1,1-dimethylurea
DDB1	Damaged DNA binding protein 1
DEK	Defective kernal
DEL	DP E2F like
DET	Deetiolated
DL	Dark to light
DMSO	Dimethyl sulfoxide
DNA	Deoxyribonucleic acid
dNTP	Deoxyribonucleotide triphosphate
DP	Dimerisation partner
dp	Decimal place
DTT	Dithiothreitol
E.coli	Escherichia coli
e.g.	exempli gratia/for example
E2F	E2 factor
EDF	Extended depth of focus
EDTA	Ethylenediaminetetraacetic acid

EdU	5-ethynyl-2′-deoxyuridine
EIN3	Ethylene insensitive3
et al.	et alia/and others
etc	et cetera/and so forth
F	Forward
FC	Final concentration
FIL	Filamentous flower
FR	Far red
G1	Gap 1
G2	Gap 2
GA	Gibberellic acid
gDNA	Genomic DNA
GFP	Green fluorescent protein
GLPACd	Global leaf pair axis curvature downward
GRF5	Growth promoting factor5
GTP	Guanosine-5'-triphosphate
GUS	β-glucuronidase
h	hour
H2A	Histone-2A
H_2O	Hydrogen-2 Oxygen-1 bond/Water
HA	Hemagglutinin
HD-ZIPIII	Class III homeodomain leucine zipper
hEBP1	Human ErbB-3 epidermal growth factor receptor Binding Protein1
HL	High light
HRP	Horseradish peroxidase
HXK	Hexokinase
HY5	Elongated hypocotyl 5
HYH	HY5 homologue
i.e.	Id est/that is
IAA	Indole-3-acetic acid
IC	Initial concentration
ICK	Interactors of cdc2 kinase
IPA	Isopropylalcohol
IPZ	Inner peripheral zone
KAN	Kanadi
KNOX	Class I knotted-like homeobox
KOH	Potassium hydroxide
KRP	Kip related protein
L	Light
L	Number-Litres
L1/2/3	Layer 1/2/3
LACs2	Long-chain fatty acid synthetase2
LAX	Like AUX1

LCd	Longitudinal curvature downward
Ler	Landsberg *erecta*
LHY	Late elongated hypocotyl
LL	Low light
LRD2	lateral root development2
LRR	Leucine rich repeat
LTS8	Lethal with sec-13 protein8
M	Mitosis
M	(number)Molar
MCM	Minichromosome maintenance
MES	2-(*N*-morpholino)ethanesulfonic acid
MFS	Major facilitator superfamily
mg	Milligram
$MgCl_2$	Magnesium chloride
MID	Midget
min	Minutes
MiR165-166	MicroRNA165-166
ml	Millilitre
mLTS8	mammalian lethal with sec-13 protein8
mM	Millimolar
mm	Millimietres
mRNA	MessengerRNA
MSA	Mitosis specific activator
mTORC	Mammalian target of rapamycin complex
mV	Millivolts
N	Number of chromosome sets
$N_{2(l)}$	Liquid nitrogen
NaCl	Sodium chloride
NL	New leaf
OC	Organisating centre
OP	Organ primordia
OPZ	Outer peripheral zone
ORC	Origin recognition complex
ORF	Open reading frame
P	Phosphorylated
P-RBR1	Phosphorylated retinoblastoma related 1
p53	Tumour protein53
PAT	Polar auxin transport
PCR	Polymerase chain reaction
pgm	Phosphoglucomutase
PHB	Phabulosa
PHOT	Phototropin
PHV	Phavoluta

PHY	Phytochromes
PIC	Protease inhibitor cocktail
PID	Pinoid
PIF	Phytochrome interacting factor
PIN	Pin formed
pmol	Picomole
PMSF	Phenylmethylsulfonyl fluoride
PNPP	p-nitrophenyl phosphate
POD	Peroxidase
PRDA1	Pep-related development arrested1
PVDF	Polyvinylidene flouride
Q-RT-PCR	Quantitative real time PCR (RNA)
QC	Quiescent centre
R	Reverse
R-light	Red light
RAM	Root apical meristem
RAPTOR	Regulatory associate protein of TOR
RB	Retinoblastoma
RBR1	Retinoblastoma related 1
RCO	Reduced complexity
REV	Revoluta
RNA	Ribonucleic acid
RNAi	RNA interference
RNR2A	Ribonucleotide reductase2A
ROP	Rho of plant
ROS	Reactive oxygen species
rpm	Revolution per minute
rRNA	Ribosomal RNA
RT	Reverse transcription
RZ	Rib zone
s	Second
S	Synthesis
S6K	S6 kinase
S6RP	S6 Ribosomal Protein
SA	Shoot apex
SAM	Shoot apical meristem
Sap	Shoot apex +primordia
SCF	Skip1/cullin/f-box related
SCR	Scarecrow
SDS-PAGE	Sodium dodecyl sulphate polyacrylamide gel
SHY2	Short hypocotyl2
SI	Stomatal index
SIM	Siamese

SNF1	Sucrose non-fermenting 1
SnRK1	Sucrose non fermenting related kinase 1
SPA	Supressor of phyA-105
STM	Shootmeristemless
T_0	Time point 0
T1	Transformation 1
T6P	Trehalose-6-phosphate
TAA1	Tryptophan aminotransferase of Arabidopsis1
TAE	Tris acetic-acid EDTA
TAIR	The arabidopsis information resource
TAR	Tryptophan aminotransferade related
TB	Transfer buffer
TBE	Tris boric-acid EDTA
TBST	Tris buffered saline with tween
TCA	Tricarboxylic acid
TCd	Transverse Curvature downward
TCP	Teosinte branched1/cycloidea/proliferating cell factor
TDNA	Transfer DNA
TE	Tris-EDTA
THR	Threonine
Tm	Temperature
TOR	Target of rapamycin
TPP	Trehalose-6-phosphate phosphatase
TPS	Trehalose phosphate synthase
TPS	Trehalose-6-phosphatase synthase
TYR	Tyrosine
UTR	Untranslated region
UV	Ultraviolet
UV-A	Ultraviolet-A
UVR8	UV resistance locus 8
V	Volts
v/v	Volume/volume
vac	Vacumm
vs	*versus*
WEI8	Weak ethylene insensitive8
Whi5	WHISKEY5
WT	Wild type
WUS	Wuschel
X-gluc	5-bromo-4-chloro-3-indolyl-β-D-glucuronic acid
α	Alpha
β	Beta
γ	Gamma
µg	Micrograms

µl	Microlitres

Chapter 1: Introduction

Plant development is continuously shaped by external and internal cues, two pivotal ones among them being light and sucrose. In plants such as *Arabidopsis thaliana* light drives leaf initiation and growth. Understanding light action on growth can help elucidate core leaf growth control mechanisms. Photosynthesis happens in leaves during the light period and plays an important role in the biosphere. Leaves utilise the light energy and convert it to chemical energy, in essence this process drives plant growth. Understanding how leaves are made is clearly important. Leaves are analogous to 'solar panels', perceiving light energy and are attuned to the light environment. Because in dicotyledonous plants leaves are only made in the light, understanding how light controls leaf development can be illuminating. I begin by exploring at the cellular level what drives leaf growth, the role of light, amongst other factors, in initiating and maintaining growth of leaves and how light can affect leaf anatomy.

1.1 Light perception

Light exposure precedes organogenesis at the shoot apices and in the absence of light leaf initiation ceases. Changes in gene expression levels in dark versus light grown seedlings clearly show that groups of genes are upregulated in the light or downregulated in the dark (Ma *et al.*, 2001). Interestingly the same light stimulus triggers photomorphogenic growth upon first light exposure whilst simultaneously inhibiting further growth of the hypocotyls (Koornneef *et al.*, 1980).

1.1.1 **Photoreceptors**

Light is perceived via photoreceptors and the three main classes are: Phytochromes, cryptochromes and phototropins. Within each photoreceptor family the number of members can vary in different plants. *Arabidopsis* has five phytochromes, PhyA-PhyE, which maximally absorb Red, (R-light), and Far Red, (FR) light (Franklin and Quail, 2010). Phytochromes are synthesised in the dark in their inactive form and are

reversibly activated in R-light wavelengths (due to photon excitation) and inactivated in FR. PhyA exclusively accumulates in the dark, absorbs FR and is barely photo-reversible (Shinomura *et al.*, 1996).

Cryptochromes and phototropins detect blue and Ultra-Violet-A (UV-A) light (Liscum *et al.*, 2003). Cryptochromes are flavoproteins and thought to be evolved from photolyases (DNA repair enzymes). In *Arabidopsis* two cryptochromes are encoded by *CRY1* and *CRY2*. Cryptochromes are nuclear proteins whose primary action is in the control of gene expression. Phototropins are also encoded by two genes, *PHOT1* and *PHOT2,* in *Arabidopsis* and are flavoproteins too. Apart from regulating phototropism, PHOT1 and PHOT2 also regulate chloroplast movement (Sakai *et al.*, 2001; Kagawa *et al.*, 2001; Jarillo *et al.*, 2001) and stomatal opening (Kinoshita *et al.*, 2001). Phototropins are plasma membrane-associated protein kinases, whose actions involve membrane or cytoskeletal responses.

A UVB receptor has also been identified known as UVR8 (UV Resistance Locus8) that is involved in UV protective responses and regulates over a hundred genes in *Arabidopsis thaliana* (Brown *et al.*, 2005). The UVR8 receptor is not discussed further here but in summary, exposure to UV-B causes accumulation of UVR8 in the nucleus (Kaiserli and Jenkins, 2007) and its interaction with Constitutively Photomorphogenic1 (COP1) regulates initiation of transcriptional responses (Oravecz *et al.*, 2006).

Additionally, perception of green light by *Arabidopsis* is thought to mediate vegetative development, stomatal opening, photoperiodic flowering and chloroplast gene expression, amongst many other responses, but no green light photoreceptor has been elucidated (Folta and Maruhnich, 2007).

1.1.2 **Skotomorphogenesis**

During etiolated or dark-dependent growth, a pattern of development known as skotomorphogenesis occurs (Josse and Halliday, 2008). Hypocotyl elongation is the most prominent feature. *Arabidopsis* seed germination requires light but absence of light in germinated seedlings causes the hypocotyl's extension growth (Gendreau *et al.*, 1997), an investment in order to reach optimal light conditions. During

skotomorphogenesis the apical hook forms, cotyledons remain closed and yellowish in appearance and cells typically contain etioplasts or proplastids

1.1.3 **Regulators of skotomorphogenesis**

In an attempt to understand light signalling mechanisms, photo-biologists undertook genetic screens searching for mutants which behaved as light-grown even in the absence of light. This led to the identification of negative regulators of light responses, or "regulators of skotomorphogenesis". The CONSTITUITIVELY PHOTOMORPHOGENIC1 (COP1) protein has a RING domain and is an E3 ubiquitin ligase (Yi and Deng, 2005). In the dark, COP1 is located in the nucleus and ubiquinates other proteins for degradation to suppress their (positive) photomorphogenic role. The best example is the degradation of ELONGATED HYPOCOTYL5 (HY5), a basic leucine zipper (bZIP) transcription factor (Osterlund *et al.*, 2000). For a recent review see (Huang *et al.*, 2014).

Well known regulators of skotomorphogenesis are the PHYTOCHROME INTERACTING FACTORs (PIFs), these proteins are from the basic-helix-loop-helix (bHLH) family of transcription factors. PIFs accumulate in very young dark grown seedlings. It was the examination of mono, double, triple and quadruple mutants that revealed their *COP* like phenotype in dark conditions, hence they promote elongation growth of the hypocotyls in the dark (Leivar *et al.*, 2008). PIFs 1, 3, 4 and 5 have been shown to positively regulate hypocotyl extension (Leivar and Quail, 2011) but each PIF can have a different positive and negative regulatory role which is why single mutant phenotypes appeared weak in their *COP* like phenotype. PIF1 negatively regulates seed germination and chlorophyll biosynthesis (Huq *et al.*, 2004; Oh *et al.*, 2004). PIF3 negatively regulates chloroplast development and chlorophyll biosynthesis (Monte *et al.*, 2004). Moreover, Lorrain and colleagues (Lorrain *et al.*, 2008) published a study on PIF4 and PIF5 and their negative regulatory role in phytochrome mediated inhibition of shade avoidance. They showed that PIF4 and 5 are abundant in the dark as well as in shade mimicking conditions and are otherwise degraded in a Phytochrome B (PhyB) dependent manner in (sufficient) light. PIFs have also been shown to regulate hypocotyl growth in other processes, independent of dark induced conditions. For instance PIF4 in

deetiolated seedlings causes elongation of the hypocotyl under high temperature (Koini *et al.*, 2009).

1.1.4 **Photomorphogenesis**

Phytochromes and cryptochromes perceive light at the shoot apical meristem/shoot apex resulting in expansion of the cotyledons with maturation of chloroplasts, inhibition of hypocotyl extension and formation of new leaf primordia (López-Juez and Devlin, 2008; Jiao *et al.*, 2007). This phenomenon is known as deetiolation or photomorphogenesis.

1.1.5 **Regulators of photomorphogenesis**

Gene expression changes upon first light exposure are primarily due to phytochromes and cryptochromes (Ohgishi *et al.*, 2004; Ma *et al.*, 2001). Both phytochromes and cryptochromes inhibit hypocotyl elongation and promote cotyledon expansion in deetiolated seedlings. Also both contribute to regulation of leaf blade expansion and inhibition of petiole elongation in the light (Kozuka *et al.*, 2005).

Light exposure causes photon excitation/activation of phytochromes (they are auto-phosphorylated) and their translocation from the cytoplasm to the nucleus (Nagatani, 2004). In the nucleus phytochromes interact with PIFs (1, 4, 5, 6 and 7), reviewed by (Leivar and Quail, 2011; Duek and Fankhauser, 2005; Toledo-Ortiz et al., 2003). This then initiates changes in gene expression that allow photomorphogenic responses to take place (Jiao et al., 2007). All PIFs are reported to have a conserved Active PhytochromeB (APB) motif at the N terminal region that specifically binds PhyB but only PIF1 and PIF3 have an Active PhytochromeA motif that specifically binds PhyA (Leivar and Quail, 2011). The active PhyA and PhyB proteins have been shown to rapidly phosphorylate and degrade the PIFs in many studies.

Mentioned under skotomorphogenic regulators was the shade avoidance response and how PhyB suppresses shade avoidance via direct phosphorylation, and then degradation, of PIFs 4 and 5. This is due to PhyB playing a major role in detecting light quality (Devlin *et al.*, 1999; Lopez-Juez *et al.*, 1992).

HY5 is a key transcription factor driving light responses. HY5 transcription is promoted by phytochromes and cryptochromes and its abundance is also regulated at the protein stability level as it regulates photomorphogenesis. In light HY5 targeting for proteolytic degradation (by COP1) is inhibited. CRY1 and CRY2 have been shown to interact with COP1 in the nucleus in the dark and possibly play a role in its degradation upon blue light perception (Wang *et al.*, 2001; Yang *et al.*, 2001). Apart from HY5, and its close homologue HYH, there are other regulators of photomorphogenesis, for example B-Box zinc finger, (BBX), basic region/leucine zipper motif, (bZIP) transcription factors, reviewed by (Wu, 2014).

The *CONSTITUTIVELY-PHOTOMORPHOGENIC/DEETIOLATED/FUSCA* (*COP/DET/FUS*) genes encode proteins that are, as mentioned above, negative regulators of photomorphogenesis (Ma *et al.*, 2002). COP1 is part of the COP1-SPA (SUPRESSOR OF PHYA-105) complex and DET1 (DEETIOLATED1) is part of the CDD (DAMAGED DNA BINDING PROTEIN1(DDB1)/DET1/COP10) complex. At the RING finger domain COP1 interacts with the CDD complex (Yanagawa *et al.*, 2004; Suzuki *et al.*, 2002). The remaining COP genes encode proteins of the COP5 signalosome complex (CSN). The CDD complex and CSN ubiquitin-mediated proteolysis are evolved mechanisms whereby plants have adopted the ability to etiolate via degrading photomorphogenic proteins. Moreover, it is an example of post-translational regulation of photomorphogenic development. *Arabidopsis* mutants of *deetiolated (det)* and *constitutively photomorphogenic (cop)* can overcome skotomorphogenic growth in the absence of light; in fact they resemble photomorphogenic seedlings, (Deng *et al.*, 1991; Chory *et al.*, 1989). This is because light is perceived by photoreceptors, and photoreceptors are targeted into the nucleus (Chen, 2008; Fankhauser and Chen, 2008; Kaiserli and Jenkins, 2007; Wu and Spalding, 2007) where they inhibit COP1 function (Yi and Deng, 2005), with the exception of UVR8, whose action requires COP1 (Kaiserli and Jenkins, 2007). Inhibition response of COP1 can be long term, where COP1 is exported out the nucleus over 24 hours (von Arnim *et al.*, 1997), or short term where R/FR or blue light impose rapid gene expression changes within an hour (Tepperman *et al.*, 2004; Jiao *et al.*, 2003; Tepperman *et al.*, 2001). The mechanism by which photoreceptors rapidly inactivate COP1 function in the nucleus, before it is exported, remains unknown.

1.2 Monocotyledon and dicotyledon plants

The distinction of mono- and di-cotyledon (monocot, dicot) plant classes was established by John Ray, 1686. Monocots diverged from dicots approximetaly 150 million years ago (Jurassic-early cretaceous) (Chaw *et al.*, 2004).

Monocots and dicots differ in phenotype. In dicots, such as *Arabidopsis,* the embryo has two cotyledons as opposed to one, petals appear in multiples of four or five as opposed to three and pollen has (in their largest group, the eudicots) three furrows or pores as opposed to one in monocots.

Specifically in the leaf symmetry is isobilateral in monocots but dorsiventral in dicots. Stomata are equally distributed in monocot adaxial and abaxial surface but dicots have more stomata on the abaxial surface. In monocots the cells of the adaxial epidermis are bulliform-shaped whereas in dicots this shape is absent. Additionally, monocot mesophyll layer consists of a uniform parenchyma unlike dicot that has palisade (tightly packed) and spongy mesophyll (with larger intracellular spaces). Cells of bundle sheath in dicots are made of parenchyma above and below the vascular bundle where some cells are parenchymatous, some collenchymatous, and present up to the epidermis. In monocots the bundle sheath is made of parenchyma above and below vascular bundles, whose structural cells are sclerenchymatous.

The developmental gradient of young proliferating cells to differentiated and expanded cells on the leaf surface exists in dicots (Gonzalez *et al.*, 2012) and monocots (Fournier *et al.*, 2005). Developmental gradients can be observed in both spatial and temporal terms, with a few subtle differences in rates and duration but the size of the proliferation zone is relatively constant for a few days prior to cessation (Nelissen *et al.*, 2016). In monocots and dicots some regulators of leaf growth are similar, such as transcriptional/translational regulators, hormone and other signalling pathways and additionally cell wall mechanics, detailed in (Nelissen *et al.*, 2016). Despite similarities in spatial and temporal leaf development and existence of common regulatory mechanisms the monocot leaves, often larger, are not preferred over the tiny *Arabidopsis* leaves. One reason is that in monocots the mature leaves prior to emergence hide the new leaves, at early stages of development. Thus, study of a comparative developmental time point is achieved more easily in *Arabidopsis* at

a given chronological point, and an early point in a monocot leaf matching to *Arabidopsis* for example, would be hidden by more mature leaves prior to emergence.

1.3 Leaf initiation

Plants photosynthesise during the day and produce sucrose as a primary product. This process occurs in leaves that have adapted a light energy capturing upper surface (adaxial side) and lower surface (abaxial side) designed for gaseous exchange. Enveloping both sides is the upper and lower epidermis between which are the palisade and spongy mesophyll cells (Fig 1.1).

1.3.1 **Shoot apical meristem vs root apical meristem**

Plant meristems comprise of self renewing populations of cells, just like animal stem cells, they are undifferentiated. Plants are able to differentiate new organs from self-renewing meristematic cells at two different locations, or types of location, called the shoot apical meristem (SAM) and root apical meristem (RAM) (Bäurle and Laux, 2003; Sablowski, 2007).

1.3.2 **Shoot apical meristem organisation**

The SAM gives rise to the aerial organs of the plant, importantly the leaves. In plants the progeny of proliferating (stem) cells is organised in a precise spatial orientation at the SAM. Stem cells are a plants reserve of undifferentiated cells that are spatially maintained by extracellular signals (Sablowski, 2007). Daughter cells of divided stem cells differentiate but also note that initiation of leaves also involves cell division and differentiation, as a developmental gradient along the leaf blade axis (Andriankaja *et al.*, 2012; Donnelly *et al.*, 1999).

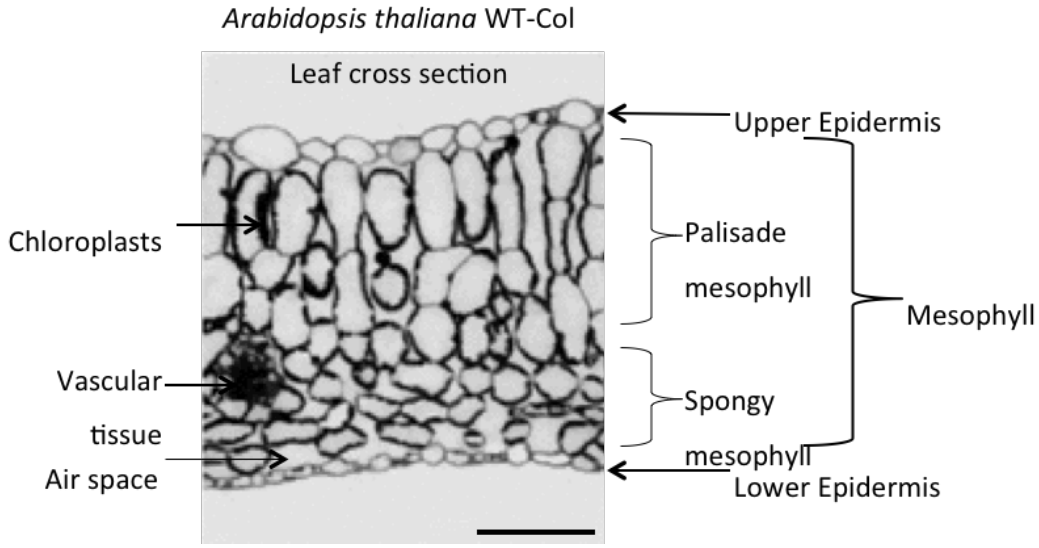

Figure 1-1 Basic *Arabidopsis thaliana* leaf anatomy

Arabidopsis WT-Col leaf cross section showing basic anatomical structures. (From plants grown under continuous light, at 150 µmol m^{-2} s^{-1}, for two weeks then at 400 µmol m^{-2} s^{-1} for 1 day followed by 600 µmol m^{-2} s^{-1} for 5 days). Scale bar = 100 µm. Adapted from Weston *et al.,* 2000.

The final fate of a plant cell is determined, as is the fate of an animal cell, but plant cells do not migrate during the developmental process of pattern formation. Thus, organisation of the meristem region and cells that differentiate from it is maintained spatially.

Organisation of the SAM can be explained by zones and layers (Fig 1.2). At the centre of the SAM is the central zone (CZ), below which is the organising centre (OC) and rib zone (RZ) and these are flanked by the inner peripheral zone (IPZ) that is further flanked by the outer peripheral zone (OPZ). At both OPZs are the organ primordia (OP). Cells in the CZ divide at a low rate, remaining undifferentiated, and surrounding cells divide faster in the PZ as they differentiate to form organs (Braybrook and Kuhlemeier, 2010). In dicotyledonous plants like *Arabidopsis* three layers form the SAM, namely layers 1, 2 (the tunica layers) and 3 (the corpus layer) (L1, L2, L3). The LI is the outer epidermal layer, L2 is the sub-epidermal and L3 is the inner most layer (where the RZ is) (Satina *et al.*, 1940). Understanding this organisation helps explain how the SAM is maintained and organs initiate.

1.3.3 **Maintenance of the shoot apical meristem**

To keep stem cells separated from those cells that differentiate tight regulation is needed. Cells must be aware of when additional growth is required in order for cells to differentiate as well as when not to over divide (not to form tumours). Stem cells maintain their fate with long range and localised signals (from neighbouring cells) and distancing from this maintenance signal causes cells to differentiate. In roots the quiescent centre (QC) maintains stem cells preventing their differentiation. In plants external cues from the environment have a major role in the decision to grow further (form new organs) yet the size of the meristem and number of stem cells must be kept constant. One way in which plants do this is by anticlinal division of cells in L1 and L2 whereas cells in L3 divide periclinally and anticlinally (Braybrook and Kuhlemeier, 2010). Lateral cell expansion pushes these cells to the periphery and the anticlinal division of cell layers maintains the layer as single cell thick (Tilney-Bassett, 1986).

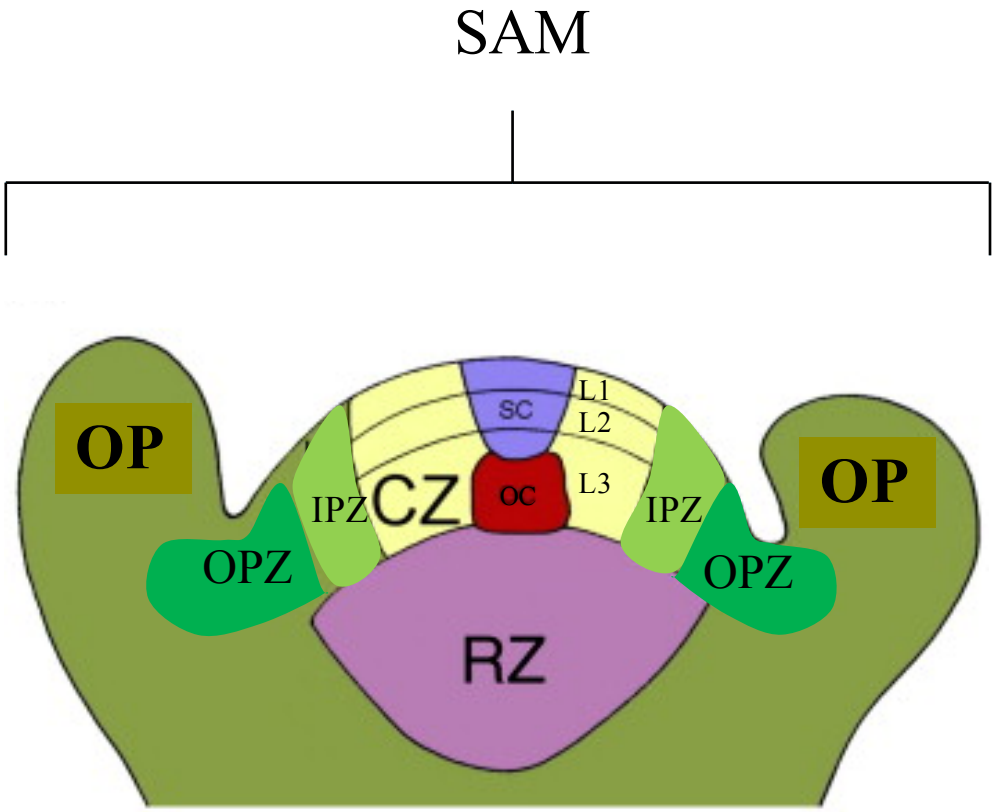

Figure 1-2 Organisation of the shoot apical meristem (SAM)

Zones of the SAM; central zone (CZ), stem cells (SC), organising centre (OC), inner peripheral zone (IP), outer peripheral zone (OPZ), rib zone (RZ) and organ primordia (OP). Layers 1-3 are shown as L1, L2 and L3. Adapted from (Dodsworth, 2009).

A second mechanism by which plants maintain the SAM is via gene expression circuitry as well as phytohormones. The WUSCHEL (WUS) transcription factor (in the RZ) and *CLAVATA* gene products (*CLV1*, *CLV2* and *CLV3*) (expressed in the CZ) are the best studied circuit in the SAM (a similar mechanism operates in the RAM but remains incompletely understood). WUS activity in L3 produces a non-cell autonomous signal that moves to the stem cells to activate CLV3. It appears that this movable signal is the WUS protein itself (Daum *et al.*, 2014; Yadav *et al.*, 2011). CLV3 encodes a small peptide that acts as a ligand, it is produced in L1 and L2 and diffuses to the L3 where it binds to its receptor. These receptors are CLV1, CLV2 and CORYNE (CRN) (Somssich *et al.*, 2016) and inhibit WUS activity. CLV2 (a receptor like protein) and CRN potentially interact molecularly as a heterotrimer where as CLV1 (a Leucine Rich Repeat, LRR, receptor like kinase) acts independently as a homomer (Bleckmann *et al.*, 2010) at the plasma membrane. The CLV1 and CLV2/CRN receptors can also interact as a multimer in CLV3 peptide perpception (Bleckmann *et al.*, 2010). Thus, CLV3 is a negative regulator of WUS. In summary, the CLV3 peptide is secreted at the CZ where self-renewing stem cells divide slowly. The CLV3 peptide initiates a signal cascade that restricts synthesis of the WUS protein to the OC and adjacent cells, whilst further initiating CLV3 expression (Brand *et al.*, 2000; Schoof *et al.*, 2000).

Further studying of WUS/CLV has introduced the role of phytohormones in maintaining the SAM. Cytokinin has been reported to positively regulate *WUS* expression and WUS represses ARABIDOPSIS TYPE-A RESPONSE REGULATORS (ARRs) that are in fact cytokinin signalling inhibitors, reviewed by (Kalve *et al.*, 2014).

In addition to the above, the prevention of early cell differentiation, at and throughout the meristem, is maintained by the class I KNOTTED-LIKE homeobox (KNOX) gene called *SHOOTMERISTEMLESS* (*STM*) (Hay and Tsiantis, 2010; Lu *et al.*, 1996). As the name suggests the mutant has no meristem because differentiation also reaches otherwise meristematic cells. This suggests that KNOX transcription factors repress differentiation, which explains why their expression is at the CZ and PZ but not in OP zones. KNOX also maintain the balance between cytokinin (a phytohormone that positively regulates cell division) and gibberellin (a phytohormone that positively regulates cell elongation, associated with

differentiation), hence, a high cytokinin and low gibberellin ratio maintains stem cell fate by preventing differentiation of the cells (Braybrook and Kuhlemeier, 2010). To date details on the maintenance of the niche remain incompletely understood and complex despite multiple analyses.

1.3.4 **Leaf initiation at the SAM**

The L1 of the SAM also forms the single cell layer of the epidermis of the leaf and L2 and L3 contribute towards the inner organ body. But what processes determine leaf initiation at a region that is strictly controlled for cell division and differentiation?

Leaf initiation involves auxin. It has been postulated that AUXIN RESISTANT1 (AUX1, an auxin influx transporter) is involved in auxin accumulation in L1. In the L1 polarized auxin transport, via PIN FORMED1 (PIN1), transports auxin from the epidermis to the leaf primordia founder cells in the meristem, at the periphery (Reinhardt *et al.*, 2003; Reinhardt *et al.*, 2000). It has also been simulated that auxin drainage via PINs in L1 towards the base of the shoot is induced by vascular strand differentiation in the L2 and L3 layers (Kalve *et al.*, 2014; Heisler *et al.*, 2005; Scarpella *et al.*, 2006). The complexity of the regulatory network in the SAM that governs leaf initiation remains incomplete and many recent reviews focus on computer based models and simulations, in other organs too, to help our understanding (Grieneisen *et al.*, 2007; El-Showk *et al.*, 2013; Vercruyssen *et al.*, 2015).

Separation of leaf primordia cells from the rest of the meristem is also facilitated by a subset of MYB transcription factors (Byrne *et al.*, 2000). Among those MYB transcription factors, ASYMMETRIC LEAVES1 (AS1) (part of the ASYMMETRIC LEAF/ROUGH SHEATH2/PHANTASTICA, ARP, protein family) represses *KNOX1* genes in leaf primordia cells allowing differentiation and development of the leaf (Guo *et al.*, 2008; Byrne *et al.*, 2001). The *STM* gene (a *KNOX* gene) acts antagonistically to *ARP* gene products controlling leaf initiation. Also, *STM* activates the expression of *CUP SHAPED COTYLEDON1* (*CUC1*, one amongst *CUC1*, *2* and *3*). Their expression separates the cell zones of organ primordia and meristem (Rodriguez *et al.*, 2014).

The leaf primordia founder cells are defined due to the local auxin maximum and this helps achieve the spiral phyllotaxy of *Arabidopsis* rosettes where new leaves emerge at angles of 137° (Heisler *et al.*, 2005; Reinhardt *et al.*, 2003; Stieger *et al.*, 2002). This process also involves the drainage of auxin from the midvein of young leaves (Deb *et al.*, 2015). Moreover, the number of cells incorporated from the meristem is a contributing factor to the final size of a leaf (Gonzalez *et al.*, 2012).

1.3.5 **Leaf polarity**

Leaves that comprise the adult *Arabidopsis* rosette have petioles (the stem like attachment of the leaf), whereas cauline leaves lack petioles (Tsukaya *et al.*, 2000). The petiole is only apparent after leaf primordia initiation and cells of the petiole arise from a pre-existing proliferative junction between the leaf blade and petiole; from this junction leaf blade cells are supplied acropetally and petiole cells basipetally (Ichihashi *et al.*, 2011).

The basal leaves of *Arabidopsis* are determinate and form a rosette as they emerge from the meristem. Each leaf is configured to three dimensional axis; proximodistal, dorsoventral and mediolateral. The dorsaventral axis of the leaf is established in the early developmental stages of the primordia at the SAM (Waites and Hudson, 1995). The adaxial side of the leaf faces the meristem, is determined by expression of *PHABULOSA* (*PHB*), *PHAVOLUTA* (*PHV*) and *REVOLUTA* (*REV*) (class III homeodomain leucine zipper proteins, HD-ZIPIII) (McConnell *et al.*, 2001) and differentiates to form mesophyll cells. Alternatively, the abaxial side is determined by expression of *KANADI* (*KAN*) and *YABBY* genes and differentiates to form spongy mesophyll cells (Tsukaya, 2005). These genes act antagonistically in order to maintain adaxial-abaxial sides. In addition to adaxial-abaxial side maintenance mechanisms others exist too. The microRNA dependant mechanism of maintaining dorso-ventrality, that is also a conserved mechanism in plants (Floyd and Bowman, 2004) (for a detailed review see Kalve *et al.*, 2014). At the rim of the adaxial-abaxial boundary changes, not yet molecularly identified, result in rod shaped leaves changing into a spatula-like organ (Donnelly *et al.*, 1999). Other genes involved are the *AS1* and *AS2* genes, they are involved in determining the adaxial side of the leaf, as well as *AUXIN RESPONSE FACTOR* (*ARF*) genes for the abaxial side (Rodriguez *et al.*, 2014).

Like our understanding of maintenance of the SAM, leaf polarity still remains unclear and complex as there appears to be a clear overlap in genes regulating SAM cell fate and leaf polarity. A good example of this is the role of auxin, its maxima are needed to initiate leaves yet it is not understood how exactly the same hormone spatially regulates leaf positioning, phyllotaxy. The role of *ARF*s in adaxial-abaxial side determination highlights the role of auxin in leaf polarity too, but this may be more complex than assumed as during leaf outgrowth auxin flows from the epidermis to the leaf tip but is also drained by vasculature of the stem (mid vein). So how does auxin simultaneously maintain adaxial-abaxial polarity (Braybrook and Kuhlemeier, 2010)? Polarity plays a role in differentiation of vasculature tissue as an increase in auxin flow allows differentiation of the pre-procambium cells and the xylem forms on the adaxial side and phloem on the abaxial side. This is due to the antagonistic role of HD-ZIPIII and KAN at the adaxial and abaxial sides respectively (Kalve *et al.*, 2014).

1.4 Leaf Growth

Establishment of SAM and leaf primordia boundaries produces protrusions at flanks of the meristem, the leaf primordia. The initial stages of the primordia involve cell division where all cells appear constant in size as growth and division are tightly regulated. When the leaf primordia first emerges they are very curled in shape, forming a cone shape around the meristem, and as this growth continues, division is restricted to the base of the leaf and distal cells eventually exit proliferation (cell division) and enter expansion (often coupled with differentiation). Reportedly, growth of leaf laminas in *Arabidopsis* is asymmetric, as auxin distribution is unequal resulting in the left side growing more than the right (phyllotaxy of *Arabidopsis* is spiral) (Chitwood *et al.*, 2012). Here leaf growth is addressed and the factors that contribute to the final size (and shape) are discussed below.

1.4.1 **Cytoplasmic and turgor-driven growth**

Cell expansion increases the vacuolar volume of a cell in contrast to cell division that causes partitioning and growth by increasing cytoplasmic volume. Turgor driven growth occurs mainly in differentiated cells that increase their volume by increasing

vacuole size, associated with water uptake but is not limited to this, consider meristematic cells. The uptake of water increases turgor. Thus, the cell wall must be flexible and act as a control point, this is referred to as cell-wall relaxation (Wolf and Greiner, 2012). The loosening of the cell wall is often associated with EXPANSINS (commonly known to assist cell wall expansion), amongst other processes that facilitate cell wall loosening. Once extension/expansion has been achieved a firm wall is reinstated with addition of cell wall components, notably cellulose microfibrils, for details see (Sablowski and Carnier Dornelas, 2014). Braybrook and Kuhlemeier, 2010, suggested the L1 of the SAM may have different mechanical properties when deciding on organ initiation suggesting that cell wall mechanics may not be limited to the growing leaf but also to organ initiation at the SAM (Dumais and Steele, 2000).

Cytoplasmic growth contributes to most of the growth (in terms of cell volume) in meristem and organ primordia. Cytoplasmic growth requires energy to be invested in macromolecule synthesis. Recent reviews have highlighted the role, in this process, of TOR, a kinase known for its role in sensing nutrient status (see later section 1.7.3) (Kalve *et al.*, 2014; Sablowski and Carnier Dornelas, 2014). The latter review highlights repression of growth and translation in carbon limiting conditions; in yeast and mammals this repression, among other responses, is regulated by yeast SUCROSE NON-FERMENTING1 (SNF1) and mammalian AMP ACTIVATED PROTEIN KINASE (AMPK), key growth regulators (see later section 1.7).

1.4.2 **Proliferative and expansion growth**

Differentiation of leaf cells takes place at the flanks of the meristem, known as leaf primordia, giving rise to two true new leaves (NLs) that undergo primary and secondary morphogenesis (Donnelly *et al.*, 1999). Primary morphogenesis involves successive cell division that leads to anatomical structures, such as vasculature, stomata and trichomes. Trichomes are exclusive to new leaves and absent from the embryonic leaves of *Arabidopsis*. Secondary morphogenesis involves cell expansion and cell wall loosening, reviewed by (Cosgrove, 2005). Hence, primary and secondary morphogenesis are a reflection of proliferative and expansion growth phases respectively. Proliferative growth mainly involves cell division and growth is a result of an increase in cell number. Notably, post division daughter cells are not

smaller in size than the parent cell. Cell expansion is often associated with an exit from proliferation into differentiation where cells increase in size, also termed differentiation-associated-expansion. In most cells of *Arabidopsis* differentiation is coupled with endoreduplication (where DNA synthesis occurs but mitosis, M, does not). It should be noted that proliferation can occur simultaneously with cytoplasmic growth and cell expansion with endoreduplication and turgor driven growth but all may occur independently too.

Growth due to an increase in cell number or an increase in cell size has been considered to be under the control of a compensatory mechanism governing final organ size (Beemster *et al.*, 2003; Tsukaya, 2002). An increase in the rate of proliferative growth or delays in the exit from proliferation are two "organ size control points", (Gonzalez *et al.*, 2012; Bogre *et al.*, 2008). The development of the leaf and the transition between these two growth phases is complex. Typically, proliferation ceases at the tip and gradually proceeds down the longitudinal axis to the base or, in other words, the differentiation gradient is of a basipetal direction (Andriankaja *et al.*, 2012; Kazama *et al.*, 2010; Bogre *et al.*, 2008; Donnelly *et al.*, 1999). Duration of each phase affects transition to the other. For instance, exiting proliferation sooner would produce fewer cells. Early entry into endoreduplication would mean the final organ size would be met by an increase in cell size. This compensation is a possible growth regulation mechanism of plants but is not essential. Thus, an abrupt inhibition to the first growth phase leads to the second and is non-detrimental to the organ (Beemster *et al.*, 2003; Tsukaya, 2003; Dengler and Tsukaya, 2001; De Veylder *et al.*, 2001). It has been established that the transition from proliferation to cell expansion is in fact a relatively abrupt process. The onset of pavement cell expansion towards the tip being a result of retrograde signalling and differentiation of the photosynthetic apparatus in chloroplasts of the differentiating mesophyll (Andriankaja *et al.*, 2012). This reinforces the complexity of leaf growth control mechanisms.

1.5 Light and growth

During germination transcript changes in numerous genes, particularly those involved in cell cycle entry, in the RAM lead to radicle protrusion out of the seed coat (Masubelele *et al.*, 2005). The role of light in regulating meristem activity and cell proliferation is much less understood and only recently has been a focus of attention. In the absence of light the meristem activity is repressed in the shoot (Yoshida *et al.*, 2011; Lopez-Juez *et al.*, 2008) and is less active in the root. However, while root meristem activity appears only to depend on sucrose availability (Stitt and Feil, 1999), leaf growth depends both on sucrose and light as a signal. Dissected tomato shoots still arrest leaf emergence in the dark that cannot be rescued on a sucrose-containing medium (Yoshida *et al.*, 2011). However, it was previously reported that etiolated seedlings in the dark initiated leaf development on sucrose containing medium, but only when the meristem was in direct contact with the medium, suggesting that access to sucrose is regulated by light (Roldan *et al.*, 1999).

Plants are anchored to the ground by their roots and must adapt to the environment that surrounds them. Most of a plant's energy comes from light capture and resources can be stored in the form of starch, which can be catabolised and utilised during the dark when light is absent. This means plants must be optimised in their light harvesting capacity that is achieved by leaves, so plants must first be able to sense changes in the environment and then change accordingly to optimise cellular roles. The ability of a plant to optimise, via chloroplast composition, leaf and root anatomy, carbon utilisation and storage, and the reflection this has on the health of the plant is perhaps what I mean by plants being "robust". Here I focus on the ability of leaves to acclimate to HL, how photoperiods regulate carbon utilisation and storage as well as highlight the fundamentals of a key transcript profiling study on the shoot apex in a dark to light transition.

1.5.1 **High light acclimation**

In dicotyledonous plants, light exposure initiates leaf organ growth at the SAM. Light is perceived by photoreceptors and a signalling cascade takes place that negatively regulates (represses) negative regulators, and positively regulates (activates) positive regulators of photomorphogenesis. For instance phytochromes that detect R/FR wavelengths become activated in R wavelength. However, not only do they become active upon light exposure (the correct quality of light) but can act in a light quantity dependent manner too to modulate the nucleo-cytoplasmic distribution of PHYA–PHYE, a process that is essential in their signalling (Kircher *et al.*, 2002).

In comparison to low light fluence rates, high light fluence rates clearly increase the thickness of the leaf and its palisade cell layer by an additional one or two layers (Lopez-Juez *et al.*, 2007; Weston *et al.*, 2000). The quantity of light affects the growth of the leaf. In conjunction, red light alone distorts the morphology of the leaf structure whereas blue light appears to facilitate the correct elongation of the palisade mesophyll cells (Lopez-Juez *et al.*, 2007). Therefore both light quality and quantity affect the cellular anatomy of a leaf. The anticlinally elongated palisade cells in high light and the isodiametric cells in low light position their chloroplasts differently for efficiency of light capture (under low light) or to maximise light utilisation and minimise photo-damage under high light (Weston *et al.*, 2000).

Increasing chloroplast number alone does not maximise light capture and photosynthesis. In any case, maximising light capture may be counterproductive in excess light, leading to photo-oxidation. In short, no single leaf anatomy is optimal at every light level; different developmental anatomies are ideally suited for different irradiances. Plants attempt to optimise carbon fixation per unit area. In high light chloroplasts decrease granal thylakoids per chloroplast and increase starch accumulation (Weston *et al.*, 2000) typical of sun-type chloroplasts (Anderson *et al.*, 1995), but prevent photo-inhibition by shading of chloroplasts in the lower cell layers. In contrast, low light chloroplasts move parallel to the leaf surface, increase their granal stacking and light harvesting complex content in order to maximise light capture (Weston *et al.*, 2000). Changes in the level of RUBISCO (large subunit) in

high and low light leaves are minimal and blue photoreceptor mutants produce shade and sun-type chloroplasts in low and high light, respectively (Weston *et al.*, 2000).

Light quantity affects chloroplast composition as well as the leaf anatomy but the sensor responsible for this anatomical plasticity remains uncertain. In addition, when a variegated mutant produces leaves that are part green and part albino, the anatomy of the leaf illustrates a "robust", thick structure (with a multilayer palisade of periclinally-elongated mesophyll cells), in the green half and a thin tissue appearance (with a single layer of cells which are not elongated) in the albino half where high light, only very moderately, increases mesophyll cell elongation. Moreover, plastids are necessary for mesophyll cell divisions in high light acclimatory responses (Tan *et al.*, 2008) (Fig 1.3). This indicates that chloroplasts affect high light acclimatory responses to an extent; at least they are necessary for the response to take place. In summary, a multiple palisade cell anatomy is a feature of leaves grown in high light and, although it requires the sensing of blue light specifically, arguing for an involvement of blue photoreceptors, it only occurs in the presence of viable chloroplasts.

1.5.2 **Light and carbon assimilation**

First etiolated growth takes place in the natural environment upon seed germination within the soil (in the dark). Light allows embryonic-leaf (cotyledon) growth and these are the initiators of a diverse growth regulatory source sink relationship. Subsequent developing leaves (denoted New Leaves, NL) store carbohydrates in the form of starch that can be catabolised when the plant senses reduced carbohydrate availability; these NLs can then become sources for subsequent NL pairs. Irrespective of carbohydrate availability, till date much conflicting literature has indicated that dicotyledonous leaves present highest growth rates in either the day or night. In contrast, monocotyledonous leaves reportedly have highest growth rates during the day but this was related to air temperature (Gallagher, 1979).

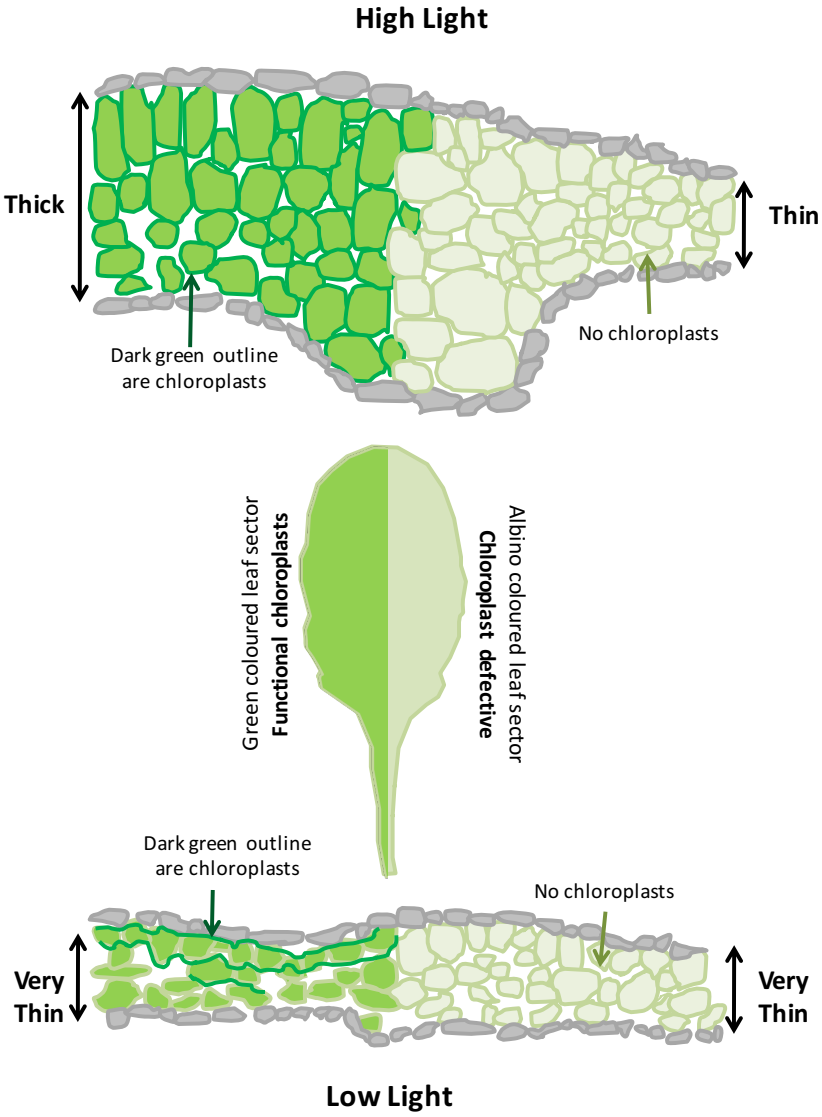

Figure 1-3 High light treatment and the role of chloroplasts in mesophyll morphogenesis

The middle leaf represents a chimeric mutant in which half the leaf is green (shaded green on the left), with functional chloroplasts, and the other half is albino (shaded grey on the right), lacking chloroplasts. On the top and bottom are cross sections of this leaf under high light (top panel) and low light (bottom panel) conditions. Under high light the leaf is generally thicker compared to low light leaves. The functional chloroplast side (left, green cells) is thicker than the albino half of the leaf (right side, greyish cells); these cells are lined with chloroplasts (thick dark green outline of cells on left). Note that in low light these chloroplasts are lined up parallel to the leaf surface (bottom panel, dark green line on left side). Cells lining leaf cross sections in grey represent the upper and lower epidermis and the mid vein has been excluded for simplicity. Not to scale. Based on the work of Tan *et al.*, 2008.

The study on the leaf of different dicotyledenous plant species such as *Nicotiana tabacum, Nicotiana attenuata, Arabidopsis thaliana, Ricinus communis* (castor-oil plant) as well as *Populus deltoides* (poplar tree) has highlighted that the discrepancy in the literature can be explained by 2 types of maximal growth 'phases': (1) High growth at the beginning of the day, most likely due to proliferative/cytoplasmic growth (Hummel *et al.*, 2007; Wiese *et al.*, 2007; Walter and Schurr, 2005); (2) High growth during the end of the day, most likely due to differentiation and expansion, (Matsubara et al., 2006; Walter et al., 2005). Despite the lack of connection between carbohydrate availability and maximal leaf growth in process (1) and (2) an association between leaf growth transitions, from proliferation to cell expansion, has been deduced: Prior to reaching final leaf size, those leaves that retain proliferative activity (a lack of transition) throughout their development appear to fit the first hypothesis (1). This includes leaves of *Populus deltoides* (Van Volkenburgh and Taylor, 1996). Alternatively, those leaves that transition (Arabidopsis thaliana) (Beemster et al., 2005), or even cease proliferation, like *Nicotiana tabacum* (Walter *et al.*, 2003) or *Ricinus communis* (Roggatz *et al.*, 1999) before reaching full size, have growth maxima as in hypothesis (2) but during early leaf development of these plants, the alternative hypothesis (1) also applies, reviewed by (Walter *et al.*, 2009). These findings indicate a link between proliferative and expansion growth and diurnal cycles, however, there is a lack of literature focused on the association of leaf growth (proliferation), carbohydrate availability and diurnal cycles.

Diurnal leaf growth patterns can be attributed to phytochrome and circadian regulatory signals, biomechanical signals or metabolic signals. The best candidate is metabolic control of leaf growth as there is substantial evidence to support why carbohydrates may affect leaf proliferative growth. For example, *Arabidopsis* seedlings grown on 4% sucrose medium will only produce larger leaves if the leaf is in contact with the surface of the medium (Tsukaya, 2003). Detachment of the shoot meristem alone also produces large cotyledons (Tsukaya, 2003) indicating that carbohydrate accumulation affects leaf size.

Plant cells in high light accumulate more starch in chloroplasts and this coincides with a greater number of cells, consistent with additional divisions, and growth of the leaf palisade (Weston *et al.*, 2000) but little is known about the mechanisms coordinating carbon (C) supply and use. Moreover, it has proven difficult to

understand carbon assimilation and its effect on growth rate as traditionally carbon assimilation is associated with source and supply to non-photosynthetic sink regions of plants (Smith and Stitt, 2007). Undoubtedly carbon availability in the form of sugar has a profound effect on growth of the plant. In water limited conditions resources are allocated towards root growth and extension rather than shoot or vegetative growth (Smith, 1982). In light limited conditions sugars are diverted towards investment into stem elongation and development of leaves and plastids (Poorter and Nagel, 2000).

During the light photo-period plants mainly allocate their assimilated carbon into sucrose and starch. The starch is utilised during the dark periods when photosynthesis cannot take place. Extraordinarily, this diurnal pattern is orchestrated so that plants adjust their storage of starch during the day so that it may be precisely utilised just before the end of the night (Stitt and Zeeman, 2012; Graf *et al.*, 2010; Gibon *et al.*, 2009; Matt *et al.*, 1998; Geiger and Servaites, 1994; Zeeman *et al.*, 1998; Fondy and Geiger, 1985). Starch turnover is regulated by an intrinsic timing mechanism known as the circadian clock where starch reserve is exhausted 24 hours after the previous dawn (Stitt and Zeeman, 2012; Graf and Smith, 2011; Graf *et al.*, 2010); the consequences of its malfunction are observed in a starchless (*phosphoglucomutase, pgm*) mutant (Graf and Smith, 2011). Starchless mutants are unable to store starch, leading to increased sugars by the end of the light period and a severe depletion at the end of the dark period (Caspar *et al.*, 1985) which results in poor growth. A simple extension of the dark period by 6 hours, in wild type plants, causes a significant number of growth-related genes to be downregulated (Thimm *et al.*, 2004). Extending the dark period, of seedlings grown on sucrose-free medium, directly inhibits root growth within the first 2 hours, further indicating the implications of starch turnover on growth (Gibon *et al.*, 2004).

The use of clock oscillator mutants *CCA1* and *LHY* confirms clock regulation of starch degradation (Graf *et al.*, 2010). Carbon utilisation in response to changes to the light period has been substantially studied. A shorter light period increases starch synthesis rate and slows down starch degradation (Smith and Stitt, 2007; Stitt *et al.*, 2007; Gibon *et al.*, 2004), this is also true for plants other than *Arabidopsis,* for example, soy bean (Chatterton and Silvius, 1979). Moreover, carbon allocation, protein content and metabolism changes are coordinated in short light photoperiods

allowing growth at a slow rate (Lu *et al.*, 2005; Gibon *et al.*, 2009). Hence, *Arabidopsis* can adjust its timing mechanism in order to tune into the length of the relevant photo period (of 24 hour cycles). A light period as short as 2 hours results in similar starch, sugar and amino acid levels at the end of the night as in longer photo-periods but this is at the expense of very limited growth (Gibon *et al.*, 2009).

Light and carbon assimilation are of importance as they are associated with growth. The dicotyledonous plant *Arabidopsis* is a tractable example that illustrates the interlinking of circadian clock, light signalling and carbon metabolism in growth performance, recently reviewed (Muller *et al.*, 2014).

1.5.3 **Light dependent leaf initiation: A key transcriptomic study**

In the past numerous studies have attempted to understand the light dependent transcriptomic changes in order to understand light perception and signalling. Some of these genome-wide transcriptomic studies utilise changes in the light type (R/FR/Blue), a light transition (dark to light), a photomorphogenic mutant (*cop1, phyB*) or a combination of these on young seedlings (Jiao *et al.*, 2003; Ma *et al.*, 2002; Ma *et al.*, 2001).

A combination approach on wild type and a *phyA* mutant in continuous FR (cFR) light transition (in whole seedlings) showed early response genes act within 1 hour of FR exposure; genes potentially regulated by PhyA are those involved in photomorphogenesis, chloroplast biogenesis, metabolism, genes thought to be involved in transcriptional regulation, stress and defence and some involved in signalling and hormone pathways (Tepperman *et al.*, 2001). Later the same lab confirmed that these early response genes define a clear association between light perception (primarily through PhyA and PhyB) and signal transduction, through a light responsive transductional network that positively regulates photomorphogenesis (Tepperman *et al.*, 2006). Light based responses are numerous and tissue specific. As previously mentioned, light causes inhibition of hypocotyl extension but positively regulates growth of cotyledons. It is plausible that because of differential growth regulation past studies that have made use of whole seedling tissue yielded complex responses. Tissue specific responses upon light exposure have proven to be more informative and a key study of our lab is described below.

Light affects growth, as is apparent from a wealth of photo-biological experimentation. Our lab previously focused on a similar dark to light transition, and sought the transcriptome-based signature that underlines the growth control mechanisms and constraints, but sought to identify the changes taking place exclusively in the shoot apical meristem, (SAM) and its surrounding leaf primordia, upon deetiolation (light exposure) of dark-grown or etiolated seedlings (Lopez-Juez *et al.*, 2008). Wild type seedlings were grown for 3 days in dark (after an initial light-stimulated germination treatment for 1 hour (h), then transferred to continuous light (CL) and cotyledon and shoot apex tissue was collected at time 0 and over 1, 2, 6, 24, 48 and 72 h in the light. Note that here Sap (Shoot Apex + primordium) based on the study by Dr Lopez-Juez and colleagues, refers to dissection of the shoot apex that in later time points also consists of the miniscule NL primordia. The gene signature changes of the embryonic leaf (cotyledon) upon dark to light transition are expected to be less dramatic, but undoubtedly growth of the cotyledons also requires cell expansion and endoreduplication (including S phase) and development of chloroplasts (Lopez-Juez *et al.*, 2008). In contrast, light irradiation in the SAp was found to first upregulate genes associated with the growth of the newly recruited cells that will form the NL tissue, as indicated by the coordinate upregulation of translational and ribosome biogenesis gene groups in the SAp, after which chloroplast biogenesis and cell wall modification genes for cell expansion proceed (Lopez-Juez *et al.,* 2008). In the dark the SAM is repressed and the cell cycle arrested; unlike in the cotyledon tissue, light exposure induces S phase and M phase activity, as early as 6 h although primordia appear 2 - 3days after light exposure (Lopez-Juez *et al.*, 2008). Representations of the responses involved in this study are shown in Fig 1.4.

Transcriptome analysis showed obvious differences in the light dependent growth responses of the cotyledon and shoot apex (Lopez-Juez *et al.*, 2008). The cotyledon undergoes cell division and growth in the embryonic phase, during seed formation (Lindsey and Topping, 1993), and cell division is almost absent in post-embryonic growth (Fridlender *et al.*, 1996; Bewley and Black, 1978).

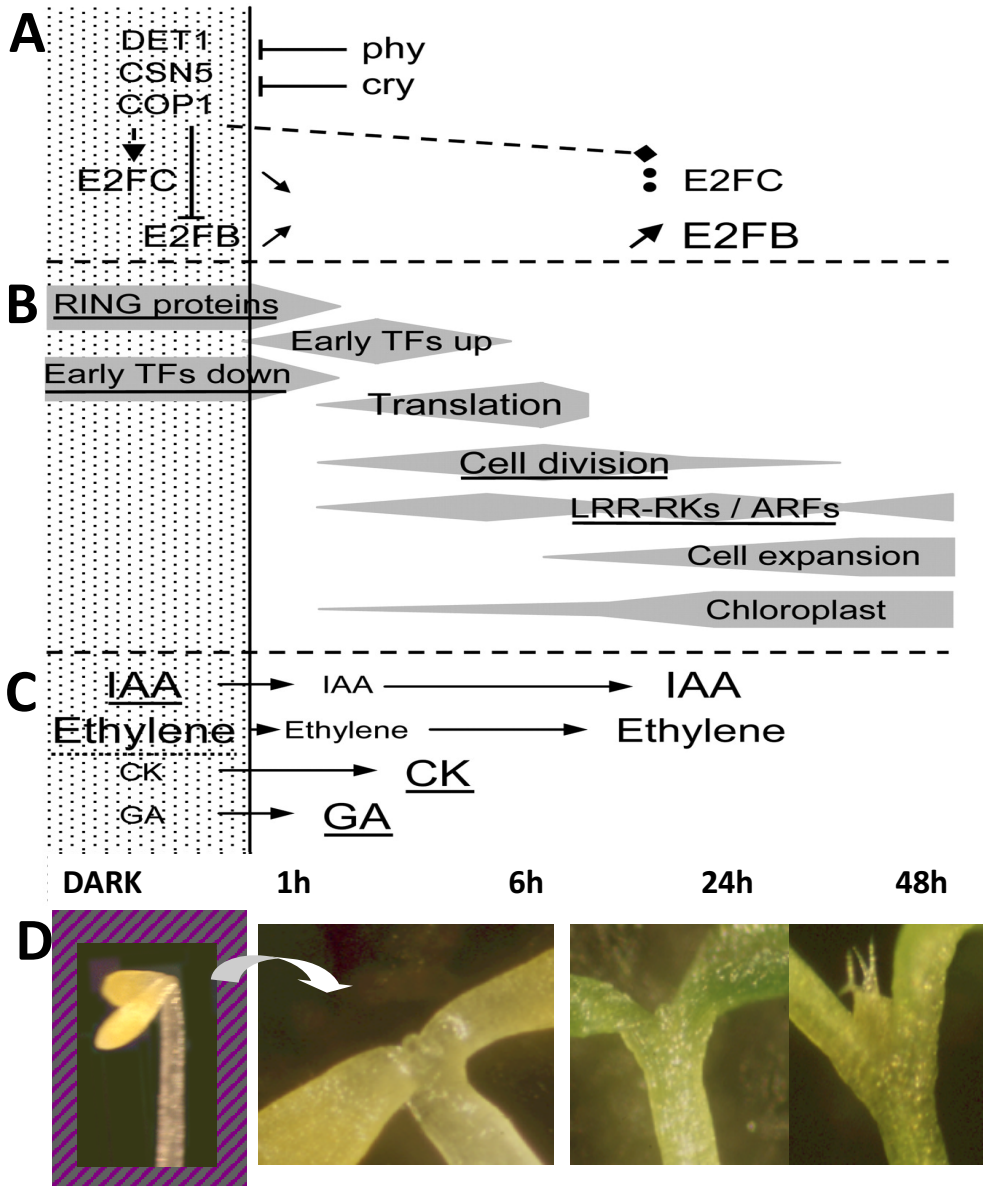

Figure 1-4 Responses involved in the dark to light transfer of Shoot-Apex$_{(+primordia)}$ tissue

D Images show closed yellowish cotyledons and apical hook in dark grown *Arabidopsis thaliana* (Col) seedlings. White arrow represents transfer to light and the images show no emergence of leaf primordia at the shoot meristem until ~48 hours (h) later (though cotyledons do unfold). Above are the key intrinsic cellular responses upon dark (shaded on left) to light (white background after vertical solid line) during the time course indicated. **A** shows changes in protein levels. In the dark DET1, COP1 and CSN5 cause reduced E2FB levels (blocked arrow) but elevated E2FC levels (arrow). In the light (right side) phytochromes and cryptochromes repress responses that otherwise occur in the dark; E2FB levels are elevated (upwards arrow and large font) and E2FC levels reduce (downwards arrow and small font compared to E2FB) due to formation of a different mobility protein form (represented by two dots and diamond arrow). **B** shows changes in mRNA expression where the width of the grey bar represents expression levels. **C** shows changes in genes associated with hormone action. Large font size represent increases and small font sizes represent decreases. Modified from Lopez-Juez *et al.*, 2008.

The subsequent leaf pair, the first true leaves, form *de novo* (denoted New Leaf 1/2, NL 1/2) and in *Arabidopsis* contain trichomes (branch-like hair structures) on the adaxial epidermis. In the SAM, at the peripheral zone, leaf primordia cells are found. These domains remain under gene expression patterns that indirectly represent the dynamic balance of hormones, particularly auxin and cytokinin in leaf initiation (Traas and Moneger, 2010; Shani *et al.*, 2006). Interestingly, application of exogenous cytokinin to whole seedlings causes a photomorphogenic response (Chory *et al.*, 1994). As for the hormone auxin, auxin levels are high at the flanks and at the dome of the SAM (de Reuille *et al.*, 2006).

In the study involving a transcriptome analysis in the light, a careful examination of signature genes responsive to only one hormone, led to the following observation: a high auxin maximum in the SAM in the dark, and low cytokinin, coincides with the repression of the SAM and lack of emergence of leaf primordia in the dark. The perception of light, in contrast, causes auxin responsive genes to be downregulated, concurrent with an increase in cytokinin responsive genes which is subsequently followed by cell division, ribosome biogenesis and chloroplast biogenesis (Lopez-Juez *et al.*, 2008).

1.6 Cell cycle regulation and its role in development

The cell cycle occurs in a precise sequence of events that consists of the following phases: Gap-1 (G1 phase); doubling of DNA by Synthesis (S phase); Gap-2 (G2 phase) and a Mitotic phase separated into prophase, metaphase, anaphase and telophase (M phase). The cell cycle helps build plant architecture and its control is central to the decision of proliferation-dependent growth or expansion/differentiation-dependent growth (Fig. 1.5). This process is regulated by checkpoints (G1/S and G2/M) that act as control mechanisms to ensure correct cell division and is influenced by external cues (Reichheld *et al.*, 1999; Shen, 2001). Additionally checkpoints help in the decision of cells to become quiescent or terminate the cycle.

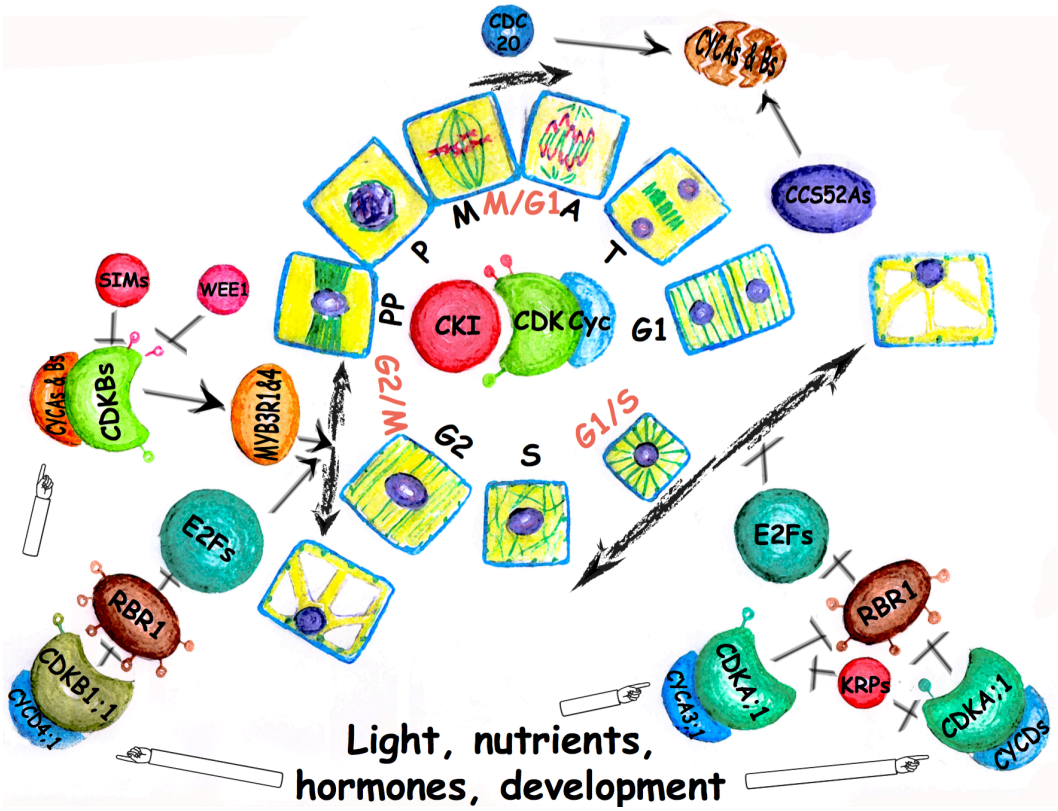

Figure 1-5 Cell cycle regulations by external cues

Regulatory components of the three main cell cycle transitions, G1/S, G2/M and M/G1. At the centre of the conserved cell cycle regulation is CYCLIN DEPENDENT KINASE (CDK) in complex with the phase-specific cyclins, and opposed by CDK inhibitors (CKI) and further regulated by positive (P-Thr161) and inhibitory (P-Thr14; P-Tyr15) phosphorylations (P). At the G1/S transition, D-type cyclins (CYDs) preferentially interact with CDKA;1, and these complexes overcome the opposing CDK inhibitors (KRPs, KIP RELATED PROTEINs). The main target of CYCD-CDKA;1 complex is RBR1, which is inactivated through CDKA;1 phosphorylation leading to the release of E2F transcription factors (primarily E2FB) to activate genes for G1/S transition. CYCA3;1 cyclin has also been shown to interact with CDKA;1, phosphorylate RBR1 and be involved in the G1/S transition. G2/M is preferentially regulated by B-type CDKs (CDKBs) in complex with A- and B-type cyclins (CYCA and CYCB). The plant-specific CDK inhibitor, SIAMESE (SIM), opposes these mitotic CDKs. The role of inhibitory phosphorylation on CDKB is not well understood. Interestingly, CYCD4;1 can associate with mitotic CDKB1;1 and has been shown to trigger mitosis, possibly through RBR1 phosphorylation. Exit from mitosis at the meta- to anaphase transition is triggered by the degradation of CYCA and CYCB through the activation of the ANAPHASE PROMOTING COMPLEX (APC) by CDC20 during the M/G1 transition and later in G1. CYCA and CYCB levels are kept low by the activation of the APC by CCS52 proteins. In plants, cells can exit from proliferation, enter into a G0 state and differentiate both at G1/S and G2/M transitions. Both these transitions are regulated by external signals such as light, nutrient availability, hormones and developmental cues. Arrows indicate activation, hammers repression, pointing fingers show regulatory inputs to the cell cycle. (Illustrated by *Binish Mohammed*, as published in (Magyar *et al.*, 2013)).

The core components of the cycle machinery are the CYCLIN-DEPENDENT KINASE-CYCLIN (CDK-CYC) complexes that regulate transition of cell cycle phases and phosphorylate the RETINOBLASTOMA-RELATED1 (RBR1) protein (Inzé and De Veylder, 2006; De Veylder *et al.*, 2007). This in turn allows transcription of genes that drive DNA synthesis via the E2-FACTOR-DIMERISATION PARTNER (E2F-DP) transcription factor (Desvoyes *et al.*, 2006; Magyar *et al.*, 2013). Here I describe the core components of the cell cycle machinery, how they regulate cell cycle transitions and how they themselves are regulated.

1.6.1 **Cyclin dependent kinases and cyclins**

As in all eukaryotic cells, the cell cycle commitment and then progression is regulated by catalytic units called CYCLIN DEPENDENT KINASEs (CDKs) in combination with activator CYCLINs (CYCs); a common and conserved cyclin binding signature in CDKs is PSTAIRE, but this is not found in all CDKs. This involves different types of CDKs and CYCs to progress through the different phases of the cell cycle. In *Schizosaccharomyces pombe* CDK activity is shown to be lowest at G1, transiently increase at S and peak at M, thus, CDK activity levels trigger phase progression of the cell cycle (Coudreuse and Nurse, 2010). Phase progression also involves timed proteolysis via ubiquitination of CYCLINS (see later) (Genschik *et al.*, 2014).

In budding yeast (*Saccharomyces cerevisiae*) and fission yeast (*Schizosaccharomyces pombe*) a single CDK, cdc28 and cdc2 respectively, with a PSTAIRE motif is sufficient to drive the entire proliferation cycle (Morgan, 1997). In plants the proliferation cycle is driven by D type (G1-S), A type (S-M) and B type (G2-M) CYCLINs (Inzé and De Veylder, 2006). However, specific CDK functions amongst classes have evolved; cdk1 in metazoans drives mitosis whereas cdk2 (in combination with cdk4 and cdk6 (that are distantly related to cdc2 and cdc28) drives S phase in human, mouse (*Mus musculus*), *Xenopus* and *Drosophila* (Satyanarayana and Kaldis, 2009b; Satyanarayana and Kaldis, 2009a; Malumbres *et al.*, 2009).

Plants possess a greater number of CYCs and CDKs (Inzé and De Veylder, 2006; Inagaki and Umeda, 2011). The *Arabidopsis* complement consists of 10 A and D

type CYCLINs (CYCAs and CYCDs) and 11 B type CYCLINs (CYCBs) as well as several A type CDKs (CDKAs) and plant specific B type CDKs (CDKBs), the interactive combination of which allows cell cycle phase progression (Wang *et al.*, 2004; Komaki and Sugimoto, 2012). The pivotal role of CYC-CDKs is not limited to proliferation but also differentiation due to their inactivation (Boudolf *et al.*, 2004a; Beemster *et al.*, 2005) this is because CYC-CDKs are regulated at the transcriptional and post-translational level.

1.6.2 **Regulators of cyclin-cyclin dependent kinases**

Despite their discovery 35 years ago the complexity of the CYC-CDK molecular network remains incompletely defined but what is known is of great significance: the cell cycle entry check point is at G1, deciding upon the G1 to S transition and is regulated by CYCLINs. CDKs positively regulate CYCDs that in turn regulate the RBR1-E2F pathway with changes in chromatin structure.

Proteolytic destruction of proteins, via marking them with an ubiquitin tag, allows these proteins to be degraded by the 26S proteosome. This allows unidirectionality of the cell cycle. Examples of such proteins are ANAPHASE PROMOTING COMPLEX/CYCLOSOME (APC) and SKIP1/CULLIN/F-BOX RELATED (SCF) complex (Vodermaier, 2004). CYCAs and CYCBs allow exit from mitosis due to their destruction by the APC (Marrocco *et al.*, 2010; Sullivan and Morgan, 2007).

As in yeast and animals, plant CYC-CDKs are also regulated by phosphorylation and dephosphorylation. Plants have a WEE1 kinase, that has a role in inhibiting entry into mitosis and negatively regulates the activity of CDKs. Expression of *Arabidopsis* or maize (*Zea Mays*) WEE1 in *Schizosaccharomyces pombe* causes cell cycle arrest (Inzé and De Veylder, 2006). Cdc25 is a phosphatase that activates the CYC/CDK in *Ostreococcus tauri* (a unicellular green alga) and *Schizosaccharomyces pombe* but has not been confirmed to have a cell division related role in *Arabidopsis* (Inzé and De Veylder, 2006). CYCs are also subject to phosphorylation as shown in sucrose starved conditions for CYCD3;1 (Planchais *et al.*, 2004).

Inhibitors of CDK bind and inhibit cell cycle progression and are called CDK-Inhibitors (CKIs) (Morgan, 1997), in plants better known as KIP-RELATED-PROTEINs (KRPs) and also known as INTERACTORs OF Cdc2 KINASE, ICK. *Arabidopsis* has seven KRPs all of which interact with CYCDs. In maize KRPs interact with D and A type cyclins. Moreover, *Saccharomyces cerevisiae*, *Schizosaccharomyces pombe* and mammals have 3, 1 and 7 CKIs respectively (Inzé and De Veylder, 2006). Additionally, the SIAMESE (SIM) family in plants (SIM and SIAMESE RELATED, SMR) were identified in mutant lines (*sim)* that are unable to initiate endoreduplication (Peres *et al.*, 2007).

In summary, CDKs are positively regulated by CYCs and negatively regulated by WEE1 kinase and KRPs in their commitment to the cell cycle. Modification of CYC/CDK alters cell division and consequently morphogenesis of an organ (Jasinski *et al.*, 2002; De Veylder *et al.*, 2001; Wang *et al.*, 2000) including the leaf (Wyrzykowska *et al.*, 2002). The role of CYC-CDKs is reviewed in greater depth by (Harashima *et al.*, 2013) and (Scofield *et al.*, 2014).

1.6.3 **G1/S and G2/M transition**

Plant CYCDs (1-4) are important in communicating external cues to cells, hence the commitment to enter the cell cycle. CYCD3 is important for development, regulation of cell cycle entry, as shown in *Arabidopsis* and the *Antirrhinum majus* (snapdragon) *CYCD1;1,* expressed in *Nicotiana tabacum (Koroleva et al., 2004)*. Overexpression of cell cycle regulators can help understand their function. Overexpression of CYCD3;1 in *Arabidopsis* causes numerous small cells and curling of the leaf (Meijer and Murray, 2001). Boniotti and Griffith (Boniotti and Griffith, 2002) argue that overexpression of E2F and DP gives a more extreme phenotype than CYCD3;1 overexpression (based on the work of Dirk Inzé) whereas inhibitors of CDK (KRP1 and KRP2), when overexpressed, cause fewer but larger cells (De Veylder *et al.*, 2001).

During late G2 CYCBs trigger entry into M phase. CYCBs have a mitosis specific activator (MSA) sequence in their promoter and in *Nicotiana tabacum* MYB transcription factors have been shown to bind to these sequences (Ito *et al.*, 2001). However, not all G2/M genes have a MSA element. Exit from M is regulated by a

destruction box (D-box) that is recognised by an ubiquitin proteolytic pathway involving the APC for cyclins that regulate M. D box-mediated degradation of cell cycle regulators is not restricted to plants and in humans can occur in post-mitotic neurons that are in fact differentiated cells (Gieffers *et al.*, 1999).

Endoreduplication can be seen as a result of activating APC earlier so M may be skipped. A study (Schnittger *et al.*, 2002) showed that CYCB1;1 and CYCB1;2 are not detectable during development of the trichome, a cell that endoreduplicates producing 3 branches. ORIGIN RECOGNITION COMPLEX (ORC) and CDC6 are part of the pre-replication machinery, and DNA synthesis occurs in endoreduplication too. In the case of CDC6 its overexpression has been shown to induce endoreduplication in *Arabidopsis* leaves, indicating its potential role in re-initiation of DNA synthesis (Castellano *et al.*, 2001).

1.6.4 **RBR1 as a core cell cycle regulator**

RETINOBLASTOMA (RB) belongs to a family of pocket proteins, including p107 and p130. *Arabidopsis* has only a single RB (RBR1) whereas the model organism *Drosophila melanogaster* has two, RBF1 and RBF2, and so does the maize plant. Additionally, RBR1 physically interacts with chromatin remodelling proteins affecting dynamics of the chromatin structure, (Kuwabara and Gruissem, 2014; Zhang *et al.*, 2000; Brehm *et al.*, 1998; Luo *et al.*, 1998; Magnaghi-Jaulin *et al.*, 1998).

The RBR1 protein interacts with CYCDs via their LxCxE motif whereby the CYC-CDK complex, following its interaction, phosphorylates RBR1. This is most critical for the initial checkpoint, cell cycle commitment and G1 to S transition. RBR1 when not phosphorylated acts as a stall to cell cycle progression but the protein abundance of the phosphorylated RBR1 protein (P-RBR1) is associated with cell cycle progression. At the G1 checkpoint P-RBR1 transiently increases, mirroring the progression of the cell cycle and diminishes towards the end of mitotic exit. The change in the RBR1 and P-RBR1 form regulates cell division. Moreover, there is accumulating evidence for the role of RBR1 in controlling symmetry of division as reviewed by (Desvoyes *et al.*, 2014).

1.6.5 **E2Fs and growth**

Arabidopsis has 3 E2-Factor (E2F) transcription factors, E2FA, E2FB and E2FC, which share domain organisation to the human E2Fs 1-3. Additionally, *Arabidopsis* has 3 DP-E2F-Like (DEL1-3) proteins that have 2 domains homologous to the DNA-binding domains of typical E2Fs but lack other highly conserved domains, notably the transcription activation domain. Therefore, the DEL proteins are unable to function as classical E2Fs and in fact compete for E2F target sites (Shen and Xu, 2009; Kosugi and Ohashi, 2002). Moreover, in the nucleus E2Fs bind to DIMERISATION PARTNER (DP) proteins, DPa and DPb in *Arabidopsis* with a preference to E2FA-B and E2FC, respectively (Magyar *et al.*, 2000). The E2F-DP dimers can bind to E2F *cis*-elements and activate gene transcription whereas the DELs bind to E2F sites but lack DPs and are unable to activate gene expression (Mariconti *et al.*, 2002). RBR1 binds to E2F transcription factors via its pocket domain and consequently represses E2F action; repression can be removed via phosphorylation of RBR1 by CYC-CDK, a conserved RB-E2F function (Van Den Heuvel and Dyson, 2008) (Fig 1.6).

Overexpression experiments of *Arabidopsis* E2FA-C have led to the notion that E2FA and E2FB are transcriptional activators and E2FC is a repressor of transcription (Magyar, 2008) with regards to the G1 to S transition. Genes transcribed by the E2F-DP heterodimer include those involved in chromatin reconfiguration and DNA replication and repair (Vandepoele *et al.*, 2005; Ramirez‐Parra *et al.*, 2003).

1.6.6 **Canonical *versus* non-canonical regulation of cell cycle**

In contrast to the canonical RB-E2F module, where E2Fs were assumed to transcribe genes for cell division, E2FA positively drives endoreduplication (Magyar *et al.*, 2012). Endoreduplication can be described as an “incomplete” cell cycle, with its mitotic stage repressed. Genes transcribed by E2FA include those needed for endoreduplication; in constitutively-expressed E2FA lines (with the RBR1 binding domain absent, so RBR1 may not suppress E2FA activity) cells entered premature expansion and increased their ploidy levels considerably compared

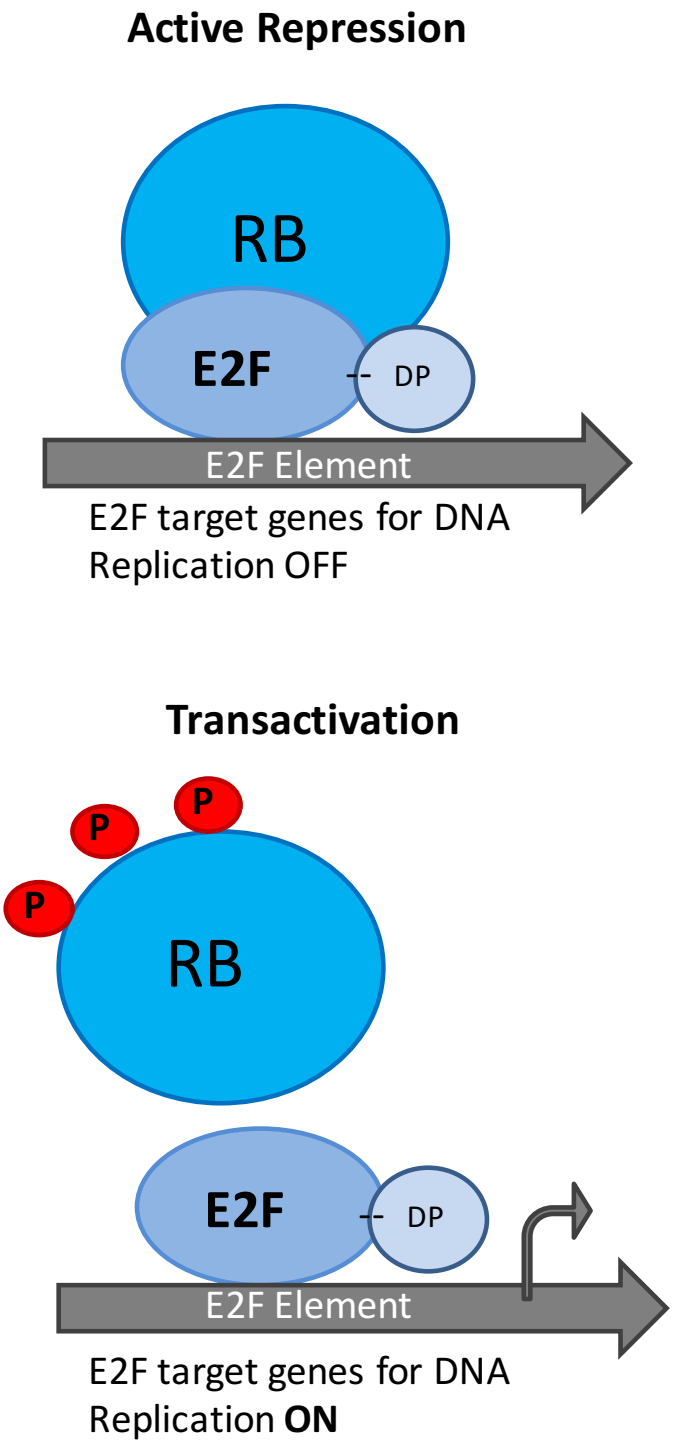

Figure 1-6 The canonical RB/E2F/DP pathway

Top shows E2F and its DIMERISATION PARTNER (DP) binding at *cis*-element of E2F target gene. Binding of RETINOBLASTOMA (RB) to E2F via its pocket domain represses E2F transactivation function. Consequently, the E2F target gene is not transcribed and cell division does not occur. Bottom shows that phosphorylation of RB (Red) frees E2F, allowing transactivation and transcription of E2F target genes. This allows cell division to proceed.

to the wild type (Magyar *et al.*, 2012). In support of this, E2FA has been shown to activate S phase genes in response to activation of the TARGET OF RAPAMYCIN (TOR) pathway. However, contrary to the canonical RB-E2F module, E2FA is also a direct phosphorylation target of TOR in the presence of glucose in the root meristem, (Xiong *et al.*, 2013).

1.6.7 **Light and cell cycle proteins: An evolutionary perspective**

Light affects the cell cycle and consequently growth, in the process of photomorphogenesis and beyond. I have mentioned how blue light has a significant role in the expansion of cells as well as the anticlinal elongation of adaxial mesophyll cells of leaves in high light (Lopez-Juez *et al.*, 2007). Light and dark conditions and their regulation of the cell cycle have been studied in phytoplankton (Vaulot *et al.*, 1986), and the effect of light on cell cycle progression has been shown in diatoms (Huysman *et al.*, 2013); the diatom specific cyclin2 (*dsCYC2)* transcripts peak 15 minutes after light exposure and behave in a blue light fluence rate dependent manner for the G1-S checkpoint. Beyond photosynthesising organisms, light and circadian rhythms regulate cell cycle genes in vertebrates such as the zebrafish (Dekens *et al.*, 2003). Surprisingly food and light entrain the circadian clock and cell cycle genes in the intestine of zebrafish (Peyric *et al.*, 2013). Artificial light has been used to disrupt circadian cycles of cell division: it alters transcription levels of genes associated with formation of cancerous tissues in mouse, highlighting the importance of the association of light and the cell cycle (Ben-Shlomo and Kyriacou 2009).

In the green lineage an association has been established between light exposure and an array of transcript changes in cell cycle-related genes (Nishihama and Kohchi, 2013). Chlorophyte green algae have no known red light photoreceptor but in *Chlamydomonas reinhardtii* a phototropin and a plant and animal-like cryptochrome have been reported; contrary to this charophyte green algae (an evolved lineage with multicellular body plans) do have a plant type phytochrome, the origin of which remains unconfirmed (Nishihama and Kohchi, 2013). As chlorophytes have no sink tissues in principle, and therefore no source/sink relationships, they produce energy and increase in size during the light period prior to dividing in the night. However, this process is not mediated by photosynthesis but by photoperception, particularly of

blue light. It has been speculated that photosynthesis or photosynthate are needed for cell cycle entry as transfer from CL (continuous light) to dark causes a G1 arrest and is reproduced by DCMU (3-(3,4-dichlorophenyl)-1,1-dimethylurea) treatment in light (Spudich and Sager, 1980). Also, the role of the circadian clock in gating the cell cycle has been reported in *Ostreococcus tauri* (Moulager *et al.*, 2007) and *Chlamydomonas reinhardtii* (Goto and Johnson, 1995).

Evolution of land plants brings greater complexity with multicellular organs and the fact that the control of light regulated growth must take into account photosynthetic and non photosynthetic organs (for instance, roots). This introduces source/sink tissues and the importance of sugars and their translocation. Basal land plants include bryophytes (those that lack a true vasculature) and pteridophytes (plants with vasculature that reproduce by spores), including mosses and ferns respectively. Light studies in ferns have shown that light affects different phases of the cell cycle as well as planes of cell division (Ito, 1969; Furuya, 1984). Studies in bryophytes have led to the speculation that there is a link between sugar and CYCD genes (Nishihama and Kohchi, 2013). Seed plants evolved to have secondary cell walls and adapted to growth at different fluence rates; for example, hypocotyls elongate in low light and also during shade avoidance responses induced by reduced phytochrome activity (Martínez-García *et al.*, 2014).

Recent advances have focused on the link between photo-perception and the proliferation-dependent growth driving machinery, cell cycle related genes. Bioinformatic analysis of *cis*-regulatory elements in core cell cycle genes in *Arabidopsis* shows that 35.71% of core cell cycle genes to have light responsive elements in their promoters (Nejad *et al.*, 2013). Specifically for the E2Fs, in *Arabidopsis* seedlings it has previously been established that the cell proliferation driver, E2FB, accumulates in whole seedlings in the light, in contrast to E2FC that is destabilised in the light, and both actions require COP1 and DET1 (Lopez-Juez *et al.*, 2008). This study also illustrates that E2FA regulated genes are also positively regulated by light during a dark to light transition in the shoot apex.

Based on the study in our lab it was also found that in the dark-to-light transition class I *TEOSINTE BRANCHED1/CYCLOIDEA/PROLIFERATING CELL FACTOR* (*TCP*) genes were downregulated but class II *TCP* genes were upregulated. The class

II TCP transcription factors also target some cell cycle genes (Martín-Trillo and Cubas, 2010) and this work highlights the possibility of the *TCP* genes being involved in regulating cell cycle genes needed for leaf initiation (Lopez-Juez *et al.*, 2008).

Light and cell cycle have also been linked via other studies, perhaps more indirectly. A component of a complex involved in endoreduplication (MIDGET, MID, part of DNA topoisomerase VI complex) binds to COP1 too but little is known about how these two components regulate endoreduplication (Schrader *et al.*, 2013).

1.7 Energy signalling pathways and growth control

Sugars contribute to the growth of plants. This process is so important that plants have adopted the ability to store some of their carbon for times when light is absent. Sugars act as metabolic intermediates as well as signals themselves of carbohydrate availability but exactly how energy status and growth is coordinated in a cell is not understood.

1.7.1 **Sugars and enzymes as growth modulators: Hexokinase and trehalose-6-phosphate**

Sucrose is systemically transported in a plant. Transfer of sucrose from source to sink regions allows growth of newly forming organs, such as leaf primordia, as well as growth of organs that do not have the ability to photosynthesise, for example roots.

HEXOKINASE (HXK) is the first enzyme involved in glycolysis (where glucose is converted to glucose-6-phosphate). The *Arabidopsis HXK1* gene product is a glucose sensor (Moore *et al.*, 2003). HXK stimulates growth and this involves hormone signalling, particularly auxin and cytokinin based on mutant seedling analysis (Ramon *et al.*, 2008).

Trehalose-6-phosphate (T6P) is precursor of the disaccharide trehalose biosynthesis pathway: UDP-glucose and glucose-6-phosphate form T6P, this involving the TREHALOSE PHOSPHATE SYNTHASE, TPS. T6P is dephosphorylated by

TREHALOSE PHOSPHATE PHOSPHATASE (TPP) to form trehalose and trehalose is eventually hydrolysed to give two glucose molecules (Elbein *et al.*, 2003; Cabib and Leloir, 1958). *Arabidopsis* has class I (*TPS1-4*) and class II (*TPS5-11*) *TPS* genes but class II function remains elusive as they have a synthase and phosphatase domain, yet they show no such biochemical activity in vitro (Ramon *et al.*, 2009). These authors indeed hypothesise a role for these class II *TPS* genes in T6P-sensing. *Arabidopsis* has 10 TPP genes.

T6P is very low in abundance in plants yet its role as regulator of growth and development is often speculated upon (Lunn *et al.*, 2014; O'Hara *et al.*, 2013a; Schluepmann *et al.*, 2012; Ponnu *et al.*, 2011). Extra T6P causes growth inhibition but it is not fully understood how this occurs, although extra T6P supply is shown to cause extra starch accumulation (a change in carbon flux) that perhaps contributes to the growth inhibition; addition of sucrose also overcomes this inhibition suggesting that carbon availability is needed alongside T6P to promote growth (O'Hara *et al.*, 2013b). In other words, T6P may act as a signal of sucrose abundance, so excessive T6P may wrongly divert carbohydrate towards storage and so cause a deficiency in sucrose availability for growth. In support of this, absence of T6P also affects growth as shown by *tps1* mutant, where growth is retarded at the embryo stage (Eastmond *et al.*, 2002). TPS1 is also shown to interact with CDKA;1, showing evidence for regulation in cell cycle progression (Geelen *et al.*, 2007). O'Hara *et al.,* (2013), highlight the possible role of T6P in pathogen infection of plants from the region where the pathogen initially infect (roots), causing trehalose accumulation as well as in other tissues/organs where pathogens normally do not, such as stems and leaves.

1.7.2 **Sucrose non fermenting related kinase1: SnRK1 as an energy sensor**

Plant SUCROSE NON FERMENTING1 RELATED KINASE1 (SnRK1) is an energy sensing kinase (Baena-González *et al.*, 2007) composed of three subunits, the catalytic α subunit encoded by genes *AKIN10* and *AKIN11*, β (encoded by three genes) and γ (encoded by a single gene) (Ramon *et al.*, 2013). The work of Ramon and colleagues used chromatin immunoprecipitation, yeast mutant complementation and phylogenetic analysis to show that plants have a unique βγ (KINβγ) subunit. The

hybrid subunit (KINβγ) acts as a canonical γ subunit that forms a heterotrimeric complex with the α and β subunits (Ramon *et al.,* 2013).

Plant SnRK1 shares homology to yeast Sucrose Non-Fermenting1 (SNF1) and mammalian AMP ACTIVATED PROTEIN KINASE (AMPK). These heterotrimeric kinases are activated when energy levels are low, a phenomenon now shown to be shared by plants (Baena-González *et al.*, 2007; Baena-González and Sheen, 2008). Yeast and mammal proteins (SNF1 and AMPK) have a role in chromatin remodelling but this is not yet known in plants (O'Hara *et al.*, 2013a).

Plant SnRK1 has been shown to phosphorylate and inactivate enzymes involved in metabolism. In studies of plants other than *Arabidopsis*, SnRK1 has been involved in starch synthesis and breakdown but the complexity of this regulatory mechanism in source/sink tissues is yet to be discovered. Moreover, in whole seedlings SnRK1 is inhibited by T6P, suggestive of its role in starvation responses, but this could not be repeated for mature leaves (Zhang *et al.*, 2009) suggesting an unknown protein factor is involved in the T6P-SnRK1 interaction that is found in young tissue (O'Hara *et al.*, 2013). This interaction means that when sucrose is abundant, a high T6P response blocks SnRK1 activity but when sucrose is low or scarce, T6P levels also remain low and SnRK1 becomes active.

1.7.3 **TOR kinase in regulating ribosome biogenesis, metabolism, autophagy and cell cycle**

The TARGET OF RAPAMYCIN (TOR) kinase is a master regulator that is evolutionarily conserved among yeasts, plants, animals, and humans. Two TOR kinases were first identified in budding yeast (*Saccharomyces cerevisiae*) but only one TOR kinase has been identified in the photosynthetic organism lineage (based on *Arabidopsis* and *Chlamydomonas reinhardtii*) as well as mammals. The yeast and mammalian TOR form two unique complexes: mechanistic (or mammalian) TOR Complex1 and 2 (mTORC1and mTORC2). The core components of mTORC1 are mTOR, mammalian Lethal with sec-13 protein8 (mLTS8) and REGULATORY ASSOCIATE PROTEIN OF TOR (RAPTOR) and the complex integrates nutrient and energy signalling to promote cell proliferation and growth. The best characterized substrates of mTOR are the S6 Kinase (S6K, represses cell proliferation in limiting conditions) and eukaryotic translation initiation factor 4E

BINDING PROTEIN1 (4E-BP1). The S6K is conserved in plants, while no homologue of 4E-BP1 is known.

Arabidopsis TOR has been linked to nutrient availability and the glucose-TOR pathway has been reported to play an important role in the growth of new leaves, cotyledons, petioles and root (Xiong and Sheen, 2012). AtTOR complex comprises of AtLTS8 and AtRAPTOR, so TORC1 is conserved in plants while no TORC2 has been found. Earlier it was mentioned that TOR plays a role in regulating cytoplasmic growth and a key target of TOR is ribosome biogenesis (Sablowski and Carnier Dornelas, 2014). TOR directly binds to the 45S rRNA and regulates its transcription (Ren *et al.*, 2011) and has been shown to regulate ribosomal proteins in *Arabidopsis*, yeast and mouse (Xiong *et al.*, 2013; Huber *et al.*, 2009; Martin *et al.*, 2004). Moreover, *Arabidopsis* EBP1 (ortholog of human EBP1) expression correlates with the expression of TOR (Horvath *et al.*, 2006). In addition TOR initiates translation of plant mRNAs at their small upstream Open Reading Frames (ORFs) and this pathway is integrated with phosphorylation of S6K1 and with auxin action, with the translation of auxin induced genes (Xiong *et al.*, 2013; Xiong and Sheen, 2012; Schepetilnikov *et al.*, 2013).

The TOR kinase also regulates metabolism and is thought to do this by affecting carbon fluxes (TCA cycle and its intermediates) but this is not fully understood (Xiong and Sheen, 2012). However, this aspect of TOR regulation is perhaps dependent on developmental stage and physiological context. TOR most likely redirects carbon storage to starch and lipids in order to adjust plant growth, developmental transitions or stress tolerance in different organs, as suggested by a recent review (Xiong and Sheen, 2014).

In *Arabidopsis* TOR downregulation leads to activation of autophagy (Liu and Bassham, 2010), a universal regulatory role of AMPK (Baena-González and Sheen, 2008). Overexpression of At*KIN10* activates some genes that are involved in autophagy (Baena-González *et al.*, 2007). Interestingly, however, downregulation of TOR activity reduces growth but promotes extension of the lifespan of plants (Ren *et al.*, 2012).

Amongst many findings of a functional over-representation analysis (based on plants with reduced TOR activity), key is that TOR signalling activates genes involved in

cell wall modification, cell cycle, carbon and nitrogen utilization, photosynthesis, and nutrient transport: these are termed anabolic pathways and TOR negatively regulates catabolic processes such as autophagy, senescence, and protein and lipid metabolism. TOR inhibition causes changes in the expression of genes involved in chromatin structure, hormone metabolism, signalling, and stress-related processes (Xiong and Sheen, 2014). Recent findings have directly linked TOR to the cell cycle. Glucose from source tissue (leaf) is the main nutrient that regulates (at a systemic level) gene expression and root growth where TOR phosphorylates E2FA to induce S phase genes in the root meristem. This finding, mentioned earlier, shows an unexpected control of an E2F transcription factor that is not mediated by CDKs. Moreover, in this study the absence or presence of the RBR1 binding domain in E2FA does not affect TOR phosphorylation of E2FA (Xiong *et al.*, 2013). Such a finding highlights the close connections between light, energy availability and cell growth and cell cycle, and shows us how much remains to be uncovered.

1.8 Aims

The aims and objectives of this work are described below (1.8.1-1.8.4) and all apply to work on the plant *Arabidopsis thaliana*. Details of all aims are further provided in the relevant chapters.

1.8.1 **E2FB in the promotion and exit from proliferation to differentiation**

In chapter 3 I aim to better understand the role of E2FB in promoting proliferation and how E2FB maintains the exit from proliferation to transit into differentiation in young cells. With the use of modified E2FB levels in different lines I aim to observe the developmental implications of the actions of E2FB on leaves.

1.8.2 **Establishing a link between light, sugar and the cell cycle**

In the first part of chapter 4 I aim to show that exogenous sucrose availability positively regulates cell cycle transcripts and attempt to reproduce this response using a previously published 4hour extended-dark assay that utilises an endogenous

acute carbon starvation response. I aim to provide a clear association between light, carbon availability and the cell cycle with detection of phosphorylated-RBR1 (P-RBR1) in a starchless mutant under 12 h light: 12 h dark cycles.

1.8.3 **Establishing an accessible system to reassess the role of light *vs* dark in the control of cell proliferation and growth in young leaves**

In the latter part of chapter 4, I aim to use a three day dark-to-light transfer (upon first new leaf pair emergence) assay, to assess how light and dark control cell proliferation and growth in developing leaves at the shoot apex. I intend to do this with the use of a mitotic reporter and DNA content analysis (flow cytometry). Upon establishment of the dark-to-light transfer response I aim to understand the light perception response in this phenomenon and its effects on other potential key regulatory processes, highlighted by our lab in a previous study, and compare this to the earlier (published) responses observed in the shoot apex in which new leaves had not yet appeared in the dark.

1.8.4 **How light quantity effects cellular development of leaves**

To evaluate the physiological relevance of light/energy control of growth, I study the effect of an increase in the fluence rate of light on the cellular development of rosettes using the mitotic reporter. In chapter 5, with the use of a low light-to-high light procedure, I aim to initiate the exploration of the sensory and regulatory mechanisms involved, with particular attention to the potential role of energy signalling and the RBR1/E2F pathway.

Chapter 2: Materials and methods

All methods described are as accurate as possible and further experimental specificities are mentioned as and when required in results. For details of techniques and/or solutions refer to appendices where indicated. A list of the equipment mentioned can also be found in the appendix (Appendix 2.1).

Sterile water refers to autoclaved distilled water.

2.1 Plant growth conditions

2.1.1 **Seed collection and storage**

See below for conditions of plant growth in soil. Mature plants were loosely wrapped in drying bags and were not watered here on after. Plants were left in long day (16 h L: 8 h D) conditions until dried.

Seeds were released mechanically from siliques, whilst in the bags, by rubbing and scratching between hands. The bag was snipped at a corner to release seeds on to a sieve (500 µm pore size) that was placed on top of a clean A4 plain white paper. Sieving was performed 2 - 3 times and the seeds transferred into a pre-labelled 1.5 ml microfuge tube.

Seeds were stored at room temperature. Long term storage of seeds was at +4 °C.

2.1.2 **Seed sterilisation**

Seed sterilisation was carried out under a laminar flow hood. The approximate number of required seeds was placed into a fresh 1.5 ml microfuge tube; if more than ¼ of the microfuge tube was filled with seeds a subsequent microfuge tube was used. The seeds were soaked in sterile water for ~5 mins prior to sterilisation. Removal of water/solution from the microfuge tube was carried out using a heat sterilised needle attached to a vacuum pump.

Sterile water was removed and ~1 ml absolute ethanol added for no more than 1 min, followed by ~1 ml of a 50:50 household-bleach:H_2O solution (sterile water used), for 10mins. Between waiting periods seeds were placed on a rotator.

After removal of bleach:H_2O several sterile water washes were carried out to remove residual bleach. Seeds were finally left in sterile water and stored in a +4 °C fridge in the dark.

2.1.3 **Plant medium**

Unless otherwise stated, chemicals were sourced from Sigma Aldrich or from VWR indistinctly. Plant medium of 1 L consisted of 8 g phyto-agar (Duchefa), 10 ml MES (see appendix 2.2 for MES protocol) and 2.2 g Murashige and Skoog medium (Duchefa) either with or without 1% sucrose. The pH of the final solution was set to pH 5.8 using KOH. The mixture was autoclaved at 110 °C for 15 mins, cooled and poured into square or circular cell culture petri dishes. Plates were stored in +4 °C fridge for short term storage only.

2.1.4 **Plating and stratification**

Seedlings were plated using a p1000 Gilson pipette and excess water dried under the laminar flow hood prior to sealing with a micro-porous tape. If different lines were used, platting multiple lines on a single plate was favoured and square petri dishes preferred.

Plates (or sterilised seeds) were stratified for at least 18 h in a +4 °C fridge and wrapped in foil. Plates were not stratified for a period of more than 3 days.

2.1.5 **Light cabinets and growth conditions**

For any particular experiment light cabinets remained unchanged. Typically, cabinets comprised of fluorescent white light (colour 840) lamps with ~115 µmol m^{-2} s^{-1} (+/-10 %) and a constant temperature of 21 °C. A detail of the cabinets and light flux with regards to figures/chapters is tabled below: Table 1.

Table 2-1 Light cabinets and lighting conditions used.

Details of the different brand cabinets, (light chamber details), light quantity (µmol m^{-2} s^{-1}) and light/dark cycle hours are listed in reference to the results chapters they apply to. h=hours. L=light. D=dark. CL=continuous light. CD=continuous dark.

Light chamber details	Light intensity (µmol m^{-2} s^{-1})	Light Dark cycle	Relevance to
Percival I-36 (I)	~110 (+/-15 %)	Long day (16 h L: 8 h D)	Chapter 3
Shelf and lighting (II) in constant temperature room	~110 (+/-10 %)	(12 h L: 12 h D)	4h ext dark
Percival I-35(III)	Bottom shelf: 60 Middle: 120 Top: 400	CL	Chapter 4 Chapter 5
Percival I-30 (IV)	~90 (+/-10 %)	CL	Chapter 5
LMS cooled incubator (V)	Dark	Dark/CD	Chapter 4

2.2 Transgenic Lines of *Arabidopsis thaliana*

2.2.1 **TDNA insertion lines, *e2fb-ko***

Two E2FB TDNA insertion lines were obtained from the Arabidopsis Biological Resource Centre (ABRC), Ohio State University. The lines were denoted as follows: SALK_120959 as *e2fb-ko 959* and SALK_103138(C) as *e2fb-ko 138*. Homozygous seeds were generated by Dr Zoltan Magyar, seeds were backcrossed, heterozygous seeds further propagated and genotyped via a selective marker. For line *e2fb-ko 959* and *e2fb-ko 138* a C-terminal E2FB antibody could not detect any protein being present, hence, these are a loss of function mutant (confirmed by Dr Zoltan Magyar, personal communication). The knockout lines have previously been published in (Berckmans *et al.*, 2011).

2.2.2 **E2FB-GFP, translational fusion**

The line E2FB-GFP was generated by Dr Zoltan Magyar via three-way Gateway ® cloning; pE2FB:gE2FB::gGFP. The T1 lines were selected and genotyped, single insertions were further propagated to homozygous lines. A GFP antibody was used for the presence of the protein and independent lines, 72, 114 and 61 were found to be strongest, medium and very weak lines, respectively.

2.2.3 **35S::HA-E2FB/DPa**

The 35S::HA-(N terminal-tag)-E2FB was generated by Dr Zoltan Magyar. The T0 was selected via Kanamycin (Gateway vector: pK7WG2, Ghent University). Western blot against the HA antibody was performed on T1 and the three strongest overexpressors propagated and the homozygous lines identified. Line 35S:DPa, homozygous, was kindly provided by Professor Lieven De Veylder, Gent University, (De Veylder *et al.*, 2002). The 35S:DPa was transformed with 35S::HA-E2FB and strong lines (via Western blot) propagated and the homozygous lines identified, i.e line 35S::HA-E2FB/DPa 10/15, see Chapter 3.

2.2.4 **35S::HA-E2FB$^{\Delta RBR1}$/DPa**

E2FB$^{\Delta RBR1}$ is a description for the truncated E2FB (1-385) with an absent RBR1 binding domain, at the C-terminal end, and the transactivation domain is also partially absent (see appendix 2.3). Similarly to the above, this line was generated by Dr Zoltan Magyar and analysed via Western blot on the 35S::HA-E2FB$^{\Delta RBR1}$, using the HA antibody. The pK7WG2 (Ghent University) gateway vector was used. The antibiotic resistance used was Kanamycin. Homozygous lines were generated. The 35S:DPa line (De Veylder *et al.*, 2002) was transformed with 35S::HA-E2FB$^{\Delta RBR1}$ and the T1 analysed via HA antibody for presence of the transgene. 5-10 % of seedlings produced 3 cotyledons (Z. Magyar, personal communication). Lines 1/10 and 10/x/8 were used and propagated if needed.

2.2.5 **RBR1-GFP, translational fusion**

The pRBR1:gRBR1::gGFP, homozygous line, was kindly provided by Dr Beatrice Horvath, Ben Scheres Lab. RBR1 protein levels were 10-15x higher as confirmed using RBR1 antibody than the endogenous level in the RBR1-GFP line (Z. Magyar, personal communication). Previously published (Magyar *et al.*, 2012).

2.2.6 ***pgm*, starchless mutant**

The *phosphoglucomutase* (*pgm*) starchless mutant (Caspar *et al.*, 1985) was a kind gift of the laboratory of M. Stitt (MPI Golm).

2.2.7 **CYCB1;1::GUS, (pCDG)**

The CYCB1;1::GUS line was provided by Dr Peter Doerner, Edinburgh University, (Colón‐Carmona *et al.*, 1999). The Promoter and first 3 exons of *CYCB1;1* were translationally fused to the *E.coli uid*A (GUS) gene.

2.3 Images of seedlings

Images were taken on the Nikon SMZ stereo microscope with the addition of an external lighting source. Images were captured on a DXM1200 camera using the NIS elements software, NIS Freeware 2.10.

2.4 Flow cytometry

Flow cytometry analysis was used to determine DNA content of cells. Flow solutions were always stored in +4 °C conditions.

2.4.1 **Harvesting samples**

New leaves or cotyledons were harvested from seedlings using micro-fine tweezers. The petiole tissue was removed.

For plants younger than 10 days old 2 - 4 cotyledons and 4 - 6 new leaves were harvested. Extremely small leaves were harvested by flattening the seedling on the agar, holding out the cotyledons with one tweezer and pinching at the base of both new leaf pairs with the second tweezer. Upon harvesting leaves were immediately placed into a circular petri dish (9 cm diameter) containing nuclei extraction buffer.

2.4.2 **Preparation of samples**

The Partec 2 step kit (CyStain® UV Precise P kit) comprises of two ready-made solutions (the details of which are kept confidential by the manufacturer): 1) Nucleus extraction buffer 2) DAPI staining solution. Flow solutions were decanted into smaller volumes and placed on ice. Contamination between the two solutions was avoided and contamination of sample prep and solution was particularly carefully avoided.

For cotyledon samples, ~6 drops of nucleus extraction buffer were placed onto the inner side of the petri dish using a plastic Pasteur pipette. For new leaves younger

than 10 days ~3 drops of nucleus extraction buffer was used. Samples were not left on the nucleus extraction buffer for longer than 5 min.
The samples were prepared using only double edged razor blades (Boots, Wilkinson sword or Tesco brands). Leaves were centred on the petri dish with the nuclei extraction buffer, any excess buffer was run down the sides of the petri dish. Leaves were chopped using a gentle but firm tapping motion, avoiding sawing and tearing of tissue, and rotation of the angles of chopping was necessary. The mid region of the blade was used to chop larger samples and the ends of the blades were used to chop very small samples. Samples were chopped until they appeared as a smear, or in the case of larger samples as tiny dots.

Chopped samples were left for no longer than 5 min prior to adding ~1.0 - 1.5 ml of DAPI solution with a plastic Pasteur pipette. A few drops of the DAPI solution were run down the used edge of the blade increasing the volume of the sample. Blade edges were wiped using a tissue, re-used up to four times and the edge changed for genetically different lines.

The sample was pre-mixed on the petri dish, by pipetting, and collected into a plastic cuvette with a fine filter placed on top. Samples remained incubated on ice prior to running and were left wrapped in foil in the +4 °C fridge to be run the following day if needed (samples were left for a maximum of 2 days in +4 °C).

2.4.3 **Running of samples**

Samples were placed in a plastic seed box on ice to keep cuvettes dry. Upon turning on the flow cytometre a clean was carried out as follows: decontamination solution x1; cleaning solution x2; sterile water x1; cleaning solution x1; final water left running. Water washes were always carried out between samples.

The lower threshold for fluorescence intensity was ~30, higher threshold at ~999 and the gain set at ~485 (as of December 2013). The first peak (2N) was set at a fluorescent intensity of 50 and the second peak (4N) at 100 using a flower sample as a control (endoreduplication does not occur in those samples). With these parameters up to five peaks (2N, 4N, 8N, 16N, 32N) could be detected in any case. Samples were run at ~50 cells/second.

The gain was readjusted if necessary to meet the 50 and 100 intensity mark. This was always reconfirmed by a control sample.

2.4.4 **Data Analysis**

Data was presented as peaks using the Flomax program. Data analysis was also achieved with the use of the Flomax software, values obtained were based on the area calculations of each peak via the software indicating the cell distribution as a percentage of DNA content.

Primarily, analysis was carried out via the automated 'peak analysis' tool: Analysis → Peak Analysis → Fit Gaussian peaks. Where peak analysis could not be achieved by the software, 'gating' was carried out to manually identify peak regions: Analysis → Gating → new →left border → right border. A minimum of three replicates were used and the data averaged and plotted as a '100% stacked column'.

Where only 2N and 4N peaks were present, 'cell cycle analysis' was additionally carried out, if desired. This indicated percentage of cells in G1, S and G2/M phases, where G1 is equivalent to the 2N cell population and G2/M is equivalent to the 4N cell population and S phase as the valley of cells in between G1 and G2/M. (As mentioned in 2.4.3 the boundaries for peaks were set up using the flower sample but the area under the peaks was determined by the Partec software).

2.5 Epidermal cell analysis

A frequency distribution graph on epidermal cell size of cotyledons, 10 dag (days after germination), was achieved based on three replicates. Additionally, the stomatal index was also calculated.

2.5.1 **Preparation of samples**

Whole seedlings were soaked in absolute methanol for 12 - 36 hours, or longer until seedlings became clear in colour. Methanol was replaced by lactic acid permanently.

Leaves were pinched at the petiole and placed on a microscopic slide, adaxial side up, with lactic acid. A cover slip was gently placed on top.

2.5.2 **Microscope and functions**

Images of the adaxial epidermis were taken using a Nikon Optiphot-2 microscope using Nomarski optics, a DXM1200 camera and NIS-elements AR program. Using the x20 magnification half the leaf epidermis was imaged using the 'Grab Large Image' tool.

The first image captured would start at the tip of the leaf and the subsequent image would be right to the previous captured image, with aid of a twenty five percent transparency function, the image was grabbed ('Grab') if transparency was manually met. The focus was also adjusted if needed. This process was repeated until the outer most edge of the leaf was anticipated, the following image was below ('Meander') and moved in the left direction ('Grab'), as described above, until the first image was directly above and again the following image was below the image captured; Right/*Grab*→ Down/*Meander*→ Left/*Grab*→ Down/*Meander*→ Right/*Grab*→ Down/*Meander* etc. The process was completed towards the petiole of the leaf and upon completion all images were collaged into a single image of half the leaf epidermis ('Finish').

2.5.3 **Measurement protocol**

Epidermal cell walls were manually drawn using the 'Paint' program, on images from section 2.5.1. If cell walls were not clear in a particular region then the region was avoided in such a way that the absence of cell walls would be apparent, this would avoid that area being considered a large cell and being measured incorrectly.

Cell size measurements of epidermal cells were carried out using the free downloadable software 'ImageJ'-'http://imagej.nih.gov/ij/'. Using an image of a graticule the scale was set using the straight line drawing tool to draw a line of known distance: on the 'Set scale' function the known distance and units of measure were inserted. The pixel value was noted for future use and the 'Global' tab selected if subsequent images were to be measured.

The paint edited epidermal images were opened in ImageJ, changed to an 8 bit grey scale image and converted to a binary image. (using tools → make binary). Types of measurements were set using the 'set measurement' functions; area, limited to threshold and values up to 3 decimal places (dp) were selected. Measurement of individual cells, excluding guard cells, was made by selecting the cell using the wand selection tool and measuring (Ctrl + M) the area. The cell was dotted using the draw tool to indicate that a measurement had been taken. This was done for all cells; the measurements appeared in a new window and were copied and pasted into Excel.

The cell areas were sorted in ascending order and the number of cells falling into a particular frequency distribution range noted/tabled. Data was based on triplicates.

The frequency distribution ranges were not selected at random: Two different wild types were used and cells were grouped into what appeared to be cells of similar size (a colour based technique) and what the actual cell areas for cells in each colour group were (a mathematical approach). Overlaps and clear boundaries were noted and the frequency distribution range values selected on this basis.

2.5.4 **Stomatal index measurement**

Stomatal index measurements were based on cotyledons in sections 2.5.1 - 2.5.2.

The formula used was:

$$SI = \frac{S}{S + E} \text{X } 100$$

SI = Stomatal Index

S = number of Stoma

E = number of Epidermal pavement cells

Stomata were manually counted and the number of epidermal pavement cells (epidermal cells other than guard cells) noted from section 2.5.3. These data were based on triplicates.

2.5.5 **Stomatal clustering analysis**

Based on the analysis by (Guseman *et al.*, 2010) and (Abrash *et al.*, 2011) stomata clustering was classed by the number of stoma adjacent to another (with no other cell type spacing the two stoma) and this was plotted on the *x* axis as 2-mer, 3-mer, 4-mer, 5-mer, 6-mer and 6+mer. How frequently this occurred was plotted on the *y* axis as the percentage of stomata in each cluster size class. The equation used was:

$$\%\ Stomata\ in\ each\ class\ size = \frac{Number\ of\ stoma\ in\ class\ size}{Total\ number\ of\ stoma}\ X\ 100$$

2.6 CYCLINB1;1::GUS Assay

The CYCB1;1::GUS assay was used as a mitotic reporter. The product of the enzymatic reaction is a blue precipitate that indicates that a particular cell is undergoing mitosis. Below is a schematic outline of the protocol (Fig 2.1) that is further described in detail.

2.6.1 **Harvesting of samples**

Seedlings were collected straight into ice-cold 90% acetone, ~1 ml in a 1.5 ml microfuge tube. The assay was fully carried out and the leaves dissected (excluding Fig 5.1, where rosettes were dissected and numbered prior to the assay but immediately put into 90% acetone after dissection). The numbers of seedlings harvested were greater than desired, however, no more than 3 - 4 seedlings were in a 1.5 ml microfuge tube if seedlings were older than 13 dag.

2.6.2 **X-gluc reaction solution**

Prior to adding the GUS substrate, 5-bromo-4-chloro-3-indolyl-beta-D-glucuronic acid (x-gluc), plants were harvested into 90% acetone (ice cold) and incubated for 15 - 30 min in +4 °C, subsequent steps were carried out in the same microfuge tube and volume of solutions used was ~1 ml. Samples were then washed twice with sodium phosphate buffer (pH 7) (see appendix 2.4) and the x-gluc reaction solution added.

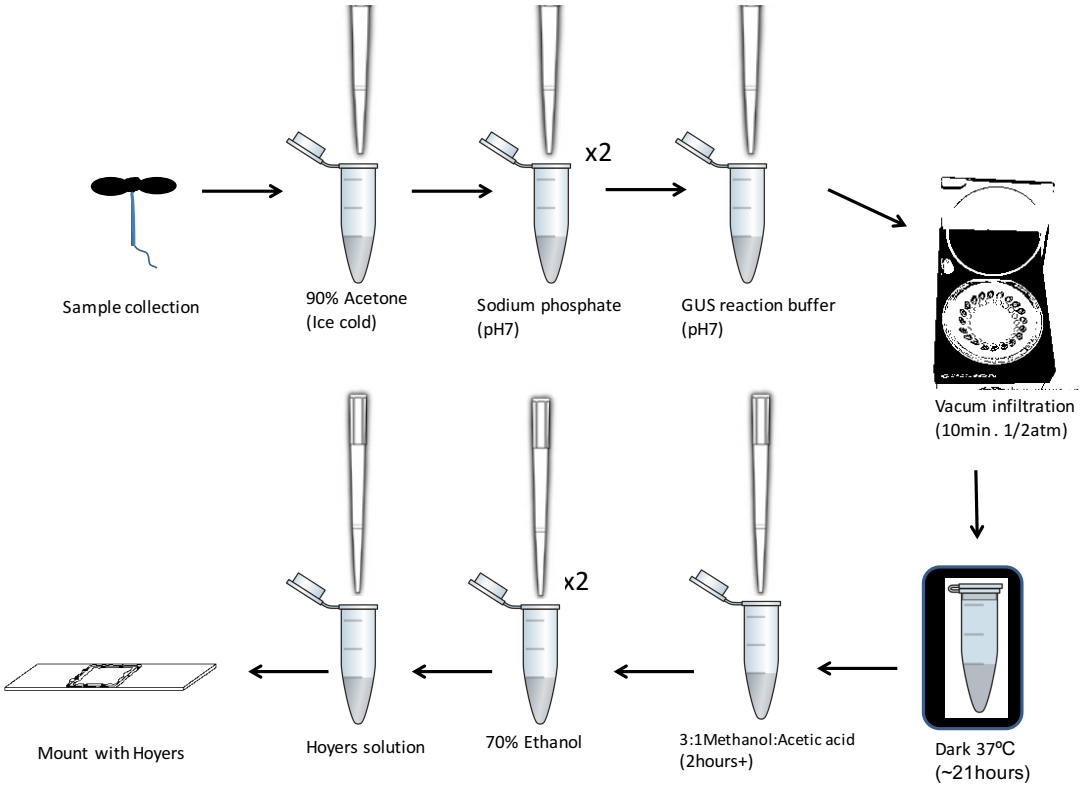

Figure 2-1 CYCB1;1::GUS protocol.

Method illustrating the key steps for obtaining punctuated CYCB1;1::GUS histochemical analysis, based on *Arabidopsis thaliana* seedlings. Adapted from; Jim Murray Lab (*personal communication*) (Donnelly *et al.*, 1999; Uchida *et al.*, 2007).

The x-gluc reaction solution used was according to the Jim Murray Lab (personal communication) (applicable to Fig 5.1) and was further adapted from Uchida *et al*., 2007 (applicable to Fig 4.6), see Table 2.2 below. Further details can be found in appendix 2.5.

The substrate used was x-gluc (sodium salt) and the reaction solution was always made to minimum of 25 ml and is recommended. The x-gluc reaction solution was added (~1 ml) after the last sodium phosphate wash, see section 2.6.1.

Table 2-2 The two methods used for x-gluc solution.

At first the protocol from the Jim Murray Lab was used for Fig 5.1. A further protocol was then adapted based on Uchida *et al.*, 2007, used for Fig 4.6. A more detailed description of calculations and volumes used can be found in the appendix, see appendix 2.5. (IC = Initial Concentration, FC = Final Concentration).

	J.Murray Lab		**N Uchida (2007)**		
	IC/stock	**FC/working**	**IC/stock**	**FC/working**	
X-Gluc	50mg/ml	0.3mg/ml	0.1M 50mg/ml	1mM	**X-Gluc**
Sodium Phosphate Buffer	0.2M	100mM	0.2M	50mM	**Sodium Phosphate Buffer**
Potassium Ferricyanide	0.1M	0.5mM	0.1M	0.5mM	**Potassium Ferricyanide**
Potassium Ferrocyanide	0.1M	0.5mM	0.1M	0.5mM	**Potassium Ferrocyanide**
Tween 20	10%	0.1%			
			10%	1%	**Triton x-100**
			0.5M	10mM	**EDTA**
			10%	1%	**DMSO**

2.6.3 **Vacuum infiltration and incubation**

After addition of x-gluc reaction solution a vacuum infiltration was performed. An ordinary speed vacuum (unknown pressure) was used except for Fig 4.6 where a speed vac with known ½ atm pressure was used, for 10 min, as recommended by Donnelly *et al*., 1999. Microfuge tube lids were closed and punctured after infiltration. The samples were incubated in the dark at 37 °C for ~21 hours.

2.6.4 **Post (x-gluc) incubation protocol**

After ~21 hours of incubation the reaction was stopped by removal of x-gluc reaction solution and addition of a 'stop' solution; 3:1 methanol:acetic acid (v/v). Samples remained in this solution for ~2 hours, or longer for more mature seedlings so the chlorophyll cleared. Two washes with 70% ethanol were then carried out and finally the samples remained in Hoyer's solution (for details of Hoyer's solution see appendix 2.6).

2.6.5 **Mounting of samples**

Samples were mounted as soon as possible and left for no longer than two weeks in the 1.5 ml microfuge tube consisting of Hoyer's solution. Seedlings were dissected under a stereo microscope with the use of fine tweezers. Samples were mounted on a microscope slide with Hoyer's solution. Additional Hoyer's solution was added, if needed, once the cover slip was gently placed and the slip sealed with clear nail polish for long term use.

2.6.6 **Microscope and functions**

Images were taken via the Nikon SMZ stereo microscope and transmitted white light (built in and from below where the specimen was placed). Use of a graticule was essential.

Alternatively, whole leaves were also imaged via use of Nikon Optiphot-s microscope in addition with an Optiscan device to perform z-stacks and an Extended Depth of Focus (EDF) image was created (see appendix 2.7 for comparison). It was confirmed that both methods work equally well, the former being less time consuming. The latter is also limited to small sections of the leaf as opposed to the whole leaf.

2.6.7 **Quantitation**

Quantitation of the blue precipitate was carried out using the ImageJ software - 'http://imagej.nih.gov/ij/'. Quantitation was based on percentage GUS per leaf area:

$$\%GUS = \frac{Area^{GUS}}{Area^{Leaf}}$$

The graticule image was used to set the scale, as described in section 2.5.2 and the measurement options set as: Area, limited to threshold and to 3 dp. For each leaf the area was calculated via use of the 'oval' draw tool to measure (Ctrl + M) the leaf area from tip to base. Prior to measuring $Area^{GUS}$ outliers were manually removed, including, dirt, debris, trichome branches, stems/petioles and some vascular structure. The image was converted to an 8 bit grey scale and further converted to a binary image. Additional outliers were removed via the 'despeckle' function. The binary image was thresholded and the area measured. It was then confirmed that thresholding the 8 bit grey scale image, adjusting the threshold and then manually removing outliers was equally sufficient.

2.7 Gene Expression Analysis

Relative gene expression profiling in *Arabidopsis thaliana* was carried out via Q-RT-PCR.

2.7.1 **Harvesting of samples**

Seedlings were harvested directly into a fresh pre-labelled 1.5 ml microfuge tube, afloat on $N_{2(l)}$ via a polystyrene microfuge tube holder. Leaves were pinched at the base whilst on plates and harvested as quickly as possible. The following sufficed for good RNA yields: ½ microfuge tube of young seedling; full microfuge tube of older seedlings; ½ - full microfuge tube of leaves from 11+ dag seedlings; ¼ - ½ microfuge tube of leaves younger than 10 dag. For experiments with a fine time course (chapter 4 and 5) requiring collection of new leaf of very small size (0.5 - 1.5

mm) whole seedlings were directly harvested into a well plate consisting of RNAlater solution (RNAlater was used to stabilise RNA at 4 ºC for up to a week). Seedlings were fully submerged in RNAlater and stored in +4 °C for up to a week to obtain good quality RNA (for evidence of RNA integrity see appendix 2.8). As far as possible seedlings were dissected after no longer than 3 days in RNAlater, dissection was carried out on a clean microscopic slide under the stereo microscope using fine tweezers. The slide was covered with RNAlater solution and a few seedlings at a time dissected and immediately frozen into a microfuge tube afloat on $N_{2(l)}$, as described above. Approximately 50 - 100 seedlings (7 dag) were sufficient.

Samples were stored in - 80 °C after harvesting. Samples harvested via the RNAlater procedure were strictly stored in - 80 °C.

2.7.2 **Grinding of material**

Harvested samples that were greater than ½ a 1.5 ml microfuge tube were always ground in $N_{2(l)}$ using a pre-cleaned and pre-chilled pestle and mortar. Equipment was reused by thoroughly cleaning with 70% ethanol and distilled H_2O. Samples were ground until a fine powder formed and topped with $N_{2(l)}$ if needed. Upon completion of grinding, the powder was carefully decanted back into the same microfuge tube (afloat on $N_{2(l)}$) using a pre-chilled and pre-cleaned fine spatula.

Where samples harvested were of a small amount (1/5 of a microfuge tube) $N_{2(l)}$ was decanted into the microfuge tube and the sample ground manually using a blue pestle (pre-chilled and pre-cleaned). More $N_{2(l)}$ was decanted until a fine powder was apparent.

Samples harvested via the RNAlater procedure required additional force via use of a fine spatula to dislodge samples as well as use of the blue pestle. A fine powder was not necessarily apparent due to the sample size but samples were ground for a greater time to ensure isolation of RNA.

All samples of the same experiment were ground in the same way.

2.7.3 **RNA extraction**

RNA was isolated using the Qiagen RNeasy PlantMini Kit, (Qiagen, U.K). Some modifications were made to the standard protocol (see Fig 2.2 below) and are described below.

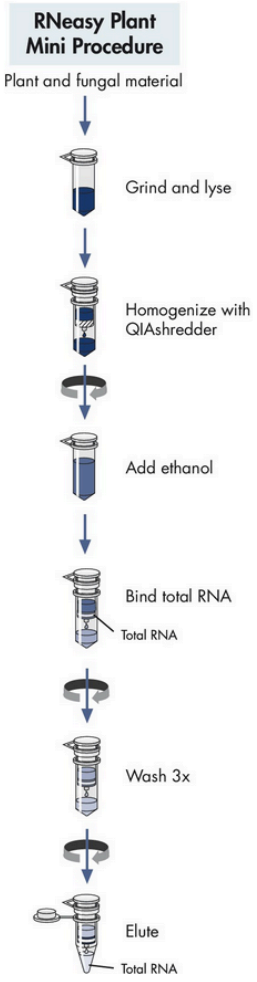

Figure 2-2 RNA isolation based on RNeasy Plant Mini Kit, Qiagen.

Taken from www.qiagen.com

A 100 mg of plant material was not used as recommended in the protocol, excess was required in order to isolate sufficient RNA, and the extra young tissue material used did not decrease yield (see section 2.7.2). Firstly, plant material was ground (see section 2.7.3). Samples were removed from the - 80 °C onto ice and 450 µl of lysis buffer (1 ml RLT buffer: 10 µl β-mercaptoethanol) immediately added. Buffer RLT consists of a high concentration of guanidine isothiocyanate. The microfuge tube was vortexed vigorously and additionally incubated at 56 °C for 3 min. All of the lysate was pipetted into the QIAshredder spin column (lilac) (columns were always placed on a 2 ml collection tube) centrifuged at 13,000 rpm for 2 min. The supernatant was carefully pipetted into a fresh 1.5 ml microfuge tube, 225 µl of absolute ethanol was added, mixed and pipetted into an RNeasy mini spin column (pink). Centrifugation at 10,000 rpm, for 15 s, was followed by decanting the flow through, adding 700 µl of RW1 buffer and re-centrifuging at 10,000 rpm, 15 s. The flow through was decanted, 500 µl of RPE buffer added, centrifuged at 10,000 rpm, for 15 s, this was repeated but the spin was for 2 min. The RNeasy mini spin column was carefully placed into a fresh 2 ml collection tube and the membrane dried by centrifuging at 13,000 rpm for 1 min. The RNeasy mini spin column was placed into a fresh pre-cleaned and pre-chilled (on ice) 1.5 ml microfuge tubes for RNA elution. RNA was eluted using RNase free H_2O provided in the kit.

The elution volume used was 30 µl but for smaller sample sizes volumes of 50 – 100 µl were used. RNase free H_2O was always added using filter tips and was pipetted directly on to the white column membrane. Samples were left to sit for ~1 min and then centrifuged at 10,000 rpm for 1 min. Samples were immediately put on ice. A small aliquot of the total elution volume was stored separately at - 20 °C and was used as the working stock for quantifying total RNA, checking quality and synthesising cDNA. The remainder of the RNA volume was stored at - 80 °C.

The quantity of total RNA eluted was determined by a fluorometric absorbance reading, using the Nanodrop instrument. The ng/µl was noted as well as the absorbance 260/280, for purity of RNA a ratio of ~2.0 was accepted.

2.7.4 **RNA quality – Agarose gel electrophoresis**

Depending on the concentrations of RNA eluted 0.5 – 1 µg of RNA was used for the gel. The calculated volume of RNA was pipetted into a microfuge tube consisting of 10 µl sterile H_2O and 2 µl loading dye. Samples were vortexed, spun down and kept on ice.

Low melting temperature agarose was used to prepare a 0.8% gel with either TAE (Tris, Acetic acid, Ethylenediaminetetraaceitc acid (EDTA) or TBE (Tris, Boric acid, EDTA) buffer (x50) (composition see appendix 2.9). Ethidium bromide stock (10 mg/ml) was carefully added as 5 µl per 100 ml.

Upon cooling the gel comb was removed and the gel loaded to a clean electrophoresis tank consisting of buffer TAE/TBE. Hyperladder I was incubated at ~50 °C for a few minutes prior to loading into the well. The gel was run at ~80 – 120 mV (dependent on the distance between the electrodes) for 20 - 30 min. The gel was checked under UV light.

2.7.5 **cDNA synthesis**

cDNA was synthesised using the Qiagen Quantitect Reverse Transcriptase/Transcription (RT) Kit. Samples were kept on ice for the procedure.

Previously, total RNA was isolated using the Qiagen RNeasy Plant Mini Kit (see section 2.7.3) and 1 µg of this was used as the template/input for the two-step reaction of cDNA synthesis. The total volume of the template RNA and RNase free H_2O was 12 µl. To this 2 µl of gDNA wipe-out buffer was added and the samples incubated at 42 °C for 2 min. The RT enzyme was removed from - 20 °C at this point and added to a pre-prepared master mix consisting of: RT buffer – 4 µl and RT primer mix – 1 µl / per 20 µl total reaction volume, see below:

Template RNA + RNase free H2O	12 µl
gDNA wipeout buffer	2 µl
RT buffer	4 µl
RT primer mix	1 µl
RT enzyme	1 µl
TOTAL	20 µl

To the reaction tube containing template RNA 6 µl of the master mix was added and the tubes incubated at 42 °C for 16 min. After incubation tubes were immediately incubated at 95 °C for 3 min, to inactivate the RT enzyme.

In cases of testing many genes, the input RNA was doubled to 2 µg and the volumes of all reaction components were doubled for a final 40 µl reaction volume. When cDNA was diluted for Q-RT-PCR this was taken into consideration (see section 2.7.8).

2.7.6 **Designing primers - Quantprime**

Most cell cycle Q-RT-PCR primers (Chapter 3) were designed using Quantprime software (www.quantprime.de). The organism selected was '*Arabidopsis thaliana* (TAIR release 10)' and the quantification protocol selected 'SYBR Green real-time qPCR (accept splice variant hits)'. The typical parameters used by default, as described in (Arvidsson *et al.*, 2008), were: 50 – 150 bp amplicon length, 60°C annealing temperature and strict primer criteria for G/C content and melting temperature (Tm). 'Primer finding' was started and the results displayed ('Results'). Primers were selected based on ability to span exon-exon borders and a high specificity rank score ("as calculated based on Primer3") for the primer pair. Other possible amplicons were detailed in the 'Primer pair information' and the rank score was taken into consideration, for primer pairs with lower rank scores too. Primers were supplied by Eurofins- MWG (https://ecom.mwgdna.com/services/oligo/).

2.7.7 **Designing primers – Primer3**

Primers designed by Primer3 (http://bioinfo.ut.ee/primer3-0.4.0/primer3) were first analysed for regions of homology in the 'full length cDNA seq' using the default 'WU-Blast' function. The desired sequence was copied and pasted into Primer3 with the following parameters; Product size range: ~80 - 150; Maximum self complementarity: 5; Maximum 3' self complementarity. The 'pick primers' tab was selected and from the output the most desirable primer was chosen based on amplicon size, melting temperature, avoiding hairpin structures and 3' self complimentarity. Selected primers were checked via WU-Blast (TAIR) and sourced from Sigma-Aldrich (chapters 4 and 5).

2.7.8 **Preparation of Q-RT-PCR**

All dilutions were done using good grade H_2O (BPC, see appendix 2.1). The cDNA was diluted 1:5. If the total reaction volume for cDNA synthesis was 40 µl, with 2 µg template RNA, cDNA was diluted as 1:10. Primers were diluted 1:10 to achieve 10 pmol.

The PCR reaction volume was 20 µl and consisted of the following: 10 µl Sybr Green, 6 µl H_2O, 1 µl R primer, 1 µl F primer and 2 µl sample/cDNA. A mastermix was prepared and added to the strip tubes. If the pipetting was done by the QIAgility robot only duplicates were run per sample. Most Q-RT-PCR preparation was done manually in triplicate samples under a laminar flow hood. To avoid pipetting error cDNA was diluted as 1:20 and 8 µl pipetted into a prepared mix of Sybr Green and F and R primers, 10 µl and 2 µl, respectively.

2.7.9 **Data Analysis**

Data was analysed using the Rest2009 software (http://www.qiagen.com/products/catalog/automated-solutions/detection-and-analysis/rotor-gene-q#resources). The 'standard mode' was selected and default settings used. The take-off values and amplification efficiency values of the

reference (ubiquitin and/or actin) were copied and pasted and the expression value noted. For Q-RT-PCR analysis in chapter 4 two reference genes (*UBIQUITIN10*, AT4G05320, and *ACTIN2,* AT3G18780) were used, a function of multiple reference genes being averaged by Rest2009 was an advantage. Additionally, the software output provides statistical analysis.

2.8 PCR

2.8.1 **DNA extraction**

Rosettes were harvested, pooled for each genetically different line, into microfuge tubes. Samples were manually ground by decanting $N_{2(l)}$, and quickly adding 0.5 ml of DNA extraction buffer (Edwards *et al.*, 1991) (see appendix 2.9 for details of solutions/buffers) and disrupting the tissue with the use of an autoclavable *blue* polypropylene pestle with an abrasive surface at the tip. Samples were then vortexed, centrifuged at full speed for 5 min and the supernatant carefully pipetted (~450 µl) into a new microfuge tube. To this tube 450 µl Isopropylalcohol (IPA) was pipetted, the tube vortexed and placed on the bench for ~10 min for the DNA to precipitate prior to centrifugation at full speed for 7 min. The supernatant was decanted and the microfuge tube best ensured to be dry (paper towel used for edges). A wash was performed by pipetting ~800 µl of cold ethanol, pipetting it out and placing tubes on a 65 °C heat block, briefly, to remove residual ethanol. The DNA pellet was resuspended by addition of 50 µl TE (Tris: EDTA, appendix 2.9) DNA suspension buffer and placed on a vortex shaker if needed. These samples were frozen at - 20 °C if not immediately used.

2.8.2 **PCR**

Before setting up the PCR primers were diluted 1:5 and the FR and BR primer pair tubes pre-labelled. Samples were kept on ice. The PCR reaction components were as follows but a master mix was prepared for each primer pair:

PCR Reaction mix (for 500 µl PCR tube)	Required Volume (µl)
H_2O	14.4
GoTaq® Buffer (Promega)	5
dNTPs	0.4
$MgCl_2$	2.5
Primer 1	0.25
Primer 2	0.25
GoTaq® polymerase (Promega)	0.2
DNA/sample	2
	Total Volume: 25 µl

The PCR cycle was performed as follows: Step 1: all reaction components heated and melted fully (94 °C, 2 min); Step 2: denaturation (94 °C, 30 seconds, s); Step 3: annealing of primers (60 °C, 30 s); Step 4: extension (72 °C, 2 min); Step 5: back to step 2. 35 cycles were performed on average and changes in annealing temperature and duration of extension phase changed based on set of primers used and product size, respectively. Samples were analysed using agarose gel electrophoresis (see section 2.7.4) and a suitable ladder.

2.9 Protein analysis: Western blot

Western blot was used for the detection of the Phosphorylated-RETINOBLASTOMA RELATED1 (P-RBR1) protein. All washing and incubation steps used a mixer (very gentle setting) and details of buffers and gels can be found in appendix 2.10.

2.9.1 **Protein extraction**

Samples were harvested using flash freezing in $N_{2(l)}$ as described in earlier methods. Samples (Fig 5.3) were ground using a drill with a metal pestle attached at the end (designed for 2 ml tubes). The drill was safely mounted on fixative stand. It was also possible to grind samples using manual blue pestle disruption of tissue (Fig 5.4). In both cases $N_{2(l)}$ was decanted into microfuge tubes during grinding to prevent thawing of tissue. Efforts were made to ensure samples consisted of similar volumes of tissue.

The ground tissue powder volume was estimated and an equivalent volume of extraction buffer (see appendix 2.10) added. Centrifugation at 16,400 rpm was carried out for ~6 min at +2 °C and the supernatant removed to another microfuge tube. SDS buffer (5x) (appendix 2.9) was added (2.5 µl SDS added for a 10 µl sample) to the supernatant and boiled for 5 min at 100 °C. Samples were frozen at -20 °C if not used further.

2.9.2 **Protein Quantification**

To 2 µl of the supernatant, from section 2.9.1, 800 µl distilled water and then 200 µl Bradfords dye reagent (see appendix 2.1) was added. Samples were mixed well prior to decanting into cuvettes for spectrophotometer analysis. For a blank 2 µl of Lacus buffer (see appendix 2.9) was used instead of sample.

2.9.3 **Protein separation**

Sodium Dodecyl Sulphate Polyacrylamide Gel (SDS-PAGE, see appendix 2.10) was used to separate proteins. First a running gel was prepared and poured between the two glass plates mounted on a gel caster platform, upon drying a stacking gel was prepared, poured and a comb put in place. Once dried, samples of equal protein amounts were carefully loaded into the wells as well as a Ladder. Running buffer was added and the gel run at 95 mV until samples reached the end of the gel.

2.9.4 **Western blotting**

The SDS-PAGE gel when complete was dismantled from the caster, carefully lifted, the stack gel removed and the remaining gel placed into blotting buffer (also called Transfer Buffer, appendix 2.9). The Polyvinylidene Flouride (PVDF) membrane was cut to size and pre-soaked in methanol for a few seconds and then placed in Transfer Buffer. Preparation of the nitrocellulose transfer blot was done in the following order from bottom to top (in the holder); Holder, foam pad, Whatman paper x3, gel, PVDF membrane, Whatman paper x3, foam pad, holder. All were pre-soaked in TB. The holder was sealed and placed in the correct orientation (cathode to anode) into the electrophoresis tank and TB poured till the top. This was left running at 20V overnight with a magnetic stirrer at the bottom (tank placed on top of stirrer platform) in a cold room.

The apparatus was dismantled and the membrane stained with reversible Ponceau stain (5 mins on shaker) to check equal loading and transfer onto the PVDF membrane. The stain was removed by washing out with 1% Tris Buffered Saline (TBS, appendix 2.9) with Tween (TBST) and milk added (2.5 g for 50 ml, 1% TBST), for blocking protein binding sites for an hour. Milk was removed and the primary Antibody (Ab) (P-RBR1, Rabbit Ab, appendix 2.1, made up with milk-TBST, 1:500) added and incubated overnight. A 10 mins wash with TBST (1%) was performed three times and the secondary antibody added (Anti-Rabbit-POD, 1:4000) and incubated for 1.5 hours. The TBST (1%) washes were repeated as before.

2.9.5 **Detection of protein**

All detection procedures were performed in the dark. The Horseradish Peroxidase (HRP) substrate (appendix 2.1) was prepared fresh (1:1 ratio) and the membrane was briefly dipped and carefully placed between two pre-cut transparency sheets (pre-aligned in the cassette). The film (appendix 2.1) was placed on top and the cassette (appendix 2.1) closed for ~10 mins before development of the film. Upon visualisation of desired band densities (in the dark) the film was briefly transferred from the developer solution to water and then fixer.

2.10 Statistical analysis

Standard deviation or standard error of the mean was calculated and plotted on graphs for all relevant data. This was based on the mean of at least triplicate samples. Details of biological replicates, technical replicates, independent repeats and statistical tests used are in the text but below is a summary table (table 2.3) of the data for each chapter and Fig. 2.3 shows an example of what is meant by 'pooled' data.

Table 2-3 A summary of the experiments, data type and the relevant statistical tests carried out.

Chapter	Experiment	Data type	Statistical Test	Error Bars	*n*
3	Flow cytometry	Percentage	*t*-test	SD	12 averaged from 2 experiments
	Epidermal cell layer	Qualitative	--	--	WT *n=6* Others *n*=3
		Frequency	Shapiro-wilk test	SEM	
	Q-RT-PCR	Quantitative	REST2009*	SD	3 technical replicates
	Seedling phenotype	Qualitative	--	--	--
	Leaf curvature	Qualitative	--	--	20 averaged from 2 experiments
		Quantitative	*t*-test	SD	
	Stomatal clustering	Qualitative	--	--	WT *n=6* Others *n*=3
		Percentage	*t*-test	SD	
	Stomatal Index	Percentage	*t*-test	SD	
	Plastid	Qualitative	--	--	--
4	Q-RT-PCR	Quantitative	--**	SD	3 technical replicates
	Flow cytometry	Percentage	*t*-test *where shown*	SD *where shown*	3
	Western Blot	Qualitative	--	--	--
	GUS staining	Qualitative	--	--	3< technical replicates
		Percentage	*t*-test	SD	
5	GUS staining	Qualitative	--	--	3 technical replicates
		Percentage appendix 5.2	*t*-test	SD	
	Flow cytometry	Percentage	*t*-test	SD	3
	Western blot	Qualitative	--	--	--

*randomisation and bootstrap
**repeated experiments in appendix 4.1

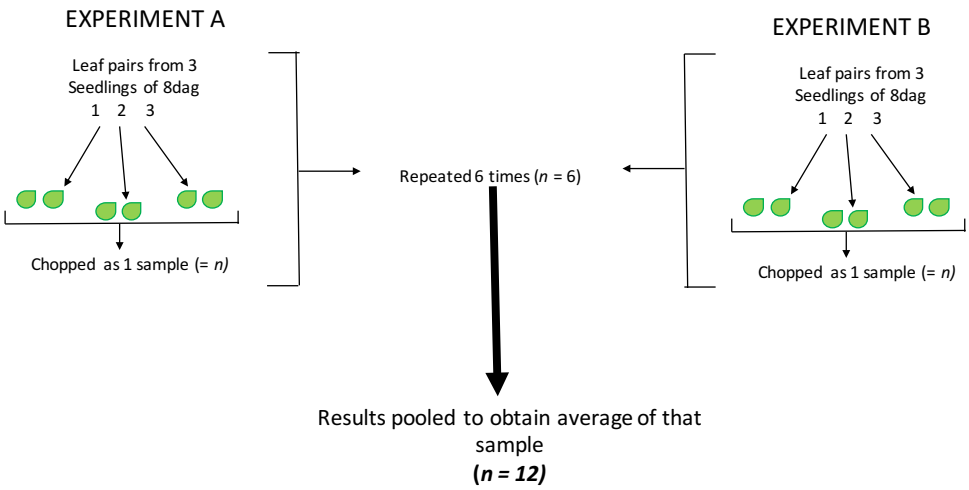

Figure 2-3 Example of 'pooled' flow cytometry data for Chapter 3.

2.11 Primer sequences used

Primer sequences for all primers in this work are in appendix 2.11. I would also like to thank Paul Devlin for the use of his *CCA1* and *PIF5* primers as well as Safina Khan for primers *MCM3* and *ORC1*.

2.12 Measuring leaf curvature

Analysis of leaf curvature was extrapolated from (Liu *et al.*, 2010) and (Wu *et al.*, 2007). The equations used for analysis of transverse curvature downward (TCd), longitudinal curvature downward (LCd) (Wu *et al.*, 2007) and the extrapolated global leaf pair axis curvature downward (GLPACd) are below.

$$TCd = \frac{pressed\ width - lateral\ margin\ width}{pressed\ width}$$

$$LCd = \frac{pressed\ length - base\ tip\ length}{pressed\ length}$$

$$GLPACd = \frac{pressed\ leaf\ pair\ axis\ length - leaf\ pair\ axis\ length}{pressed\ leaf\ pair\ axis\ length}$$

Further detail is in the relevant text and a visual aid in Fig. 3.13. It should also be noted that these experiments were conducted at the John Innes Centre, Norwich.

Chapter 3: E2FB positively acts on cell proliferation in meristematic cells and inhibits the re-entry to mitosis in differentiated pavement cells

3.1 Introduction

The proliferation of cells increases cell number that, together with cytoplasmic and elongation growth, contributes to final organ sizes. Proliferation is associated with the first phase of organ growth and is coupled to cytoplasmic growth fuelled by macromolecule synthesis (Bogre *et al.*, 2008). The second phase of growth coincides with the onset of cell differentiation, where cells expand in size, and in *Arabidopsis* is coupled to the endoreduplication cycle. Both proliferation and endoreduplication cycles require DNA synthesis but in the latter mitosis is skipped. The initiation of differentiation in the leaf moves in a basipetal direction from the tip, intricately shown by (Andriankaja *et al.*, 2012) by individually tracing each cell on the leaf epidermis. Overexpression of positive cell cycle regulators, such as CYCD3;1, leads to continued cell proliferation and reduced cell size leading to altered leaf anatomy with failure to develop distinct spongy and palisade mesophyll cell layers (Dewitte *et al.*, 2003). The cell cycle machinery regulates proliferation and endoreduplication-dependent growth with particular emphasis on the RBR1/E2F switch that is regulated by CYCLINS (CYCs) and CYCLIN DEPENDENT KINASES (CDKs) (CYC-CDKs). The heterodimeric kinases CYC-CDKs regulate progression through the course of the cell cycle. CDK(s) primarily in association with D-type cyclins phosphorylate the RETINOBLASTOMA RELATED1 (RBR1) protein at multiple sites. The phosphorylation results in inactivation of RBR1 and consequently E2F-DP dependent transcription of genes, which allows progression through S and M phases of the cell cycle.

The E2F transcription factors are traditionally divided into activators and repressors, dependent on whether they are able to transactivate gene expression when released from RBR1 or only have functions together with RBR1 to make a repressor complex, respectively. The classifications of E2Fs to activator/repressor types are not fully

understood in plants, but E2FA/B are thought to be activators while E2FC a repressor in *Arabidopsis*. E2FA is most active to regulate DNA synthesis both during the normal cell cycle, and during endocycle (De Veylder *et al.*, 2002). The work of (Magyar *et al.*, 2012) shows that RBR1 represses endocycle through E2FA while the freed E2FA can stimulate endocycle, but only DNA binding but not transactivation function is required for this activity. This led to the suggestion, that E2FA functions together with RBR1 to maintain the meristem through the repression of the exit to endocycle. The overexpression of E2FB simultaneously with its DIMERISATION PARTNER type a (DPa), but not that of E2FA-DPa, results in an increase in the CDKA;1 and CDKB1;1 protein levels, indicating that E2FB is a positive regulator of cell proliferation (Magyar *et al.*, 2005). It is known that ectopic overexpression of E2FB induces S and M phase but represses endocycle (Sozzani *et al.*, 2006). The Sozzani lab (2006) also described that ectopic overexpression of E2FB led to smaller seedlings at 4 days old but at 16 days old the cotyledons were larger than the WT with reduced cell size and the appearance of increased cell number. However, further studies of using combinations of ectopic overexpression, RBR1-binding mutants and knock out mutant lines, similar to what was used for E2FA (Magyar *et al.*, 2012) and a finer time course to follow leaf development, one that is more tuned to the developmental switch from proliferation to endocycle/differentiation during leaf development (Andriankaja *et al.*, 2012), may be more appropriate in inferring the role of E2FB during leaf development. E2FC is a repressor of cell proliferation as overexpression leads to enlarged cells that do not divide as well as reduced expression of S phase genes (Del Pozo *et al.*, 2002).

In *Arabidopsis* leaves, specifically the first new leaf pair, provide a tractable developmental system for this transition. In this system leaf cells are typically small in size and proliferate until the leaf reaches a few mm in length (Dewitte *et al.*, 2007). At this point cells near the tip of the leaf begin to increase in size with a concomitant exit from cell proliferation (Qi and John, 2007). When this exit is abrogated leaf development will be compromised, for example, leaf flatness is disrupted because it is precisely controlled via genetic regulation of the cell cycle arrest (Nath *et al.*, 2003).

To study how E2FB regulates the transition from proliferation to expansion/endoreduplication dependent growth our lab utilised a loss of function mutants (*e2fb-ko*), lines with elevated E2FB expression within its own expression

domain by introducing a functional GFP fused form of E2FB under the control of its own promoter (E2FB-GFP) and producing lines with ectopic overexpression (35S::HA-E2FB/DPa). In animal cells it was shown that the deletion of the C-terminal part of activator E2Fs that encompasses the overlapping RB binding and trans-activation domains abrogated the cell cycle exit but not the cell proliferation. This suggested in animal models that the recruitment of RB is important for cell cycle exit, but the E2F transactivation function is dispensable for maintaining cell proliferation (Zhang *et al.*, 1999). This was surprising as it was thought that the transcriptional activation of genes required for the G1 to S phase transition is the most important function of E2Fs. To test whether this also holds for activator E2Fs in plants I used, previously constructed, similar C-terminal deletion constructs for E2FB and overexpressed them together with DPa (35S::HA-E2FB$^{\Delta RBR1}$/DPa). These lines were used for phenotypic analysis, flow cytometry and Q-RT-PCR.

3.2 Aims and objectives

In summary, the hypotheses reflect the assumption that the level of E2FB is a critical determinant of the developmental transition from proliferation to differentiation/endoreduplication. This hypothesis is primarily based on previous reports that E2FB induces mitosis in cultured cells and represses endocycle (also called endoreduplication). Should this hypothesis not be met for loss of function mutant, I shall consider redundancies with the other E2F proteins.

Hypothesis 1:

Elevated E2FB levels (E2FB-GFP lines) and ectopic overexpression (35S::HA-E2FB/DPa) would promote cell proliferation. This would lead to increased number of cells due to either the accelerated cell proliferation or the delay in the exit from proliferation.

On the other hand, early exit from the cell cycle and entry to differentiation would result in large expanding cells.

Hypothesis 2:

The T-DNA insertion loss of function mutant lines of E2FB would compromise cell proliferation. This could lead to the onset of differentiation.

Hypothesis 3:

It is not known, whether E2Fs are absolutely necessary for transcriptional activation of their target genes, or their main role is the repression with RBR1. If the second scenario is the case, the knock out mutant may not be compromised for the expression of cell cycle genes and therefore cell proliferation in meristematic tissues.

Hypothesis 4:

The transgenic E2FB$^{\Delta RBR1}$/DPa lines (labelled as 1-385, see schematic diagram in appendix 2.3) would interfere both with the activation and repression mechanisms. If the repression is important, I expect cells to over-proliferate. If transcriptional activation is fully necessary for cell proliferation, I expect compromised proliferation leading to fewer and larger cells. Also, if there is a cell type specific requirement for these functions, I can expect to observe both effects in different cells.

In the case of negative results to my hypothesis, I shall also consider some technical problems, such as the possible effect of the genomic insertion site of the construct, stability of the mRNA or protein folding or function compromised by the introduced tags.

The described transgenic lines were generated by our collaborator, Zoltan Magyar (see section 2.2). New leaves form *de novo* from the shoot meristem, as pairs, while cotyledons have an embryonic origin. Cells in cotyledon only proliferate for a short period of time before they switch to endocycle. The first new leaf pair (NL 1/2) typically emerge at 7 dag in my growth conditions. Because new leaves have trichomes on the leaf surface whereas cotyledons do not, it was technically more feasible to use cotyledons for epidermal cell size analysis whereas flow cytometry and gene expression analysis was carried out on the NL 1/2 series, 8, 10, 12 and 15 dag. Selected cell cycle marker genes were used for gene expression analysis, detailed in Table 3.1.

Table 3-1 Gene annotation for Q-RT-PCR

Gene	Annotation
E2FB	The E2FB protein is a transcription factor that binds to DNA with its Dimerisation Partner (DP) via an E2 recognition site, products of this are cell cycle genes. Involved in G1-S progression.[a]
CYCD3;1	The product of *CYCD3;1* plays a role in phosphorylating RBR1 to balance the entry into cell proliferation and differentiation.[b]
CDKB1;1	CDKB1;1 is a M phase promoting gene and is inactivated when endoreduplication begins; this occurs via the proteolytic destruction of its cyclin partner, CYCA2;3[c d]
CYCA2;3	Gene *CYCA2;3* encodes an M phase enhancing cyclin.[e f]
RBR1	RETINOBLASTOMA RELATED1 (*RBR1*) protein is regulated by CDK-CYCs and forms a repressive complex with E2Fs.
MCM3	Minichromosome Maintenance3 (*MCM3*) is involved in initiation of DNA replication.[g]
ORC1	Origin of Replication Complex1 (ORC1) is also involved in the initiation of DNA replication.[h]

[a] (De Jager *et al.*, 2001)

[b] (Dewitte *et al.*, 2003)

[c] (Boudolf *et al.*, 2004b) [d](Boudolf *et al.*, 2009)

[e] (Imai *et al.*, 2006) [f](Boudolf *et al.* 2009)(Boudolf *et al.*, 2009)

[g] (Vandepoele *et al.*, 2005)

[h] (Vandepoele *et al.,* 2005)

3.3 E2FB T-DNA insertion, *e2fb-ko*

Two independent T-DNA insertion lines were identified for *E2FB* from the SALK collection (*e2fb-ko 959* and *e2fb-ko* 138). Using an E2FB-specific antibody targeted against the C-terminal region in Western blot (performed by Dr Zoltan Magyar) confirmed that in both lines a full length E2FB protein is missing. PCR was performed on *e2fb-ko 959*. Epidermal cell analysis was performed on *e2fb-ko 959* and gene expression analysis was performed on both *e2fb-ko 959* and *e2fb-ko 138*.

3.3.1 **Confirmation of T-DNA insertion in *e2fb-ko 959* (salk)**

Genotyping with PCR was performed on pools of WT-Col and *e2fb-ko 959* leaf tissue (Fig 3.1A). The T-DNA insertion was confirmed by use of genomic DNA (gDNA) for PCR amplification with Forward (F), Reverse (R) and Border (B) primers the one specific for the insertion carried out as separate reactions (see methods). For the FR primer pair the amplicon of anticipated size (~1000bp) was present in the WT-Col but absent in the *e2fb-ko 959*. The primer pair BF showed a band (~800bp in size) for *e2fb-ko 959*, which could indicate that the *e2fb-ko 959* has two T-DNA insertions as an inverted repeat (not shown). These results show that the *e2fb-ko 959* has a T-DNA insertion in the *E2FB* gene and is homozygous for the T-DNA insertion (no FR product/band observed). Note, the uknown band as possible contamination as these WT-Col plants were used multiple of times without such observation (indication of T-DNA insertion).

3.3.2 ***e2fb-ko* promotes early endoreduplication onset**

Flow cytometry (DNA content/ploidy) analysis was carried out for both *e2fb-ko 959* and *e2fb-ko 138* lines (Fig 3.1B). All the flow cytometry data in this chapter is a pool of two individual experiments consisting of an average of six technical replicates in each case, additionally the WT-Col is a pool of two biological replicates. All flow cytometry graphs in this chapter show statistical significance (*) for the relevant N/peak against the WT-Col, $p<0.05$, *t*-test.

The WT-Col NL 1/2 consisted of 2N and 4N nuclei content at the earliest stage of leaf development at 8 dag, indicating that cells alternate between G1 and G2 phases of the cell cycle (Fig 3.1B). 8N became apparent at 10 dag, indicating that some cells entered endoreduplication. At 12 dag 8N further increased while 16N became apparent at 15 dag.

At 8 dag there was very little difference in the DNA content of the *e2fb-ko* lines, compared to the WT-Col. Further on, at 10 dag, *e2fb-ko 959* had an increased proportion of cells with 8N, though this was less pronounced and statistically insignificant ($p<0.05$) in the *e2fb-ko 138* line. A difference was observed at 12 dag

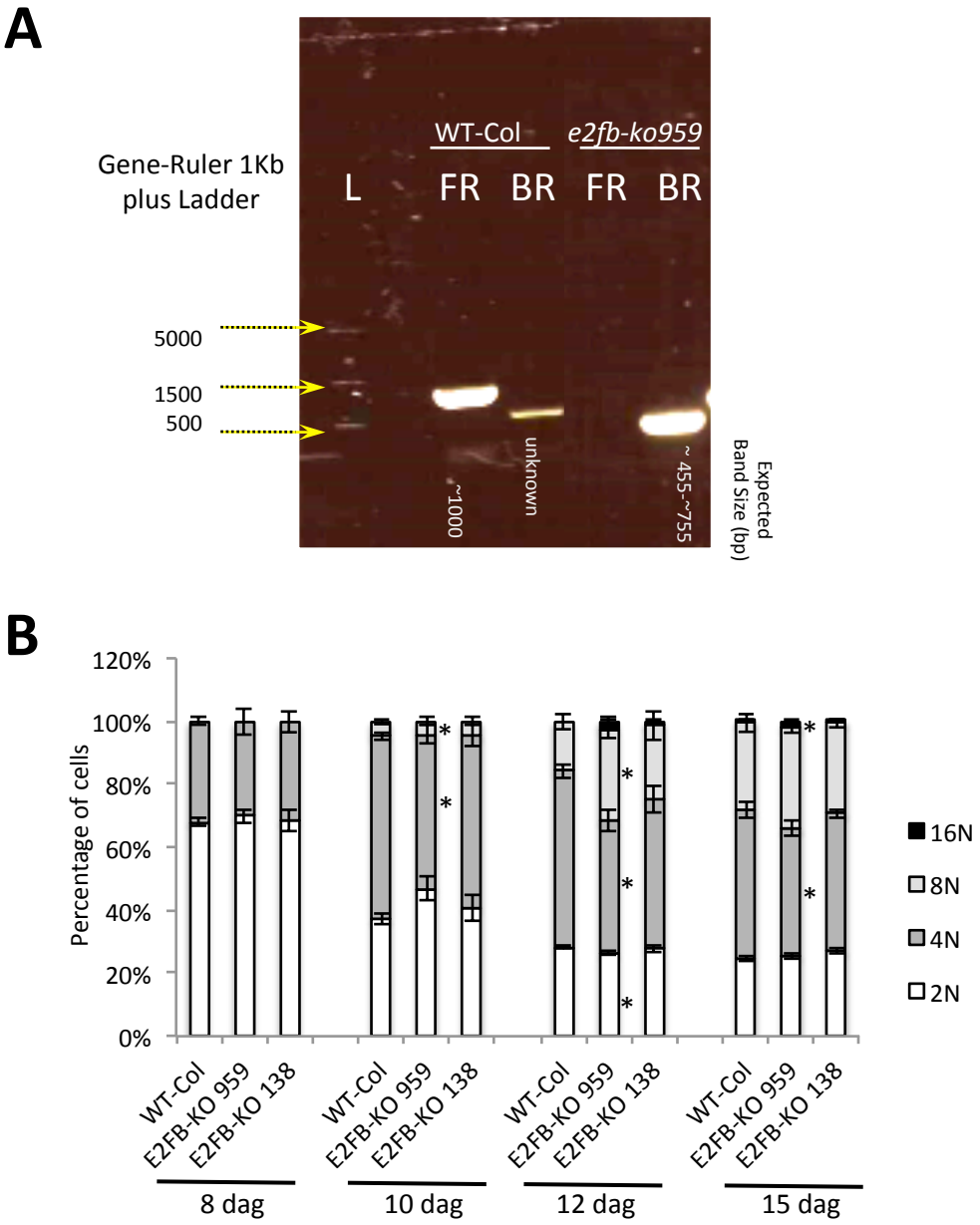

Figure 3-1 Absence of E2FB in the *e2fb-ko 959* leads to early onset of endoreduplication

A) PCR analysis shows absence of the E2FB gene in the T-DNA insertion line *e2fb-ko 959*. Samples harvested were pools of 3-5 *Arabidopsis* rosettes. Forward-Reverse (FR) and Border-Reverse (BR) primer pairs were used. These results confirm homozygous *e2fb-ko 959*. **B)** Flow cytometry analysis of the first new leaf pair in WT-Col and *e2fb-ko 959* over 8, 10, 12 and 15 dag (days after germination). A mean of two independent experiments, average of 12 technical replicates. Bars = standard deviation. * = significance, *t*-test, $p<0.05$.

where WT-Col lacked 16N but both *e2fb-ko's* had a 16N peak. This was statistically significant in the *e2fb-ko 959* 2N, 4N and 8N where as 16N only just entered this ploidy level with more deviation in the data. Notably at 15 dag the cells entering 16N is significant in the *e2fb-ko 959* as compared to the WT-Col 15 dag. At 15 dag the DNA content of WT-Col and *e2fb-ko 138* appeared similar. Thus, during the NL 1/2 development the *e2fb-ko* lines entered endoreduplication early in comparison to the WT-Col, evident at 10 - 12 dag.

3.3.3 **Distinct large epidermal cells in the *e2fb-ko 959* cotyledon**

Cotyledons from 8 dag seedlings were cleared with methanol and fixed in lactic acid for analysis of the adaxial epidermis of half the cotyledon (base to tip direction; Fig 3.2A). The WT-Col epidermis consists of pavement cells with a jigsaw like appearance that increasingly become more lobed as cells differentiate. Guard cells that make up the stoma and meristemoid cells in the guard cell linage are a distinct population of cells in the leaf epidermis. In the *e2fb-ko 959* pavement cells appeared larger; which was confirmed by measuring the area of all cells except the recognisable guard cell linage (Fig 3.2A). The frequency distribution graph showed a majority of cells in the WT-Col of being 1000 - 3000 μm^2 and cells above 6000 μm^2 were lowest in abundance. In contrast, cells of the *e2fb-ko 959* showed a different distribution where a large proportion of cells were above 9000 μm^2. The frequency distribution graph in Fig 3.2B shows a bell curve or Gaussian shape for the WT-Col with the *e2fb-ko 959* having a larger bar to the right of the bell curve shape, appreciating that the graph has intervals on the x axis a Shapiro-Wilk test was performed on the empirical data. As $p<0.05$ for WT-Col, and calculated W below the critical W, the null hypothesis (that the data is from a normal distribution/population) is rejected. Because the test could potentially be biased for sample size a Quantile-Quantile (Q-Q) plot was used and validates that the data is not from a normal distribution. For Shapiro-Wilk test values and graphical Q-Q plot see appendix 3.1. The Q-Q plot shows that the data is heavy tailed to the left and skewed on the right for WT-Col where as *e2fb-ko 959* shows less of this skewedness on the right (*e2fb-ko* 959; $p<0.05$, W calculated<W critical). Overall, this indicated that some cells of the *e2fb-ko 959* became exceptionally large in comparison to those of the WT-Col.

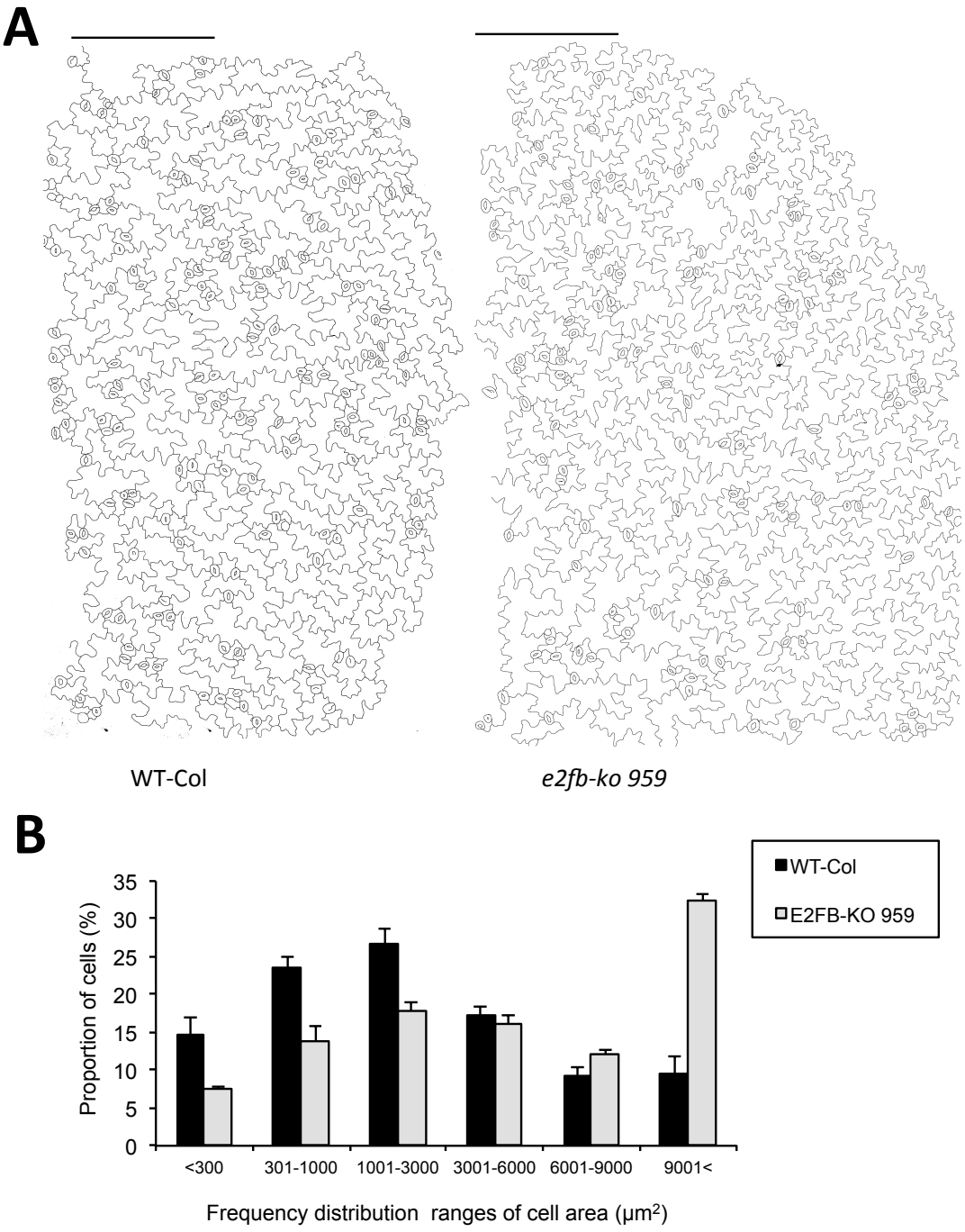

Figure 3-2 Epidermal cells are larger in the *e2fb-ko 959*

A) Epidermal cells for half the cotyledon (of 10 dag) were manually drawn as described in methods. Scale represents 1000 µm. **B)** Frequency distribution of epidermal cells shown in A. Based on triplicate samples, two biological replicates were used for WT-Col. Larger cells (above 9000 µm2) are greater in the *e2fb-ko 959* (grey bars), large bar on right. Error bars represent standard error.

3.3.4 **Putative E2F-target cell cycle genes are down in the *e2fb-ko* lines**

Size analysis revealed cells to be larger in the *e2fb-ko 959* adaxial epidermis of the cotyledon. In agreement I found by flow cytometry in NL 1/2 an early exit to endoreduplication. To see whether these phenotypes correlate with altered expression of cell cycle genes during the development of the leaf, I selected RETINOBLASTOMARELATED1 (RBR1) and a few E2F target genes, (CYCD3;1, CDKB1;1, CYCA2;3; annotated in Table 3.1). All four genes were found to have canonical E2F cis-elements (see appendix 3.2). Two other putative E2F target genes involved in DNA initiation were selected, MINICHROMOSOME MAINTENANCE3 (MCM3) and ORIGIN OF REPLICATION COMPLEX1 (ORC1).

All Q-RT-PCR in this chapter are based on 3 technical replicates and asterisks on figures simply represent statistical analysis of this sample carried out by REST2009 software, which employs randomised bootstrapping to test for significance between the two groups. The reference gene used was *UBIQUITIN10* (*UBQ10*) (see appendix 2.11).

In agreement with previous studies all cell cycle genes in the WT-Col followed a pattern where expression was greatest in young leaf at 8 dag and declined over 10, 12 and 15 dag (with the exception of CYCA2;3 at 10 dag) (Fig 3.3). The E2F target genes (all genes shown in Fig 3.3) followed a similar pattern in the *e2fb-ko 959* and *e2fb-ko 138* lines, however, these genes were significantly downregulated in comparison to the WT-Col, most evidently at the earliest time point, 8 dag, where the largest proportion of proliferating cells are present. RBR1 was the only gene downregulated at 8 dag, but not at subsequent time points in the *e2fb-ko* versus WT-Col. Genes *MCM3* and *ORC1* were slightly elevated at 15 dag in *e2fb-ko 959* but on the contrary were significantly downregulated (in *e2fb-ko 959*) at 8 dag compared to WT-Col. Overall, these results showed that E2F target cell cycle genes were down-regulated in the *e2fb* mutant T-DNA insertion lines. The REST 2009 software was used for the analysis of these data, the statistical output from the software (Pfaffl *et al.,* 2002) also shows the data to be significant in all cases.

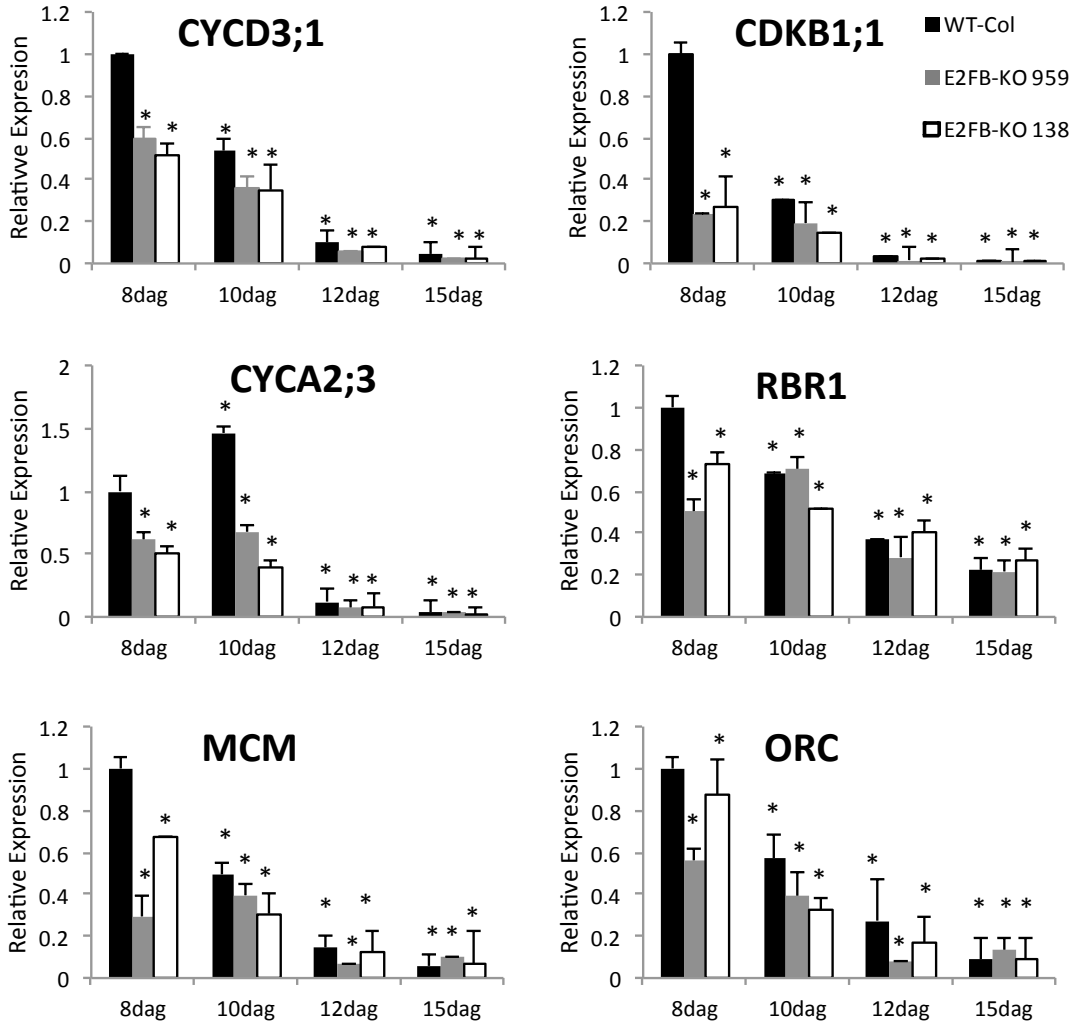

Figure 3-3 Q-RT-PCR analysis of key cell cycle genes in *e2fb-ko*: genes are downregulated

First new leaf pair in WT-Col (black bars), *e2fb-ko 959* (grey bars) and *e2fb-ko 138* (white bars) were harvested over 8, 10, 12 and 15 dag. The reference point in each gene is the WT-Col 8 dag. Cell cycle gene transcripts decline over time in the WT-Col (exception of *CYCA2;3* 10 dag). Cell cycle gene transcripts are down in the *e2fb-ko* compared to the WT-Col, notably this is most obvious at the early time points, 8 dag. Error bars represent standard deviation. Asterisks (*) represent statistical significance (95% confidence interval) based on randomisation and bootstrap tests by the REST2009 software (Pfaffl *et al.* 2002). Data is based on 3 technical replicates.

3.4 Elevated E2FB levels in different pE2FB:gE2FB::gGFP lines

To identify the intracellular localisation and developmental distribution of E2Fs and RBR1, our lab previously constructed translationally fused C-terminal Green Fluorescent Protein (GFP) lines (Zoltan Magyar), of interest is the pE2FB:gE2FB::gGFP line (E2FB-GFP lines). The expression of the E2FB gene is under the control of its native promoter but the transformed lines have an extra pair of genomic copies of the E2FB gene at a single insertion site in addition to the endogenous ones in the homozygous lines. We selected 15 independent transformed lines and in detail characterised three; E2FB-GFP lines 72, 114 and 61 that were found to show high, medium and low expression of E2FB-GFP, based on Western blotting with the GFP-specific antibody (this was conducted by Zoltan Magyar and is shown in appendix 3.3). In this part I present the phenotypic and gene expression analysis of these lines. Flow cytometry and Q-RT-PCR was carried out on all three lines and observation of pavement cells only on the strongest overexpressor (line 72).

3.4.1 **Greater E2FB levels cause greater curvature of the cotyledon**

Cotyledons of WT-Col seedlings exhibited a typical flat surface, whereas the strong E2FB-GFP 72 overexpressor cotyledons had a convex adaxial side (Fig 3.4A). In contrast, the weak overexpressor, E2FB-GFP 61 had cotyledons similar to the WT-Col but appeared slightly larger in size. New leaves of E2FB-GFP 72 also showed similar curvature whereby 15 dag seedlings appeared shrivelled and small due to curving of the leaves. At first these subjective results were noted but a more quantitative approach is discussed in section 3.7 (Fig 3.13) to comparatively discuss leaf curvature as well as leaf size amongst all the transgenic lines used here. No obvious developmental delays in the growth of the adult plant, or production of seeds, was observed except that the E2FB-GFP 72 appeared to form a smaller rosette area in adult plants.

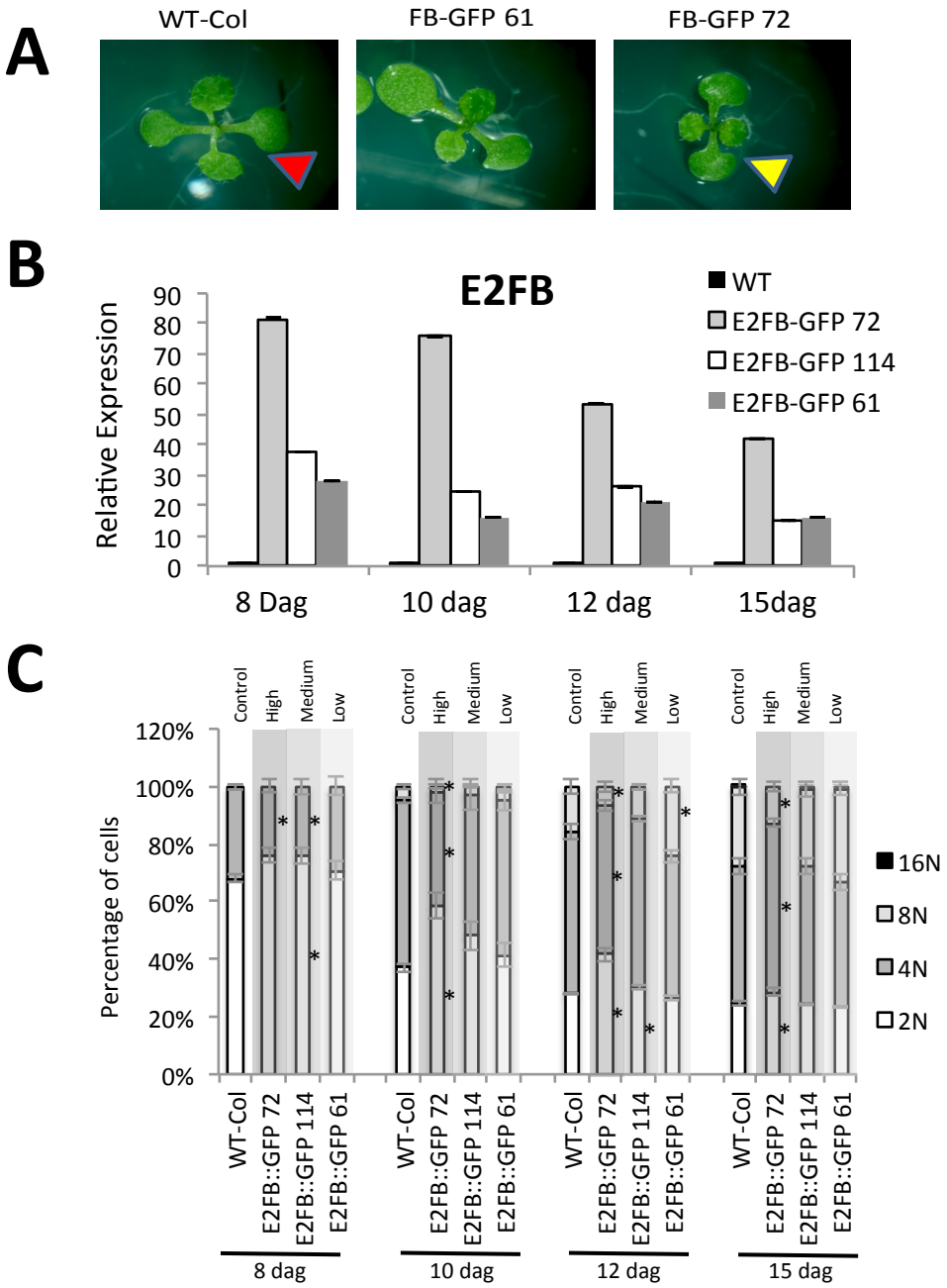

Figure 3-4 Analysis of E2FB-GFP lines

A) 12 dag seedlings show an increase in the level of E2FB (left to right, WT-Col, low E2FB-GFP overexpression line and high E2FB-GFP overexpression line) Yellow arrow heads show curled cotyledons (contrasted by red arrow head in WT-Col). **B)** Q-RT-PCR analysis of E2FB gene transcripts in the first new leaf pair over 8, 10, 12 and 15 dag in E2FB-GFP 72, E2FB-GFP 114 and E2FB-GFP 61 as high, medium and low E2FB (protein) expressing lines. The WT-Col is the black bar and WT-Col 8 dag is the reference point. Error bars represent standard deviation of 3 technical replicates. **C)** Flow cytometry analysis of the first leaf pair over 8, 10, 12 and 15 dag. WT-Col (control) and high, medium and low E2FB-GFP expression lines (as labelled and shaded from dark grey to light grey in background). All error bars represent standard deviation of data from two individual experiments with an average of 12 technical replicates. * = significance, *t*-test, $p<0.05$.

3.4.2 **Confirmation of E2FB levels in E2FB-GFP lines via Q-RT-PCR**

Transcript levels of E2FB were measured using Q-RT-PCR in NL 1/2 series. An E2FB primer designed towards the 3 prime end shows elevated E2FB levels in the E2FB-GFP lines (Fig 3.4B). The previously mentioned Western blot showed high, medium and low expressors at the protein level, this was confirmed at the mRNA level but additionally over a leaf time series. In the WT-Col, E2FB levels decline over time, however, they remain elevated in the E2FB-GFP lines (up to ~55fold for E2FB-GFP 72).

3.4.3 **The exit from proliferation into endoreduplication was delayed in correlation with the elevated E2FB-GFP amounts**

Lines E2FB-GFP 72, 114 and 61 (high, medium and low expressors respectively) were analysed for ploidy levels of cells in NL1/2 at 8, 10, 12 and 15 dag. The WT-Col ploidy levels were as described earlier (3.3.2). In comparison to WT-Col at 8 dag there were a greater proportion of cells with 2N nuclei in the E2FB-GFP lines that correlated with the E2FB amounts (Fig 3.4C). Because at this early time point there is a large proportion of cells that proliferate, this change in 2N/G1 and 4N/G2 proportion indicate upon elevated E2FB expression the cells spend a longer time in G1 and shorter time in G2 phase of the cell cycle. Cells exit to endocycle from the G2 phase. In agreement, at 10 dag the larger 4N/G2 proportion was accompanied with the appearance of the 8N category of nuclei that was more in WT-Col than in the E2FB-GFP lines. The proportion of 8N further increased at 12 DAG in WT-Col but was smaller in E2FB-GFP lines in correlation to the E2FB expression levels. At 15 dag, where a very small portion of WT-Col nuclei entered 16N (0.56%), E2FB-GFP 72 did not (0%) where as E2FB-GFP 114 (0.78%) and E2FB-GFP 61 (1.07%) did enter 16N. The E2FB-GFP 72 persistently shows a statistically significant difference (greater proportion of cells in the respective N state) compared to the WT-Col whereas E2FB-GFP 114 only does at 8 dag: E2FB-GFP 61 only significantly shows a difference at 12 dag but this is due to a greater proportion of cells in 8N compared to the WT-Col. In summary, these results together with the *e2fb* mutant results suggest that E2FB suppresses the entry into endoreduplication in a dose dependent manner.

3.4.4 **Elevated E2FB levels introduces unprecedented cell wall boundaries**

As E2FB dose-dependently affects the exit from proliferation into endoreduplication, I looked to see whether there are changes in epidermal cell sizes as previously this was reported by (Sozzani *et al.*, 2006) in an ectopically overexpressed E2FB line. I had an initial observation for all three E2FB-GFP lines but detailed analysis was carried out on E2FB-GFP 72. Analysis of the adaxial cotyledon epidermis revealed cell shape and size distribution to be more heterogeneous in comparison to the WT-Col (Fig 3.5). Quantitative analysis of cell size was intended but identification of cell wall boundaries proved to be more challenging in this line as compared to others, shaded in the image (Fig 3.5). For this reason a frequency distribution may not have been a true representation of data and was not calculated based on the methods I used. Smaller cells were more abundant and, consequently, lobed cells were less frequent in the E2FB-GFP 72 line. Additionally, the cell wall boundaries appeared in an atypical fashion, i.e. straight lines in multiple instances that were never apparent in the WT-Col (represented by arrows in Fig 3.5). It was the axis at which the cell wall boundaries were present that was peculiar. For ease of description it was as though one giant lobed cell had two to six ladder steps, all perpendicular to a single axis, where the steps were cell walls. Based on the hypotheses a late entry into endoreduplication would be expected to lead to smaller and/or more cells. This was observed here for the E2FB-GFP 72 line but notably the constitutively expressed E2FB line in a previous publication was reported to have modest increase in ploidy levels despite smaller but more cells (Sozzani *et al*., 2006). Here I report that a very high level of E2FB, in a line with an extra pair of genomic copies, gives the aforementioned epidermal cell phenotype but with reduced ploidy levels. This is suggestive of an E2FB level threshold in these lines in order to effect the transition into endoreduplication (because E2FB-GFP 61 did not display smaller cells as in E2FB-GFP 72).

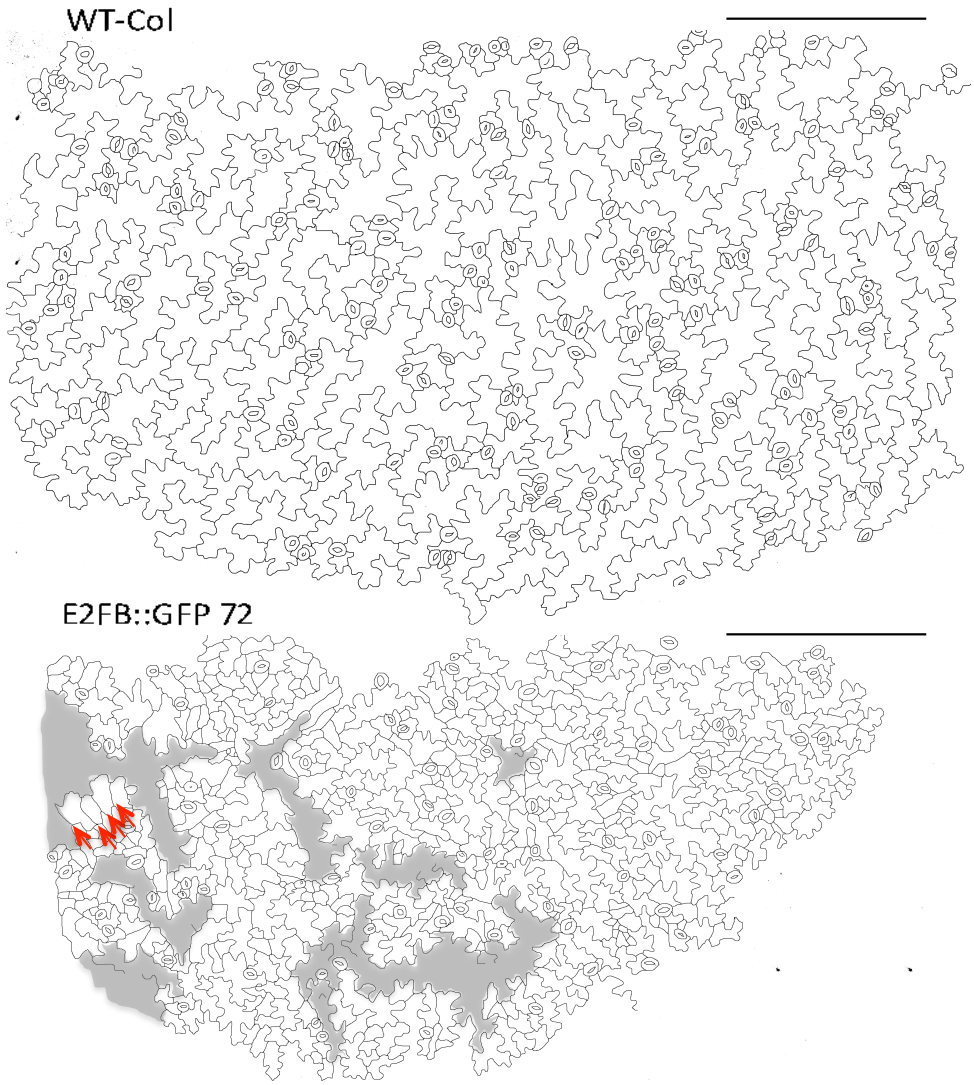

Figure 3-5 Epidermal cells are smaller in the E2FB-GFP 72 line

Half the cotyledon (10 dag) was analysed manually for epidermal cells, as described in methods. Pavement cells of E2FB-GFP 72 (bottom) lack the same jigsaw and lobed appearance as in WT-Col (top) and many small cells are apparent. Cell walls appear perpendicular to a single axis in the E2FB-GFP 72 (red arrows). Cell walls were also more difficult to distinguish as shown by shaded grey regions of uncertainty. Scale represents 1000 µm. Frequency of these divisions was recurrent in all samples observed (including independent experiments).

3.4.5 **Cell cycle genes are upregulated in the E2FB-GFP lines**

The alteration in leaf and cell geometry and the delayed entry into endoreduplication in the E2FB-GFP lines led to the expression analysis of cell cycle genes (Fig 3.6). Putative E2F target genes were used similar to those used earlier (Table 3-1).

Generally, the selected cell cycle genes showed an upregulation in the E2FB-GFP lines, as opposed to reduction that was found in the *e2fb-ko*. It was expected that the significant downregulation of genes, in all time points observed, for the *e2fb-ko 959* would perhaps lead to significant upregulation of all the tested cell cycle genes when E2FB levels are high, particularly E2FB-GFP 72 (based on ploidy and epidermal cell analysis). Interestingly, the upregulation, when compared to the WT-Col at any time point, was in general more prominent not at the youngest leaf (8 dag), but at 10 dag, when in WT-Col the exit from cell proliferation happens. The E2FB dose effects were not followed in the same way as the E2FB transcripts (Fig 3.6) by the different cell cycle genes presented here (Fig 3.6).

Genes *CDKB1;1*, *CYCA2;3* and *RBR1* showed clear increase in expression that remained dose dependent up to 12 dag, notably more significant in the case of *CYCA2;3*. It was evident in *CDKB1;1* that the strongest E2FB-GFP line (72) showed greatest expression levels (even at 15 dag expression was up compared to the WT-Col). This was also true for *RBR1* except that at 8 dag E2FB-GFP 72 and E2FB-GFP 114 were both up by 2 fold, the lowest expressing line (for E2FB protein, E2FB-GFP 61) remained relatively similar to the WT-Col for both *CDKB1;1* and *RBR1*. Both *CDKB1;1* and *RBR1* were up at 12 dag in E2FB-GFP 72. *CYCD3;1* and *MCM3* expression were only slightly up compared to the WT-Col at 10 dag. Particularly, the elevation of the two DNA-synthesis-related genes *MCM3* and *ORC1* did not correlate with the E2FB doses and was highest with medium levels of E2FB. For *ORC1* this data was not very significant except that at 15 dag *ORC1* was downregulated.

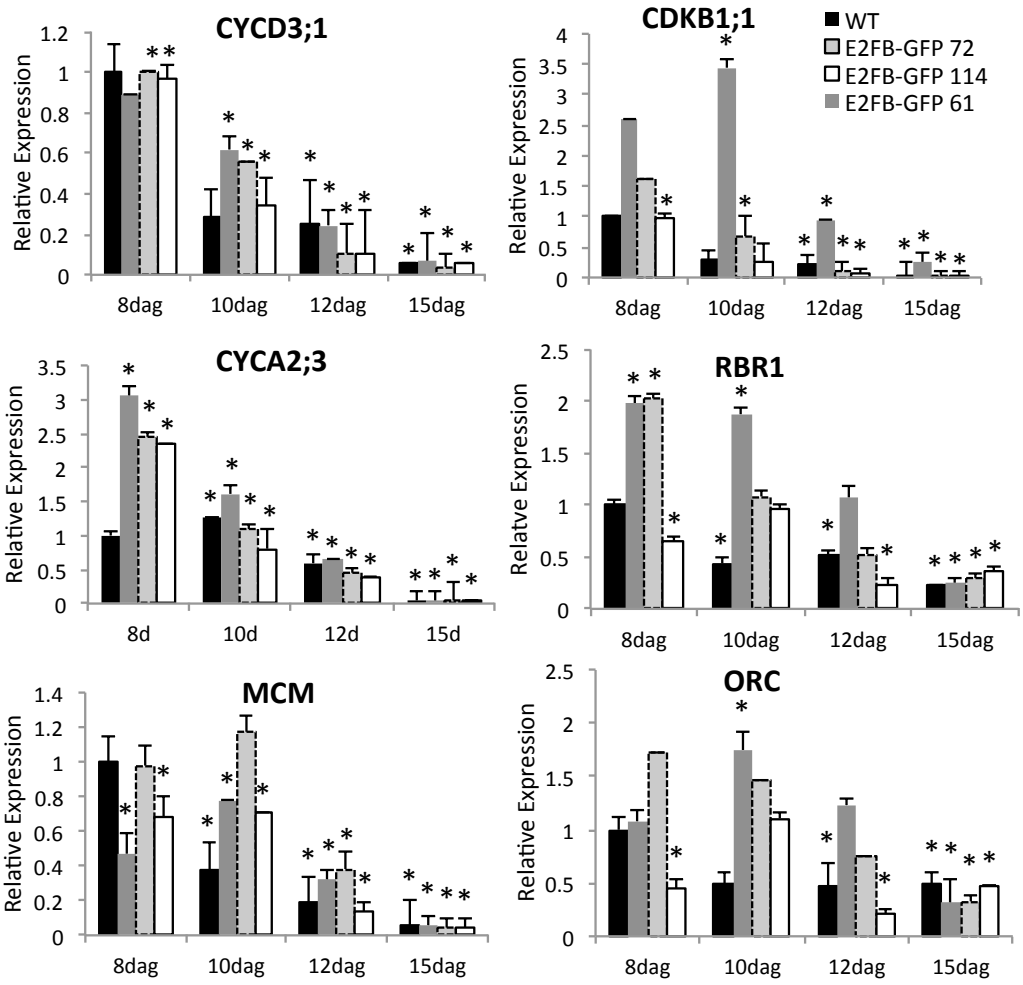

Figure 3-6 The expression of cell cycle genes in E2FB-GFP lines

First new leaf pair in WT-Col (black bars), E2FB-GFP 72, 114 and 61 (high, medium and low expressors, respectively, shown via gradient of grey bars) were harvested over 8, 10, 12 and 15 dag. The reference point in each gene is the WT-Col 8 dag. Elevated E2FB levels in the E2FB-GFP lines cause different behaviour patterns in transcripts of different cell cycle genes. Error bars represent standard deviation. Asterisks (*) represent statistical significance (95% confidence interval) based on randomisation and bootstrap tests by the REST2009 software (Pfaffl *et al.,* 2002). Data is based on 3 technical replicates.

3.5 Ectopic overexpression of E2FB/DPa using 35S-CaMV promoter

Ectopic overexpression of E2FB with the 35S-CaMV promoter, in conjunction with co-overexpression of DPa was also generated by Dr Zoltan Magyar (Magyar *et al.*, 2000; Magyar *et al.*, 2005). This line is denoted 35S::HA-E2FB/DPa. Previously this line was used to study the effects of auxin dependent cell division in tocacco BY2 cultured cells (Magyar *et al.*, 2005). With the same construct we generated transformed *Arabidopsis* plants to show how E2FB/DPa co-overexpression affects leaf development using flow cytometry in NL 1/2 series. Notably this line is different to the constitutively expressed E2FB line mentioned in (Sozzani *et al.*, 2006) as DPa was not overexpressed in that study. Epidermal cells and cell cycle related gene transcripts were analysed too. Comparison of this line was made to the WT-Col as well as to the E2FB-GFP line.

3.5.1 **Cotyledon curvature in the 35S::HA-E2FB/DPa line**

Leaf geometry, in particular curvature, was discussed earlier for the E2FB-GFP 72 line (section 3.4.1). Cotyledons of the 35S::HA-E2FB/DPa line showed greater curvature, with a more convex adaxial side (Fig 3.7A). In contrast to the E2FB-GFP 72 line, the 35S::HA-E2FB/DPa cotyledon had a different shape compared to the WT-Col; the cotyledon appeared larger but curved and greater in length in the basipetal direction evident at 10 dag and 15 dag images. As previously mentioned these observations were noted but in a follow up section of this chapter where leaf geometry phenotypes were quantified and compared with the WT-Col and other E2FB transgenic lines (section 3.7).

3.5.2 **Ectopic overexpression of E2FB does not alter ploidy level but increases the proportion of cells in S phase**

The ploidy level of cells in the 35S::HA-E2FB/DPa and WT-Col were similar at 8 dag in NL 1/2 (Fig 3.7B). At 10 dag cells enter 8N ploidy levels in the WT-Col and 35S::HA-E2FB/DPa line, the 2N and 4N nuclei percentage of cells remained similar.

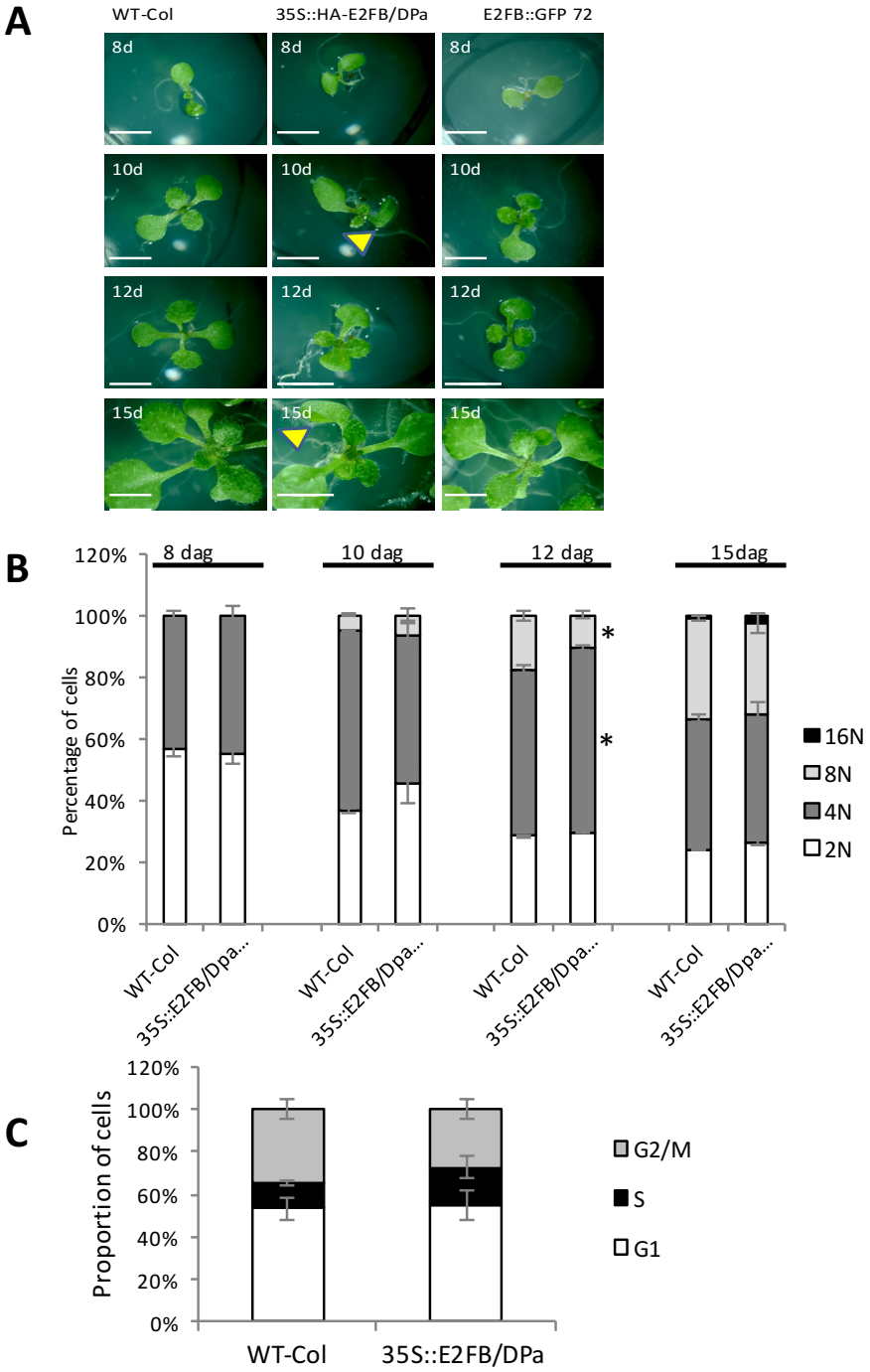

Figure 3-7 Analysis of constitutively expressed E2FB, 35S::HA-E2FB/DPa

A) Images of seedlings over 8, 10, 12 and 15 dag (top to bottom order) to show cotyledon curvature indicated by yellow arrow head in extreme case. (**B)** Flow cytometry analysis of the first leaf pair over 8, 10, 12 and 15 dag was carried out in WT-Col and 35S::HA-E2FB/DPa. All error bars represent standard deviation of data from two individual experiments with an average of 12 technical replicates. * = significance, *t*-test, $p<0.05$. Overall, ploidy status appeared not to be altered in the 35S::HA-E2FB/DPa line. However, a greater proportion of cells were in S phase (8dag) (see **C**).

Although the percentage of cells in 8N at 10 dag suggest slightly more endoreduplication in the 35S::HA-E2FB/DPa line compared to the WT-Col, this is insignificant based on *t*-test where p>0.05. However, at 12 dag the 8N proportion of cells increased in the WT-Col where as 35S::HA-E2FB/DPa remained similar to that of 10 dag and are significantly less than the WT-Col: at 12 dag the 35S::HA-E2FB/DPa line indicated a delay in the exit from proliferation, without excluding the possibility that this may coincide with a slow progression of the cell cycle and entry into endoreduplication. At 15 dag the results for ploidy levels of cells in the 35S::HA-E2FB/DPa were similar to the WT-Col. Overall, these results showed that nuclei content of cells in the 35S::HA-E2FB/DPa was similar to the WT-Col with no obvious delay in the exit from proliferation. This was anticipated because a delay in exit from proliferation was observed in the E2FB-GFP 72 line, where E2FB levels were up too. Also note that constitutive expression of E2FB alone moderately increased ploidy levels (for 35S::HA-E2FB/DPa I observe this at 10 and 15 dag but this is statistically insignificant). However, at 12 dag there is less ploidy and this is significant (based on a pool of two experiments with at least six biological replicates each). Cell cycle analysis is of the same data where cells in the S phase have an intermediate amount of DNA between 2N and 4N. Moreover, cell cycle analysis of the 8 dag sample revealed greater S phase activity in the 35S::HA-E2FB/DPa line (Fig 3.7C) inferring that the moderate increases in the ploidy levels in 35S::HA-E2FB/DPa are not due to a slow progression of the cell cycle (in time) but could in fact suggest the opposite: assuming cells progress faster or that more cells are synthesising DNA and dividing.

3.5.3 **The proportion of small epidermal cells increase in the 35S::HA-E2FB/DPa line**

Cotyledon adaxial epidermal cell analysis revealed many more small cells in the epidermis of the 35S::HA-E2FB/DPa as opposed to the WT-Col (Fig 3.8A). In comparison to the WT-Col, epidermal cells appeared smaller in size and greater in number at the same area, consequently, the number of stomata appeared increased too (but stomatal index, SI, was similar to the WT-Col, see later section 3.8).

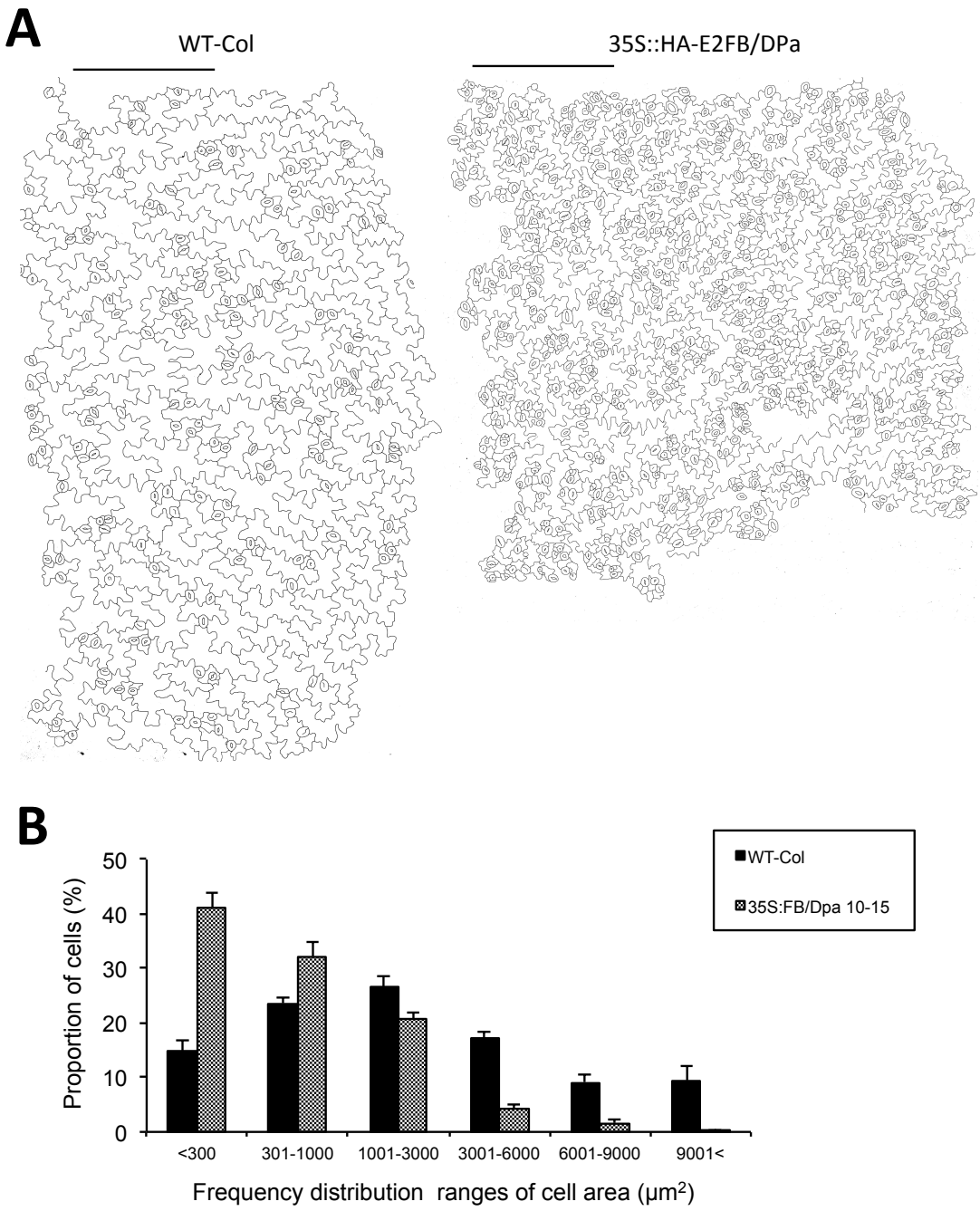

Figure 3-8 Cells are smaller in size in the constitutively expressed E2FB line, 35S::HA-E2FB/DPa

A) Epidermal cells for half the cotyledon (of 10 dag) were manually drawn as described in methods. Scale represents 1000 µm. **B)** Frequency distribution of epidermal cells shown in A, for WT-Col (black bars) and 35S::HA-E2FB/DPa. Based on triplicate samples. Error bars represent standard error. In both cases the data is not from a normal distribution (Shapiro-Wilk test, $p>0.05$, see text).

Measuring the cell area showed that the greatest proportion of cells lay within the less than 300 μm^2 range and depleted in the 3001-9000 μm^2 range to very few cells (Fig 3.8B). No cells were found above 9000 μm^2. Based on the Shapiro-Wilk test the calculated W was below the critical W and $p<0.05$ (rejecting the null hypothesis, that the data is from a normal distribution). The Q-Q plot shows the data is distributed similarly to the WT-Col but the right side has more outliers (see appendix. 3.4).

Epidermal cell analysis revealed largely increased cell numbers (twice as many) and reduced size for 35S::HA-E2FB/DPa (compared to WT-Col). It was therefore surprising that the flow cytometry data (Fig 3.7B) did not show significant differences in the timing of the entry into endoreduplication over the time course.

3.5.4 **Putative E2F target genes are upregulated upon ectopic E2FB overexpression**

Gene expression analysis was carried out on NL 1/2 at 8, 10, 12 and 15 dag. The *E2FB* mRNA was elevated, up to ~100 fold in 35S::HA-E2FB/DPa line (Fig 3.9) (notably greater than E2FB-GFP 72, Fig 3.6). The relative expression of all other genes was significantly (shown by *) higher in the 35S::HA-E2FB/DPa line (Fig 3.9). Cell cycle genes, as expected, were highly expressed during the early developmental stages of NL 1/2 in the WT-Col and were downregulated by 15 dag in parallel to the gradual cessation of cell proliferation. In contrast, with the line 35S::HA-E2FB/DPa the highest expression levels of cell cycle genes were at 10 dag; *E2FB*, *CYCD3;1*, *RBR1*, *CYCA2;3,ORC1*, at ~100, 3.5, 8, 7 and 8 fold, respectively. However, it was noted that data for *ORC1* were statistically insignificant based on the REST2009 analysis. For *CDKB1;1* 8 dag and 10 dag transcripts were both ~7 fold up and *MCM3* was up by ~3 fold with 8 dag being the peak of expression in both genes, not 10 dag as described for the other cell cycle genes. In summary, upon E2FB overexpression in the 35S::HA-E2FB/DPa line the putative E2F target genes were significantly upregulated during the development of NL 1/2. This upregulation was clearly maintained during the course of the 8 - 15 dag time period of NL 1/2 development, when E2FB was constitutively expressed.

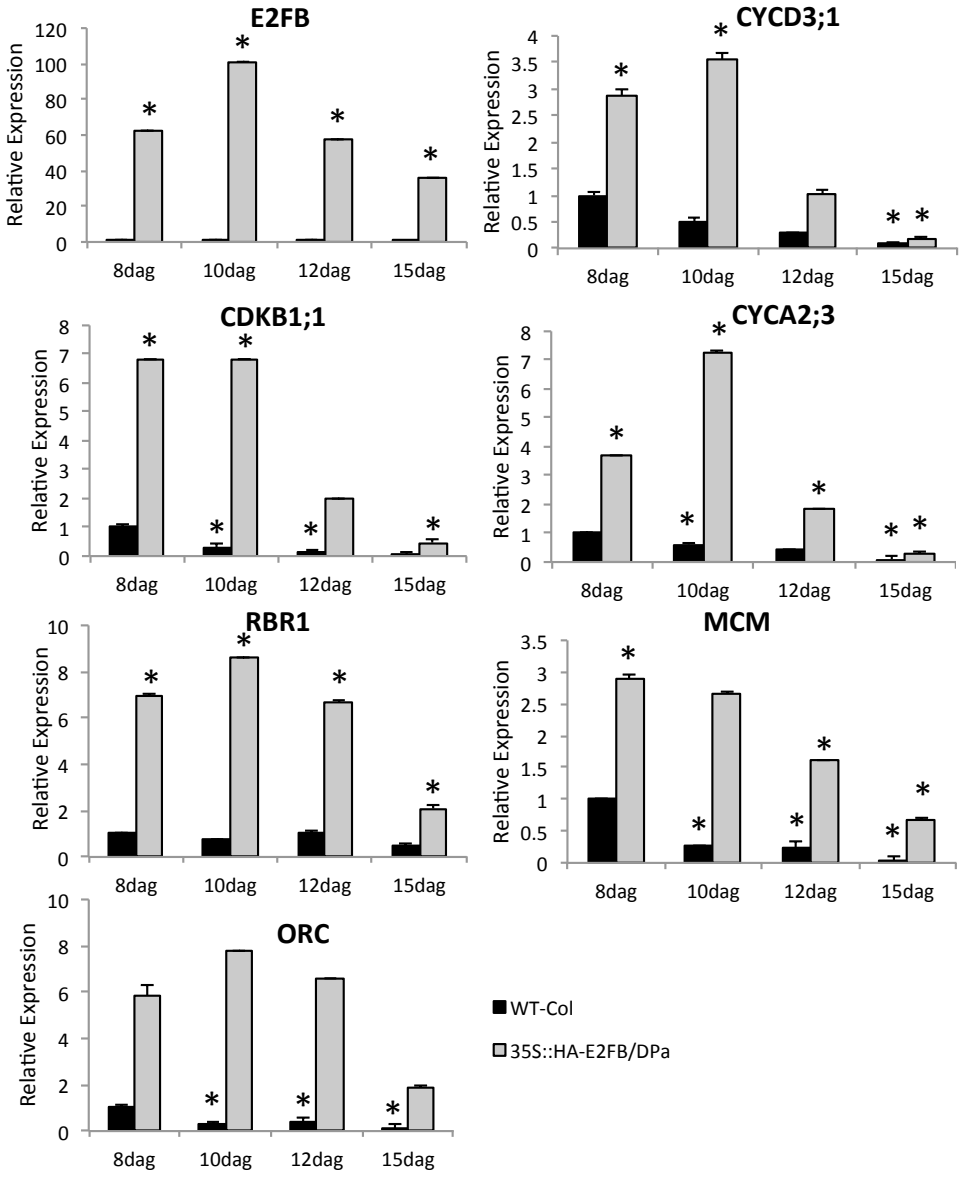

Figure 3-9 Cell cycle gene transcripts are upregulated in 35S::HA-E2FB/DPa

First new leaf pair in WT-Col (black bars) and constitutively expressed E2FB line, 35S::HA-E2FB/DPa (grey bars) were harvested over 8, 10, 12 and 15 dag. The reference point in each gene is the WT-Col 8 dag. Error bars represent standard deviation. Asterisks (*) represent statistical significance (95% confidence interval) based on randomisation and bootstrap tests by the REST2009 software (Pfaffl *et al*., 2002). Data is based on 3 technical replicates.

3.6 Overexpression of a truncated E2FB mutant form with deletion of the C-terminal RBR1 binding domain, 35S::HA-E2FB$^{\Delta RBR1}$/DPa

Truncation of E2FB (1-385) resulted in loss of part of the transactivation domain as well as the RBR1 binding domain. This construct was overexpressed under the 35S-CaMV promoter together with DPa. The discovery of plant E2Fs first relied on their amino acid sequence similarities to animal E2Fs and how homologous their domain organisation was, notably the C terminal sequence present in E2Fs for RB binding is not present in plants (Lammens *et al.*, 2009). These structural predictions for plant E2Fs were validated by many follow up studies, specifically for E2FA and E2FB transactivation function was shown to be dependent on DPa (Kosugi and Ohashi, 2002; Sekine *et al.*, 1999).

3.6.1 **Phenotype of the 35S::HA-E2FB$^{\Delta RBR1}$/DPa lines**

Both 35S::HA-E2FB$^{\Delta RBR1}$/DPa lines, 1/10 and 10/x/8 showed growth retardation phenotypes but some seedlings appeared similar to the WT-Col, suggesting an unstable phenotype. Some seedlings showed a 3 cotyledons phenotype, producing subsequent 3 true leaves (Fig 3.10A). This phenotype occurred sporadically, limiting the availability of seeds to quantify this occurrence. In 35S::HA-E2FB$^{\Delta RBR1}$/DPa seedlings that showed growth retardation the adult plant had a dwarf phenotype and consequently seed production was greatly reduced due to fewer branches and siliques.

3.6.2 **The 35S::HA-E2FB$^{\Delta RBR1}$/DPa does not enter endoreduplication earlier**

Overexpression of a truncated E2FB mutant would have resulted in two possible scenarios: 1) The absence of the RBR1 binding domain would abrogate the ability to form repressor complexes on E2FB; 2) The absence of the transactivation domain towards the C-terminus, if essential for its transactivation role, would prevent genes being activated that could compromise cell proliferation.

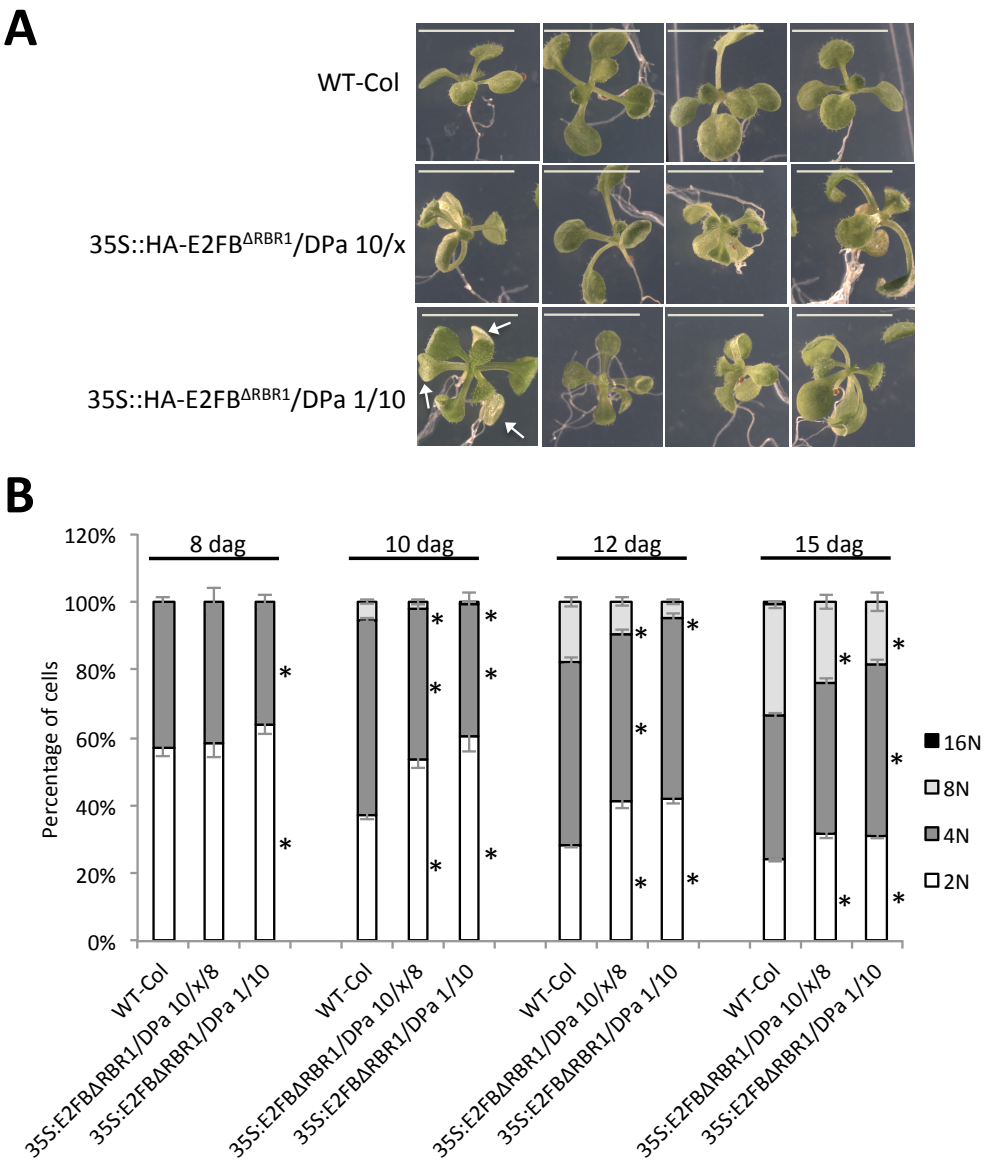

Figure 3-10 Analysis of a truncated E2FB mutant with a missing RBR1 binding domain, 35S::HA-E2FB$^{\Delta RBR1}$/DPa

A) Two independent 35S::HA-E2FB$^{\Delta RBR1}$/DPa lines (10/x/8, middle and 1/10, right) of 11 dag occasionally showed a 3 cotyledon and 3 leaf phenotype (most obvious image, bottom left, shows this with white arrows). Bar = 0.5cm. **B)** Flow cytometry analysis of the first leaf pair over 8, 10, 12 and 15 dag was carried out in WT-Col and 35S::HA-E2FB$^{\Delta RBR1}$/DPa lines. All error bars represent standard deviation of data from two individual experiments with an average of 12 technical replicates. * = significance, *t*-test, $p<0.05$.

At 8 dag the 35S::HA-E2FB$^{\Delta RBR1}$/DPa line 10/x/8 appeared similar to the WT-Col, but 35S::HA-E2FB$^{\Delta RBR1}$/DPa 1/10 had significantly greater proportion of cells in 2N, consequently significantly fewer cells in 4N (Fig 3.10B). At 10 dag both these lines had greater percentage of cells in the 2N peak (presented as a bar) in comparison to the WT-Col (10 dag) and significantly less cells entering polyploidy (low percentage of 8N). At this stage line 35S::HA-E2FB$^{\Delta RBR1}$/DPa 1/10 only entered endoreduplication (8N). At 12 dag it was more apparent that the proportion of 8N nuclei was lower in 35S::HA-E2FB$^{\Delta RBR1}$/DPa lines, line 1/10 being more prominent than line 10/x/8.

At 15 dag, in contrast to the WT-Col, both 35S:E2FB$^{\Delta RBR1}$/DPa lines did not enter further endoreduplication, as there was absence of nuclei at the 16N ploidy level (both lines had significantly fewer cells in 8N compared to WT-Col). These results indicated that partial absence of the transactivation domain delayed cells in their exit from proliferation.

3.6.3 **There are extremities of small and large epidermal cells in the 35S::HA-E2FB$^{\Delta RBR1}$/DPa**

Adaxial epidermal cells of the cotyledon were analysed for the following lines: WT-Col, 35S::HA-E2FB$^{\Delta RBR1}$/DPa 10/x/8 and 35S::HA-E2FB$^{\Delta RBR1}$/DPa 1/10 (Fig 3.11A). Pavement cells in the WT-Col appeared lobed and guard cells were evenly dispersed. In the 35S::HA-E2FB$^{\Delta RBR1}$/DPa lines cells appeared large but were less lobed, particularly for 35S::HA-E2FB$^{\Delta RBR1}$/DPa 10/x/8. The composition of the epidermis was altered with stomata appearing less evenly and in clusters, surrounded by meristemoids (the smaller cells of the epidermis). This change in spatial patterning of the epidermal cells was mirrored in Fig 3.11B of measured cell areas; both 35S::HA-E2FB$^{\Delta RBR1}$/DPa lines clearly showed two extremities, small and large cells. The first three ranges are similar to the WT-Col but in the epidermal images this similarity was less obvious as the large cells appeared to fill most of the epidermis. The data from the 35S::HA-E2FB$^{\Delta RBR1}$/DPa lines also reject the null hypothesis (null: the data is from a normal distribution) (see appendix 3.5 for Q-Q plots).

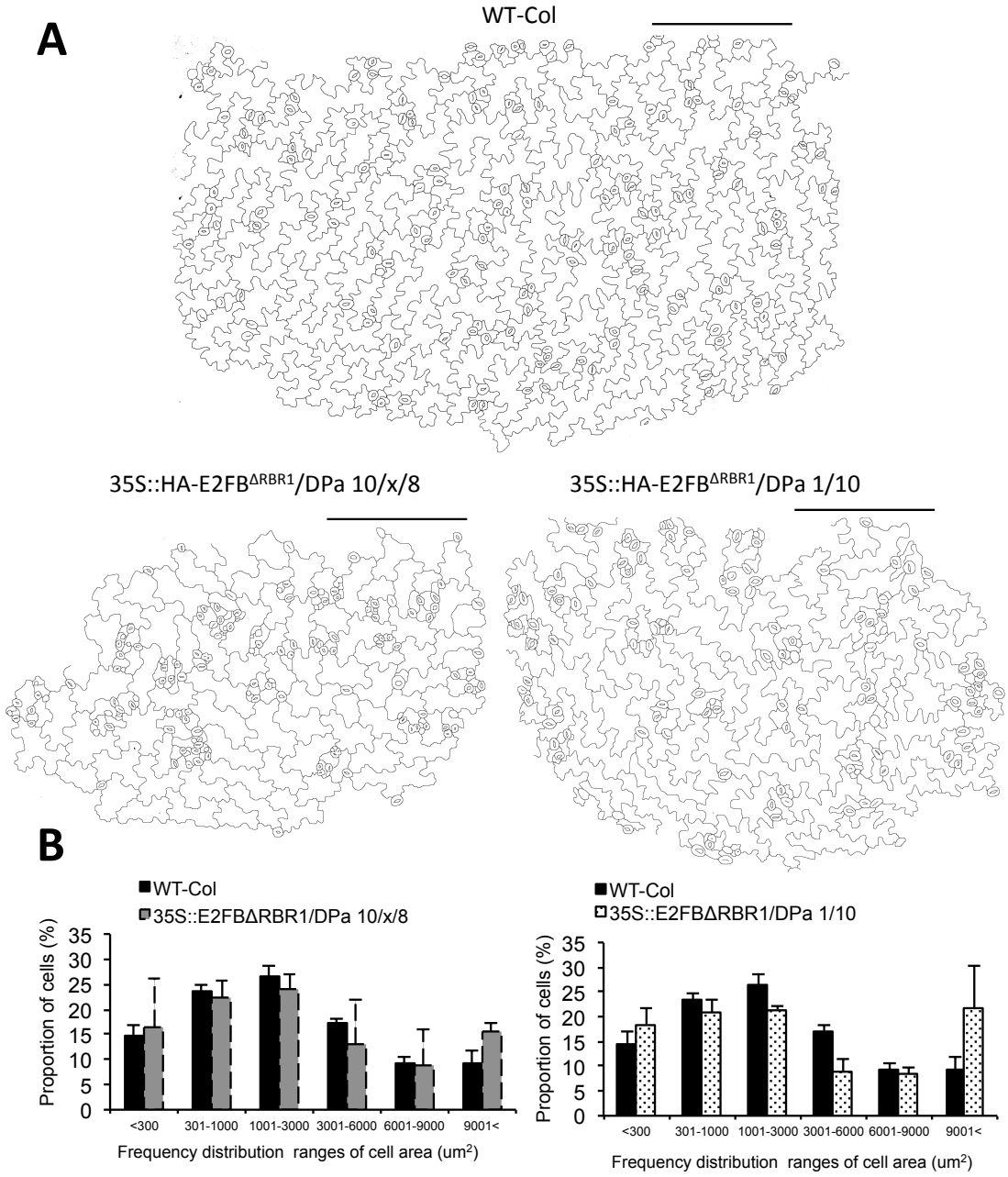

Figure 3-11 Cells are fewer but larger in the 35S::HA-E2FB$^{\Delta RBR1}$/DPa lines

A) Epidermal cells for half the cotyledon (of 10 dag) were manually drawn as described in methods. Scale represents 1000 µm. **B)** Frequency distribution of epidermal cells shown in A. Based on triplicate samples. Error bars represent standard error. In all cases data was not from a normal distribution (Shapiro-Wilk test, $p>0.05$, see text).

Also, more large cells were quantified for line 35S::HA-E2FB$^{\Delta RBR1}$/DPa 1/10, which as mentioned above had more lobed cells than the 35S::HA-E2FB$^{\Delta RBR1}$/DPa 10/x/8. Overall, epidermal cells showed clearly noticeable changes in shape and patterning in the 35S::HA-E2FB$^{\Delta RBR1}$/DPa line in comparison to the WT-Col.

3.6.4 **The expression of cell cycle E2F target genes is elevated in the 35S::HA-E2FB$^{\Delta RBR1}$/DPa line**

Putative E2F target genes were analysed via Q-RT-PCR on NL 1/2 over 8, 10, 12 and 15 dag. Genes used were the same as those used in the 35S::HA-E2FB/DPa line (annotated in Table 3.1) where all genes were upregulated.

The relative expression of both lines, 35S::HA-E2FB$^{\Delta RBR1}$/DPa 10/x/8 and 35S::HA-E2FB$^{\Delta RBR1}$/DPa 1/10, was similar except in some instances where 35S::HA-E2B$^{\Delta RBR1}$/DPa 1/10 showed slightly more upregulation compared to line 35S::HA-E2FB$^{\Delta RBR1}$/DPa 10/x/8 (Fig 3.12). This difference never exceeded more than two fold. At 8 dag, the endogenous *E2FB* levels were up at a relative expression value of ~2 for 35S::HA-E2FB$^{\Delta RBR1}$/DPa 10/x/8 but was over ~3.5 fold for 35S::HA-E2FB$^{\Delta RBR1}$/DPa 1/10. Both lines were significantly up relative to the WT-Col. At 10 dag both lines showed increased *E2FB* transcripts by ~2 fold, however, they were comparable to the WT-Col at 12 dag and only slightly up at 15 dag. In fact, this trend also applied for all genes tested but in some instances this upregulation was insignificant (*t*-test); see asterisk (*) in Fig 3.12, where $p<0.05$. Upregulation for *CYCD3;1, CYCA2;3, RBR1, MCM3* and *ORC1* was in the range of ~2.5 - 3 fold (~4.5 fold for *CYCA2;3*) at 8 dag and dropped to ~1 - 1.5 fold at 10 dag. *CDKB1;1* was the one gene with upregulation of ~4.5 fold for 35S::HA-E2FB$^{\Delta RBR1}$/DPa 10/x/8 (8 dag) and ~6.5 fold for 35S::HA-E2FB$^{\Delta RBR1}$/DPa 10/x/8 (8 dag).

The conclusions from these results can be made in comparison with the 35S::HA-E2FB/DPa line. In the 35S::HA-E2FB/DPa line putative E2F target cell cycle genes were highly upregulated throughout the 8 - 15 dag developmental time window of leaves. In the 35S::HA-E2FB$^{\Delta RBR1}$/DPa lines upregulation was also evident but it primarily happened at 8 dag and then dissipated to the level of WT-Col at 12 dag and 15 dag.

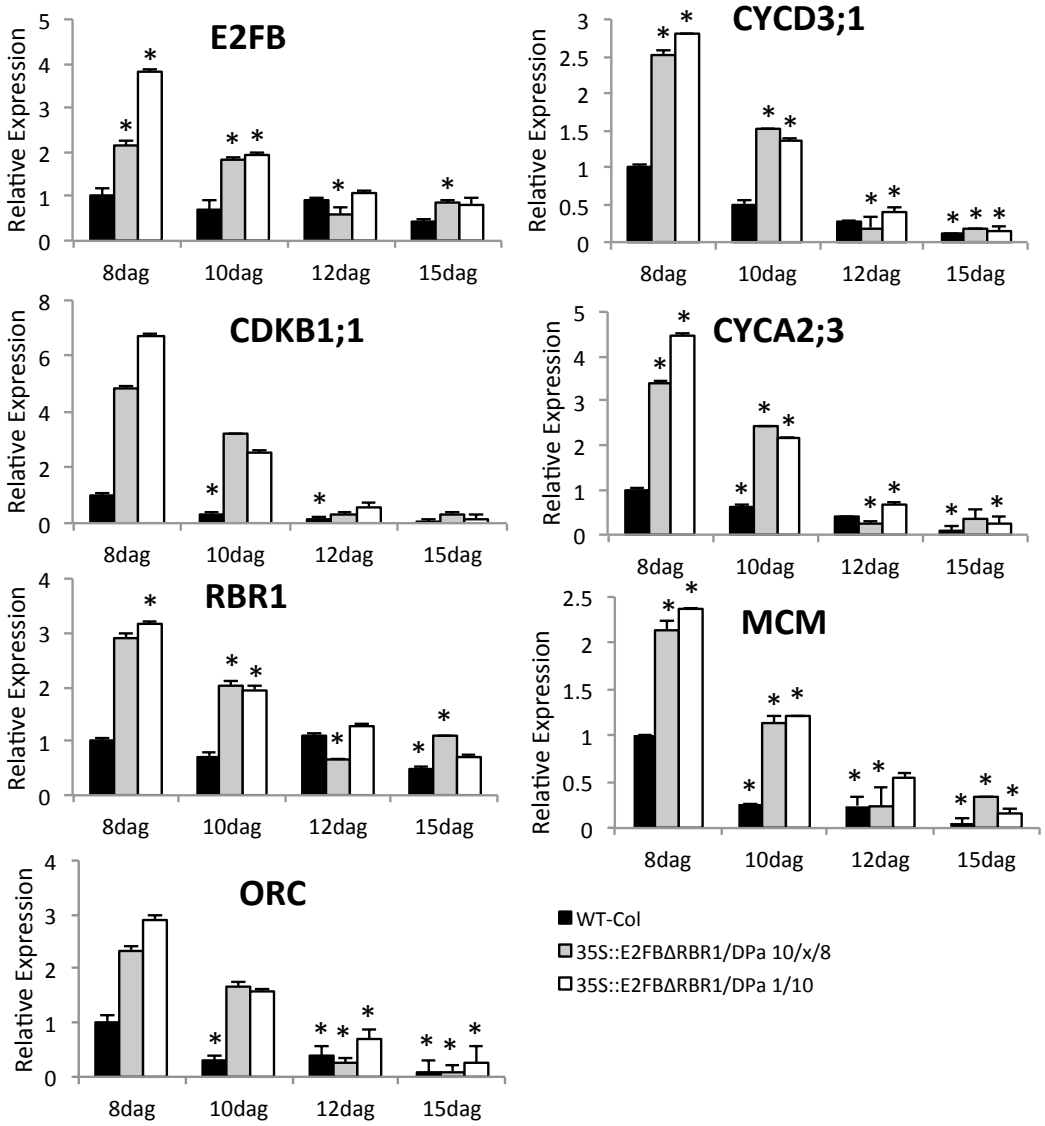

Figure 3-12 Cell cycle gene transcripts are upregulated during early leaf development in 35S::HA-E2FB$^{\Delta RBR1}$/DPa lines

First new leaf pair in WT-Col (black bars) and 35S::HA-E2FB$^{\Delta RBR1}$/DPa lines 10/x8 and 1/10 (grey and bars) were harvested over 8, 10, 12 and 15 dag. The reference point in each gene is the WT-Col 8 dag. Error bars represent standard deviation. Asterisks (*) represent statistical significance (95% confidence interval) based on randomisation and bootstrap tests by the REST2009 software (Pfaffl *et al.,* 2002). Data is based on 3 technical replicates.

These indicate that the regulation of E2FB through RBR1 binding and repression is important mainly in proliferating cells while full length E2FB level is important to determine the timing of cell proliferation. Ectopic overexpression of E2FB sustained proliferation and the expression of cell cycle genes for a longer time. The truncated E2FB could not be detected by the C terminal E2FB antibody that is used by our lab and it could detect the full length E2FB (35::HA-E2FB/DPa) (see appendix 3.6). Therefore I do not know the exact level of the truncated E2FB protein in these lines.

The increase in the proportion of both the smallest and the largest cells in the leaf epidermis in the 35S::HA-E2FB$^{\Delta RBR1}$/DPa line suggests that developmentally different cell populations might respond differently to the E2FB truncated mutant overexpression. It appears that pavement cells became abnormally large, which suggests that the abrogation of transcriptional activation function of 35S::HA-E2FB$^{\Delta RBR1}$/DPa compromised cell proliferation and led to cell cycle exit in these cells. In contrast amplifying stem cell divisions in the stomata linage appears to be sustained in the 35S::HA-E2FB$^{\Delta RBR1}$/DPa.

3.7 Quantitative analysis of leaf geometry

Previously I described the phenotypes observed in the E2FB-GFP and 35S::HA-E2FB/DPa lines as well as the growth retardations that occurred sporadically in 35S::HA-E2FB$^{\Delta RBR1}$/DPa. The leaf curving phenotype presented here is descriptive (Liu *et al.*, 2010) and quantitative (Wu *et al.*, 2007) based on the leaf Curvature Index (CI). Based on observation, the E2FB-GFP 72 line cotyledon appeared to have global longitudinal curvature (proximal-distal, base to tip) only where as 35S::HA-E2FB/DPa had global longitudinal and global transverse (mediolateral axis, middle to margin) curvature. This was not exclusive to the cotyledons. Also, the curvature in both instances was downwards.

Based on the above observation the transverse curvature downward (TCd) and longitudinal curvature downward (LCd) was calculated (based on (Wu *et al.*, 2007) (see equations below).

$$TCd = \frac{pressed\ width - lateral\ margin\ width}{pressed\ width}$$

$$LCd = \frac{pressed\ length - base\ tip\ length}{pressed\ length}$$

This was done for the cotyledons of the two aforementioned lines that were expected to have a significantly higher CI than WT-Col as well as E2FB-GFP 61. E2FB-GFP 61 was selected because visually no curvature was apparent in E2FB-GFP 61 as compared to E2FB-GFP 72 (Fig 3.13A). The averaged data (from an average of 20 biological replicates of two independent experiments) shows that TCd was significantly highest for 35S::HA-E2FB/DPa (*t*-test, where $p<0.05$) (Fig 3.13A). Both E2FB-GFP lines had a significantly higher TCd compared to WT-Col. LCd was significantly high for 35S::HA-E2FB/DPa and E2FB-GFP 61 but not for E2FB-GFP 72, with a notably large standard deviation bar (Fig 3.13B). The LCd for E2FB-GFP 72 was insignificant but unexpectedly E2FB-GFP 61 TCd was similar to that of E2FB-GFP 72 which was not evident in the descriptive curvature approach; yet the E2FB-GFP 72 seedling appeared smaller than the WT-Col and E2FB-GFP 61. Due to this discrepancy I formulated a curvature calculation based on (Wu *et al.*, 2007) to a whole seedling level (see visual aid in Fig 3.13C). This could explain the discrepancy because curvature may not be exclusive to the leaf lamina. The axis at which the petioles were aligned for the cotyledon pair was measured (and again after flattening out and pressing down, I called this global leaf pair axis curvature downward (GLPACd) (see equation below).

$$GLPACd = \frac{pressed\ leaf\ pair\ axis\ length - leaf\ pair\ axis\ length}{pressed\ leaf\ pair\ axis\ length}$$

This was done for all transgenic lines as this type of curvature was thought to easily contribute to the appearance of reduced rosette area in young seedlings. All E2FB lines, except *e2fb-ko 959*, showed significant curvature compared to the WT-Col, with E2FB 72 and 35S::HA-E2FB/DPa being similar and highest (Fig 3.13C).

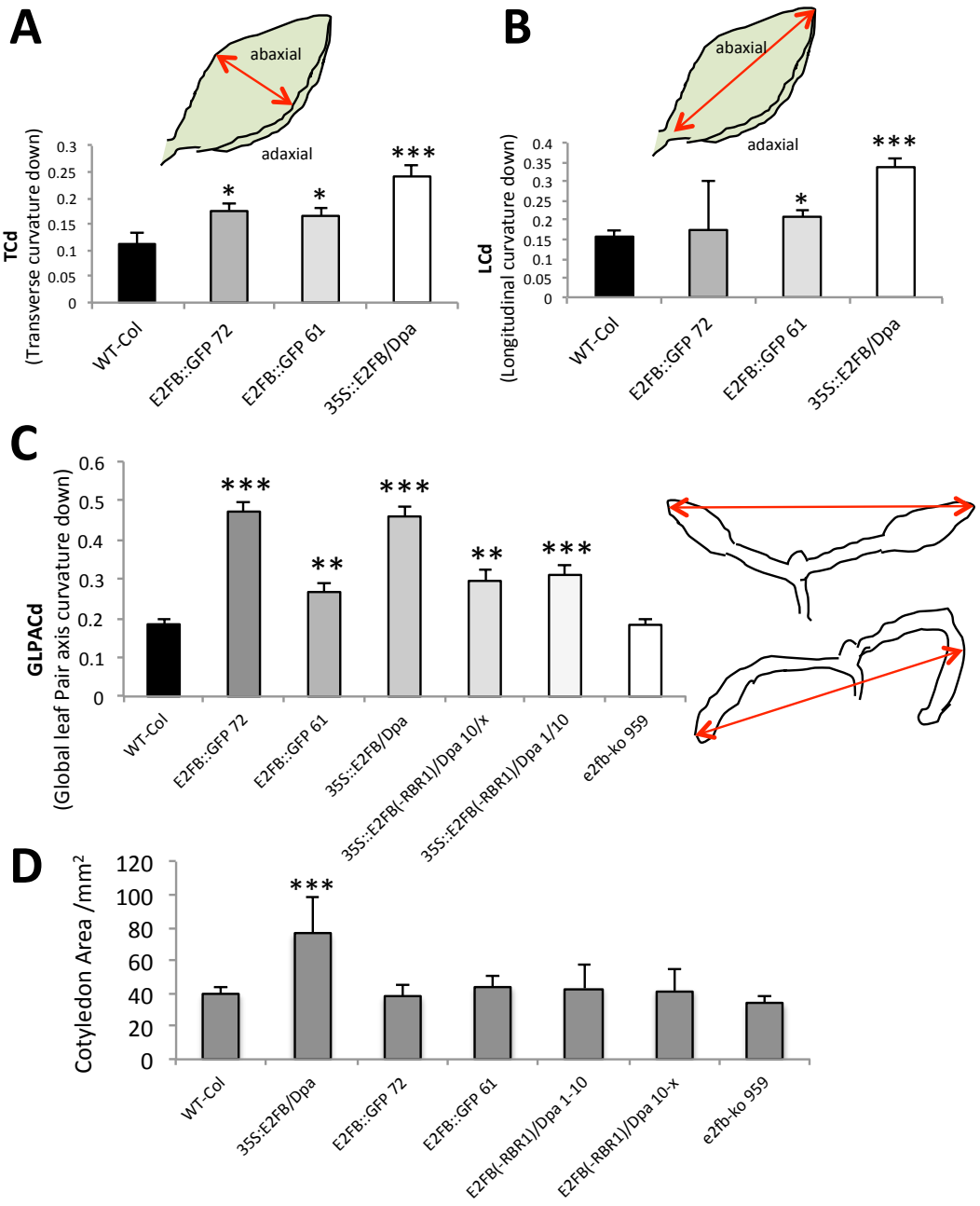

Figure 3-13 Comparison of cotyledon Curvature Index (CI) and area

The curving phenotype of leaves was measured as Transverse Curvature down/wards (TCd) **(A)** and Longitudinal Curvature down/wards (LCd) **(B)** (based on Wu *et al.* 2007) as shown in visual aid. **(C)** Global Leaf Pair Axis Curvature down/wards was measured in all lines as shown in visual aid. In A, B and C bars represent standard error of the mean of ~20 biological replicates from two independent experiments and *t*-test as $p<0.05$ *, $p<0.01$ **, $p<0.001$ ***. **D)** Cotyledon area of all lines was measured, and average of at least 20 biological replicates from two independent experiments. Bars show standard deviation and *** is where $p<0.001$, *t*-test.

Some of the initial hypotheses focused on the transition from proliferation to endoreduplication/differentiation where it was hypothesised that an early entry into endoreduplication may be associated with reduced cell number but increased cell size: a compensatory mechanism. However, this is under the assumption that the final size of the organ remains unchanged in the WT-Col and modified E2FB lines. As the epidermal images were from a cotyledon of 10 dag the cotyledon area measured was also for 10 dag seedlings so that the two may be compared. In other words one can falsely assume this as the end point (final organ size) of the given data set for which there is epidermal cell size, ploidy analysis and cotyledon area data. The data confirmed that cotyledon area in the modified E2FB lines was not significantly different to the WT-Col, except for 35S::HA-E2FB/DPa where cotyledons are significantly larger (*t*-test, $p<0.05$) (Fig 3.13D). The implications of this data and what can be inferred from it is in the discussion of this chapter.

3.8 Changes in stomata patterning

A rule of thumb is that two mature stomata must be separated by one non stomatal cell (Nadeau and Sack, 2002). I observed abnormal stomata patterning in the epidermal cell analysis of cotyledons as well as with NL 1/2. This became evident when the large area of the leaf was observed (half the cotyledon). In 35S::HA-E2FB$^{\Delta RBR1}$/DPa cells resembling stomata and meristemoids were clustered while pavement cells were large but relatively few in number (Fig 3.14A). It was also noted that 35S::HA-E2FB/DPa cells in the stomata lineage (meristemoid, guard cell precusors and guard cells) appeared greater in number and I could identify clustered stomata (Fig 3.14B). It may be assumed that this was due to the constitutive overexpression of E2FB but remarkably in the *e2fb-ko 959* it was noted that occasionally this clustering of stomata also occurred (Fig 3.14B).

It was tempting to speculate that the clustering of stomata, or its increase in number, was because of overproliferation due to abrogated RBR1 control on E2FB. Stomatal index (SI) was calculated from the half cotyledon images (Fig 3.14C) (see equation below).

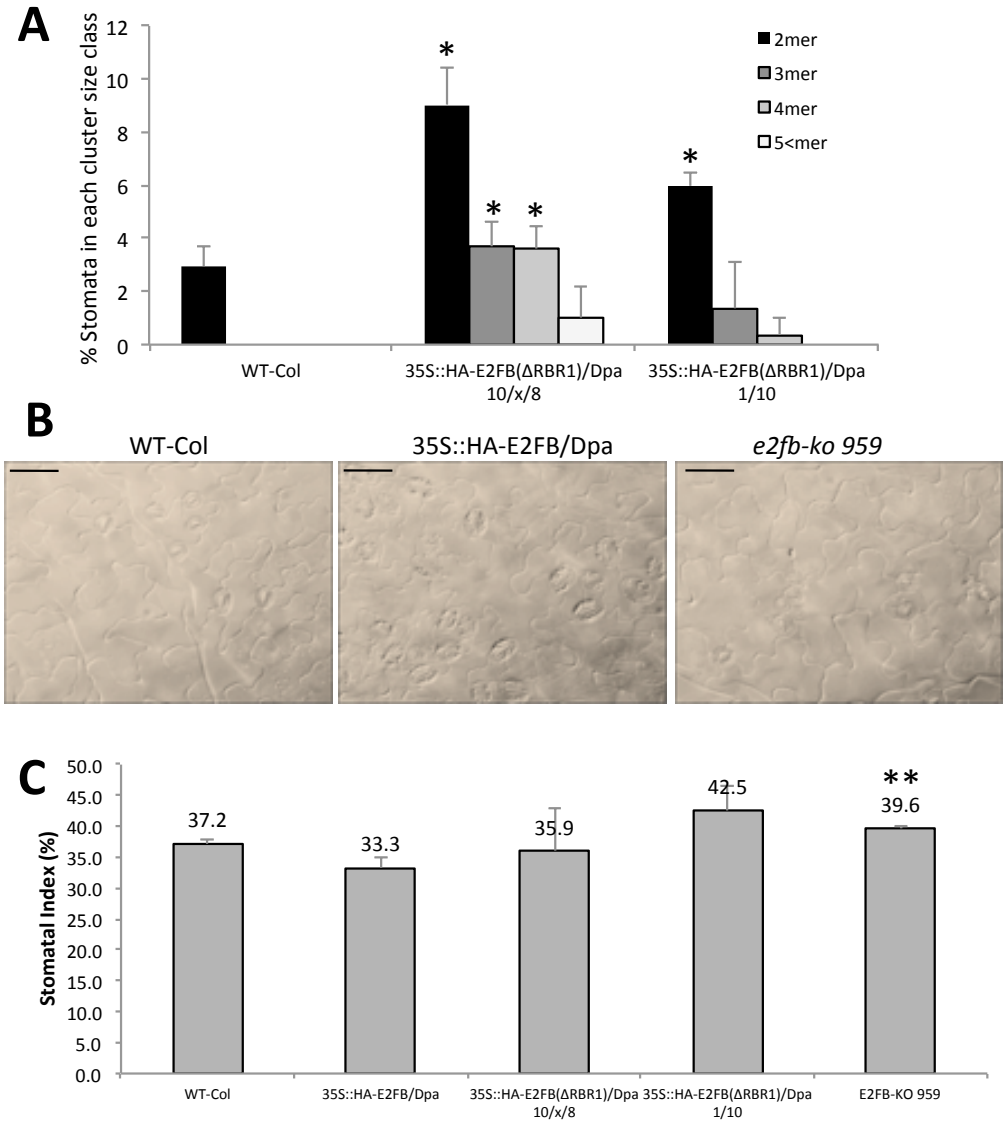

Figure 3-14 Absence, overexpression (and truncation) of *E2FB* changes stomatal patterning

A) Stomata cluster was calculated from the epidermal images for 35S::HA-E2FB$^{\Delta RBR1}$/DPa , triplicates and * = $p<0.05$, *t*-test. Bars show standard deviation. **B)** Epidermal cell analysis of cotyledons 15 dag (days after germination). Stomata appear separated, clustered and semi-clustered (not frequently) from left to right. **B)** Stomatal index was calculated for the shown lines using epidermal images used for cell size frequency distributions. Bars represent standard deviation and *t*-test performed, where $p<0.01$.

$$SI = \frac{number\ of\ Stoma}{number\ of\ Stoma + number\ of\ Epidermal} \text{X } 100$$

No significant differences in SI were found in the overexpressing E2FB lines in comparison to the WT-Col. However, *e2fb-ko 959* had a moderate but statistically significant (*t*-test, $p<0.01$) greater SI. This may be explained by the fact that although in the E2FB overexpressing lines stomata appear greater in number this is counter balanced by the increased cell number. For instance, if the number of stomata remained constant in WT-Col and 35S::HA-E2FB/DPa but only the number of epidermal cells increased in 35S::HA-E2FB/DPa, the SI would be expected to be lower for this line. Notably, in Fig 3.14B E2FB appears to affect the size of guard cells; larger in the overexpressed 35S::HA-E2FB/DPa line and smaller in the T-DNA insertion, *e2fb-ko 959*. Based on the technique I have used here quantifying this would not be accurate and feasible, also, propidium iodide staining and leaf curvature was problematic when I attempted to image leaves. By other methods this may be achieved for a large number of samples; for instance, a fluorescent tag for the plasma membrane and a microscope to easily carry out large scale imaging of the leaf area (automation of imaging and collaging leaf sectors). Additionally, the guard cells of modified E2FB level lines contained a greater number of internal structures, what appear to be chloroplasts (Fig 3.15A and B). This phenomenon was exclusive to lines where E2FB levels were up rather than down, in the *e2fb-ko 959* guard cells appeared smooth. The same observation was serendipitously made separately for 35S::HA-E2FB$^{\Delta RBR1}$/DPa 10/x/8, from a 3 cotyledon seedling (Fig 3.15B).

These data provide the first insight into the role of E2FB in guard cell patterning, and possibly their cellular differentiation. Clearly, more detailed analysis with stomata-lineage-specific markers will be required to understand the role of E2FB in stomatal development. An example would be to have the truncated E2FB line driven by two different promoters, one for the pavement cell lineage and the other for the stomata lineage. This would help to address why the two cell types respond differently in this line (and possibly others) and if crossed with a plasma membrane marker line one could solve both problems simultaneously.

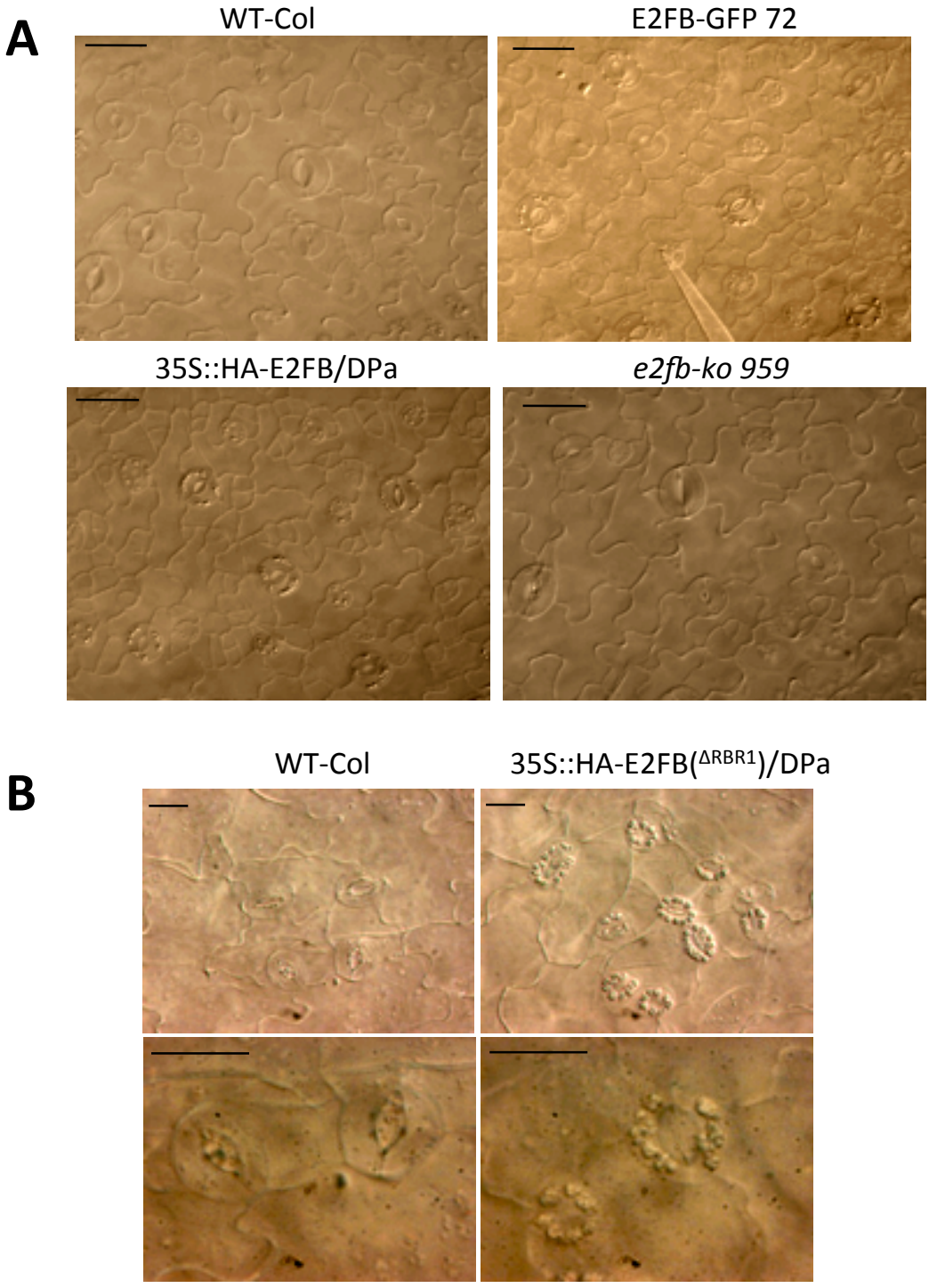

Figure 3-15 Chloroplasts in guard cells of *E2FB* overexpression lines

A) 12 dag leaf (first pair) epidermal analysis. WT-Col (top right) and *e2fb-ko 959* (bottom right) guard cells are smooth. *E2FB* overexpression causes grainy guard cells due to chloroplast accumulation (E2FB-GFP 72, top right and 35S::HA-E2FB/DPa, bottom left). **B)** 8 dag cotyledon of WT-Col (left, top and bottom) and 35S::HA-E2FB$^{\Delta RBR1}$/DPa (right, top and bottom) shows smooth guard cells in WT-Col and extensive chloroplast accumulation in guard cells of the 35S::HA-E2FB$^{\Delta RBR1}$/DPa line. Scale bar is 20 µm at x40 (top) and x100 (bottom) (B).

3.9 Discussion

The RBR1/E2F/DP transcriptional complex is regulated by CYC-CDKs and its action determines the timing of the exit from cell proliferation and the final size of an organ. In the introduction to this chapter the aims were outlined with potential hypotheses. Here I reiterate those hypotheses and the assumptions that were made are clarified and discussed further. It should be noted that some of these assumptions are described here as a result of the data and so were not anticipated at the start and in order to justify those results the assumptions have been outlined below.

The time it takes for an organ to initiate and reach its final size is called 'developmental time'. It was assumed that the length of developmental time for any organ, in this case leaf, remains constant. To clarify, this means that division (proliferation) and the transition to differentiation and endoreduplication and expansion occurs over a given time that does not change (most likely to be an *x* number of days). Based on this, the first assumption of my hypotheses is that the start (initiation) and finish (final organ size) times remain unchanged and only the time at which the transition occurs changes as a result of the levels of E2FB changing; because E2FB is hypothesised to be an activator E2F. Secondly, proliferation is assumed to cause an increase in cell number (due to division of cells) and differentiation/endoreduplication coupled with cell expansion increase cell size. The two mentioned assumptions, supported by (Bogre *et al.*, 2008; Gonzalez *et al.*, 2012), lead to assumption three: the changes in the transition time will allow compensatory mechanisms of proliferation and endoreduplication to occur (partially supported by the work of Tsukaya and colleagues). Here, for simplicity, I assume that compensation occurs without altering the final size of the organ. The fourth assumption is that RBR1 binds to E2FB via its pocket domain and supresses E2FB function. Hence, E2FB transactivation function is important for full function of E2FB to transcribe genes with an E2FB *cis*-element. Moreover, RBR1 when not bound to E2FB allows full transactivation function of E2FB where as RBR1 bound to E2FB supresses this transactivation activity; thus absence of the RBR1 binding domain (and partial transactivation domain) should prevent E2FB regulated genes from being transcribed.

With respect to hypothesis 4, the full transactivation function is necessary for E2FB to drive transcription of its regulatory genes. This is based on comparing data of 35S::HA-E2FB$^{\Delta RBR1}$/DPa lines and 35S::HA-E2FB/DPa, where genes have a low relative expression in the former (yet upregulated in comparison to WT). In 35S::HA-E2FB$^{\Delta RBR1}$/DPa it is not fully understood why cells of the same tissue type can become too large (pavement cells) or more in number and clustered, stomata and meristemoid cells (this observation is discussed below). One possible reason for partial transactivation is that some of the transcriptional activator functions are still retained in the truncated protein. My results also do not exclude the possibility that perhaps the truncated E2FB protein does not bind to DNA effectively. Contrary to this, the upregulation of selected cell cycle transcripts in my data suggests otherwise. Moreover, we know (in our lab) that CDK activity is up in this line, indicative of more cells cycling through the G1/S transition. The stability of the truncated E2FB protein can be tested in protoplasts, with the use of clycloheximide. This can be repeated with DPa co-transfection. Clycloheximide can bind to ribosomes and block the translocation step in elongation (Schneider-Poetsch *et al.*, 2010) blocking protein synthesis. By taking samples over a time course the results can be indicative of the half life and stability of the protein. An alternative method to create a truncated E2FB protein would be via the Clustered Regularly-Interspaced Short Palindromic Repeats (CRISPR) technology (Jinek *et al.*, 2012; Larson *et al.*, 2013) that can be used for targeted mutagenesis as well as truncation of a protein, discussed in this review (Barrangou *et al.*, 2015)

With respect to the primary assumption these data support the hypothesis that E2FB does affect the timing of transition (see hypotheses 1 and 2). Generally, the results indicate that more E2FB shifts the transition further, towards a delay in exiting proliferation (or as determined from flow cytometry analysis, entry into endoreduplication). This is supported by the data of *e2fb-ko 959* where cells enter endoreduplication earlier, supporting the hypothesis (3) that RBR1 repression is important. This conclusion is generalised because 35S::HA-E2FB/DPa showed subtle difference in its ploidy level in contrast to the high upregulation of transcripts. However, 35S::HA-E2FB/DPa has increased cell number, by approximately two fold compared to the WT-Col, and reduced cell size. Based on these findings the Q-RT-PCR and cellular analysis supports hypothesis 1 in contrast to the flow cytometry

data. With respect to the secondary assumption the 35S::HA-E2FB/DPa line was expected to have the greatest delay in entering into endoreduplication (as opposed to the E2FB::GFP 72) but in fact the ploidy data for 35S::HA-E2FB/DPa is very similar to the WT-Col, except at 12 dag. Differences between ploidy analysis, Q-RT-PCR and cellular analysis was not hypothesised. Another explanation may be that the cells across the leaf do not drastically change ploidy status (entry or delay into endoreduplication) over the leaf developmental time but in the given proliferation phase/window many cells of the leaf divide rapidly. This theory speculates that the length of the cell cycle changes in the sense that cells transition through phases of the cycle quickly so that more cells result from this rapid cell cycle; where 2 cells dividing in time *t* would give a total of 4 cells this would be 6 or 8 cells and *t* remains unchanged. Also, this means that the developmental time frame of the organ does not change and neither does the decision of transition into endoreduplication. In such a context it is tempting to describe this rapid description of cell cycle activity as 'hyperproliferation'.

Furthermore, based on the methods used here for epidermal cell size analysis E2FB-GFP 72 could not be measured. It would have been interesting to see if cell number increased and cell size reduced as in the 35S::HA-E2FB/DPa because E2FB-GFP 72 line entered endoreduplication much later than the WT-Col (in all time points). If the increased cell number and reduced cell size were to be observed for this line, similarly to 35S::HA-E2FB/DPa, then this observation of increased cell number and reduced cell size would be attributed to the delay in entering endoreduplication either due to constitutively expressed E2FB levels or an extra genomic copy, supporting hypothesis 1. If however in the E2FB::GFP 72 line only cell number was to increase (hypothesis 1), and no change in cell size (opposing the second part of hypothesis 1), this would be attributed to no change in the timing of the cell cycle *per se* but rather a change in the transition that allows only more cells to be produced (consider the first few assumptions). Alternatively, if cell number remains unchanged but cells become smaller then the delay in the transition to endoreduplication may be considered as a developmental delay only, with no consequence on cell compensation; more E2FB and overexpression of cell cycle genes would only affect transition time but not cell number and size, contradicting assumption 2 and opposing hypothesis 1 and 2. However, the *e2fb-ko 959* data suggests this is unlikely

because less E2FB in cells affects the transition, a faster entry into endoreduplication, and larger epidermal cells were quantified. Thus this line supports the alternate hypothesis (of hypothesis 1) and that E2FB is required with RBR1 for a repression function (hypothesis 3).

In fact most mutants of post translational regulators of CDKs and CYCs are generally reported to have leaves with fewer cells that is compensated by an increase in cell size (Blomme *et al.*, 2014) but final leaf sizes have not always been quantified in these cases. Large epidermal cells were reported in a homozygous *CDKA;1* mutant (*cdka;1*) (Nowack *et al.*, 2012). CDKA;1 is the plant homolog of cdc2 kinase (yeast) as it is the only plant CDK that contains the conserved PSTAIRE motif that is essential for CYC binding and controls DNA replication and mitotic entry of the cell cycle (Hemerly *et al.*, 1995; Ferreira *et al.*, 1991). Although the plant had large epidermal cells it appeared dwarf like too (we did not observe any changes in the development of seedlings or adult plant of *e2fb-ko*) (Nowack *et al.*, 2012). The number of cells for half the *e2fb-ko 959* cotyledons did not reduce significantly (WT-Col average cell number = 306, *e2fb-ko 959* = 221, *t*-test = 0.26, $p>0.05$). This contradicts assumption 3, as a compensatory mechanism would increase cell size but reduce cell number, although this was explicitly stated as part of hypothesis 1. In fact in 35S::HA-E2FB/DPa the increase in cell number and reduced cell size actually produces a larger cotyledon, opposing the compensation theory where by the final organ size must remain the same. This increase in cotyledon size was also reported for a similarly overexpressed E2FB line (without co-expression of DPa) but no statistical test was provided or quantification of number of epidermal cells (Sozzani *et al.*, 2006). My findings confirm that the size of the cotyledon was significantly larger and the number of cells significantly greater (WT-Col average cell number 306, 35S = 795, *t*-test = 0.04, $p<0.05$). In support of compensation, as assumed, overexpression of a dominant negative allele of CDKB1;1 (*cdkb1;1)*, that has lower kinase activity, also produces NL 1/2 with half as many cells as the WT but a compensation of very large cell sizes causes no changes in final leaf size (Boudolf *et al.*, 2004b). In agreement with my gene expression analysis data, that postulated the conclusion that cells in the *e2fb-ko* divide less than the WT-Col (due to a short proliferative phase and early entry into cell expansion) the dominant negative *cdkb1;1* overexpression line also had a lower cell division rate and cells entered

endoreduplication earlier (Boudolf *et al.*, 2004b). Notably, *CDKB1;1* expression is also down in the *e2fb-ko*. In summary these data support hypotheses 1-3 but final leaf size measurements were not considered as part of the analysis when postulating these hypotheses as part of a organ growth compensation mechanism.

Discussing the 35S::HA-E2FB$^{\Delta RBR1}$/DPa line in terms of compensatory mechanisms is difficult as growth retardation and emergence of 3 cotyledons adds complexity to data interpretation. Analysis of data that is more open to subjectivity (manually drawing epidermal cell walls or counting stomata clusters) should be carefully done and the reasons for any differences be discussed. For instance, previously it was reported that a 35S driven E2FB line lacked trichomes (Sozzani *et al.*, 2006) where as neither of the two constitutively expressed lines in these data showed such a phenotype (appendix 3.7). Whether or not this is associated with the co-expression of DPa is a possibility. E2FA overexpression alone causes ectopic divisions but co-expression with DPa causes divisions as well as endoreduplication (De Veylder *et al.*, 2002). Why E2Fs alone exert a different effect than with their DP's may be associated to dimerisation with any of the two endogenous DPs or with the co-overexpressed DP partner. Additionally, E2FB regulated under its own promoter but fused to GUS was suggested to report E2FB promoter activity at hydathodes and base of trichomes (Sozzani *et al.*, 2006). However, this must be carefully interpreted because the *in situ* observations were not so convincing in showing *E2FB* transcripts at the base of trichomes (figure 2b in *this* paper, (Sozzani *et al.*, 2006)). My experience tells me that GUS diffusion is a problem if the assay is not carried out very strictly, appendix 3.8 shows GUS at hydathodes of leaves and at the base of trichomes in the *CYCB1;1::GU*S line used in chapter 4, this is not what the reported GUS staining is like for this line (Donnelly *et al.*, 1999).

Hypothesis 4 outlined the possible dual role of E2FB by considering its activation and repression mechanism as cell type specific affects. Differences in the data do not necessary lead to the conclusion that hypothesis 4 can be supported but epidermal cell size and spatial patterning suggest there may be cell type specific affects. In any case the interpretation of ploidy level analysis, cell size and cell number data is not so straightforward because it is not necessarily correlated. As these results show compensation is not trivial and ploidy levels do not always reflect what is observed at the tissue level, for instance the ploidy levels of 35S::HA-E2FB$^{\Delta RBR1}$/DPa do not

reflect the aberrant epidermal cells spatial patterning. Shape of pavement cells should also be studied alongside pavement cell size, as pavement cells in 35S::HA-E2FB$^{\Delta RBR1}$/DPa appear less lobed. The shape factor can be calculated (Dewitte *et al.*, 2007) and plotted with cell size to show how cell roundness and size correlate. It is possible for pavement cell size to be the same in a differentiation-promoting mutant, *DEFECTIVE KERNEL1-4* (*dek1-4*), but the shape of cells is changed (Galletti *et al.*, 2015). These *dek1-4* cells also neighbour straight walls, suggesting divisions similarly to the E2FB-GFP 72. These divisions are not just limited to leaf but sepals too (Galletti *et al.*, 2015) and the paper also describes epidermal cell separation and loss of cell-to-cell contact. It would need to be confirmed if these cell wall 'malfunctions' contribute to the difficulty in cell wall identification, using the manual techniques applied in my work for epidermal cell size analysis in the E2FB-GFP 72 line. There is no certainty if this was due to the leaf placement on the slide (the focusing of the microscope) or a result of the line itself. A scanning electron microscope could resolve this as observed in a *CDKA;1* dominant negative allele (*cdka;1*), driven by a shoot meristemless promoter, with cell wall malfunctions and gaps in cell walls (Borowska-Wykręt *et al.*, 2013).

I attempted to maximise validity of the flow cytometry data presented here, at least 15,000 cells were counted per biological replicate (of which there were approximately six) and two independent experiments were pooled. In contrast to overexpression of E2FB where ploidy levels were moderately up compared to the WT-Col (Sozzani *et al.*, 2006) the data presented here show less cells entering ploidy at 12 dag only, this was the most significant result. Moreover, although the other time points show statistically insignificant data, notably more cells appeared to have entered ploidy in the other time points for 35S::HA-E2FB/DPa. Supporting the data of 12 dag overexpression of *CYCD2;1* produced leaves with smaller cells but with lower DNA content (Qi and John, 2007). In the aforementioned paper (Sozzani *et al.*, 2006) although not explicitly stated, it appears that ploidy analysis was done at 16+ dag.

Serendipitous observations lead to further analysis on stomatal clustering and index, thus they were not part of the original hypotheses. The differences observed in the WT-Col epidermal cells to the 35S::HA-E2FB$^{\Delta RBR1}$/DPa were unexpected as were the differences in guard cells of E2FB overexpressing lines. Stomatal Index (SI)

shows that E2FB does not influence stem cell divisions in the stomatal lineage but spatial distribution of stomata appears altered when E2FB levels are modified (as in 35S::HA-E2FB$^{\Delta RBR1}$/DPa). Contrary to this, absence of E2FB in the *e2fb-ko 959* has a higher SI though the data could benefit with more independent experiments. Given these data it is plausible that E2FB regulates divisions of the stomatal lineage (most likely repressing divisions as absence of E2FB increases SI) and that this mechanism may involve the ability of E2FB to form a repressor complex with RBR1 and/or DPa (the latter because 35S::HA-E2FB$^{\Delta RBR1}$/DPa has significant clustering). Similarly, both *cdkb1;1* (dominant negative mutant) and *cdka;1-ko*, (null mutant) were mentioned to have phenotypes similar to the *e2fb-ko* (in my work) and both mutants affect stomata development too. However, contrary to my findings, the *cdkb1;1* mutant shows a decrease in stomata number but does show morphological changes (Boudolf *et al.*, 2004a). The *cdka;1-ko* also shows reduced stomata number and an arrest in guard mother cells (Weimer *et al.*, 2012). This discrepancy may be due to the subjective approach in quantifying stomata and error in distinguishing guard mother cell from a smaller sized stomata. Note that *CDKB1;1* transcripts were down in the *e2fb-ko 959* (with high SI). Fortunately, the abundance of microstructures in guard cells, most extensive in 35S::HA-E2FB$^{\Delta RBR1}$/DPa lines not WT-Col or *e2fb-ko*, indicated that only guard cells were counted. These guard cells were densely packed with what are assumed to be chloroplast or chloroplast precursors, this observation was less consistent with the E2FB-GFP and 35S::HA-E2FB/DPa lines and was not observed for the WT-Col and *e2fb-ko,* as guard cells appeared smooth.

From this data it is tempting to propose that, to some extent (because they are interdependent), meristemoid/stomatal lineage cell division is independent of pavement cell division. This can be supported by the fact that kinematic analysis of leaf revealed that as cell division rate decreases over time stomatal index increases coinciding with an increase in pavement cell number early in development (5-14 days) where as guard cell number increases till day 17 (Asl *et al.*, 2011). This was further supported by their *in silico* modelling where before day 18 pavement cells had a higher relative growth rate but after this stomata grew faster than pavement cells, introducing the idea that the epidermis has differential growth rates during development. These differential growth rates may be attributed to differential growth control mechanisms by E2FB. This may explain why E2FB and RBR1 are localised

in meristemoid and guard cells shown via E2FB-GFP and RBR1-GFP (Zoltan Magyar, *personal communication*). It would need to be confirmed that the structures I have observed in guard cells are plastids. This could be done by using a fluorescent protein fused to a nucleoid-localised protein that specifically targets chloroplast nucleoids. An example of a protein that can be used is PEP-RELATED DEVELOPMENT ARRESTED1 (PRDA1), using a 35S:PRDA1-YFP construct (Qiao *et al.*, 2013). If this is validated then it may be possible that cell division and plastid/chloroplast division are not completely independent processes, they may be interdependent. Because E2FB overexpression does not increase divisions of the stomatal lineage (above I explain how this may be independent of pavement cell division) but does increase plastid structures in guard cells the argument could be as described: high E2FB dose in the cells delays entry into endoreduplication and because the exit from proliferation depends on the differentiation of the photosynthetic apparatus (Andriankaja *et al.*, 2012) one mechanism for cells to cope with this delay (or high E2FB) relies on the prevention of differentiation of plastids. So to prevent this plastids divide further, at least in guard cells of meristem layer 1. This may explain why *e2fb-ko* lacks this guard cell packing and in the instances where packing of guard cells was observed exit from proliferation was delayed or enhanced proliferation took place. The work of Andriankaja and colleagues (2012) was not based on epidermal image analysis alone but was also supported by transcriptome analysis of the leaf, which also supports the theory that photosynthesis (and chloroplast differentiation) precedes leaf cell expansion (including the mesophyll).

E2FB overexpression has previously been reported for its stimulation of cell division (Sozzani *et al.*, 2006) in a developmental context. Here I highlight that the interaction between E2FB and DPa is potentially significant in the spatial patterning of leaves, and this could not be appreciated using previous ectopically expressed E2FB lines. The use of transgenic lines with a gene dose effect, as presented here, can be more informative. Varied cell cycle gene doses have been reported in yeast (*Saccharomyces cervisiae)* (Alcasabas *et al.*, 2013), mouse (*Musmusculus*) (Abate-Shen and Shen, 2005) as well as *Arabidopsis.* This helps to further deduce the role of that gene in order to understand how the gene is involved in morphogenesis. Another example is the gene dosage effect of WEE1 (Wee1 kinase homolog) on

morphogenesis from hypocotyls in *Arabidopsis* (Spadafora *et al.*, 2012). Based on the lines used in my work the transcript level of E2FB clearly had an effect on leaf geometry, epidermal cell size, number, spatial patterning and ploidy status. A high dose of E2FB introduced curvature in the leaf organ in both the transverse and longitudinal direction, except in the case of E2FB-GFP 72 that will need more samples in order to reduce the standard error of the mean and then test for significance once this is reduced. All transgenic lines were measured for global curvature of the seedling along the leaf pair axis where high doses of E2FB increase curvature significantly and the lowered E2FB dose is similar to the WT-Col. When levels of E2FB are up cells generally delay their exit from proliferation and cell cycle transcripts were up which suggest that leaf curling is a result of increased cell division. This is supported by curling of leaf phenotype when *CYCD3;1*, (35S::CYCD3;1) is overexpressed (Dewitte *et al.*, 2003). However, where curvature exists along the leaf pair axis this does not exclude the possibility that the curvature is a result of altered cell cycle activity at the leaf blade petiole junction. The cotyledon was only larger in the 35S::HA-E2FB/DPa lines (not 35S::HA-E2FB$^{\Delta RBR1}$/DPa or E2FB-GFP) whereas constitutive expression of *CYCD3;1* (Dewitte et al., 2007) and an extra genomic copy of *CYCD3;1* (Horiguchi *et al.*, 2009) both increased leaf size.

It has previously been shown in our lab that overexpression of CYCD3;1 decreased RBR1-E2FB association but increased RBR1-E2FA association (Magyar *et al.*, 2012) and these results reiterate that CYCD3;1 and E2FB are positive regulators of cell proliferation. Overexpression of CYCD3;1 increases E2FB protein abundance (Magyar *et al.*, 2012) but here it is shown that only ectopic expression of E2FB substantially increases *CYCD3;1* transcripts, whereas the extra genomic copy of E2FB does not have the same affect, this is in fact true of all cell cycle genes tested in the ectopic E2FB line (35S::HA-E2FB/DPa).

Moreover, the data presented here are quantitative (Q-RT-PCR as opposed to semi-quantitative) and in combination with other methods, western-blot and co-immunoprecipitation for protein abundance, and Chromatin-Immunoprecipitation (ChIP), for protein-DNA interaction, can elucidate more about the behaviour of the RBR1/E2FB/DPa interaction. This work also highlights that a fine developmental time-course can prove to be more informative than ‘snap-shots’. From 8 – 15 dag

proliferation and the transition to endoreduplication is a finer but appropriate time series (Andriankaja *et al.*, 2012). Acknowledging the similarities in this work to that of (Sozzani *et al.*, 2006) a strong foundation has been set in which to study whether or not E2FB has a dual role in regulating growth and division in pavement *versus* meristemoid cells in *Arabidopsis* leaves. Such a phenomenon was elucidated for E2FA with similar constructs comparatively studied (*here;* (Magyar *et al.*, 2012). To sum up, the data presented here, although preliminary, reveals a potentially novel insight to the dual cell type specific role of the RBR1/E2FB/DP complex/pathway.

Chapter 4: Light and leaf growth

4.1 Introduction

As land plants evolved they were able to produce seeds independently of water. They nevertheless retained from their ancestors a total dependence from light as their energy source. Phytochromes are photoreceptors that were present in a common ancestor of charophyte algae and land plants (Li *et al.*, 2015). Phytochromes sense the ratio of Red (R) and Far Red (FR) light. Absorption of the FR spectra does not constitute a photosynthetic source. Nevertheless, FR light controls a specific developmental program where seeds germinate and deetiolate. This developmental programme takes an initial form, in dark conditions, known as skotomorphogenesis (Josse and Halliday, 2008). In skotomorphogenesis the apical hook does not unfold and the hypocotyl extends (Gendreau *et al.*, 1997; Vandenbussche *et al.*, 2005). Light-dependent growth is geared towards enabling photosynthesis and is called photomorphogenesis. I can define these two developmental programs as light-independent and light-dependent growth. In dicotyledonous plants embryonic leaves (namely, cotyledons) in the absence of light do not unfurl and extending the dark period does not change this. It is only in the presence of light that cotyledons unfurl and subsequent leaves emerge from the shoot apical meristem (SAM). These emerging leaves are initially defined as leaf primordia.

The deetiolation response was utilised in our lab to understand better the sequence of events underlying the development of leaf primordia (*de novo*) from the SAM (Lopez-Juez *et al.*, 2008). Our experimental set-up involved a short white light pulse (1 hour) to induce germination, transferring seeds to a total of 3 days in the dark and then transferring (the germinated, dark-grown seedlings) to light. Samples were taken upon first light exposure up till 3 days; details of this are described in chapter 1 (section 1.5.3). The ensuing global transcriptomic analysis was most informative because unlike past studies, that examined light responses but utilised whole seedlings, this involved careful dissection of a very small tissue (the shoot apex). Addressing the fundamental question as to how the light response initiates leaf growth and development, it became evident that certain genes are upregulated in the

dark and downregulated upon light exposure or *vice versa.* Some of these genes are involved, among others, in cell cycle regulation and ribosome biogenesis, demonstrating fundamental growth responses. Other genes are involved in hormonal signalling, response to energy status and transcriptional regulation, outlining potential key growth control mechanisms upon deetiolation in the shoot apex (Fig 4.1) (and cotyledon) (Lopez-Juez *et al.*, 2008) .

The work of Lopez-Juez *et al.*, 2008, best captured phytohormone responses to light, in particular the hormones auxin and cytokinin. Yoshida *et al.,* 2011, further illustrated this phenomenon in tomato shoot apices where organ initiation begins, but has not previously been shown in leaves that are re-illuminated to light from dark. Whether this phenomenon is restricted to the shoot apices or may be recapitulated in NL 1/2 (*Arabidopsis*) was asked. The AUX1/LAXI auxin import proteins are involved in vascular patterning and differentiation (Fàbregas *et al.*, 2015). In tomato leaf precise ablation of layer 3 cells causes auxin accumulation that produces wider primordia and affects phylotaxis (Deb *et al.*, 2015). Importantly, the latter is transient and with a new midvein being initiated within a few days this growth defect is quickly restored. Specifically for the leaf, low auxin establishes adaxial identity (Qi *et al.*, 2014). Clearly auxin accumulation and redistribution (drainage) is a prerequisite for leaf growth. Cytokinin response regulators include ARRs (Arabidopsis type-A response regulators) and CRFs (cytokinin response factors) (Rashotte *et al.*, 2006) that are indicative of cytokinin signalling responses even when they perform a negative, end-of-response action, for a review see (El-Showk *et al.*, 2013). Application of exogenous cytokinin to dark grown seedlings induces deetiolation (Chory *et al.*, 1994) suggesting that low cytokinin levels are needed for the dark induced etiolated growth. Understanding ethylene as a growth response regulator is more complex as it is dependent on species, tissue and cell type, see review (Van de Poel and Van Der Straeten, 2015). Ethylene positively drives cell division in the shoot, specifically in the apical hook and in combination with auxin (Raz and Koornneef, 2001). Ethylene inhibits cell division in the root apical meristem (Street *et al.*, 2015). Ethylene acts as an inducer of growth at the apical hook in the presence of light (Smalle *et al.*, 1997), specifically for EIN2 (Alonso *et al.*, 1999), as opposed to the absence of light (Bleecker *et al.*, 1988).

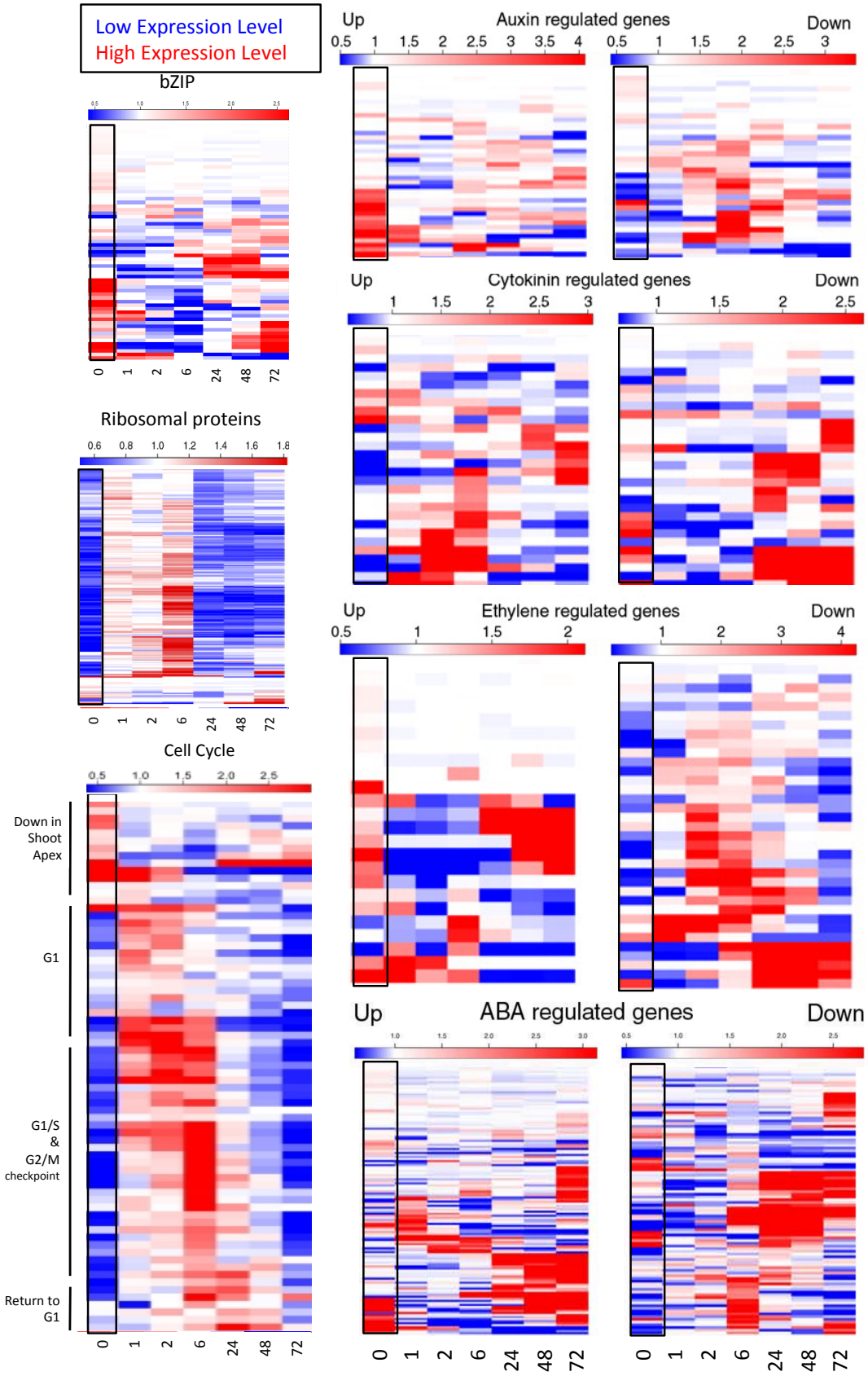

Figure 4-1 Light activated transcriptional responses in the shoot apex hypothesised to be similar to those of leaf 1/2 following a dark pretreatment (***continued on next page***)

A graphical reformatting of the heat maps (cell cycle panel maps re-drawn using R software, http://www.r-project.org/) specifically in shoot apices plus leaf primordia (SAp) during the first dark to light transfer, in the study of Lopez-Juez *et al.*, 2008. A cut off was selected prior to representing the relative expression values as heatmaps. The *x* axis represents time (hours) after transfer to light. 0 represents samples in the dark, prior to transfer, shown by a black margin for that timepoint. This representation highlights the common pattern of expression, that of to individual genes can be sought from the supplemental data of the original paper. **Left**: several bZIP were rapidly downregulated, ribosomal proteins were transiently, synchronously upregulated and cell cycle genes responded in a wave pattern during the dark to light transfer. (left, top to bottom). **Right**: auxin responsive (up) genes were up but cytokinin responsive (up) genes were down in the dark and behaved antagonistically upon light exposure. Ethylene responsive (up) genes are up in the dark and down upon light exposure. Abscisic acid genes responded to light in a less consistent manner: Some abscisic acid responsive (up) genes were transiently up upon light exposure in later time points but abscisic acid down genes were generally down in the light too. **Bottom axis** on all heatmaps reads: (SAp) 0, 1, 2, 6, 24, 48, 72 (hours) where 0 is in the dark. SAp = Shoot apex + primordia tissue.

Cloning of *TRYPTOHAN AMINOTRANSFERASE OF ARABIDOPSIS1* (*TAA1*) identified this as the original *WEAK EHTYLENE INSENSITIVE8* (*WEI8*) mutant (*wei8*) (Stepanova *et al.*, 2008). Homologues of *TAA1* are *TRYPTOPHAN AMINOTRANSFERASE RELATED1* AND *2* (*TAR1* and *TAR2*) (Stepanova *et al.*, 2008). *ABSCISIC ACID* (ABA) *DEFICIENT2* (*ABA2*) is involved in ABA biosynthesis and, once again, is representative of ABA action; as a rule of thumb ABA and ethylene are known to act antagonistically (Anderson *et al.*, 2004; Cheng *et al.*, 2009). At least in tomato endogenous ABA levels are highest in the cotyledon and hypocotyl elongation zone in dark grown seedlings (as compared to blue light grown ones) (Humplík *et al.*, 2015) suggesting that ABA drives etiolated growth and inhibits deetiolation and photomorphogenesis.

For the work in this chapter it is the behaviour of these different gene-groups that are assumed to indicate the type of responses and transcriptional reprogramming events that correlate with growth upon light perception. Although limited by the lack of knowledge of post-translational modifications, these gene expression changes suggest that these genes are regulated by a signal (light) that is perceived by the cells, the consequence of which is growth of the leaf.

Photoreceptors have redundant roles in leaf initiation upon light exposure because severe deetiolation is observed if multiple phytochromes and both cryptochromes are defective in a single plant (Lopez-Juez *et al.*, 2008). Photoreceptors are involved in light perception as sensory proteins that act as signalling intermediates in order to activate or repress the photomorphogenic response (Sheerin *et al.*, 2015).

Light is the prime environmental factor plant growth depends on and therefore light-dependent developmental processes, collectively called photomorphogenesis, are important to shape plants. Photosynthesis uses light energy to produce triose phosphate (intermediary and unstable sugar). Triose phosphates can be condensed to hexose phosphates (e.g. glucose-1-phosphate) that can later be stored as starch in the chloroplast or act as precursors of sucrose synthesis. The first few steps in either starch or sucrose synthesis is similar but the enzyme isoforms are specific to the chloroplast or cytosol. Sucrose is transported systemically in the plant and, following conversion to glucose, stored elsewhere also in the form of starch. Cells need energy to perform growth, energy that drives anabolic processes and overall growth of an

organism. Here I indistinctly use the terms 'nutritional status' and 'carbon availability' to describe the status of availability of sucrose or glucose in cells and how they are linked to growth. Low sugar levels have previously been described to induce 'starvation' genes and high sugar levels induce 'feast'' genes. For example severe carbon limiting conditions (extension of the night/dark period whereupon starch becomes exhausted) induces 'starvation' genes (as opposed to 'feast' genes) that are involved in catabolism of alternate carbon sources and limit growth (Usadel *et al.*, 2008). In the dark to light deetiolation experiment a group of basic-leucine-zipper1 (bZIP) genes was rapidly downregulated (by 1 hour, the earliest time point tested) upon light perception (Lopez-Juez *et al.*, 2008) that otherwise are expressed at very low levels. Here I describe these as starvation genes (Graf *et al.*, 2010).

Sucrose can act as a source of energy as well as a signal (Smith and Stitt, 2007). For example, photosynthetic sucrose can act as a long-range signal, from cotyledons, to regulate root elongation in early development (Kircher and Schopfer, 2012). Light can effect plant growth as a source of energy as well as a signal that is perceived by specific photoreceptors. How these two separate actions of light impact on organ growth needs to be much better understood. Because both light and sugar have dual roles, as signals and as sources of energy, both are likely to be interdependent. Light and energy-availability together can regulate carbon partitioning in a diurnal photoperiod. (Note that neither the use of the word diurnal nor photoperiod implies circadian rhythmicity). Glucose is stored in the form of starch and starch synthesis and degradation have previously been shown to be altered with changes in photoperiod (Gibon *et al.*, 2004), reviewed by (Graf and Smith, 2011). Stored starch is utilised and depleted at the end of the night (Fondy and Geiger, 1985; Geiger and Servaites, 1994; Matt *et al.*, 1998; Zeeman *et al.*, 1998). The depletion of starch is finely timed; almost all starch reserves are depleted by the time of the anticipated light period (Graf *et al.*, 2010). This is circadian clock-dependent because decreasing the length of the light period could be expected to lead to starch being consumed too soon but plants adjust the rate of starch degradation in the subsequent dark period so that starch reserves are only depleted by the anticipated light (dawn) (Scialdone *et al.*, 2013).

Leaves of dicots develop in light only, primordia initiate during photomorphogenesis. This would be consistent with a model in which extension of

the hypocotyl does not require cell division in the shoot apical meristem (in the dark) and light-dependent growth is what drives initiation of new organ primordia from the shoot apical meristem. In contrast to this, Roldan and collaborators show how the meristem can overcome the growth arrest when in contact with sucrose (Roldan *et al.*, 1999). The authors show that in the dark, if the meristem can contact the sucrose-containing agar, leaves do emerge from the meristem. However, the leaf primordia that emerge do not undergo growth as leaves would do in the presence of light, they appear poorly developed and flimsy with extended petioles (Roldan *et al.*, 1999). This shows that the meristem, when having unrestricted access to sucrose, can initiate leaf primordia (and eventually flower after the production of a number of leaves) but cannot proceed with further growth that is typical of light-dependent morphogenesis: flowering does not necessarily lead to seeds and emerging primordia do not expand or increase in size to mature leaves.

Based on this work of Roldan and colleagues (1999), carbon availability and *CONSTITUTIVELY PHOTOMORPHOGENIC* mutants are able to overcome skotomorphogenesis in the dark. However, the described further development/morphogenesis in the dark is different to that present in light (Roldan *et al.*, 1999). This suggests that some morphogenic programmes are fully light-dependent but others are not: the presence of an alternative positive signal in the dark can elicit a growth program similar to that in light-dependent growth but cannot complete it to the same extent. The implication is that a number of different growth-driving signals exist. Are there any other factors that can override the absence of light? To what extent can they do so? Understanding these potential factors can then allow experimental perturbation, similar to the one taking place when the apex directly accesses sucrose, followed by growth monitoring. One approach to solve this is to attempt to understand the molecular changes in the cells of plants upon light perception. The potential factors that cause growth are based on the gene expression analysis described earlier (Lopez-Juez *et al.*, 2008). As these data were performed on the shoot apex upon dark to light transition, these responses involved organ initiation growth, *de novo*. I wanted to test if the same responses are involved in the growth of a pre-existing organ (a partially formed leaf). This (given the larger amount of tissue present in each sample) would also overcome the difficulty posed by the fact that the method previously used is extremely time consuming. Furthermore I selected one or

two key candidate genes from the major response/factor groups (some of which are routinely used for studying a particular response) to study light dependent growth of NL 1/2. This was done similarly to the 3 day dark SAM assay (Lopez-Juez *et al.*, 2008) but was much quicker and would be easier to replicate, hence opening the door to later studies, for example enabling genetic approaches. To reiterate, the assumption here in my work is that these responses/factors correlate with growth and pertubation of these could elucidate whether these factors cause growth.

The 3 day dark period in molecular terms appears to represent a lack of carbon availability. Often proliferation-dependent growth (cell cycle activity) has been linked to exogenous sucrose availability (of intact seedlings) and the upregulation of cell cycle transcripts (Riou-Khamlichi *et al.*, 2000) or phosphorylation of RB (Hirano *et al.*, 2008). Much less is known about how cell proliferation-driven growth is regulated by light. The light signal may regulate meristem activity through regulating cell proliferation. This link was suggested by experiments that show that the light signalling proteins COP1, DET1 and CSN5 regulate the abundance (stability) of E2FB and E2FC transcription factors. For example, E2FB protein level is elevated in the light compared to the dark, and notably abundant in both light and dark in the *constitutively-photomorphogenic1 (cop1)* mutant (Lopez-Juez *et al.*, 2008). Contrary to this E2FC amount is reduced in the light. In another study it was shown that the light dependent ratio of the activator E2FB and repressor E2FC, through competition on target promoters, determines the expression of genes, such as *DEL1* which then regulates *CDKB1;1* , repressing it in a light-repressed organ (Berckmans *et al.*, 2011). Because carbon assimilation is also under light regulation (Graf *et al.*, 2010; Graf and Smith, 2011) and light can act as a signal to regulate proliferation-dependent growth (Lopez-Juez *et al.*, 2008), unravelling an association between the two was attempted and constitutes the logic behind the first part of the results for this chapter, section 4.4.

4.2 Aims and objectives

In the first part of this chapter I hypothesised that carbohydrate availability regulates cell cycle genes and cell cycle activity, and that this underlies the effect of the exposure to exogenous sucrose and also the effect of cycling light and dark (diurnal)

regulation of carbon catabolism. Exposure of intact seedlings to media +/- sucrose was used before monitoring changes in cell cycle transcripts in combination with cell cycle analysis. An endogenous carbon starvation response was induced by extending the dark period of a diurnal cycle by 4 hours (Graf *et al.*, 2010; Gibon *et al.*, 2004), and this was used as comparison for the exogenous sucrose application protocol, without a need to, for example, transfer seedlings to medium without sucrose (an experiment which would be fraught with difficulties in interpretation owing to the presence of endogenous sugar). Having established the 4 h dark-extension protocol, I hypothesised that modifying E2FB levels in *planta* would decouple the transcript behaviour of cell cycle genes from the carbon status. Lastly, I tested the contrasting hypotheses of RBR1 phosphorylation being either a direct result of light perception or a result of carbon availability, using a *plasitidial-phosphoglucomutase* (*pgm)* mutant (Caspar *et al.*, 1985) in which a defect in starch accumulation results in sugar accumulating excessively in the light and being severely depleted towards the end of the dark (Gibon *et al.*, 2004).

In the latter part of this chapter the 3 day dark protocol was establised. The hypothesis was that the light-dependent gene expression responses for morphogenesis involved in light-dependent growth of a pre-existing (but very young) leaf organ are the same as those involving organ initiation (*de novo*) in the light. If proven, one could later test genetic or external perturbations of the initiation of leaf primordia as well as of the young leaf in future studies. The alternative hypothesis would suggest that gene expression changes involved in organ initiation at the shoot apex constitute a different growth program compared to growth that occurs in a developing organ (not *de novo*), or that the first-time response to light is a unique response which cannot be replicated later on; this could possibly explain why leaves initiate in the dark when the apex has direct access to sucrose but leaves do not grow further. I have chosen to refer to the modification of the original protocol (presented in this chapter) using the term "re-deetiolation" to distinguish it from the original "deetiolation".

4.3 Short term sucrose induction in *Arabidopsis* seedlings

Two signals which are of great interest are light and nutrient (in particular sucrose) availability. Light is essential for plant growth and the availability of sugar regulates the plant cell cycle by changes in the expression of the D-type cyclins (Menges *et al.*, 2006; Riou-Khamlichi *et al.*, 2000). Sugar availability also induces changes in the phosphorylation status of RBR1 (the relative level of P-RBR1) (Hirano *et al.*, 2008). Changes in CYCD mRNA (Riou-Khamlichi *et al.*, 2000) and RBR1 phosphorylation (Hirano *et al.*, 2008) upon addition or removal of sucrose have been reported in *Arabidopsis thaliana* cell-cultures. Often, removal of a nutrient from a cell suspension culture and subsequent re-addition synchronises cells to represent specific cell cycle phases, and this has been done for sucrose (Menges and Murray, 2002). P-RBR1 positively regulates the cell cycle and its levels increase over a 24-hour period upon transfer of whole seedlings to liquid sucrose media (3%), and the reverse occurs in 0% sucrose (Magyar *et al.*, 2012).

I monitored how selected transcripts and ploidy levels change over a short time course after intact seedlings were transferred to +/- sucrose liquid media. Changes in expression of 4 key cell cycle genes (described in Table 4.1) were analysed via Q-RT-PCR and changes in DNA ploidy were analysed using flow cytometry.

Table 4-1 Gene annotation for section 4.3.1

Gene	Annotation
CYCD3;1	The product of *CYCD3;1* plays a role in phosphorylating RBR1 to balance the entry into cell proliferation and differentiation[a]
CYCA2;3	Gene *CYCA2;3* encodes an M phase enhancing cyclin [b]
CDKB1;1	The partner of CYCA2;3 is CDKB1;1, both are M phase promoting genes [c]
CYCB1;1	The B-type cyclin, *CYCB1;1*, is expressed in a more narrow window of mitosis onset, [d]

[a] (Dewitte *et al.*, 2003)

[b] (Imai *et al.*, 2006; Boudolf *et al.*, 2009)

[c] (Boudolf *et al.*, 2004b; Boudolf *et al.*, 2009)

[d] (Donnelly *et al.*, 1999; Fung and Poon, 2005)

4.3.1 **Sucrose availability upregulates the cell cycle**

Whole seedlings (7 dag) were transferred from solid medium (with 1% sucrose, under 16 h light: 8 h dark conditions) to liquid media with 1% (+) or without (-) sucrose to allow rapid access of sucrose for a short sampling timescale (before transfer, BT/0 hour (h); 6 h; 12 h; 24 h). Because absence of endogenous sucrose cannot be excluded in this experimental set up the term "sucrose deprivation" is suitable. To assess the transcriptional state of the cell cycle machinery I selected the following genes for testing: *CYCD3;1*, *CYCA2;3*, *CYCB1;1* and *CDKB1;1* (see Table 4.1).

CYCD3;1 transcripts in the sucrose-rich state were elevated at 6 h, 12 h and 24 h, and although transcript levels fell at 6 h and 12 h in the sucrose-deprived state, they increased again at 24 h (all results presented in Fig 4.2A).

CYCA2;3 expression peaks at 12 h after transfer to 1% sucrose liquid medium, after which it declined. However, in the sucrose deprived state (0% sucrose) transcript levels fell to approximately half at 6 h and gradually increased again (Fig. 4.2A). *CDKB1;1* (partner of CYA2;3) showed very subtle changes in the transcript levels upon transfer to sucrose-deprived or sucrose-rich media. For *CDKB1;1* a very subtle increase was observed at 6 h only, in the sucrose-rich (1%) state, and the greatest decline in transcripts was at 24 h post-deprivation (transfer to 0% sucrose). Similarly to *CYCD3;1*, *CYCB1;1* transcripts peaked at 6 h in 1% sucrose and in 0% sucrose transcripts declined and were least abundant at 24 h (Fig. 4.2A).

Cell cycle genes are activated in relation to the stage of cell cycle and of the four genes used here three are necessary for M phase, while *CYCD3;1* is rate limiting for the G1-S transition (Menges *et al.*, 2006). These data show that cell cycle genes, regardless of the cell cycle stage in which they are active, change in expression in response to sucrose. This suggests that sucrose signalling pathways act on both G1 and G2 checkpoint transitions. Hence, a complexity in the behaviour of the transcripts in the sucrose rich and/or deprived state was observed.

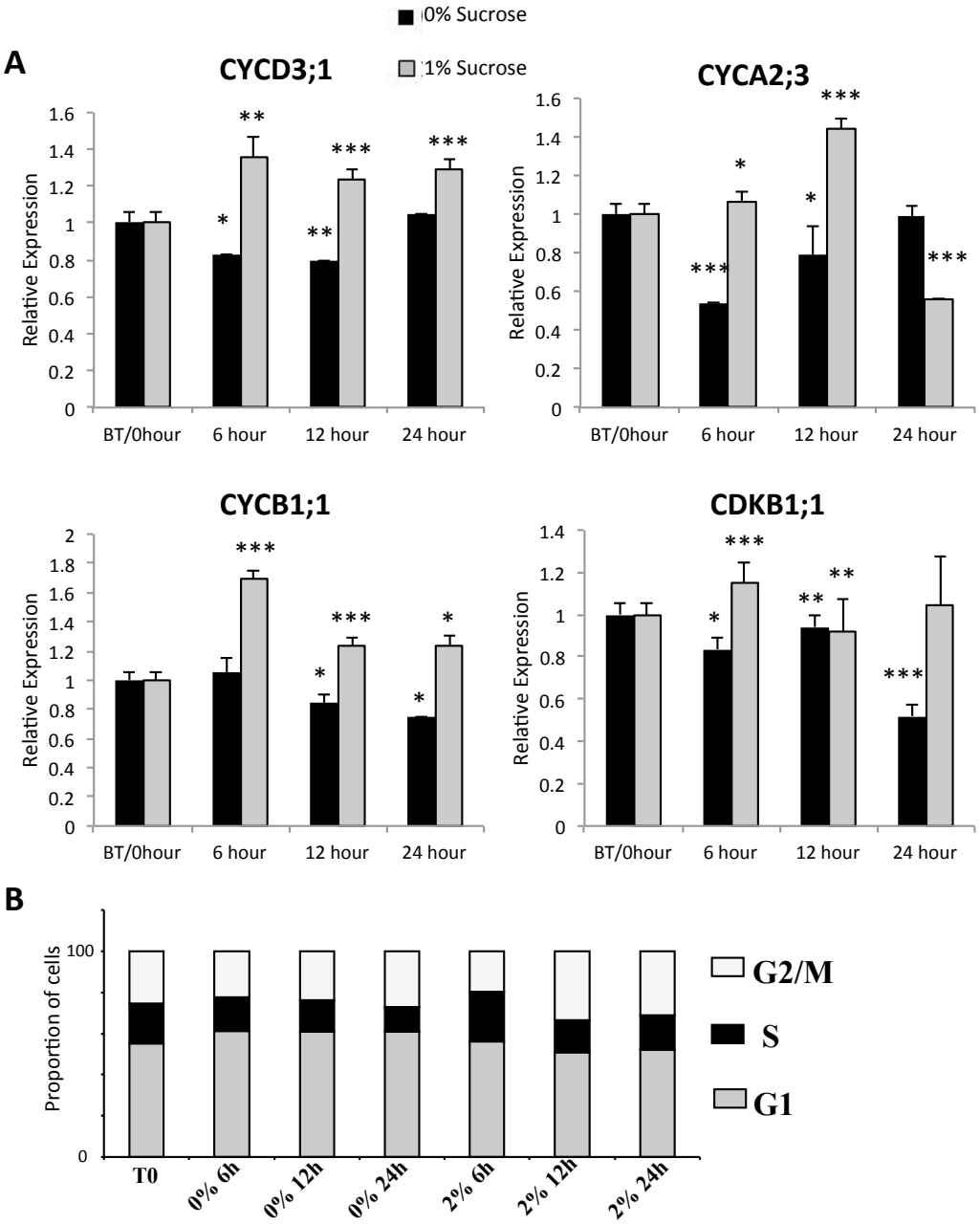

Figure 4-2 Cell cycle responses of seedlings upon transfer to +/- sucrose liquid media

A) Whole seedlings (7dag, days after germination) were transferred from solid medium (1% sucrose, under 16 h light: 8 h dark conditions) to liquid media with 1% (+) or without (-) sucrose, both in the presence of light. Transfer to 1% sucrose caused cell cycle transcripts to elevate, to a varied degree, and transfer to 0% sucrose caused transcripts to decline (some later than others). Results obtained for one sample, Significance of differences was tested for 3 technical replicates per sample, against those of the BT sample, and are therefore preliminary. $p<0.05$, $p<0.01$, $p<0.001$ as *, **, ***, respectively (*t*-test). **B)** Seedlings from (A) were also analysed for cell cycle state via flow cytometry, except 2% sucrose was used instead of 1% sucrose. Transfer to 2% sucrose caused an increase in the proportion of cells in S phase at 6 h. In 0% sucrose S phase decreased, this being most evident after 24 h. Results based on a minimum of 5 replicate samples. (Cell Cycle analysis as inferred from Partec software).

4.3.2 **Increase and decrease in S phase activity in sucrose rich and sucrose-deprived state, respectively**

Although the cell cycle genes behaved in a complex manner, it is evident that the availability of sucrose affects genes involved in mitotic activity (*CYCA2;3, CYCB1;1* and *CDKB1;1*) and the G1-S transition (*CYCD3;1*). To support the hypothesis that upregulation of *CYCD3;1* did lead to increased proliferation, flow cytometry analysis was performed and the G1, S and G2/M-phase proportion of cells inferred. The same experimental set up was used as in section 4.3.1 (except for the use of 2% sucrose instead of 1%, in parallel to the concentration used for the P-RBR1 blot analysis) (see methods) (Fig 4.2B).

Transfer of whole seedlings to sucrose-rich liquid media (2% sucrose) brought about an increase in S phase activity at 6 , followed by an increase in the G2/M proportion of cells at 12 h (Fig. 4.2B). In contrast, in sucrose deprived conditions (0% sucrose) S phase activity diminished over time and was reduced at 24 h, the G1 proportion of cells being modestly higher at 6 h.

These results show that exogenous sucrose supply to seedlings increased S phase, synonim of DNA synthesis, in parallel with the previous data which show that mitotic genes were up in the presence of sucrose too (Fig 4.2 A-B). Upon sucrose starvation cells reduced DNA synthesis, hence the cell proliferation cycle, and simply completed any mitosis earlier underway. This may result from the increased P-RBR1 in + sucrose and reduced P-RBR1 in – sucrose (Magyar *et al.*, 2012).

4.4 A 4 hour extended dark period as an acute starvation response

Previously in section 4.3 seedlings were transferred to 0% liquid sucrose medium as a method to induce carbon depleted conditions. Use of the 4 hour extended dark protocol introduced an endogenous carbon starvation period (Graf *et al.*, 2010; Gibon *et al.*, 2004) when used with seedlings grown on solid MS agar/medium. This makes it a valuable tool for analysis regarding carbon utilisation and carbon storage, highlighting diurnal regulation of starch synthesis and degradation as mentioned in

the introduction to this chapter. Here this, amongst other experimental systems, was used to associate diurnal cycles and the acute starvation response to the cell cycle.

The endogenous carbon starvation response was achieved by growing seedlings in 12 h light (L) 12 h Dark (D) cycles (12 h L: 12 h D) and extending the night period by 4 hours at 9 dag. Hence, four sampling time points arise; before dark (BD) (before the night begins), after dark (AD) (at the end of the night, just before expected dawn/light), 4 hours light (4hL) (4 hours after dawn/light) and 4 hours extended dark (4hD) (4 hours extension of the night, which would otherwise be equivalent to the 4hL), see visual aid (Fig 4.3A). Genes used to validate the 4hD experimental system are annotated in Table 4.2.

Table 4-2 Gene annotation for section 4.4.1

Gene	Annotation
CCA1	CIRCADIAN CLOCK ASSOCIATED1 (CCA1) is circadian regulated.[a], peaking at dawn. Its transcript stability is further regulated by light as it is stable in dark and far-red lightconditions but its mRNA has a short half life in red and blue light.[b]
PIF5	PHYTOCHROME INTERACTING FACTOR5 (PIF5) is a beta helix loop helix,(bHLH),transcription factor active in the dark and whichis degraded by the light activated form of phytochromeB.[c]
ATL8	ATL8 is a starvation gene with clear diurnal regulation in 4h extended dark assay.[d]

[a] (Wang and Tobin, 1998) [b] (Yakir *et al.*, 2007)

[c] (Lorrain *et al.*, 2008)

[d] (Graf *et al.*, 2010)

4.4.1 **Validation of the 4 hour extended dark experimental system**

Three genes were used to validate the 4 hour extended dark experimental system, *CCA1*, *PIF5* and *ATL8* (Fig 4.3B). Transcripts of *CCA1* were up in the AD sample (night/day transition, dawn) but were reduced in the 4hL as well as 4hD. The latter may be due to its circadian function. An important feature of the circadian clock is its ability to be entrained by environmental signals such as changes in light or temperature but this could affect transcript stability. Correspondingly to the protein stability regulation, *PIF5* transcripts are upregulated in the 4hD relative to the BD

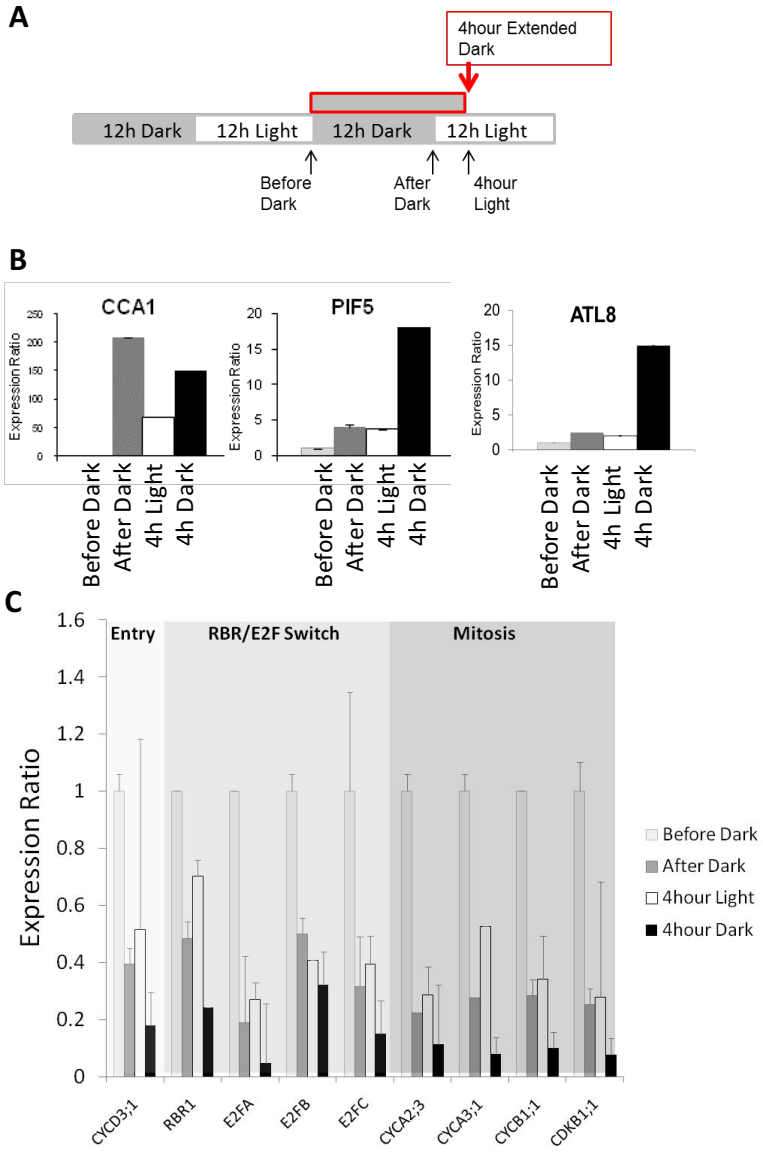

Figure 4-3 A 4 hour extension of the night links cell cycle gene transcript levels to light and endogenous carbohydrate availability

A) Schematic diagram to show sampling/time points of the 4 hour extended experimental system. (Based on the protocol by Gibon *et al.,* 2004.) The sample labelled "Before Dark" was harvested at 9dag and was used as the reference point for Q-RT-PCR analysis, shown in (B) and (C). **B)** Validation of the 4 hour extended dark system using genes *CCA1* (a circadian-regulated, morning gene), *PIF5* (a dark-induced gene whose protein is degraded in light) and *ATL8* (a starvation gene, used by Graf *et al.,* 2010). **C)** Whole seedlings were harvested as described in (A). Cell cycle transcripts behaved in a similar manner in this experiment, higher in the evening, a slight increase 4 h into light and lowest expression levels in 4 h extended dark. This pattern persists regardless of the phase of the cell cycle the gene is expressed in. Results of one sample in a single experiment. Error bars show standard timepoint (Fig 4.3B). Lastly, the starvation gene *ATL8* is significantly upregulated in the extended dark conditions (4hD) as expected because carbon starvation and deviation between 3 technical replicates. Most data in **B** and **C** have been reproduced in an independent experiment (see appendix 4.1). Plates contained 1% sucrose in both experiment.

upregulation of this gene in extended dark conditions has previously been reported (Graf *et al.*, 2010). From this data the 4h extended dark experimental system was working in our given conditions. This data has been reproduced in an independent experiment (appendix 4.1).

4.4.2 **Similar transcript behaviour of cell cycle related genes**

The 4 h extended dark system was further used to link diurnal, endogenous, carbohydrate availability to cell cycle related genes. Genes selected for this experiment played a role in cell cycle entry or were components of the RBR1/E2F switch (*CYCD3;1, RBR1, E2FA, E2FB and E2FC*) or onset of mitosis (*CDKB1;1, CYCA2;3, CYCA3;1 and CYCB1;1).* These genes were analysed for putative E2F elements in their promoter regions (for a summary table of core cell cycle genes with potential E2F elements see appendix 3.1) so that patterns in diurnal regulation of any gene may be studied in E2FB mutant or over-expressing lines (section 4.4.3).

Cell cycle genes of the RBR1/E2F pathway (*E2FA, E2FB, E2FC* and *RBR1*), mitosis onset (*CYCA2;3, CYCB1;1, CDKB1;1, CYCA3;1*) and the cell cycle entry cyclin (*CYCD3;1*) all showed transcripts to be low at the end of the night in the AD time point (Fig 4.3B). Remarkably, all appeared to show further reduction in transcript levels at 4hD when compared to the AD. Such a reduction was prevented if return to light took place (4hL).

From these results (Fig. 4.3B) it is clear that cell cycle gene transcripts tend to be at higher levels at the end of the day (BD) than the end of the night (AD). Genes are somewhat upregulated upon return to light, (4hL) and are further down regulated in the extended dark period, (4hD). Some of these data were reproduced in an independent experiment (appendix 4.1: those that were not tested are not shown not because they were not reproducible).

4.4.3 **Modified E2FB gene dose dysregulates the typical diurnal behaviour of *CYCA2;3***

It was shown in section 4.4.2 that cell cycle genes have a pattern where transcript levels are lowest in the 4hD and appear to be upregulated by light (Fig 4.3B). The 4h

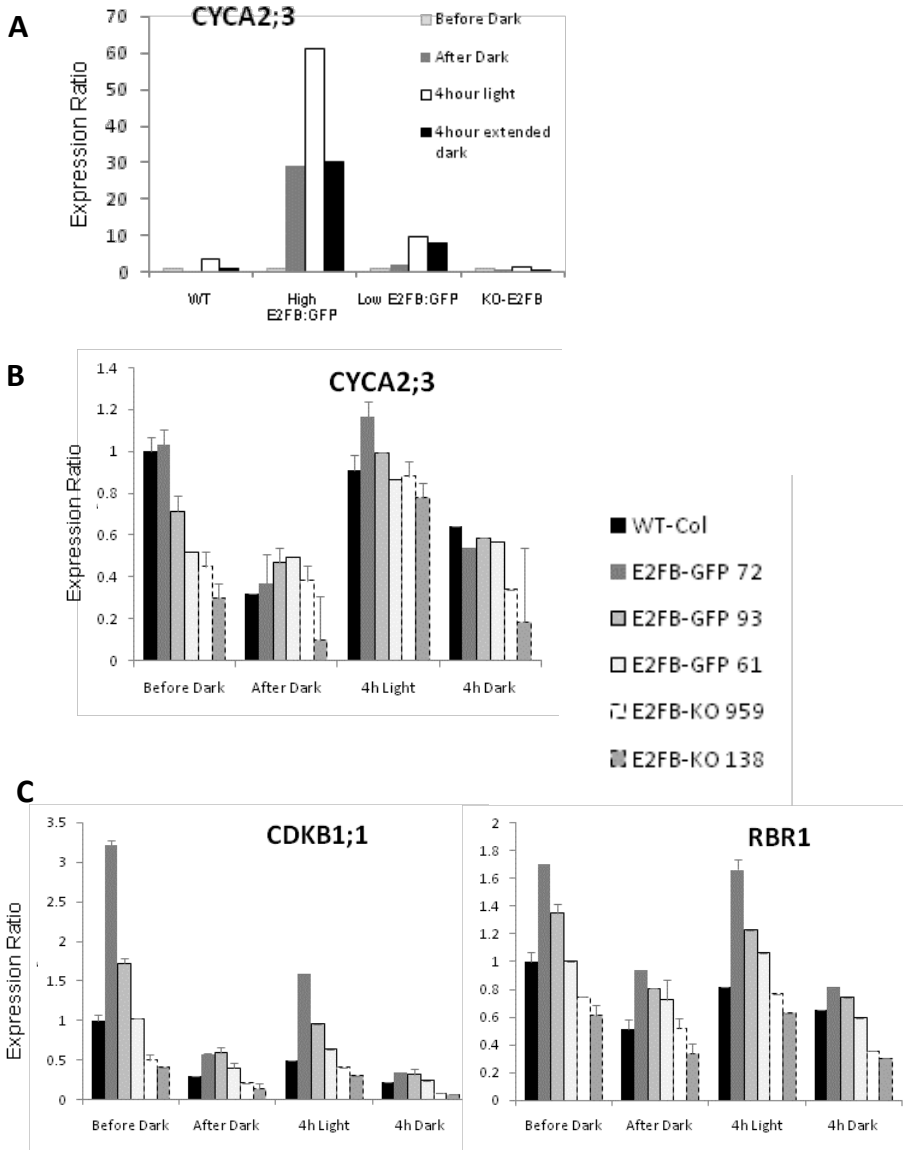

Figure 4-4 Modified *E2FB* levels dysregulate the diurnal behaviour of cell cycle transcripts (Q-RT-PCR)

A) Representation of the *CYCA2;3* gene (in whole seedling samples), following the 4hour extended dark protocol (see Fig4.3), in WT-Col and in lines with modified *E2FB* expression or activity levels. In each case the reference is the time point labelled "before dark", and therefore levels are normalised to the initial time point within each line, and cannot be compared across lines. **B)** Re-plotting of *CYCA2;3* expression made for every sample in reference to the WT-Col, "before dark" value. **C)** Cell cycle genes *CDKB1;1* and *RBR1* were also analysed as in (B) (reference point is WT-Col before dark, samples, left to right, are WT-Col, E2FB-GFP lines 72, 93, 61, E2FB-KO lines 959, 138). These results demonstrate that several cell cycle genes, when compared to WT-Col, show E2FB-GFP dose-dependency (transcripts are upregulated in a similar pattern, high, medium and low, to the pattern of overexpression of the transgene) but other cell cycle genes (such as *CYCA2;3*, shown in B) do not. In all graphs error bars show standard deviation for 3 technical replicates. Some of these results have been reproduced in an independent experiment and those not shown were simply not tested (see appendix 4.1).

extended dark experimental system was applied to different E2FB transgenic and mutant lines (for details of lines see section 2.2) and compared to WT-Col seedlings. Amongst the cell cycle genes tested gene *CYCA2;3* showed a distinct response to E2FB levels (Fig 4.4A).

The data show that in the line in which the gene expression level of E2FB is high (High E2FB-GFP; pE2FB:gE2FB::GFP) *CYCA2;3* transcripts are elevated AD and in the 4hD, by approximately 25 fold, and even more so at 4hL, at approximately 60 fold. Moreover, when a line with lower E2FB-GFP expression level was used, (based on E2FB protein detection carried out by Zoltan Magyar, see chapter 3 for details) the *CYCA2;3* transcripts in AD, 4hL and 4hD are all upregulated relative to the BD but are only up by 10 fold in comparison to the high expressing E2FB-GFP line. In the *e2fb-ko* line, AD and 4hD transcript levels are extremely low for *CYCA2;3* and even the 4hL time point shows only a subtle upregulation. Note that the reference point in each case was the BD time point for the same line, to assess exclusively the impact of the treatments. In order to assess the effect of the change of E2FB protein level, the data were reanalysed in reference to the WT-Col at each time point (Fig 4.4B). Clearly *CYCA2;3* levels are not very high in the E2FB-GFP lines compared to the WT-Col, yet *CYCA2;3* levels were altered in the light and extended dark periods within each line (as shown in the previous graph). *CYCA2;3* levels were lower in the *e2fb-ko* lines, particularly *e2fb-ko 138* (see appendix 4.1 for an independent experiment reproducing similar results). The dose dependency of E2FB could be observed at BD and 4hL but could not be observed in the AD and 4hD. This data on *CYCA2;3* show that cell cycle transcripts are regulated by modified E2F levels as well as by the treatments of light and extended-/dark.

Similar analysis of two cell cycle related genes (*CDKB1;1* and *RBR1*) showed *CDKB1;1* transcripts were elevated in the E2FB-GFP high and medium expressers (E2FB-GFP 72 and E2FB-GFP 93, respectively) and this is most obvious at BD and 4hL, though dose dependency was not displayed in AD and 4hD. The *e2fb-ko* 959 and *e2fb-ko 138* have low levels of *CDKB1;1*, particularly in the 4hD (Fig 4.4C). Similarly to *CDKB1;1*, *RBR1* transcripts were elevated when the E2FB dose level was relatively high and the *e2fb-ko* appeared similar to the WT-Col (appendix 4.1 shows an independent experimental repeat for *RBR1* in the *e2fb-ko* lines).

This showed that not only did the light dark period affect cell cycle gene transcript levels, but altering the gene dose of the cell proliferation driver E2FB dysregulated the anticipated light dark behaviour of cell cycle gene *CYCA2;3*. Whether or not this is true for all cell cycle genes, or even as circadian regulation for those genes that do show such behaviour, cannot be concluded; certainly the gene dose of E2FB does not upregulate all cell cycle genes, for instance, *CYCA2;3* and *CDKB1;1* behaved differently but their proteins together promote M phase. Understanding whether and how light and dark (diurnal or circadian) phases regulate the cell cycle is lacking in plants as compared to other organisms. This may be because disentangling the connection between light, nutrition (carbon) and growth is problematic when interpreting data. Specifically in plants, our collaborator, Rossana Henriques, is initiating work on an energy sensor (the TOR protein) and its potential role in circadian clock modulated growth.

4.4.4 **RBR1 is phosphorylated in the light but is affected by carbon utilisation and storage**

As starch turnover has been shown to be regulated by diurnal cycles in many studies, it could be speculated, based on the previous data (section 4.4.3), that regulation of cell cycle gene expression may also be associated with diurnal patterning. At least in leaves diurnal patterns show the relative growth rate to be greatest in light, the first sample was 3 h after light, similar to the 4hL in my experiment in the previous results section (Wiese *et al.*, 2007). Based on the down regulation of cell cycle transcripts (Fig 4.3) proliferative growth is most likely limited in the dark where carbon from photosynthesis is also limited. However, the breakdown of starch to provide glucose during the night, when cell cycle activity appears minimal (section 4.4.3), suggests that there is a disconnection between the photoperiod and cell cycle activity because some carbon is available. In order to distinguish between these two possibilities, the phosphorylation status of RBR1 was checked in 12 h L:12 h D diurnal conditions on whole seedlings collected over a 48 hour period, at 3 hour intervals (Fig 4.5).

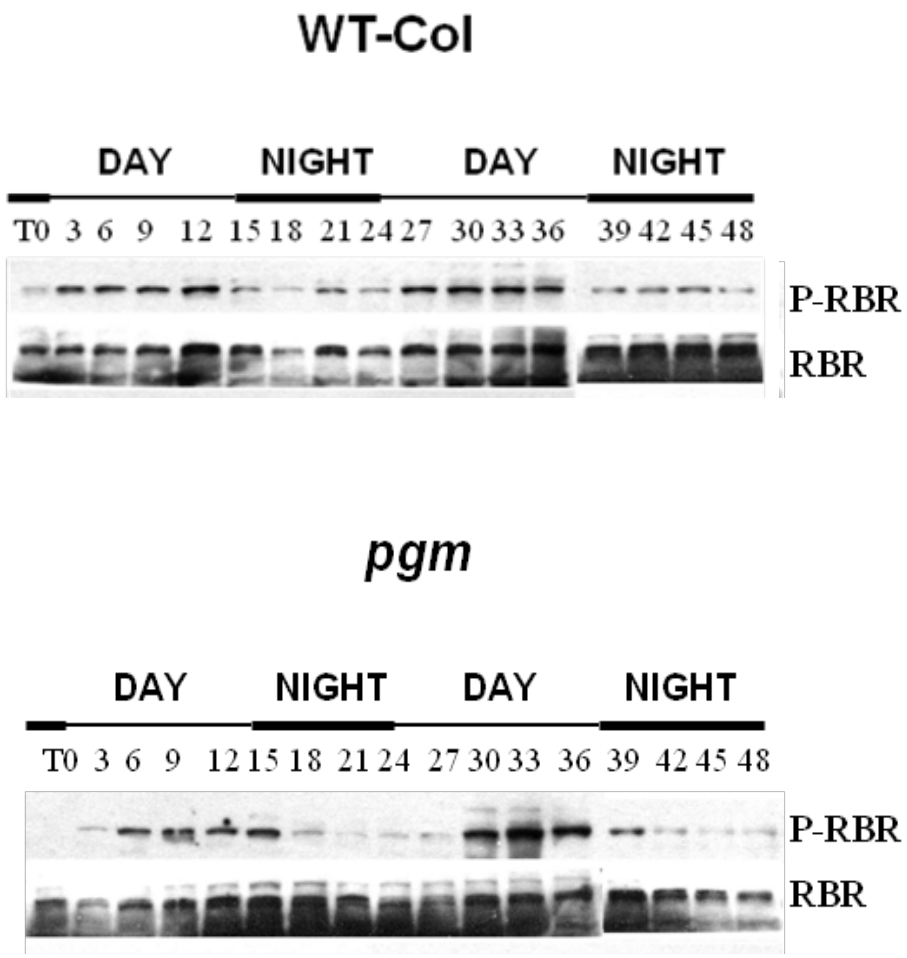

Figure 4-5 Diurnal rhythms and endogenous carbohydrate availability affect P-RBR1 abundance

WT-Col and *phosphoglucomutase* (*pgm*) mutant were grown in 12 hour light, 12 hour dark cycles and whole seedlings harvested at 3 hour intervals over 48 hours. Western blot using a Phosphorylated-RETINOBLASTOMA RELATED1 (P-RBR1, ~130kDa) specific antibody (relative to RBR, ~125kDa) was carried out. WT-Col (top) showed that P-RBR1 was abundant during the light (3-12 h time point) and in the *pgm* this pattern was observed with a 3 hour lag (6-15 h time point). (We acknowledge Zoltan Magyar for his contribution to this Western blot).

The results (Fig. 4.5) show that P-RBR1 is more abundant in the light as compared to the dark in the WT-Col. A starchless mutant (*plastidial-phosphoglucomutase -pgm*) was then used to elucidate the association of light and dark periods with sugar availability. The loss of function (*pgm*) mutant (Caspar *et al.*, 1985) accumulates at insufficient rates starch to store, has high sugar levels during the light period and is starved towards the end of the dark period, causing a repression in genes that hinders carbon utilisation in the light (Gibon *et al.*, 2004). Additionally, protein synthesis occurs at a diminished rate during the night in *pgm* perhaps to counter-balance the lack of carbon availability, (Pal *et al.*, 2013).

The Western blot analysis (Fig. 4.5) showed a 3 hour lag in the appearance of P-RBR1 during the light period and its disappearance after the end of the day, when sugar is still abundant, in the *pgm* mutant. This illustrates the fact that light and dark phases and carbohydrate availability affect the phosphorylation status of RBR1 in the *pgm* mutant, where P-RBR1 would yield free E2F for driving of cell growth. Future replication of this analysis would include a third blot with samples from a free running period (for instance, constant light) that could give clarity to whether this is circadian-regulated (as opposed to diurnal regulation, by light and dark).

4.5 Establishment of a dark growth-arrest protocol visualised with *CYCB1;1::GUS* as a mitotic reporter

Based on the findings so far I have shown that RBR1 phosphorylation is under the influence of diurnal rhythms, and the P-RBR1/RBR1 pattern lags by 3 hours in the *pgm* starchless mutant (section 4.4.4). This suggests RBR1 phosphorylation is associated with carbohydrate access, and that carbohydrate availability during the night is not sufficient to maintain it in the *pgm* mutant. Although data showing a link between energy status of the cell and phosphorylation status of RBR1 have been published in the past using sucrose application (Hirano *et al.*, 2008; Magyar *et al.*, 2012) these findings suggest that carbohydrate accessibility to/perception by the cell affects RBR1 phosphorylation over and above light perception. This does not exclude the possibility that this may be an indirect result of light presence. Moreover, in the 4hD cell cycle genes were shown to be further downregulated reiterating the link between carbohydrate availability, a starved state and the cell

cycle. Further experiments may help show if these observation are primarily due to severe depletion of carbohydrate or a disrupted light exposure. Finally, based on these experiments carried out on whole seedlings it is difficult to precisely determine how growth is affected.

An earlier study of our laboratories (Lopez-Juez *et al.*, 2008) had examined the Shoot Apex (SA), from which leaf primordia grow *de novo*, and the later associated leaf primordia, in seedlings germinated and grown for 3 days in the Dark (3dD), hence etiolated seedlings. That study found that starvation genes are strongly expressed in the dark and are almost immediately (within one hour, first time point examined) downregulated upon light irradiation; this is followed by ribosome biogenesis and increased DNA synthesis and, in parallel, mitosis (as assessed by gene expression signatures and directly by flow cytometry (Lopez-Juez *et al.*, 2008)). Inspired by the observations in the work of Dr Lopez-Juez and colleagues and to distinguish between the growth response signatures in the shoot apex *versus* leaf primordia, I carried out a re-deetiolation assay. In this procedure seedlings were first in continuous light (CL) until 7dag, when NL 1/2 primordia emerge, seedlings were transferred to 3dD and then back to light (DL; dark to light) examining them over a similar time course, 1 h, 3 h, 6 h, 12 h, 24 h, 48 h and 72 h after DL transfer. NL 1/2 were monitored for growth-related responses via a mitotic reporter, CYCB1;1::GUS (Donnelly *et al.*, 1999), and DNA content/ploidy analysis. The advantage of this revised experimental set-up is that it allows the much more rapid collection of increased amounts of material, the leaf primordia, the majority of which was still capable of undergoing active growth.

4.5.1 **Three days dark reduces mitotic activity due to growth arrest in new leaf 1/2**

The CYCB1;1::GUS construct does not alter expression of the *CYCB1;1* gene, but simply reports the presence of the protein (Donnelly *et al.*, 1999). In 7 dag seedlings, punctuated GUS expression was observed in NL 1/2, (Fig 4.6A). The expression pattern shows an acropetal (base to tip) gradient. After 72 h in Continuous Light (CL) (10dag) CYCB1;1::GUS expression was reduced, mitotic activity lost and the leaf appeared much larger in size. This may be interpreted as a result of cells having

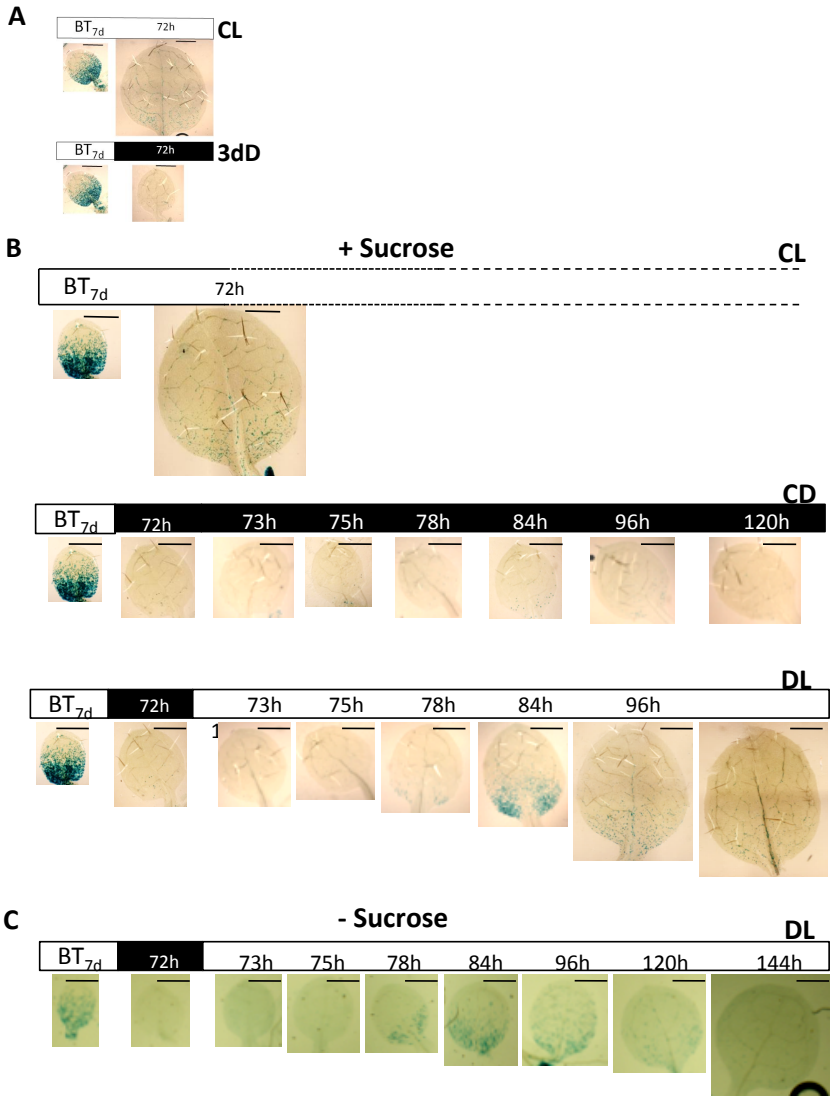

Figure 4-6 Mitotic response of the first new leaf pair in a light to dark, back to light, transition.

A) The first new leaf pair was dissected from 7dag CYCB1;1::GUS-expressing seedlings, grown in continuous light (CL), after visualising the GUS reporter. The blue GUS stain indicates cells undergoing mitosis, in an acropetal gradient, at the time point before transfer (BT_{7d}). Seedlings 3 days later (72h) show very little GUS reporter activity, but the leaf size is clearly increased. 7dag seedlings transferred to 3 days dark, 3dD (72h, 3dD) also showed no GUS staining but the leaf was not as large as a leaf grown in CL. **B)** The top panel shows a repeat of (A), as a reference, at the same scale as the rest of (B). These seedlings were grown on 1% sucrose medium (as in A). The middle panel shows an extension of (A) where seedlings were kept in the dark for 3 further days (these are called continuous dark, CD, samples, a second control). The bottom panel shows transfer of seedlings back to light 72 h after the transfer to dark, over a time course of 1 h (73 h), 3 h (75h), 6 h (78 h), 12 h (84 h), 24 h (96 h) and 48 h (120 h) labelled as dark to light (DL). **C)** This shows a repeat of the aforementioned except on medium lacking sucrose. Scale bar represents 500 µm. These observations (**A** and **B**) were made at least three times in independent experiments.

exited proliferation and entered differentiation, enhancing growth (see later). This reduction in activity over time has been reported many times but in the context of comparing an ectopic/mutant line to the WT (Van Norman *et al.*, 2011; Kang *et al.*, 2007). However, after 3dD the leaf showed complete absence of CYCB1;1::GUS expression, as previously reported for the shoot apex (Lopez-Juez *et al.*, 2008) but here I note specifically for the leaf that it increased very little in size, (compared to the control, 72 h CL). This suggests that the absence of light imposes a growth arrest on leaf primordia as they failed to increase in size and showed no mitotic activity.

4.5.2 **Cells in NL 1/2 recover mitotic activity upon light irradiance after 3dD**

Because the absence of light is hypothesised to impose a growth arrest, allowing observation of recovery back to light, and consequent continuation of growth of leaf primordia, the GUS protocol for CYCB1;1 was continued up to 3 days, as previously done for the shoot apex from which primordia emerged at later time-points (Lopez-Juez *et al.*, 2008). The top panel of Figure 4.6B shows the CL (control) where NL 1/2 grew, increased in size and decreased in mitotic activity, as described above. The second panel shows the second control (Continuous Dark after 7dag, CD) where leaves lost mitotic activity fully as observed at 72 h and this loss of mitotic activity remained the case throughout the additional 3d of darkness. The leaves remained relatively unchanged in size, displaying a growth arrest over 6 days in total. Contrary to this, seedlings that were transferred back to the light after 3dD showed a reappearance of CYCB1;1::GUS, peaking at 84 h (12 h DL) flanking the mid-vein near the petiole. This was observed as a diffused peak in staining at 6 h in the shoot apex, including petioles of cotyledon and very young primordia (Lopez-Juez *et al.*, 2008). Here I observed the GUS stain to appear strongly at a single time point (12 h). At 96 h (24 h DL) CYCB1;1::GUS expression was already lost but, notably, the leaf was substantially larger in size at 96 h and 120 h (DL). These results showed that even on sucrose-containing plates mitotic activity arrests after 3dD, but recovers 12 h after light irradiance.

4.5.3 **Seedlings on – sucrose plates show less mitotic activity at 7 dag and a slow recovery from the dark growth arrest**

It was shown above, for + sucrose plates, that NL 1/2 were growth-arrested in the 3dD but transfer back to light brought on synchronous CYCB1;1::GUS expression at 12 h DL. This disappeared in the subsequent time points, presumably as cells enter differentiation. I asked whether the sucrose available in the medium affected the DL response, in contrast to the response in - sucrose plates that were previously used in the SAM gene expression signatures by Dr Lopez-Juez and colleagues. In seedlings grown on - sucrose medium plates, NL 1/2 at 7 dag showed much less CYCB1;1::GUS expression and the recovery after 3dD was more slow (Fig 4.6C). Instead CYCB1;1::GUS reappearance upon transfer back to light occurred at 78 h (6 h DL), became abundant at 84 h and 96 h (DL) and dissipated at 120 h rather than 96 h (DL). The 144 h time point showed that the leaf continued to increase in size substantially and mitotic activity was eventually lost. Interestingly, these findings illustrated a difference in the recovery of mitosis upon deetiolation of dark-adapted seedlings, depending on the presence or absence of sucrose in the plates. Based on these differences I decided to pursue gene expression analysis of NL 1/2 in - sucrose medium growth conditions (see later).

4.6 Quantitation of CYCB1;1::GUS

The expression of GUS was quantified so that the area of GUS on the leaf was expressed as a proportion of the whole leaf area (%GUS). Although Figure 4.6 shows the most representative images, a true representation of the averages could be achieved via the %GUS calculation (see methods).

4.6.1 **A narrow or broad peak in CYCB1:1::GUS activity in + sucrose and – sucrose, respectively**

In the + sucrose medium plates between BT - 72 h %GUS decreased in the CL (Fig 4.7A), and analysis of later time points showed no new GUS activity (*not shown*). Notably, in the - sucrose medium plates %GUS in CL remained relatively constant indicative of a slow exit from mitosis/proliferation cycle. The CD %GUS remained

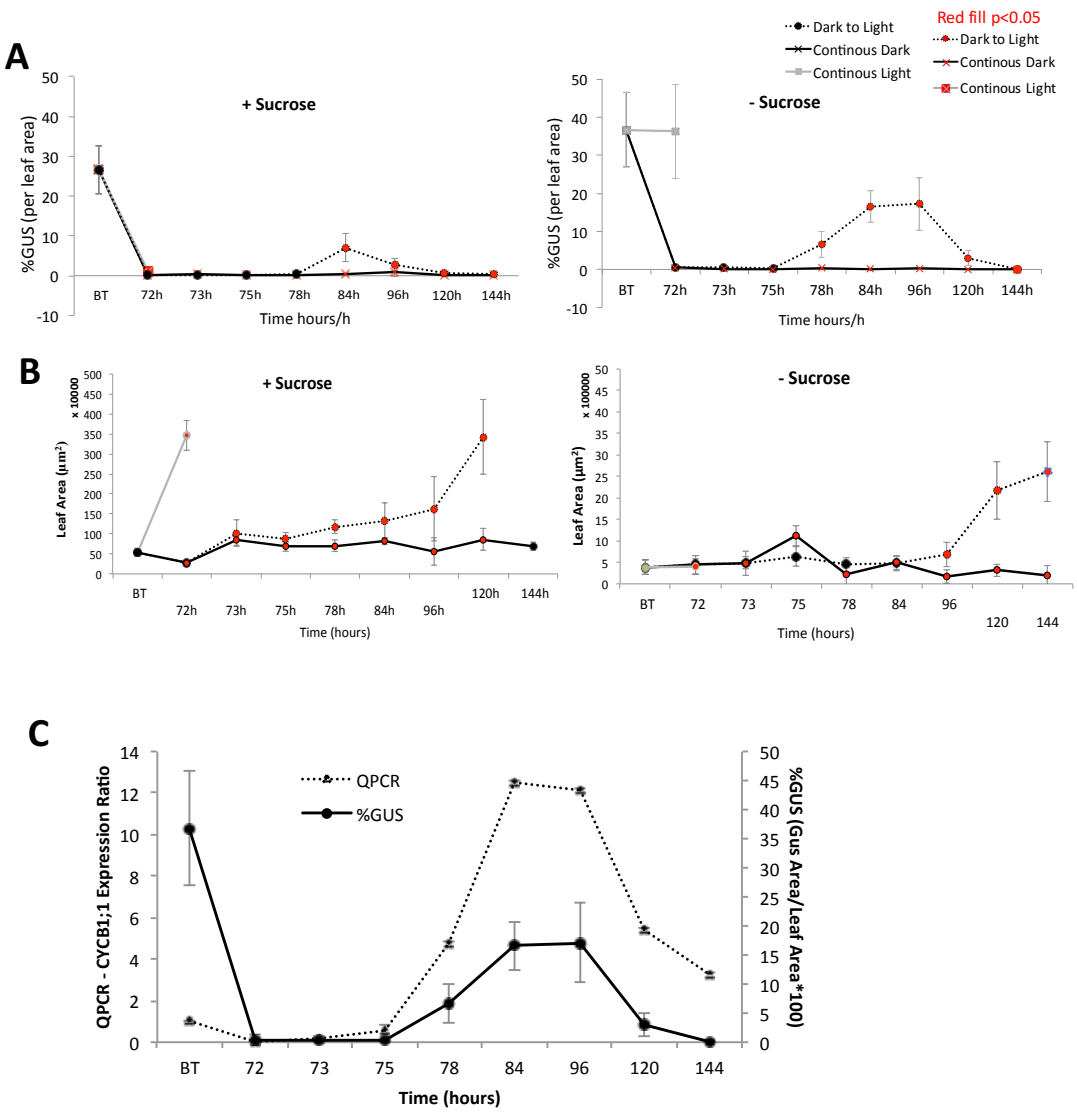

Figure 4-7 GUS quantitation in the dark to light transition

A) Quantitation of GUS activity as %GUS-occupied area per leaf area in the first new leaf pair, transferred to dark for 3 days at 7dag and then back to light (dark to light, dotted line). Controls were continuous light (no 3days dark) (solid grey line) and continuous dark (extension of 3 days dark to 6days) (solid black line). This was done for seedlings grown on medium with (+ sucrose, left) and without (- sucrose, right) sucrose. **B)** Individual leaf area, used in the determination of %GUS in (A). The + sucrose data show that the expansion of leaves contributed to a decline in %GUS in continuous light, leaves in continuous dark did not increase in size, but recovery of %GUS in the dark-to-light transfer occurred against a backdrop of increased leaf area. The broad %GUS peak in – sucrose also accompanied an increase in leaf size. **C)** Validation of the %GUS quantitation (redrawn from A, - sucrose, solid black line) using the *CYCB1;1* primers in Q-RT-PCR of identical samples (dotted line). All error bars represent standard deviation for leaf area and GUS quantitation data (n=15). In **A** and **B Red** mark/fill represents a $p<0.05$, *t*-test (where continuous conditions were tested against the BT value and Dark to Light samples were tested against the 72h value, i.e. the sample after 3 days dark). Q-RT-PCR values in **C** represent averages of 3 technical replicates of a single RNA sample.

at close to zero, hence a flat line. However, in the + sucrose condition some %GUS was unexpectedly present as a small peak at 96 h. Moreover, a peak in %GUS was far greater at 84 h (12 h DL) in the + sucrose recovery, in agreement with Fig 4.6. Also, as previously observed, in the DL transfer the response in %GUS in the - sucrose condition was slow and the broad peak occurred between 78 h - 120 h (DL) on the graph (Fig 4.7A). This result indicated a slower re-stablishment of mitotic activity taking place in the - sucrose condition but surprisingly %GUS values were greater too; I attribute this observation to the smaller leaf sizes, confirmed in section 4.6.2.

4.6.2 **An increase in leaf size is a result of dissipation of mitotic activity**

The transition from DL in + sucrose yielded a synchronous peak in mitotic activity at 12 h DL. Because a eukaryotic cell cycle takes an average 24 h, and the mitotic phase is a small fraction of that (Cooper and Hausman, 2000), the staining shows a plausible single round of cell division. Assuming the same for the – sucrose condition, the broad peak suggested a slower progression (recovery) through the cell cycle. Leaf area analysis (of those leaves used for %GUS analysis, section 4.6.1) indicated an increase in leaf size was correlative with a reduction in %GUS expression, as clearly evident in the control light (CL, +sucrose medium plates) (Fig 4.7B). For – sucrose medium plates, as mitotic activity remained steady for CL, the increase in leaf size was not observed till later on. This was reinforced by analysis of the DL transfer where leaf size increased between 96 h – 120 h (- sucrose, Fig 4.7B) and mitotic activity reduced (%GUS, Fig 4.7A). The peak in %GUS occurred at 84 h in + sucrose, and its dissipation was also followed by an increase in leaf size (Fig 4.6B), beginning at the same time point. The CD leaf sizes showed fluctuations due to the small sample size, but no evident increase in leaf sizes. It should be noted that leaf sizes in – sucrose were smaller than those in + sucrose. This was also true for CL samples, indicating that this overall difference in leaf size is not associated with the dark or dark to light transfer alone, absence of sucrose brings about this effect.

These findings showed that in the DL transfer a single (narrow or broad) peak in mitotic activity were followed by an increase in leaf size. This was later shown to be coinciding with an increase in ploidy levels (see all of section 4.7).

4.6.3 **Validating %GUS with Q-RT-PCR**

It was observed that unlike the + sucrose CD, leaf areas in the – sucrose CD showed a large variance (Fig 4.7B), particularly between 73 h - 78 h. The leaf areas affected the %GUS calculation. Thus, Q-RT-PCR was used as a gene expression analysis tool in order to further validate the GUS quantitation results in – sucrose conditions (see Fig 4.7C). Remarkably, the graph showed a gene expression pattern clearly matching that of the %GUS.

4.7 Analysis of cellular ploidy after growth dark-arrest and its relief

The growth arrest of NL 1/2 caused by the 3dD could be recovered by retransfer of seedlings to continuous light, regardless of differences in the +/- sucrose conditions (see section 4.5.3). Leaves in 72 h CL showed very little mitotic activity at this stage (assuming most mitosis has already occurred) but were assumed not to be growth arrested as they were larger in size. Leaves in the 3dD also showed no mitotic activity but were growth arrested as they did not increase in size as in the control (CL). This suggested endoreduplication and differentiation-dependent growth was occurring in leaves in CL where cells expand and increase in size and mitosis no longer occurs. To validate this, flow cytometry analysis was used for ploidy level quantitation as well as identification of the proportion of cells in S phase (for DNA synthesis). DNA synthesis is common for the mitotic cycle and the endoreduplication cycle.

4.7.1 **Recovery from 3dD causes entry into S phase, more so in the + sucrose than – sucrose plates**

Using the methods available, a Partec flow cytometer instrument and its cell cycle analysis tools, S phase could be calculated relative to the proportion of cells before (2N) and after the S phase (4N). In the + sucrose medium condition during the 3dD period the proportion of nuclei in S phase decreased (before transfer, BT – 72 h), this was also true for the – sucrose medium condition (Fig 4.8A). The proportion of cells in S phase in the control (CL) remained elevated compared to the 3dD but this was only shown at 24 h. This is because no 4N peak was observed at 24 h using peak

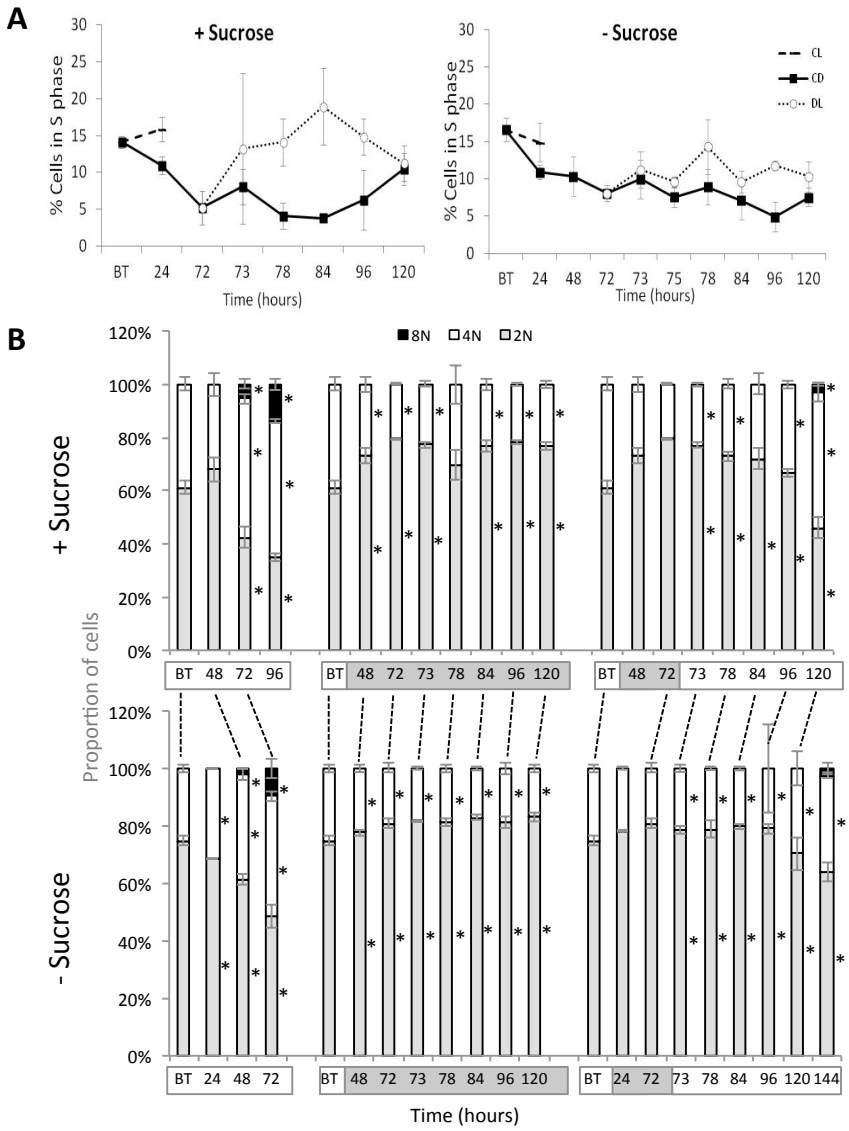

Figure 4-8 Cell cycle analysis in the dark growth arrest response and recovery upon light exposure

A) Whole seedlings were grown on + sucrose (left) or – sucrose (right) medium (continuous light, CL dashed line), transferred to 3 days dark at 7dag (Before Transfer, BT), and then back to light (dark to light, DL, dotted line). First leaf pair samples were used for cell cycle analysis via flow cytometry at 1 h (73 h), 3 h (75h), 6 h (78 h), 12 h (84 h), 24 h (96 h) and 48 h (120 h). A further control remained in continuous dark, CD (solid black line). Cells undergoing S phase reappeared after DL transfer, more so in + sucrose conditions. **B)** Ploidy level analysis of samples in (A), for + sucrose (top) and – sucrose (bottom). White bar on x axis represents CL, white to black bar represents BT at 7dag, then CD, and white to black to white bar represents DL transfer. CL leaves entered endopolyploidy (a ploidy greater than 4N) at 72 h whereas CD leaves remained growth-arrested (with 2N and 4N cells only). Notably, DL transfer resulted in the appearance of endopolyploidy (8N) at 120 h and 144 h for + sucrose and – sucrose, respectively. All error bars represent standard deviation. * show $p<0.05$ (*t*-test) when compared to BT for CL and CD or 72 h for DL. Dashed lines are used as a visual aid to show the same sampling time points in the with and without sucrose conditions.

analysis of the software. After this time point ploidy levels increase in CL, no 2N peak can be detected. While conceptually a "combined" S phase occurs between G1 and G2 and between G2 and higher ploidy levels, the instrument's software calculates S phase exclusively between G1 and G2. This renders the software unable to detect S phase after the 24 h time point (see methods). Upon transfer back to light (+ sucrose) S phase activity increased and peaked at 84 h (DL) before dissipating and matching the CD sample at 120 h. In the – sucrose condition the response was less pronounced upon recovery (DL) and, while a S phase increase upon transfer back to light (DL) was evident, both DL and CD fluctuated and their differences remained small (- sucrose).

4.7.2 **Transfer back to light after 3dD increases ploidy in the – sucrose plates but with a 24h delay compared to + sucrose plates**

The proportion of cells in S phase reflects the occurrence of DNA synthesis and was used in conjunction with the analysis of mitosis using CYCB1;1::GUS. However, DNA synthesis also occurs during endoreduplication/differentiation, when cells increase their ploidy levels from 2N, 4N to 8N, 16N, 32N and so on. I proceeded to monitor this. In CL under both +/- sucrose conditions ploidy from 4N to 8N occurred at 48 h (8dag) in NL 1/2 with a slightly greater (but significant) portion of cells acquiring increased ploidy in the + sucrose condition (Fig 4.8B). During the 3dD period cells increased their G1/2N content in both +/- sucrose conditions, suggestive of a cell cycle "completion" through mitosis and a G1-S arrest, as S phase was previously shown to decrease (Fig 4.8A). This arrest then remained present after the 3dD and the proportion of cells did not increase further for 2N and/or decrease for 4N during the course of the continuous dark period (i.e. mitosis is also arrested).

Upon transfer back to light the cell population reduced its G1/2N fraction and increased its G2-M/4N fraction. In the + sucrose DL transfer cells entered endopolyploidy at 120 h whereas in the – sucrose condition this was observed at 144 h, 24 hours later. Overall, cells that were growth-arrested in the 3dD not only recovered mitotic and S phase activity but continued to enter endoreduplication.

4.8 Gene expression analysis, Q-RT-PCR

Seedlings grown in the dark undergo skotomorphogenesis where they become etiolated in appearance but light irradiation causes the emergence of new leaf (NL) primordia from the SAM (Whitelam and Halliday, 2008). Prior to the emergence of the NL, that are only visible 2 - 3 days after irradiation, many intrinsic responses take place at the transcript level, some of which occur very rapidly, within 1 h (the first time point observed, Lopez-Juez *et al*., 2008). Seedlings of 7 dag have primordia emerging from the SAM; transfer to 3dD is here shown to cause a growth arrest but a remarkable recovery takes place upon light irradiance (sections 4.6 - 4.7). This phenomenon was further tested for similarities and differences to the 3dD (etiolation) – de-etiolation response in the shoot apices (Lopez-Juez *et al.*, 2008). This was achieved via a quick gene expression analysis of two or more selected genes, some based on the work of Lopez-Juez *et al.*, 2008, and are described further. Here I assume these genes behave in a characteristic manner in the 3dD protocol and ask whether the key signature response is similar or different from that previously published. It should be noted that – sucrose plates were used to be consistent with the work of Lopez-Juez and colleagues (2008). Section 4.1 covered details of the phenomena observed and below is a list of genes used to study these (Table 4.3).

Reference genes used in all experiments were *ACTIN2* (*ACT2*) and *UBIQUITIN10* (*UBQ10*) (appendix 2.11)

Table 4-3 Regulatory modules for light growth presented as categories for genes (and their annotations) to be tested for section 4.8

Category of analysis	Gene	Annotation
Cell Cycle/DNA synthesis	*KRP4*	KIP RELATED PROTEIN4 (*KRP4*) is a CDK inhibitor that controls the transition from the G1 to S phase of the cell cycle [a] and is the

Cell cycle/DNA synthesis		earliest cell cycle gene affected by light in a shoot apex dark-to-light transition study.[b]
	RNR2A	RIBONUCLEOTIDE REDUCTASE2A(*RNR2A*) encodes a subunit of an enzyme key for nucleotide biosynthesis and is a target of the DNA damage checkpoint.[c] Its mRNA has been shown to accumulate at S phase in tobacco BY2 cells.[d]
	H2A	HISTONE-2A (*H2A*) synthesis must necessarily accompany DNA synthesis, to provide chromatin constituents during both the mitotic cell division cycle for proliferation as well as endoreduplication
	CYCB1;1	The B-type cyclin, *CYCB1;1*, is expressed in a narrow window of mitosis onset, [e,f]
Translational capacity	*S6RP*	The S6 RIBOSOMAL PROTEIN (*S6RP*) is a component of the 40S ribosomal unit and is regulate d by the S6Kinase (S6K). This phosphorylation regulates the selective translation of ribosomal proteins that increase translational capacity.[g]
	EBP1	Localisation of human ErbB-3 epidermal growth factor receptor Binding Protein1 (*hEBP1*) suggests it has a role in ribosome biogenesis and sustaining protein translation.[h,i] This function is conserved in plants too.[j]
Energy Status/Starvation response	*TPS9*	TREHALOSE-6-PHOSPHATE SYNTHASE9 (*TPS9*) is described in TAIR as both a synthase and also a phosphatase that dephosphorylates Trehalose-6-Phosphate (T6P), an intermediate of the trehalose biosynthesis pathway, but it is more likely to have a role in sugar sensing.[k]
	bZIP1	basic leucine Zipper1 (*bZIP1*) is itself one of several bZIPs described to be involved in the plant carbohydrate starvation response,[l] and with bZIP63 is hypothesised to transduce low energy signals in order to reprogram primary

		metabolism as part of the starvation response.[m]
RBR1/E2F switch components	*RBR1*	RETINOBLASTOMA RELATED1 (*RBR1*) protein is regulated by CDK-CYCs and forms a repressive complex with E2Fs.
	E2FA	E2FA is a transcription factor. Genes positively regulated by E2FA are also positively regulated by light, and encode DNA synthesis-related factors, whereas genes encoding plastid proteins and some metabolic enzymes are initially repressed by E2FA upon light perception and induced later in waves of activity.[n]
RB/E2F switch	*E2FB*	Transcription factor E2FB is a positive regulator of cell proliferation, (see chapter 3), and the protein is abundant in light and constitutively present in *cop1* mutants grown in the dark.[o]
	E2FC	E2FC is a transcriptional repressor of the G1 to S transition,[p] and has a high mobility form in the presence of light.[q]
Hormone balance	*AUX1*	AUXIN RESISTANT1 gene (*AUX1*) encodes an auxin influx transporter and is known to have a role in apical hook development.[r] It serves as a marker of auxin response.
	ARR5	ARABIDOPSIS TYPE1 RESPONSE REGULATOR5 (*ARR5*) was originally identified as a cytokinin induced gene.[s],
	EIN3	ETHYLENE INSENSITIVE3 (*EIN3*). A marker for ethylene action.
	ABA2	Abcisic acid (ABA) DEFECIENT2 (*ABA2*) encodes a protein involved in biosynthesis of ABA whose signalling pathway has been linked to sugar signalling pathways.[t]

[a] (Zhao *et al.*, 2012) [b] (Lopez-Juez *et al.*, 2008)

[c] (Huang *et al.*, 1998) [d] (Philipps *et al.*, 1995)

[e] (Donnelly *et al.*, 1999) [f] (Fung and Poon, 2005)

[g] (Henriques *et al.*, 2013)

[h] (Squatrito *et al.*, 2004) [I] (Squatrito *et al.*, 2006) [j] (Horvath *et al.*, 2006)

[k] (Paul *et al.*, 2008)

[l] (Usadel *et al.*, 2008) [m], (Dietrich *et al.*, 2011)

[n] (Lopez-Juez *et al.*, 2008)

[o] (Lopez-Juez *et al.*, 2008)

,[p] (Magyar, 2008) [q] (Lopez-Juez *et al.*, 2008)

[r] (Vandenbussche *et al.*, 2010)

[s], *reviewed by* (To and Kieber, 2008).

[t] *reviewed by* (León and Sheen, 2003)

4.8.1 **Light upregulates genes involved in DNA synthesis**

Light irradiance was shown to immediately increase S phase activity in the shoot apex (Lopez-Juez *et al.*, 2008) as well as in NL 1/2 (Fig 4.8A). To further establish that light irradiance and growth were associated with cell cycle progression at the transcript level, in NL 1/2, I hypothesised that cell cycle transcripts would increase in a manner similar to CYCB1;1::GUS. *CYCB1;1* transcripts were previously shown to mimic CYCB1;1::GUS expression in the DL transfer (Fig 4.7C); here the control treatment (CL) (denoted light on graph, Fig 4.9) was shown to exhibit a gradually reduced expression of *CYCB1;1*, but not as dramatically as the dark grown sample (Fig 4.9). *RIBONUCLEOTIDE REDUCTASE2A* (*RNR2A*) expression declined in the light and 3dD condition (labelled dark on graph), more dramatically so in the latter. Light irradiance caused an increase in *RNR2A* transcripts within a few hours and peaked at 78 h (6 h DL) and then dissipated; notably *CYCB1;1* peaked at 84 h (12 h DL) and 96 h (24 h DL) indicating onset of mitosis after S phase (although the two processes can occur in parallel in different cells). *HISTONE-2A* (*H2A*) expression again decreased over time in the CL, but dropped dramatically in the 3dD within 24 h (at 24 h D) as observed for *CYCB1;1* and *RNR2A*. Upon DL transition, *H2A* expression peaked at 96 h (24 h DL) in NL 1/2. Contrary to other cell cycle genes, during the dark treatment *KIP RELATED PROTEIN4* (*KRP4*) transcript levels were variable but elevated relative to light. Upon transfer from dark to light *KRP4* transcript levels declined, albeit transiently. In summary, there was an increase in cell cycle gene transcripts in the 3dD DL transfer but this response appeared as a broad wave (in transcript behaviour) in NL 1/2. In contrast, in the study of etiolated seedlings (Lopez-Juez *et al.*, 2008), where the shoot apex was examined, transcript based responses peaked (a narrow peak) at 6 h after light irradiance. As for the cell cycle repressor, KRP4, results were also as hypothesised, high in the dark.

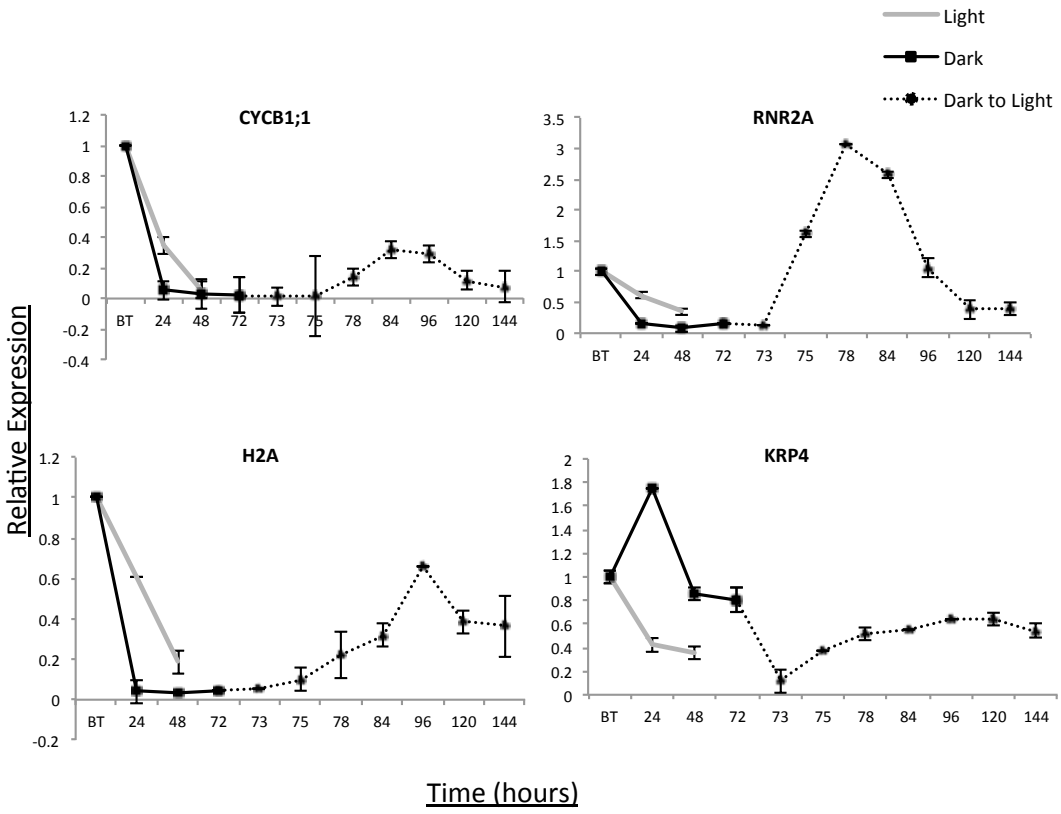

Figure 4-9 Cell cycle response in the dark to light growth response

Analysis of expression of the genes indicated, obtained by Q-RT-PCR) in first new leaf pair tissue, following the light treatment indicated. Whole seedlings were grown in – sucrose medium plates under continuous light. At 7 dag (before transfer, BT) seedlings were transferred to 3 days dark (dark, solid black line, 24 h, 48 h and 72 h), continuous light was a control (light, solid grey line, BT – 72 h). After 3 days dark (72 h) seedlings were transferred back to light (dark to light, dotted line, 72 -144 h). Time points of dark to light transfer correspond to 1 h (73 h), 3 h (75h), 6 h (78 h), 12 h (84 h), 24 h (96 h), 48 h (120 h) and 72 h (144 h), as shown on the *x* axis (in hours, h). BT is the reference point. Bars show standard deviation of 3 technical replicates of one RNA sample.

4.8.2 **Light expands the cells' translation capacity**

As well as transcription, translation is a key aspect of growth in eukaryotic cells as the investment of cells in ribosome biogenesis is concurrent with cell cycle gene transcription in light-mediated growth of the SAM (Lopez-Juez *et al.*, 2008).

In the dark RIBOSOMAL PROTEIN S6 (*S6RP*) transcripts declined rapidly as compared to light. In the DL transfer *S6RP* expression increased, peaked at 84 h – 96 h (12 h – 24 h DL) and then declined (Fig 4.10). In comparison to *S6RP, EBP1* expression did not decline as dramatically in the dark but transfer to light elicited upregulation within three hours and remained relatively elevated throughout the ensuing light period. These results illustrate that growth of NL 1/2 during the 3d DL transfer involved upregulation of cell cycle gene expression as well as translation capacity and ribosome biogenesis. These gene signature responses reflected those of the SAM and associated primordia (Lopez-Juez *et al.*, 2008).

4.8.3 **Dark and the starvation response**

Light is a source of energy for leaves through the photosynthetic production of organic carbon. I showed earlier that under sucrose induction conditions cell cycle activity is enhanced (see section 4.3.1 - 4.3.2). However I also showed that 3dD in NL 1/2 introduces a growth arrest irrespective of sucrose availability in the medium even when the only source of sucrose is the seedling's cotyledons (- sucrose medium plates) (see section 4.5.1). Transcript analysis of cell cycle and translation-related genes validated the role of light in imposing a growth arrest in the dark and reinitiating growth responses upon transfer back to light in NL 1/2 (see section 4.8.1 - 4.8.2). As this resembles the gene expression signature of the etiolated/de-etiolated shoot apex I hypothesised that starvation responses based on the presence or absence of light would be recapitulated too: The analysis of de-etiolation of the shoot apex had observed a strong starvation response in the dark. This response was very rapidly lost upon exposure to light, within 1 h, well before chloroplast development or photosynthesis could take place (Lopez-Juez, *personal communication,* based on data in Lopez-Juez *et al.*, 2008 and the starvation genes selected by Usadel *et al.*, 2008) (Fig 4.11). Indeed, two characteristic starvation genes were examined. These genes were *TREHALOSE-6-PHOSPHATE SYNTHASE9* (*TPS9*) and *BASIC LEUCINE ZIPPER1* (*bZIP1*). Both genes were upregulated in the dark and remained

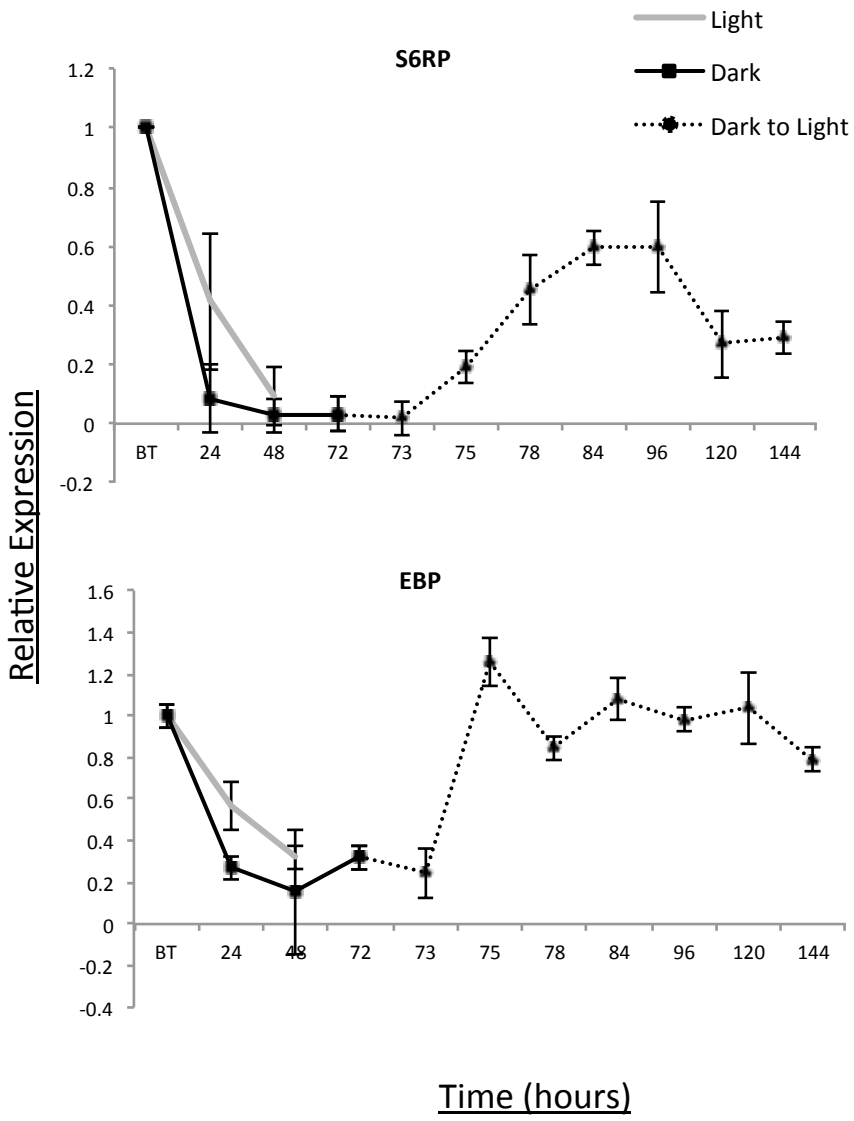

Figure 4-10 Gene expression associated with translational capacity expands during the dark-to-light growth recovery response

Analysis of expression of the genes indicated, obtained by Q-RT-PCR) in first new leaf pair tissue. Whole seedlings were grown in – sucrose medium plates under continuous light. At 7 dag (before transfer, BT) seedlings were transferred to 3 days dark (dark, solid black line, 24 h, 48 h and 72 h), continuous light was a control (light, solid grey line, BT – 72 h). After 3 days dark (72 h) seedlings were transferred back to light (dark to light, dotted line, 72 -144 h). Time points of dark to light transfer correspond to 1 h (73 h), 3 h (75h), 6 h (78 h), 12 h (84 h), 24 h (96 h), 48 h (120 h) and 72 h (144 h), hence the labelling of the *x* axis (in hours, h). BT is the reference point. Bars show standard deviation of 3 technical replicates of one RNA sample.

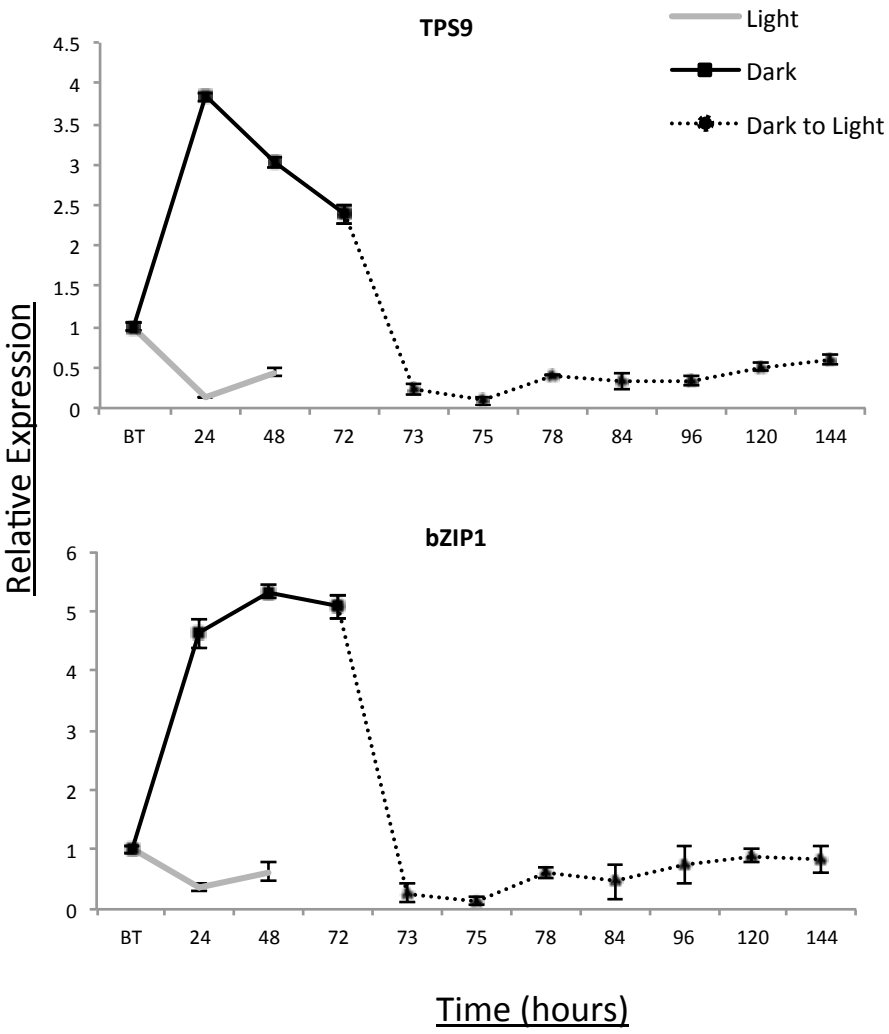

Figure 4-11 The starvation response in the dark is rapidly reversed upon light exposure

Analysis of expression of the genes indicated, obtained by Q-RT-PCR) in first new leaf pair tissue. Whole seedlings were grown in – sucrose medium plates under continuous light. At 7 dag (before transfer, BT) seedlings were transferred to 3 days dark (dark, solid black line, 24 h, 48 h and 72 h), continuous light was a control (light, solid grey line, BT – 72 h). After 3 days dark (72 h) seedlings were transferred back to light (dark to light, dotted line, 72 -144 h). Time points of dark to light transfer correspond to 1 h (73 h), 3 h (75h), 6 h (78 h), 12 h (84 h), 24 h (96 h), 48 h (120 h) and 72 h (144 h), hence the labelling of the *x* axis (in hours, h). BT is the reference point. Bars show standard deviation of 3 technical replicates of one RNA sample.

low in expression in the light. Upon light perception they were rapidly downregulated within an hour and remained relatively low in expression during the remaining of the light period (Fig4.11).

4.8.4 **Light and the RBR1 and E2F genes**

The cell cycle is regulated by the RBR1/E2F/DP pathway, a transcriptional regulatory switch. Unlike the previously examined CYCB1;1 gene, these genes *(RBR1, E2FA, E2FB* and *E2FC*) do not show transcript accumulation at given phases of the cell cycle. However, their altered protein abundance in response to light, and evidence for the role of COP/DET in influencing E2Fs and the cell cycle, led us to analyse transcripts of the RBR1/E2F module in the 3dD experiment (Fig 4.12). In brief, the results showed that transcripts fell in the light (as differentiation takes place) but more so in the dark. With the exception of *E2FB*, all transcripts fell gradually as differentiation occurs in the light, or rapidly if growth was arrested in the dark, and the DL transition elevated them, again with the exception of *E2FB*, which perhaps showed a transient drop in expression. Interpretation of this data alone is less informative due to the post-translational regulation of the RBR1/E2F switch, for instance RBR1 phosphorylation status that yields free E2F. The data does indicate that transcripts fell in the dark and were re-elevated when transfer back to light took place. Hence, these data complement the findings of the 4hD, extended-night experiment (see section 4.4.1 - 4.4.2).

4.8.5 **Light and dark and the involvement of hormone pathways**

Our findings presented so far established that light, cell cycle and translation responses in the SAM/very early primordia and NL 1/2 are similar, highlighting the role of light-mediated growth, albeit with the use of a few key genes. Furthermore, the dynamic roles of hormones affect many growth responses and potentially play a role in the dark repressive and light active state of the SAM. Based on the work of (Lopez-Juez *et al.*, 2008) and (Yoshida *et al.*, 2011) the four genes used here, representative of the four hormonal response types (auxin, cytokinin, ethylene and abscisic acid) assumes their action/biosynthesis and cross talk with light can be tested here (Fig 4.13).

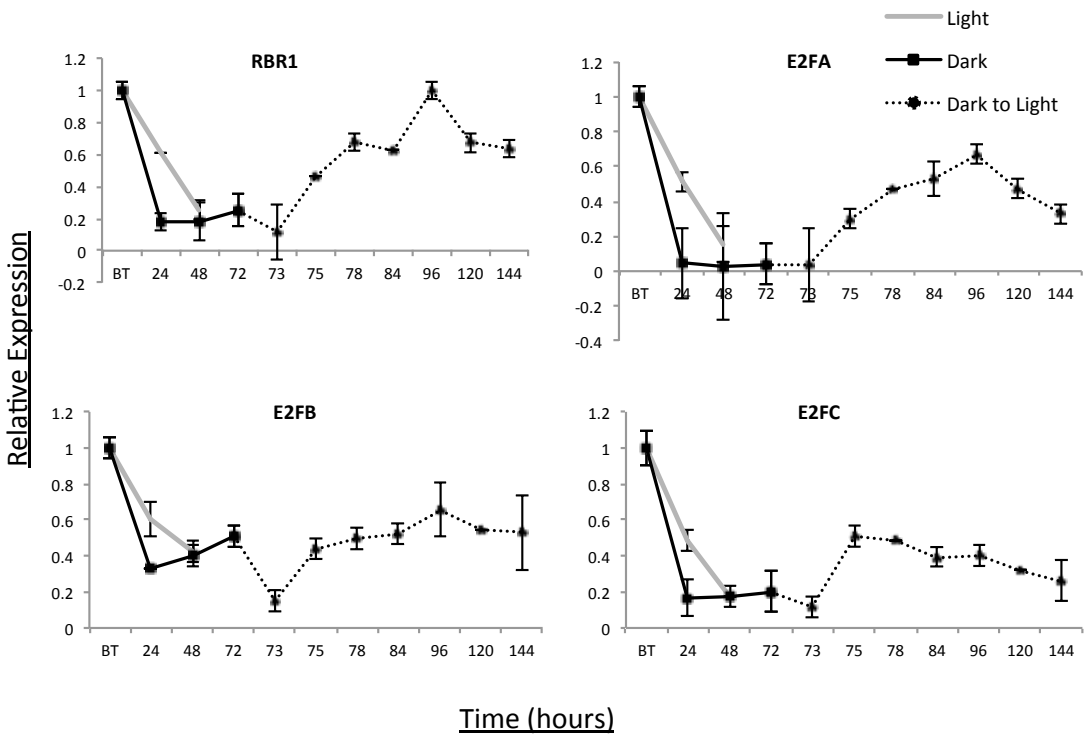

Figure 4-12 Transcript abundance of the proteins involved in the RBR1/E2F/DP pathway varies

Analysis of expression of the genes indicated, obtained by Q-RT-PCR) in first new leaf pair tissue. Whole seedlings were grown in – sucrose medium plates under continuous light. At 7 dag (before transfer, BT) seedlings were transferred to 3 days dark (dark, solid black line, 24 h, 48 h and 72 h), continuous light was a control (light, solid grey line, BT – 72 h). After 3 days dark (72 h) seedlings were transferred back to light (dark to light, dotted line, 72 -144 h). Time points of dark to light transfer correspond to 1 h (73 h), 3 h (75h), 6 h (78 h), 12 h (84 h), 24 h (96 h), 48 h (120 h) and 72 h (144 h), hence the labelling of the x axis (in hours, h). BT is the reference point. Bars show standard deviation of 3 technical replicates of one RNA sample.

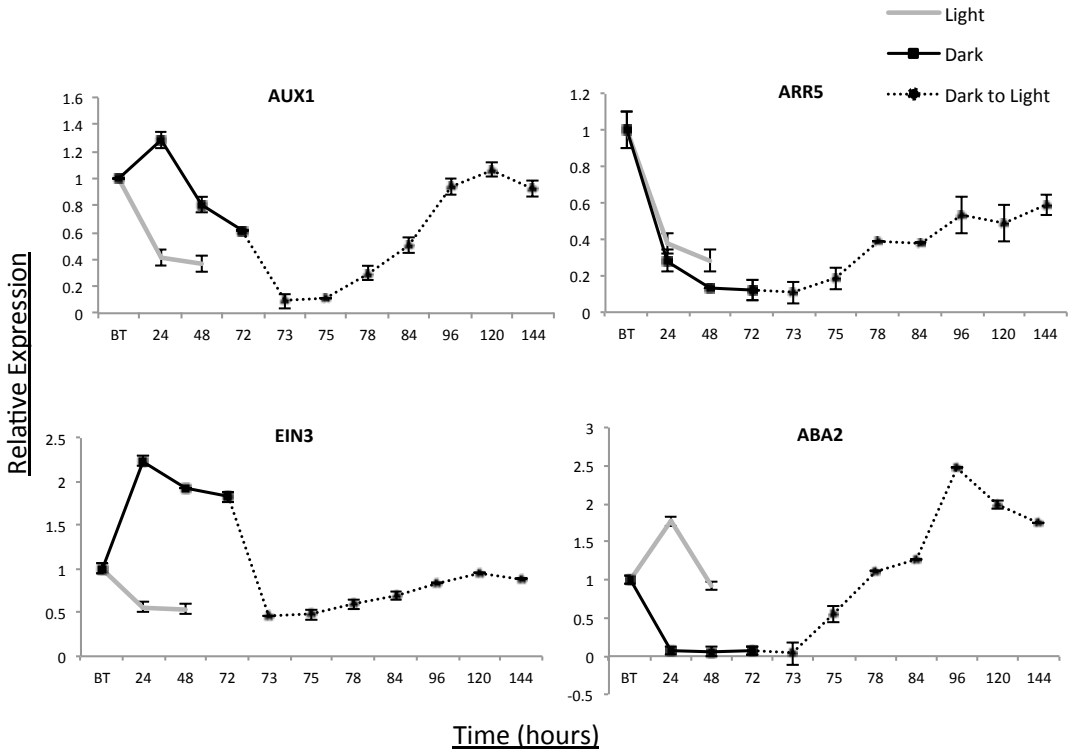

Figure 4-13 The dark to light growth response involves hormone pathways

Analysis of expression of the genes indicated, obtained by Q-RT-PCR) in first new leaf pair tissue. Whole seedlings were grown in – sucrose medium plates under continuous light. At 7 dag (before transfer, BT) seedlings were transferred to 3 days dark (dark, solid black line, 24 h, 48 h and 72 h), continuous light was a control (light, solid grey line, BT – 72 h). After 3 days dark (72 h) seedlings were transferred back to light (dark to light, dotted line, 72 -144 h). Time points of dark to light transfer correspond to 1 h (73 h), 3 h (75h), 6 h (78 h), 12 h (84 h), 24 h (96 h), 48 h (120 h) and 72 h (144 h), hence the labelling of the x axis (in hours, h). BT is the reference point. Bars show standard deviation of 3 technical replicates of one RNA sample.

The *AUXIN RESISTANT1* gene (*AUX1*) encodes an auxin influx transporter but was here used as a well-characterised auxin-responsive gene. In Fig 4.13, expression behaviour shows *AUX1* increased in the dark and remained low in the light.

Light perception after dark caused a transient decrease in *AUX1* expression in the first hour followed by a recovery and later a broad peak in expression, 96 h-144 h (24 h-72 h DL/day2-3 after re-transfer to light), at the time of cell expansion.

ARABIDOPSIS THALIANA RESPONSE REGULATOR5 (*ARR5*) expression was lost in light but more rapidly so in dark, and was upregulated within six hours after transfer back to light. Cytokinin is typically described as a cell division-promoting hormone, at least in aerial tissues (Shani *et al.*, 2006). This is consistent with its rise upon DL transfer and its gradual decline in the light control, where leaves continue to grow and differentiate, and stronger decline in the dark, where growth arrest occurs.

The tryptophan dependent auxin biosynthesis is downstream of ethylene response, (Swarup *et al.*, 2007; Stepanova *et al.*, 2008), this prompting us to monitor the response to ethylene. *ETHYLENE INSENSITIVE3* (*EIN3*) expression, representative of ethylene action, mirrored the behaviour of *AUX1*, high in the dark, light repressed and becoming gradually upregulated as cells exited division.

ABA drives etiolated growth and inhibits deetiolation and photomorphogenesis (Humplík *et al.*, 2015). Contrary to this, *ABA2* expression (Fig 4.13), constant in light, was downregulated in the dark although opposite to *EIN3*. In the DL transfer *ABA2* transcripts increased after a few hours and peaked approximately at 96 h, (24 h DL). A plausible explanation is that *ABA2* is induced by glucose application (Cheng *et al.*, 2002). One could describe the status of ABA responses as being the almost exact opposite to those of the "starvation genes".

These results reiterated the importance of phytohormones, their possible interaction with sugar signalling pathways, and their role in regulating growth and development of organs. Inevitably this adds greater complexity to our understanding of growth.

4.9 Direct access of sucrose

Darkness causes a growth arrest in both + and – sucrose conditions (Fig 4.6). However, notably in the + sucrose %GUS quantitation experiments, a small peak of mitotic activity was occasionally observed in the continuous dark condition at 96 h. Upon returning to these samples it was found that the new leaf petioles were etiolated and there appeared to be a pattern to this observation in the + sucrose plates that did not occur in a similar fashion in the – sucrose plates, explaining the flat line observed for CD %GUS. Direct access of sucrose to the shoot SAM, via vertically grown plates in the dark, produced a similar phenomenon (Roldan *et al.*, 1999). Based on this seedlings that were occasionally found to have fallen flat on the agar were separated from those standing upright and the CYCB1;1::GUS assay carried out.

4.9.1 **Direct access of the shoot apex to sucrose leads to initiation of new leaf 3/4**

Over time seedlings in the dark began to have slightly elongated hypocotyls as well as etiolated appearance of petioles of NL 1/2. This observation was made regardless of the presence of sucrose in the medium, and eventually caused some seedlings to fall onto the medium. In the – sucrose plates neither seedlings that had fallen 'flat' nor those that remained 'upright' showed CYCB1;1::GUS activity. When visualising the mitotic staining, those seedlings that were flat in the + sucrose plates showed CYCB1;1::GUS staining while those that were upright showed no or negligible staining (Fig 4.14). This serendipitous observation recapitulated the observation by Roldan *et al*., (1999), but with the added tool to visualise those cells that were dividing in the absence of light. It appeared that the staining was more specific to the SAM and NL 3/4 (indicative of an active meristem). In fact NL 1/2 lacked staining except for a few punctuated dots at the junction between the leaf lamina and the petiole, suggestive of an elongation response. Appearance of NL 3/4 occurred without growth recovery in NL 1/2 of these same seedlings, suggesting that the growth promoting-signal was restricted to the meristem and the organs that then emerged from it.

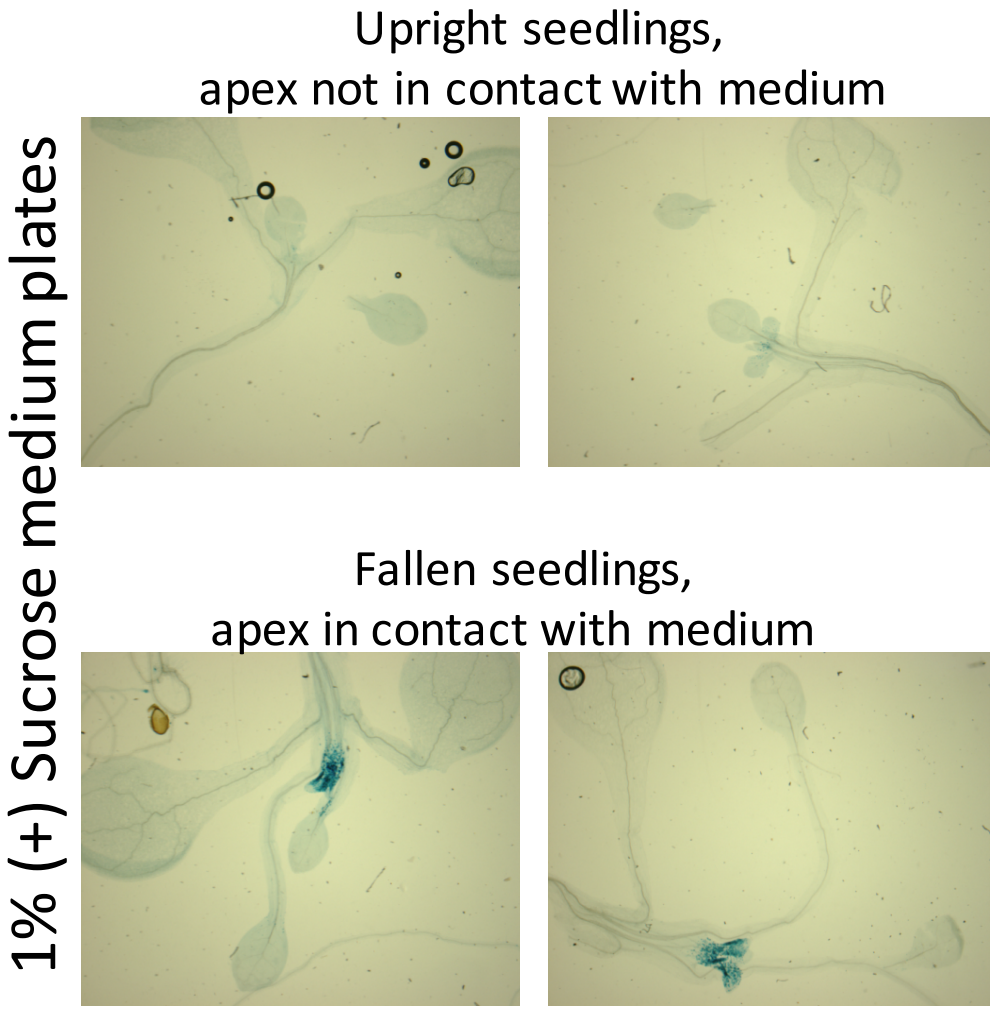

Figure 4-14 Access of sucrose to the shoot apex initiates new leaf 3/4 primordia in the dark

CYCB1;1::GUS seedlings were grown on + sucrose medium, under continuous light, and at 7dag were transferred to continuous dark. Approximately 7 days later seedlings were examined for GUS activity. Seedlings which had fallen and whose apex, as a result, was in direct contact with the medium (**bottom**) were separated from those that remained upright (**top**). No GUS staining was observed in the upright seedlings. Seedlings that had fallen and whose apex contacted the medium showed GUS staining at the SAM and new leaf 3/4 (close to the SAM).

4.10 Discussion

Through the series of experiments described in this chapter, I tried to address two sets of key questions concerning the possible role of energy (carbohydrate) signalling pathways in the control of cell proliferation and growth. Acknowledging that there is cross talk between carbohydrate and light signalling pathways I addressed the question how energy/nutritional status of a cell effects cell cycle regulators. Secondly, what signatures responses are common in a re-deetiolation of very young leaf and the dark imposed arrest at the meristem, and then its transfer back to light.

In the experiment involving exogenous application of sucrose (or absence of it) not all four cell cycle genes responded as quickly to the treatments, some responses took place at 6 h and some at 24 h. Sucrose application onto intact, whole seedlings does not yield similar results to experiments involving liquid cell culture, CYCD3 levels were down 2 fold after 24 h when sucrose was removed from the liquid cell culture and up by 4 fold within 4 h when sucrose was reapplied (Riou-Khamlichi *et al.*, 2000). Application of exogenous sucrose is experimentally useful but in the natural environment plants produce sucrose in the leaves and transfer via the phloem to other organs, such as roots. However, this does not exclude the possibility that some sucrose can be taken up from the plate medium at the aerial tissues and consequently can affect lateral root emergence in WT, and this process is enhanced in cutin defective mutants *lateral root development2* (*lrd2*) and *Long-Chain Fatty Acid Synthetase 2* (*LACS2*) (MacGregor *et al.*, 2008). The observation of CYCB1;1::GUS staining at the apex and NL 3/4 in the dark, when seedlings had fallen and contacted the sucrose containing medium, can be attributed to this too. A carbon incorporation assay, via radioactive labelling, would confirm this phenomenon.

Alternatively, in the 4 h extended dark/night experiment, cell cycle genes exhibited behaviour whereby transcripts were up in the light, when carbon is available, and down in the dark, particularly once carbon is depleted. When E2FB levels were modified in plants this observation was dysregulated, with respect to the relative transcript fold change and light and carbon availability. These findings reiterate the notion that some cell cycle genes are activated depending on the phase of the cell cycle, others are activated in response to signals such as light and/or sucrose and perhaps a combination of the two. As a general rule for cell cycle gene transcripts,

"light equals more, dark equals less", but whether transcript abundance *per se* or the lengths of light and dark periods carry a stronger influence awaits clarification, as only E2FB levels were modified here.

Because it appeared that cell cycle transcripts were to some extent regulated by light and carbon availability and could also be upregulated by abundance of another cell cycle protein (E2FB), post-translational modifications were looked into. Monitoring of the master regulator RBR1 and its phosphorylation state revealed the fact that carbon availability correlates better than light perception with RBR1 phosphorylation (the state that drives cell cycle progression at the G1 checkpoint, better termed as restriction point). This was because the *pgm* mutant, at times when it lacked available carbon, yet was in the presence of light, showed lack of RBR1 phosphorylation. To truly confirm that carbon availability leads to growth progression via cell division a CDK activity assay could be used.

The role of light in leaf initiation at the apex was elucidated in the 3 day dark grown seedling-deetiolation study previously mentioned (Lopez-Juez *et al.*, 2008). The key gene signature responses assumed to be involved in the light dependent organ initiation (primordia) at the SAM were found to be similar for organs (NL 1/2) already present that were then transferred to 3 days dark. Although only one or two key genes were used to monitor each component of the response, the fact that all behaved as in the shoot apex organ initiation response suggests the gene expression programming in the two growth phenomena to be similar.

To reiterate, light can act as a signal that is perceived via photoreceptors and as a source of energy where carbon availability and assimilation produces sucrose. That said, sugar (specifically sucrose) itself can also act as the source of energy, as it is systemically transported in the plant, and as a signal (based on my observation recapitulating those reported by (Roldan *et al.*, 1999)). Thus, it is difficult to distinguish whether the key growth responses observed in this chapter, albeit similar to (Lopez-Juez *et al.*, 2008), are due to light perception or to light as a source of energy, which inevitably yields sugar. Undoubtedly there appears to be cross talk between light and sugar signalling pathways but in the future these could be separated through simple experiments, at least in the context of this work. The growth responses observed for the leaf primordia here are similar to those for the

shoot apex in the earlier study (Lopez-Juez *et al.*, 2008), in the initial time points of which no leaves were present, and even the cotyledons were photosynthetically incompetent and therefore unable to generate new sugar. This strongly suggests the growth responses to be dependent on light perception by photoreceptors that signal to downstream factors and cause the responses observed at the mRNA level. The sensing pre-eminence of photoreceptors and their signalling pathways can be tested by repeating the current 3 day dark assay in NL 1/2 but with the use of constitutive light perception mutants, for example *cop1* (Deng *et al.*, 1991) and *det1* (Chory *et al.,* 1989), for a recent review see (Lau and Deng, 2012). Both *cop1* and *det1* mutants were identified in an *Arabidopsis* screen displaying light grown phenotypes in darkness. While their roles are not limited to photomorphogenesis, they are both involved in the targeted degradation of light response-transcription factors (HY5, HYH) in darkness, i.e. such transcription factors are preventing from acting in the dark, becoming active in the light, or when COP1 or DET1 are absent. If indeed photoreceptor signalling rather than photosynthesis turns growth-related genes on, one would predict such genes to behave in the dark in those mutants as they do after light perception in the wild type. However, given that the mutants are photosynthetically competent, if photosynthesis, and not photo-perception, is responsible for the changes in gene signatures during re-deetiolation, such gene expression signatures in *cop1* and *det1* mutants would parallel those of the wild type.

A recent study (Pfeiffer *et al.*, 2016) has revealed that both light and energy signaling act independently in activating WUS expression at the SAM, and that both are needed in synergy for full photomorphogenesis to take place as does in the light. The authors' work also concluded that light perceived through phytochromeB as well as the cryptochromes influences the SAM as determined by WUS induction in a reporter line. Notably, they reiterated that light was not perceived by the SAM but other distant tissues and suggested an unknown mobile signal. Examination of *cop1* and *det1* would confirm that this secondary signal, which it is tempting to speculate could play a permissive role allowing or disallowing sugar/energy signaling, is itself controlled by classic light signaling.

In the absence of light, sucrose at the aerial tissue can induce mitotic activity that is absent under the same condition in the absence of sucrose in the MS medium plates. One possible explanation for this phenomenon is that the shoot apical region is

deprived of access to sucrose, which would otherwise be available through the phloem, in the absence of light. This would explain why the starvation gene expression response is so rapidly ended by the presence of light, regardless of the photosynthetic competence of the cotyledons or the existing young leaves. It is unclear from this study whether the sucrose accessibility control would be specific to the region where the GUS staining was observed or whether accessibility to sucrose occurs across all aerial sink tissues. If the latter were true it is plausible that sucrose allows for an unknown secondary signal to exert its effect specifically at the apex and newly emerging primordia. This would explain why access of sucrose to the aerial tissue does not bring about morphological changes in the pre-existing NL 1/2 in the dark but only to *de novo* leaf initiation.

Growth of plants is regulated by many factors and at the SAM, the organ generating centre of the aerial part of the plant, these have been highlighted in the work of Dr Lopez-Juez and colleagues, 2008: cell proliferation, boost of translation capacity, energy availability, the antagonistic role of hormones. Each factor requires a deeper understanding of how it regulates growth. As far as cell cycle activities are concerned, cells undertake decisions related to entry, undergoing proliferation *vs* endoreduplication, and exit. The decision to enter appears associated with that of increasing translation capacity, as reflected by increased ribosome biogenesis. Increasing cell division drivers (E2FB, chapter 3) enhances growth in terms of increasing cell number, but not necessarily organ or plant size. Whether or not more E2FB protein in the plant will bring about the same response in the 3 day dark assay was not analysed here. However this experiment could be done to test whether enhanced mitotic drivers will delay mitotic arrest (shown by the disappearance of CYCB1;1::GUS staining), if at all, and cause a faster recovery when brought back to light (staining would be expected to appear before 12 h upon seedling transfer back to light). Similarly, one could test whether the presence of sucrose (preferably provided as liquid media) could replace the transfer back to light (in a protocol with no lights on but seedlings being transferred to sucrose-containing liquid media). This could be done with the CYCB1;1::GUS expressing line, an experiment which would extend the data obtained in the related work by Roldan *et al.* (1999) in which they exposed seedlings on vertical sucrose-containing plates. The experiment would address to what extent sucrose can replace the absence of light and this is why the

other signature responses would also be useful. My findings show that the original observations made by Roldan and colleagues involves a cell division/mitotic response. However, this now poses the question why morphogenesis in the dark is still very different and specific because it appears that cell division and elongation take place, yet phenotypically seedlings exhibit skotomorphogenic growth. Again, this directs further study into spatial regulation of developmental signals/regulators. Another experimental strategy could test whether possesing a high auxin but low cytokinin state (and *vice versa*), by genetic means, affects growth of the SAM and emerging leaves. Thus, the follow up hypotheses of this study emphasise the value of the key signature responses involved in organ initiation (SAM) and primordia growth, as established in this work (see schematic summary, Fig 4.15).

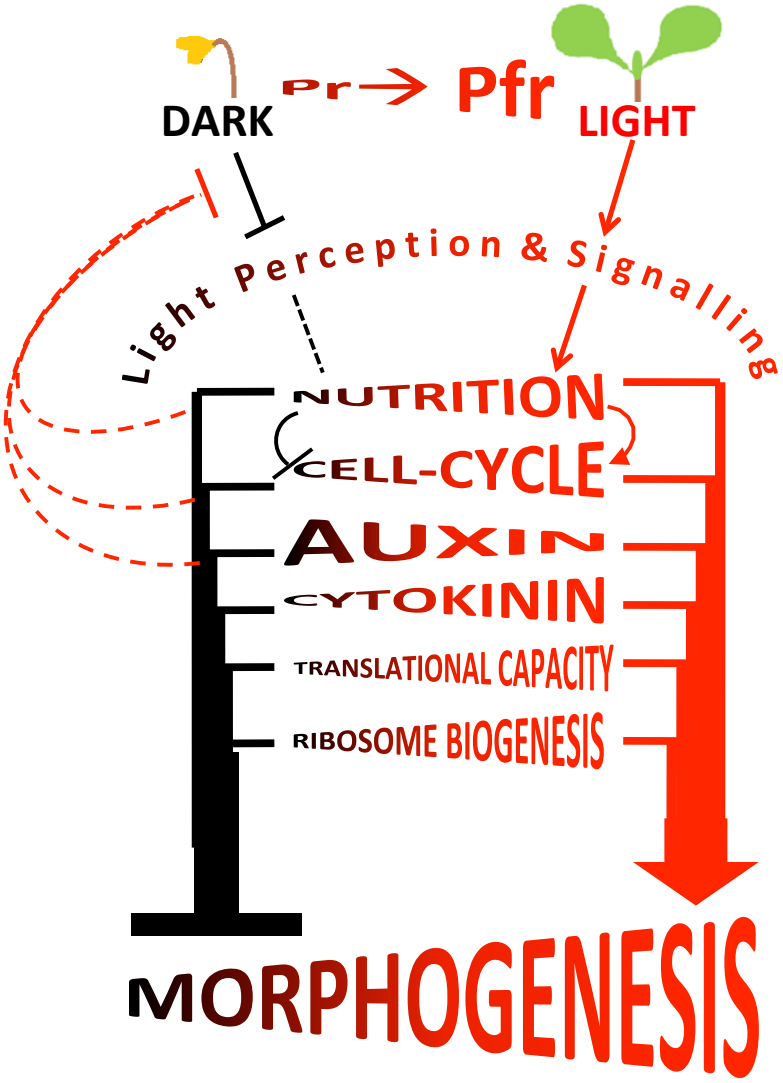

Figure 4-15 A schematic diagram to represent the reprogramming events associated with dark and light morphogenesis

Arrows represent promotion, blocked arrows represent repression and dotted lines represent theoretical promotion/repression or neither (a gap in knowledge). Font enlargement shows degree of promotion of the process referred, aided with colour gradient (black to red) for dark to light reprogramming and promotion of morphogenesis.

Dark (with Pfr absent) equals absence of light perception and causes the associated signalling cascades to be blocked ultimately preventing photomorphogenesis (shown by the presence of apical hook and the absence of leaf development). This is due to a low nutritional status of cells (low carbon availability), low cytokinin (but high auxin) responses, low translational capacity and ribosome biogenesis and reduced cell cycle activity. Light promotes all of the aforementioned except for auxin responses which are transiently reduced upon transfer to light; this is due to light perception and signalling. Availability of reduced carbon (nutrition) promotes cell cycle activity whereas lack of it prevents cell cycle progression. It remains unclear whether the absence of light perception in the dark is directly responsible for the downstream events. Whether reversing the degree of promotion of the events shown as text independently of light perception is or is not sufficient to induce photomorphogenesis in the dark (red dotted blocked arrows on left) is yet to be known.

Chapter 5: High light acclimation and leaf growth

5.1 Introduction

In chapter 4 I focused on light irradiation and how this affects sugar metabolism. Then I associated growth with light, the absence of which caused a growth arrest. In this chapter I focus on, not the presence or absence of light, but the quantity of light and how this affects growth. This will be referred to as a light acclimation.

Plants acclimate to their changing environmental conditions aiming to optimise growth. Well known light acclimatory responses are phototropism, that effects leaf movement, shade acclimation, that affects chloroplast composition in order to improve light capture as well as other changes in leaf orientation, morphology and chloroplast positioning. The words 'sun' and 'shade' are typically used to describe the results of high light (HL) and low light (LL) acclimatory responses, respectively, and can be used to describe plants, as used in (Lepisto and Rintamaki, 2012), or leaves and chloroplasts, as used in (Weston *et al.*, 2000). Shade light can also refer to the altered light quality (spectral composition) which occurs when direct sun light is filtered by a plant canopy: this leads to a selective removal of visible light, particularly blue and red, and as a result a selective enrichment in far-red light wavelengths (Casal, 2013). Such an enrichment inactivates light-stable phytochromes and this triggers a shade avoidance syndrome, involving stem elongation. I study only the impact of altered light quantity. In continuous light and unchanged light quality (spectrum), sun plants, unlike shade plants, have thicker leaves, longer palisade cells, higher stomatal index, small grana, higher chlorophyll content and high CO_2 assimilation per leaf area (Lepisto *et al.*, 2009). Similarly, chloroplast composition in high light involves more starch granules (larger in size) and fewer stacked granal thylakoids (Weston *et al.*, 2000).

Leaves in HL have a greater photosynthetic capacity per unit leaf area because they are adapted to maximising the efficiency of light capture. Under HL conditions leaves use that light to, among other things, increase palisade cell divisions, increasing the number of cells per unit area. Consequently, the number of

chloroplasts per unit area also increases. In *Chenopodium album* (a herbaceous plant) HL responses were observed in young leaves of the same plant under two different conditions: 1) Only mature leaves were exposed to HL and the shoot apex shaded; 2) Only the shoot apex was exposed to HL (mature leaves were shaded). In the first condition a multi-cell palisade (i.e. more cells in palisade than are typically observed in the leaf) was observed in the young leaves but in the second condition only a single palisade layer was observed, suggesting that young leaves are influenced by signals from mature leaves (Yano and Terashima, 2001). Indeed it has been shown in *Arabidopsis* that primordia of HL-exposed plants already contain a multi-layer palisade at the earliest stage that can be observed (Kalve *et al.*, 2014). This suggests that the HL action impacts the meristem itself and causes the recruitment of a greater number of meristematic cells for each primordium.

It was shown that blue light is needed for cell expansion in WT-L*er* (Lopez-Juez *et al.*, 2007). Other studies have observed that in HL sub-epidermal palisade cells elongate (becoming described as cylindrical, greater in length than width) but this did not occur in red light (devoid of blue light). However, in the PHOTOTROPIN (PHOT) (*phot1* and *phot 2*) double mutant or the *phot2* single mutant palisade cell elongation in HL was still observed (Lopez-Juez *et al.*, 2007). In another study it was confirmed that sub-epidermal palisade cell height (anticlinal direction) was blue light dependent (in HL) and increase of width of cells (in the periclinal direction) was only observed in red HL (height increases were also observed in red HL) (Kozuka *et al.*, 2011). Kozuka and colleagues (2011), also showed that this response was primarily PHOT2 dependent as constitutively expressed PHOT2 caused anticlinal palisade cell elongation independent of blue light. In the presence of blue light PHOT2 also caused anticlinal positioning of chloroplasts in palisade cells, as part of a protective avoidance response (Kong *et al.*, 2007; Kagawa *et al.*, 2001). Notably chloroplasts in low light were at a periclinal orientation (Lopez-Juez *et al.*, 2007; Trojan and Gabrys, 1996) but Kozuka and colleagues (2011) showed palisade cell development to be independent of chloroplast position.

A variegated mutant, with functional chloroplasts (in a green half of the leaf) and defective chloroplasts (albino half of the leaf) within the same organ, showed that the increase in leaf thickness and palisade cell elongation in HL occurred only on the "functional-chloroplast" (green) side. Emphasis in this study (using the variegated

mutant) was on the role of chloroplasts in altering leaf morphology, independent of the light signal. For instance, a multi-layer palisade in HL was only observed in the green (functional-chloroplasts) leaf sectors suggesting the involvement of retrograde signalling in the HL acclimation of the leaf (Tan *et al.*, 2008). In this work retrograde signalling specifically refers to signalling between subcellular organelles, from plastid to nucleus. It was in my interest to try to understand this phenomenon because I was interested in light and proliferation-dependent growth; the impact of the presence of viable chloroplasts suggested that a chloroplast-derived signal is involved in this response. I further hypothesised this signal is based on energy status and it is most likely photosynthate which causes this photosynthetic acclimation of the leaf in HL.

It is important to note that cell proliferation in the periclinal direction, i.e. to generate extra layers of palisade, is not the only form of proliferation possible. Under HL larger organs (with a greater area) are also generated, and this form of cell proliferation could also be controlled by photosynthate availability. The term photosynthate is broadly used to refer to photosynthesis-derived sugars in the plant.

5.2 Aims and objectives

My interests were specific to the HL acclimation response of leaves becoming larger and forming multi-palisade cell layers. I tested the hypothesis that this response involves proliferation of cells from a differentiated cell/tissue stage (i.e. the palisade cells return to division in HL). To answer the question "when does this proliferation-dependent response take place?", I repeated a LL to HL transfer experiment on 13 dag soil-grown seedlings (germinated on MS medium plates up till 6 dag and then transferred to soil) and used a mitotic reporter (CYCB1;1::GUS) over a time course in *Arabidopsis* rosettes.

To elucidate the role of RETINOBLASTOMA RELATED1 (RBR1) in the HL acclimatory response, young new leaf (NL) tissue was used to detect the abundance of Phosphorylated-RBR1 (P-RBR1). P-RBR1 was used as an indication of E2Fs being freed from RBR1 suppression and it was hypothesised it would be more abundant in HL.

I hypothesised that photosynthate was the signal that stimulated the HL acclimation response in green sectors of the variegated mutant leaf (Tan *et al.*, 2008). To test this I used a photosynthesis specific inhibitor 3-(3,4-dichlorophenyl)-1,1-dimethylurea (DCMU) in the LL to HL transfer and again monitored the abundance of P-RBR1 protein.

It should be noted that experimental set ups (use of plates or soil) and tissue (NL pair used) varied among these experiments and are described in detail for each section. Continuous Light (CL) conditions, of a constant spectrum, were used in all experiments and only changes in light intensity were made.

5.3 Proliferation-dependent growth in acclimation to high light

Unlike endoreduplication (expansion) –dependent growth, proliferation-dependent growth does not skip mitosis (M). I used a M phase cyclin to report mitotic activity (CYCB1;1::GUS) in all leaves of 13 dag seedlings when transferred from LL (60 μmol m^{-2} s^{-1}) to HL (400 μmol m^{-2} s^{-1}). Observations were made over 2, 6, 12, 24 and 48 hours (h).

5.3.1 **An increase in CYCB1;1::GUS activity occurs in HL but only in 'young' tissue**

Whole seedlings were used for the CYCB1;1::GUS assay and NL were dissected afterwards. In untreated leaves (those that remained in LL) the natural CYCB1;1::GUS staining existed, displaying a high to low gradient from base to tip (Fig 5.1, leaf number 4/5). No staining of mitotic activity was observed in cotyledons (LL) and these are not shown in Fig 5.1. However, on our experimental set up no staining was observed in NL 1/2 (LL) either, even at the earliest time-point (2 h) where up to NL 5 could be dissected (Fig 5.1). I found that the increase in mitotic activity could be observed as early as 2 h.

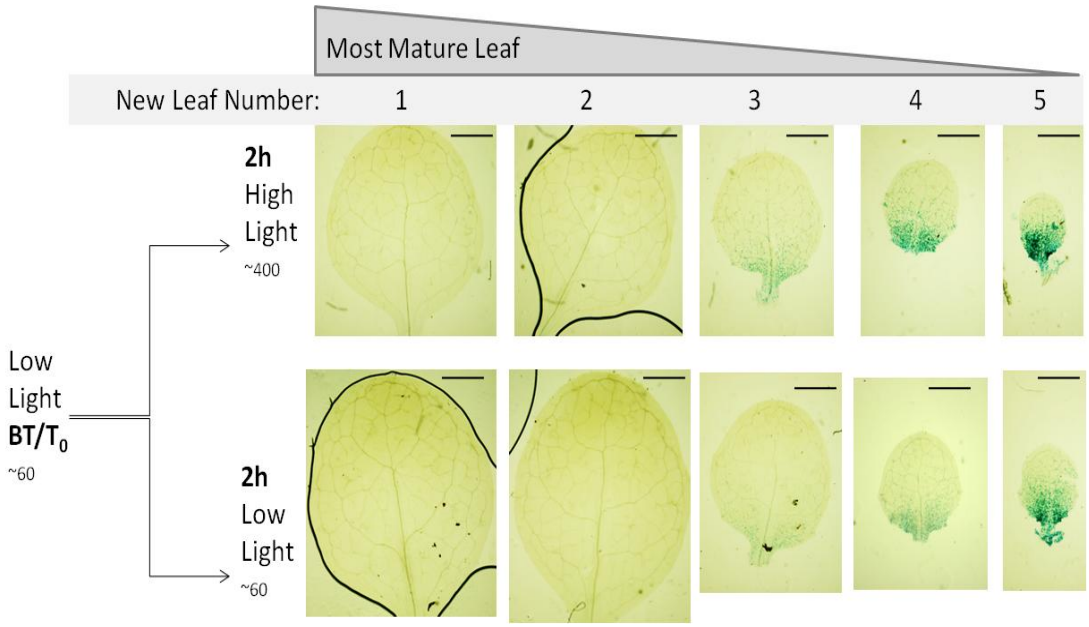

Figure 5-1 *Arabidopsis* new leaves stained by the CYCB1;1::GUS reporter 2 hours after transfer to high light.

13dag (days after germination) soil-grown seedlings under continuous light (~60 µmol m^{-2} s^{-1}) (BT/T_0, before transfer) were transferred to high light (~400 µmol m^{-2} s^{-1}) and analysed 2 hours (h) later for mitotic activity with use of the CYCB1;1::GUS reporter system. High light samples (top panel) were compared to low light samples (bottom panel). The younger the leaf, the greater the staining (left to right, both panels). Also refer to appendix 5.2 for quantitative data analysis.

These findings show that those leaves that had no staining in LL did not ever have staining upon transfer to HL (these leaves include the cotyledons and NL 1/2). However, wherever staining was observed in LL, even though it may have been very sparse (usually just above the blade-petiole junction), an increase occurred in HL (see NL 3, Fig 5.1 and appendix 5.2).

5.3.2 **Ploidy levels increase sooner under HL conditions**

Using the same experimental conditions as in section 5.3.1 DNA content analysis was carried out at 1, 3, 6, 12, 24, 48 and 72 h, using flow cytometry. This was done for NL 3/4 and NL 5 (I observed that these leaves were present from the T_o timepoint, subsequent leaves emerged during the course of the experiment and were not measured). Notably, NL 3/4 were developmentally mature in comparison to NL 5 (Fig 5.2).

The LL to HL transfer shows very little change in the proportion of cells in 2N, 4N and 8N over the first 6 hours (Fig 5.2A). In the case of NL 5 only 2N and 4N peaks were observed as expected (Fig 5.2B). NL 3/4, at 12 h, show the ploidy status of cells to be increasing in the HL conditions: the proportion of cells in 4N is greater in HL, after 12 - 24 h, followed by more cells in 8N, after 48 h HL, and then a 16N peak was present only in HL, at 72 h (Fig 5.2A). These differences were less obvious for NL 5, they were evident only at 24 and 48 h, but I noted the variability of the data, shown by the standard deviation bars, to be greater when working on NL 5, particularly at 48 h (Fig 5.2B).

I aimed to look at the DNA synthesis, S phase, activity of cells in the LL to HL transfer (Fig 5.2C). It was noted that evidence of endoreduplication was present in LL and HL, NL 3/4, at the 3 h time point (Fig 5.2A). Cells had greater S phase activity as early as 1 h in the HL conditions (Fig 5.2C) and this difference was more pronounced towards 24 - 72 h. In summary, analysis of these results showed that NL 3/4 enter endoreduplication early in HL conditions and this coincides with an increase in S phase activity.

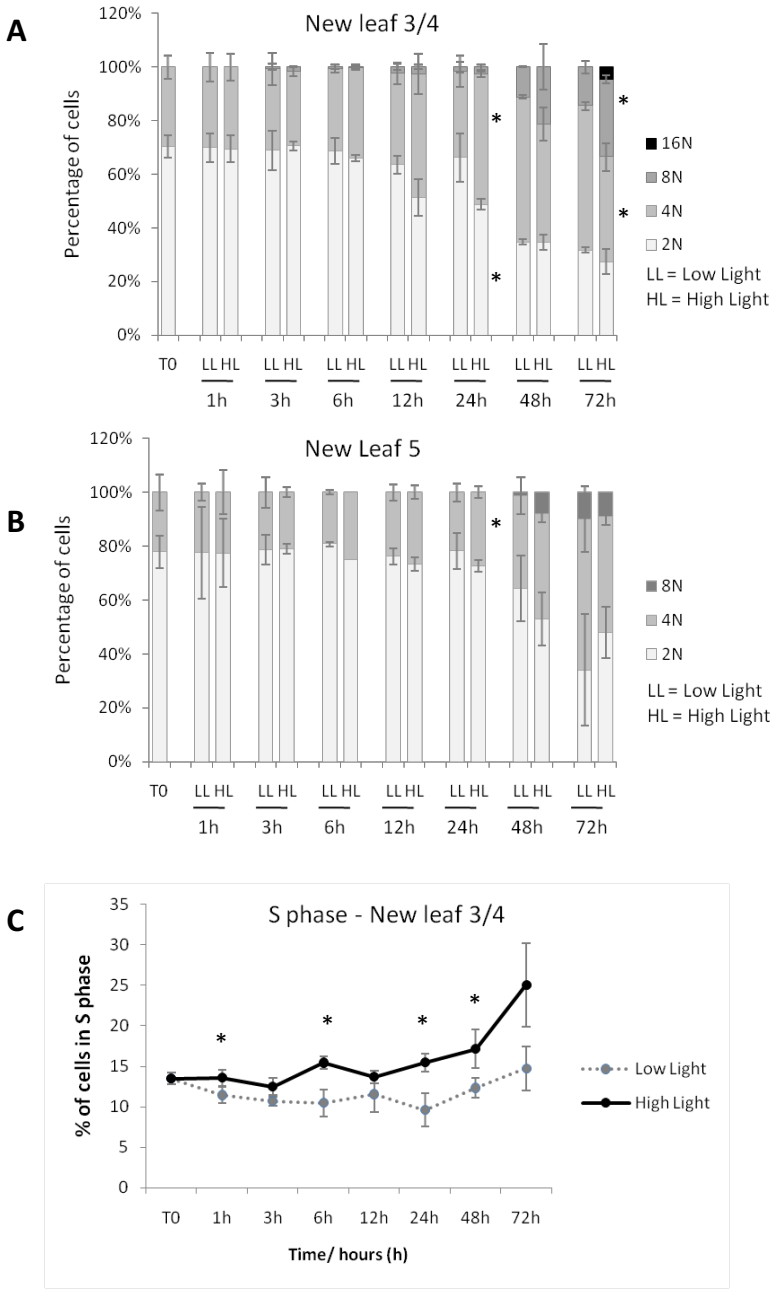

Figure 5-2 DNA content analysis of cells in new leaves under low light *vs* high light conditions

13dag (days after germination) soil-grown seedlings under continuous low light (LL) (~60 µmol m^{-2} s^{-1}) were transferred to high light (HL) (~400 µmol m^{-2} s^{-1}) and selected new leaf tissue was prepared for flow cytometry analysis over 1, 3, 6, 12, 24, 48 and 72 hours (h) after transfer. (A) New leaf 3/4 under HL increased ploidy levels sooner than LL samples (beginning at 12 h). A 16N peak was present in HL, 72 h, but absent in LL. (B) New leaf 5 (developmentally younger than new leaf 3/4) only showed early exit from proliferation at 48 h (HL, note the 8N value). (C) Analysis of S phase activity in new leaf 3/4 showed a greater proportion of cells in S phase in HL as early as 1 h. The greatest differences were observed at 48 – 72 h, when ploidy increases by endoreduplication as observed in (A). Bars represent standard deviation, based on a minimum of 3 biological replicates (with a pool of at least 4 leaves from different plants in each case). * marks statistical significance, $p<0.05$, *t*-test.

5.4 The phosphorylation status of RBR1 in the HL acclimation of new leaves

The phosphorylated form of RBR1, P-RBR1, was abundant in growth-favouring conditions, when sugar is present (Zoltan Magyar, *personal communication*). I anticipated higher P-RBR1 levels in HL compared to LL because I had confirmed that mitotic activity increases in HL, in NLs that had not yet exited proliferation. To assess this, the same experimental set up was used as in section 5.3, over a shorter time course, and NL 3 along with all other leaf material emerging from the shoot meristem was collected (I call this NL 3+ tissue, which excludes NL 1/2 and cotyledons). The RBR1-GFP line was used to facilitate detection of the P-RBR1 protein, because it was anticipated that such a line harboured a higher amount of RBR1 protein than its wild type. As a control NL 1/2 material was collected separately. Surprisingly I observed more P-RBR1 in HL in NL 1/2 (Fig 5.3), in spite of the absence of CYCB1;1::GUS in HL or LL. In NL 1/2 it was observed that P-RBR1 levels increased in HL and dissipated at 24 h HL (Fig 5.3A). I acknowledge that the before transfer (BT) P-RBR1 levels were greater than those at 2 h LL, in spite of the conditions having remained unchanged, and currently have no explanation for this fact. In LL P-RBR1 levels remained relatively unchanged between 6 – 12 h and then decreased at 24 h but notably P-RBR1 levels appeared higher in 24 h LL than 24 h HL. Detection of P-RBR was unsuccessful for NL 3+ tissue. The cause of this could not be identified as it was carried out simultaneously to NL 1/2.

5.5 Inhibiting photosynthesis (with DCMU) decreases levels of P-RBR1

To test whether a photosynthate based signal was responsible for the multi-palisade layers in HL acclimation I treated whole seedlings (grown on MS medium) with a photosynthesis inhibitor, DCMU. Seedlings were grown in 6 welled plates on liquid medium containing 0.25% sucrose, to minimise starvation responses inflicted by DCMU treatment, and allow seedling physiology to continue, but to still prevent responses elicited by high light if they are of a photosynthetic nature.

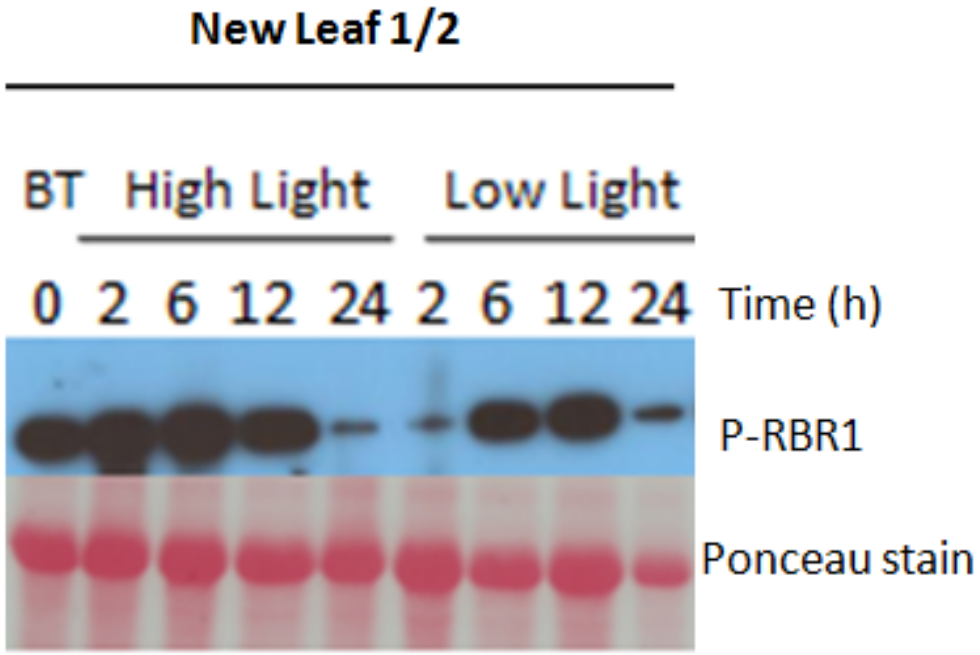

Figure 5-3 Phosphorylated-Retinoblastoma1 (P-RBR1) levels in the first new leaf pair under low and high light conditions

13dag (days after germination) soil-grown seedlings under continuous low light (LL) (~60 µmol m^{-2} s^{-1}) were transferred to high light (HL) (~400 µmol m^{-2} s^{-1}) and the first leaf pair tissue collected for Western blotting. A P-RBR1-specific antibody was used. This was done for 2, 6, 12 and 24 h after transfer, where low light samples were the control. Between 2 – 6 h P-RBR1 levels were greater in HL and similar at 12 h for LL and HL. At 24 h P-RBR1 was more abundant in LL compared to HL, note that at 24 h LL loading seems unequal/less (according to Ponceau stain). Reversible Ponceau stain (bottom, red) was used as a loading control. BT = Before Transfer. 40 µg protein was loaded. RBR1-GFPseedlings were used.

Seedlings (8 dag) were transferred to +/- DCMU liquid for an hour (still under CL, 60 µmol m^{-2} s^{-1}) and then transferred to HL (300 µmol m^{-2} s^{-1}) and whole shoot material harvested at 30, 60 and 120 min for LL and HL in +/- DCMU treatment. Again, the RBR1-GFP expressing line was used.

Firstly, I noted that the BT for +/- DCMU appear different but can attribute this to the unequal loading or non-uniform protein running from the well (observed by the reversible Ponceau stain) (Fig 5.4). Contrary to the observations in Fig 5.3 HL samples did not show more P-RBR1 levels compared to LL in – DCMU conditions, however, these samples comprise of whole shoot (not NL pair) (Fig 5.4). In + DCMU, HL samples showed slightly more P-RBR1 levels (evident at 30 and 120 min) but generally, compared to – DCMU , P-RBR1 levels were lower in DCMU treated seedlings (whole shoot tissue).

5.6 Discussion

Two of the main conclusions drawn from my current work on HL acclimation are: (1) young leaves that still showed mitotic activity, via the mitotic reporter staining (CYCB1;1::GUS), had the ability to increase mitotic activity in 2 h upon transfer to HL and (2) the P-RBR1 levels in HL did not mimic the mitotic response as anticipated: NL 1/2 showed increases in P-RBR1 in HL despite no increase in mitotic reporter staining being observed. This made it difficult to come to conclusions about P-RBR1 in HL and rationale for the observations is attempted below.

Due to time constrains the blot could not be repeated but reasoning is provided under the assumption that the data may be reproduced (3-10 biological replicates, individual seedlings, were used in each sample). The P-RBR1 protein was more abundant in HL than LL in NL 1/2, in which no mitotic activity was observed (Fig 5.1 and Fig 5.3). According to the mitotic reporter data, NL 1/2 are expected to have exited proliferation and entered into differentiation (endoreduplication/expansion). Thus, absence of cell division that is otherwise driven by E2FB would lead us to expect lower levels of P-RBR1 in LL than HL for NL 1/2. So why was more P-RBR1 present at 2 h in NL 1/2 HL when no mitotic activity was observed?

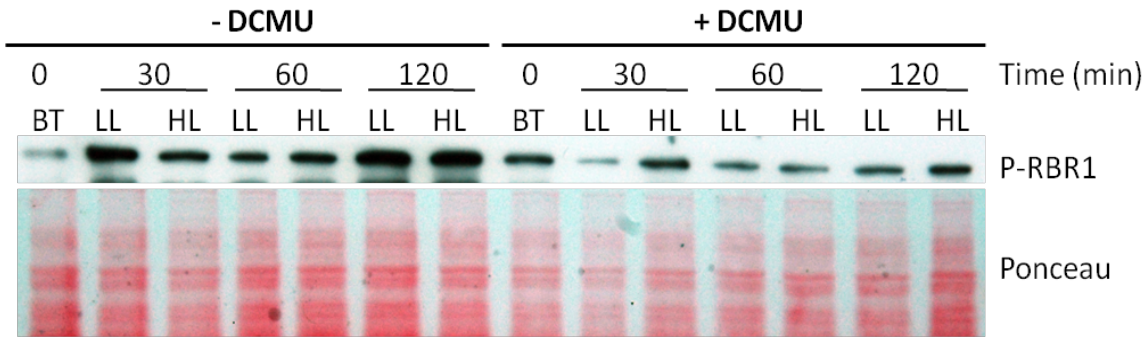

Figure 5-4 Phosphorylated-RETINOBLASTOMA RELATED1 (P-RBR1) under low and high light conditions in the presence and absence of DCMU treatment

Seedlings of 8 dag grown on liquid media under continuous light (BT, before bransfer) (~60 µmol m^{-2} s^{-1}) were transferred to +/- DCMU for an hour before transferring to high light (HL) (~300 µmol m^{-2} s^{-1}). Only shoot material was harvested at 30, 60 and 120 min, low light (LL) was used as a control. Western blot was carried out using a P-RBR1-specific antibody. In the absence of DCMU P-RBR1 levels were greater compared to DCMU-treated seedlings. HL samples did not show more P-RBR1 levels in – DCMU shoots but despite lower P-RBR1 levels in + DCMU, HL samples had more P-RBR1 levels compared to LL. Reversible Ponceau stain was used as a loading control. 30 µg of protein was loaded. RBR1-GFP seedlings were used.

I hypothesise that P-RBR1 releases free E2FA that drives the endoreduplication cycle, rather than cell division as does E2FB (Magyar *et al.*, 2012). This facilitates the fast proliferation-to-differentiation transition in HL leaves, later causing emergence of the subsequent leaf pair. Also, because no mitotic activity was observed, E2FB could not have driven cell division in NL 1/2. It remains unknown why the same response in NL 3/4 in HL would enhance cell division. This speculative hypothesis would require further work but provides an insight into how light signals may affect RBR1 post-translationally, yet by unknown mechanisms result in different growth responses at different stages of organ development. Additionally, in Fig 5.3 P-RBR1 levels were greater in LL 24 h, compared to HL 24 h. If this result is reproduced one explanation for this is based on a slower developmental progression in LL leaves as compared to HL leaves, due to which the 24 h LL sample exhibits higher P-RBR1 than the 24 h HL one. However, this is very specific for the NL number observed (in this case the primordia of the first leaf pair, which have exited proliferation) and the sampling time point. The slower developmental progression in LL leaves (as compared to HL leaves at the same time point, that enter and exit the cell cycle faster) is discussed later in this section.

It was also shown that P-RBR1 levels were generally higher in the - DCMU treated seedlings, irrespective of LL or HL conditions (Fig 5.4). The blot was reprobed to exclude the possibility of artefacts (see appendix 5.1). I anticipated that inhibiting photosynthesis would lead to less P-RBR1 in DCMU-treated seedlings. This would be due to a loss of the signal from chloroplasts. Based on the work of (Tan *et al.*, 2008) this treatment would be the equivalent of examining the albino leaf sector of the variegated mutant (Tan *et al.*, 2008). As a result, HL acclimation would not occur and cell division would be absent as no multilayer palisade would form. To understand these unexpected data the work of Yano and Terashima is appropriate. Their experiments (Yano and Terashima, 2001) on *Chenopodium album* (a herbaceous plant) showed that when the shoot apex was shaded, but mature leaves were under HL, the subsequent leaves arising from the meristem were sun-type with 2 palisade layers. Alternatively, a high light exposed shoot apex and shaded mature leaves produced single-palisade, shade type leaves. Chloroplast composition was nevertheless shade type suggesting that sugar may be the signal from mature leaves regulating leaf development of new leaves, while it is not the signal regulating

chloroplast composition (Yano and Terashima, 2004). The follow up study of Yano and Terashima, 2004, revealed that the periclinal divisions occurred mostly when cells were actively dividing (to form the two cell layered palisade), thus, light signals alter polarity of cell divisions. Moreover, they concluded that mesophyll growth and lamina expansion was not synchronous because palisade cells could elongate and expand (causing thickening of the leaf) after full lamina expansion. Perhaps this work is what led to the work of Kalve and colleagues (Kalve *et al.*, 2014) in taking their kinematic analysis of leaf cells to further understand the low light *vs* high light phenomenon (see below).

My initial hypothesis was that the additional palisade cell layer in HL is due to extra cell divisions. To address this I first discuss the experimental observations of the mitotic CYCB1;1::GUS staining and then (based on my observations and the work of Kalve *et al*., 2014) the plausible reasoning for why transfer to HL does cause extra divisions (which may in full or in part be periclinal and lead to additional layers) but only in newly emerging leaves in HL.

Mitotic activity in young leaves refers to those leaves in which staining was observed, as little as this may have been, and when observed, the staining was at the base of the leaf near the petiole. In chapter 4 I discussed that transition from proliferation-dependent growth to endoreduplication/expansion-dependent growth in *Arabidopsis* can be observed in the leaf with a cell cycle arrest front (distal-to-proximal or tip-to-base) and larger, less 'circular' (isodiametric) cells being present at the tip of the leaf (Andriankaja *et al.*, 2012). Thus mitotic activity remained near the base of the leaf and (based on my observations) as long as the entire leaf had not passed the transition state, HL acclimation could re-elicit further mitotic activity. In other words, it is plausible that the increased mitotic reporter staining observed in the same region of the leaf, under HL, is due to these cells (near the base) re-entering cell division. Notably, this enhanced staining in HL remained within the same region of the leaf as in LL (for instance, staining near the base in LL was observed to be greater in area in HL but was still present near the base, not the entire leaf surface). One can speculate that the same cells observed for mitotic activity (or being under proliferation-dependent growth, at any stage of the cell cycle) could be pushed into another round of cell division; on the other hand, possibly some cells at early phases of the cell cycle are made to "run through" and exit it faster contributing to the

observation of more mitotic activity. This may be explained by my observation, during the sampling of particular leaf numbers at the given time points, that leaves in HL appeared to emerge faster (based on size of young leaf) than LL leave (see appendix 5.2, I calculated %GUS for leaves in the same experiment as in section 5.3.1 and Figs 5.1 and 5.2, based on three biological replicates). The best example of how this is evident in the %GUS analysis of new leaf 6 (appendix 5.2). New leaf 6 shows that at 24 h and 48 h leaves in HL have less %GUS compared to LL leaves, owing to the fact that HL leaves are larger in size and this correlates with a smaller proliferation zone (GUS staining) where as LL leaves are smaller in size and most of the leaf is stained. Another example is new leaf 7 at 48 h (appendix 5.2) but results such as new leaf 7, 24 h, simply show leaves in HL have a greater ability to divide despite the fact that they may have emerged earlier, compared to the LL leaf of the same number and time-point. Hence, in summary, in the early experimental time points HL leaves show greater %GUS when compared to LL leaves of that time point. However, in the later experimental time points in NLs that still displayed mitotic activity, %GUS was greater in LL compared to HL (appendix 5.2). Importantly, I observed that plants in HL produced NL at a faster pace than those in LL and this explained the high %GUS values for LL leaves in later time-points. LL primordia remained at the mitotic stage even when HL ones had already exited. Because this observation may explain the staining patterns in this experiment, it would be necessary to track rosette leaf emergence quantitatively in the two light conditions. It appears that although exact experimental "times" after transfer were compared, "developmental times" may have differed for the two treatments. HL accelerates leaf initiation and exit from proliferation so the extra staining observed is most likely not due to a slowing of the cell cycle, a consequence of which would be more cells at that particular stage, but to a cell cycle acceleration. Overall, I concluded that %GUS differences in LL to HL transfer were most apparent in 'young' NL, i.e. in cells that were newly recruited into leaf primordia and observed soon afterward. This explained why NL 3 and 4 showed clear differences between LL and HL at 2 h. In contrast, NL 7 did not appear different at 24 h (in LL *vs* HL), as it emerged between 12 and 24 h, faster in HL and with a quick transition from proliferation-dependent to differentiation/expansion-dependent growth. So the stage at which NL 7 in HL shows a greater extent of proliferation than LL was probably missed (appendix 5.2).

The extra cell division observed following the transfer from LL to HL suggested that these divisions occurred when cells were about to transition to a differentiated state. Future work in our lab will require resin embedding and transverse sectioning, but this was not possible in the course of my work. Thus, my conclusions are limited but reasonable considering other recent observations (Kalve *et al.*, 2014). Certainly in HL conditions leaves produce an additional palisade cell layer (Lopez-Juez *et al.*, 2007; Tan *et al.*, 2008; Kalve *et al.*, 2014; Kim *et al.*, 2005; Yano and Terashima, 2001; Dengler, 1980; James and Bell, 2000) and in supplemental fig.1 of (Heyneke *et al.*, 2013). The recent work of Kalve *et al.,* 2014, is discussed as it describes kinematic data on the expansion rates of the whole-leaf lateral, longitudinal and anticlinal axis but also in the context of LL *vs* HL. In their experiments plants were grown in LL or HL (not transferred) and their findings confirmed that the mature LL leaf thickness was reduced by 45%. In agreement, HL leaves were thicker, mainly due to the thicker spongy and palisade mesophyll, and quantified to be larger in area too (Kalve *et al.*, 2014). An important finding was that tissue layer number was established early after germination (LL *vs* HL were applied from the start) but later anticlinal expansion rates contributed to the thickness of the leaf, so leaves transitioned early from HL to LL were thinner than those transitioned early from LL to HL, but had an extra palisade tissue layer. In the context of my work this suggests that the mitotic activity observed in young (already emerged) leaves, upon transfer to HL, was indicative of anticlinal divisions (divisions in which the new wall is formed with an anticlinal orientation). These anticlinal divisions most likely increase lateral/area growth of the leaf. Alternatively, leaves that then emerged in HL underwent early periclinal divisions. It is plausible that the rapid disappearance of mitotic staining in emerging HL leaves was due to anticlinal expansion coupled with endoreduplication (no M phase). Because periclinal division precedes anticlinal expansion (Kalve *et al.*, 2014) this may explain why HL NL 1/2 had increased P-RBR1 levels (at 2 h) (for DNA synthesis) but no mitotic staining (as M phase is skipped).

The quality of light affects flowering time. A low R:FR ratio accelerates flowering (Wollenberg *et al.*, 2008) as a survival mechanism of plants to rapidly produce seeds. However, this is typical of a shade avoidance response, not necessarily light intensity. Nevertheless, in five other long day plant species high irradiance was

shown to induce early flowering (Jalal-Ud-Din *et al.,* 2012) , an observation I made too for *Arabidopsis* in the transfer from LL to HL. As previously mentioned, leaves emerged faster in HL (appendix 5.2) and consequently plants flowered earlier. When a leaf primordium first emerges the leaf blade and petiole are indistinguishable for a couple of days (Kalve *et al.*, 2014) when Layers 1, 2 and 3 of the meristem are recruited to initiate the leaf primordium. I hypothesise that leaves emerging after the transition from LL to HL are influenced at this stage by HL in the decision to form an additional palisade cell layer. It is plausible this involves incorporating more cells from the meristem L2, supported by (Gonzalez *et al.*, 2012), or, alternatively, immediate periclinal divisions influenced by HL (both contributing to an additional palisade cell layer). To sum up, although preliminary, the results in this chapter reinforce the notion that light intensity can regulate proliferation-dependent, and later endoreduplication/expansion-dependent, growth in the leaf.

Chapter 6: General Discussion

6.1 Thesis Summary

The first half of my work studied the E2FB transcription factor and how important was its transcription activation function and binding to RETINOBLASTOMA RELATED1 (RBR1) as a repressor complex. Combinations of transformed lines were used and analysis of cell ploidy, cell size and number was an integral part of the analysis. Changes in plastid number and pavement cell shape were not anticipated and the analysis was limited to the transition of proliferation to differentiation in the epidermis.

The proliferation-to-differentiation transition was studied further at the whole organ level by a temporal perturbation of light. The perturbation of light and its effect on leaf initiation growth was previously characterised in our lab but in the shoot apical meristem (SAM) (Lopez-Juez *et al.*, 2008). My modified 3 day dark re-deetiolation protocol in young existing leaves was also an extrapolation of the acute endogenous carbohydrate starvation response. Thus, the growth arrest and recovery response in the re-deetiolation protocol is elicited by a light energy or light perception response that can easily be distinguished by photoreceptor mutants in a follow-up experiment. All signature responses hypothesised were tested and recapitulated responses of *de novo* leaf growth.

A further light perturbation experiment enhanced light intensity to distinguish whether or not high light induces cell proliferation in differentiated leaves. This was because high light leaves display an additional palisade as well as a thicker leaf (Weston *et al.*, 2000) (Tan *et al.*, 2008). Results from this work established that young proliferating leaf cells (not those which had exited proliferation) can proliferate more in high light but the proliferation response is likely to be axis specific.

Light presence is a prerequisite for leaf initiation and growth but my findings show that regulatory pathways involved in leaf growth are many and interlinked and

combine to overcome the effect of light absence. This discussion reiterates these mechanisms of cell proliferation control by light and beyond.

6.2 Regulation of leaf growth over multiple axes

Large and multi-lobed cells are present towards the tip of the leaf and correspond to differentiation-associated expansion growth. Contrary to this, dividing cells are small and isometric and are located at the base of the leaf. The "division growth" phase can be arrested at gap (G) phases by the absence of light or enhanced by increasing light intensity. Specifically in the latter, these findings are limited as they give no direct information about whether the cells divide to give rise to the multiple palisade or cells divide in the opposite direction, to increase leaf blade area. The conclusions made in chapter 5 can be combined with recent experiments (Kalve *et al.*, 2014).

Growth at the cellular level can be described based on axis of division, commonly known as plane of division, or axis of expansion. These dual axes of developmental regulation are an integral part of the two growth phases, proliferation and expansion-dependent growth (see Fig 6.1). Division along two different axes contributes to growth in two ways: periclinal divisions, that form the new wall in a periclinal orientation, increase cell number (increasing tissue layer number) and anticlinal divisions increase cell number to increase leaf blade area in a proliferation-dependent manner. Similar to division-, expansion-growth is also along two axes. New cell wall is not synthesised during expansion growth and this led to the question of whether or not the cell walls in the large and differentiated E2FB::GFP 72 line were truly due to a reversion back to cell division (Fig. 3.5). Expansion in the anticlinal direction thickens the leaf and periclinal expansion increases the leaf blade area in a differentiation-dependent manner.

6.3 Light as a regulator of leaf growth

Light affects division and expansion. Light perception is involved in divisions at the SAM where cells lose stem cell niche identity and differentiate into the first leaf

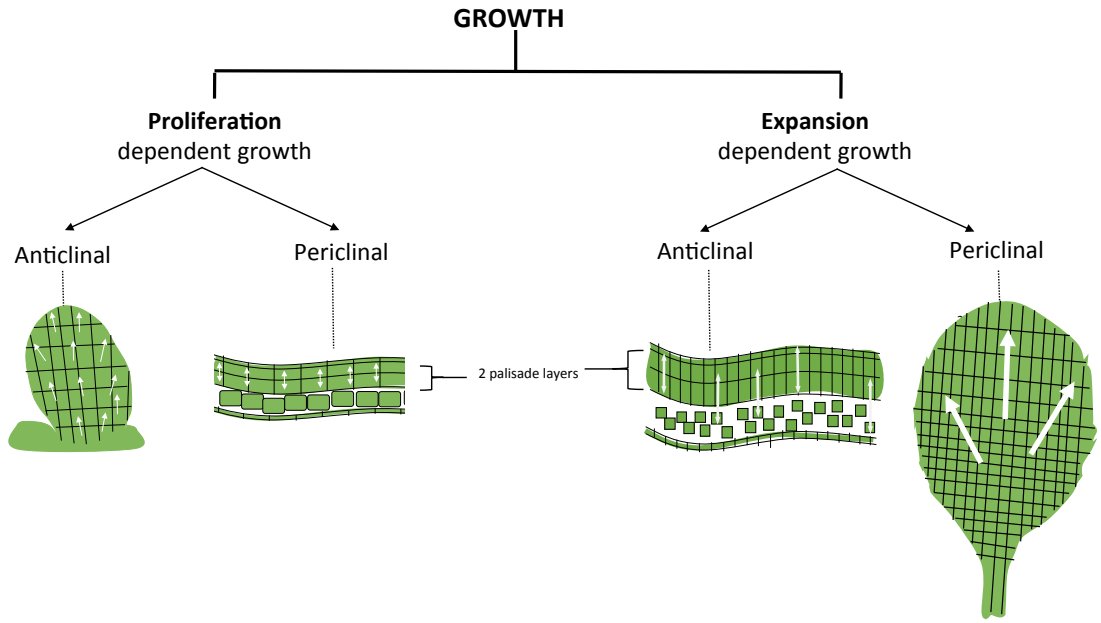

Figure 6-1 Proliferation and expansion dependent growth regulation of the leaf over multiple axes.

The first phase of leaf growth is described as being cell division/proliferation dependent and it transitions into differentiation-associated expansion growth. In both phases cell division and expansion can be over two axes anticlinal and periclinal. An anticlinal division is where the new cell wall is synthesised along the anticlinal axis, increasing leaf lamina area. A periclinal division is where new call is synthesised along the perclinal axis, adding tissue layers to the palisade mesophyll. Anticlinal expansion increases leaf thickness and periclinal expansion increases leaf lamina area. Note that early anticlinal division initiate the organ, an additional palisade is due to early periclinal divisions, leaf thickness (despite two palisade layers) is dependent on anticlinal expansion and the proliferation to differentiation gradient in the established leaf (far right). White arrows show direction of growth.

initiation cells. This describes photomorphogenic growth and *de novo* leaf morphogenesis. My work demonstrates that light absence can act as a temporary "brake" on division, the reappearance of light removes this "brake" and growth continues with cell divisions. Such a "brake" imposed by red light absence has previously been described in pea (*Pisum sativum*) as a 'photo-reversibility' of red light-induced cell cycle mRNA, where far red light exposure was used for photo-reversibility (Reichler *et al.*, 2001).

Light intensity contributes to cell number across leaf tissue layers, specifically the palisade, and it is plausible this contribution is due to regulation of cell division following germination. High light induces the presence of additional palisade layers in the leaf without excluding the alternate hypothesis that this may be due to the recruitment of a greater number of cells from the SAM (Kalve *et al.*, 2014; Gonzalez *et al.*, 2012). Leaves initiated in high light but immediately transferred to low light after germination were thin but comprised of an additional palisade layer (Kalve *et al.*, 2014). In contrast, leaves grown in a similar protocol, except from low to high light were thick but comprised of a single palisade layer (Kalve *et al.*, 2014). Based on these observations I concluded that the enhanced mitotic divisions I observed in the transfer to high light, a rapid response in young leaves in my experiment, were more likely due to anticlinal cell divisions. Future work should involve intricate observations of cells during primordium initiation in high light conditions to understand the contribution of cell division and/or recruitment of cell number. Observation of the speculated anticlinal divisions may be studied by a combination of CYCB1;1::GUS and modified Pseudo-Schiff Propidium Iodide cell wall staining (Truernit *et al.*, 2008).

Light affects cell expansion but previous studies have demonstrated this by changes in light spectra such as blue light contributing to cell expansion (Lopez-Juez *et al.*, 2007; Wang *et al.*, 2015). Light contributes more to anticlinal expansion than periclinal expansion and this is enhanced in high light (Kalve *et al.*, 2014). In summary, mechanisms of cell proliferation control occur over two axes albeit tissue-specifically, only the palisade will have multiple layers. It is not yet established which cell layers are affected in the re-deetiolation. The subsequent growth phase,

associated with expansion, is also differentially regulated by light at the tissue and cell level.

6.4 Mechanisms of cell proliferation control by light

6.4.1 **Energy status and the decision to proliferate by cell cycle regulators**

Light can act as a source of energy, associated with carbohydrate availability, or as a direct signal, transduced via photoreceptors. The availability of carbohydrate affects cell proliferation as cell cycle transcript levels begin to increase in light and levels are further reduced in extension of the dark. P-RBR1 (phosphorylated-RETINOBLASTOMA RELATED1) promotes cell division and is abundant during the light period as compared to the dark. Therefore, regulators of the cell cycle are themselves regulated by energy status of the cell. This was complemented by my experiment where carbohydrate availability and light perception were decoupled and the phosphorylation pattern of RBR1 was that corresponding to carbohydrate availability, not light and dark phases.

6.4.2 **Circadian regulation of available carbohydrate and cell division**

It is plausible that cell division in *Arabidopsis* is circadian regulated. This can be explained by the influence of the "energy" status of the cell and the fact that carbohydrate availability is under circadian regulation (Stitt *et al.*, 2007; Stitt and Zeeman, 2012; Smith and Stitt, 2007; Graf *et al.*, 2010; Graf and Smith, 2011). Alternatively, circadian regulation of the cell cycle in *planta* may be attributed to the evolutionary endosymbiosis with cyanobacteria. It is established that cell division in cyanobacteria is circadian regulated (Dong *et al.*, 2010; Rust *et al.*, 2011) and recent work provides insight into the role of the redox state of the cell and carbon flux as timers of cell division (Diamond *et al.*, 2015). Genes in plants are encoded by the plastid genome or plant nuclear genome and studies hypothesise the possible benefits for the chloroplast and nuclear gene encoding strategy, for details see (Allen, 2003; Raven and Allen, 2003). It would be very difficult to dissect what has evolved as circadian regulation due to cyanobacteria or plants *per se*. The "energy" status of a

cell would be anticipated to have an impact in both cases. Although many findings focus on the "energy" status of a cell gating cell division, the cell cycle may itself input into gating the circadian clock, based on results from a mammalian system biology approach (Bieler *et al.*, 2014).

6.4.3 **The role of chloroplasts in energy signalling and division**

In the context of cell division in the leaf the chloroplast must differentiate for proliferation to cease and expansion-growth to dominate (Andriankaja *et al.*, 2012). I observed many plastids in guard cells when aberrant cell divisions occurred in the constitutively active E2FB line, 35S::E2FB/DPa. An increase in chloroplasts due to increases in cell divisions has previously been reported (Vercruyssen *et al.*, 2015), and in that case it was suggested that this phenomenon may be associated with maintaining photosynthetic capacity of plant cells. The role of E2FB may not be exclusive to cell cycle regulation but this transcription factor may also be a key developmental regulator involved in cross talk between developmental stage, photosynthetic capacity, metabolism and cell division that has previously not been reported. This role would be analogous to GROWTH PROMOTING FACTOR5 (GRF5) that enhances cell and chloroplast division and overall photosynthetic capacity of the cells in the mesophyll (Vercruyssen *et al.*, 2015). This requires further analysis in order to observe what happens to chloroplast and cell numbers in other cell layers in the 35S::HA-E2FB/DPa line, ideally where chloroplasts are abundant unlike in the epidermis.

6.4.4 **Sucrose access at the shoot apex and cell proliferation in the absence of light**

The dark arrested meristem could initiate new leaves whilst the SAM was in contact with the sucrose-containing medium. These leaves do not develop further and have a restricted leaf size, as previously reported (Roldan *et al.*, 1999). It can be inferred that in the dark sucrose promotes cell proliferation only, and the inhibition of cell expansion contributes to the small size of leaves that initiate in the dark. I cannot exclude the possibility that the leaves initiated in the dark are completely dependent

on divisions alone. Supporting the hypothesis on the increased recruitment of cells from the meristem, during primordium protrusion, the need for concurrent periclinal divisions in the L2 during primordium protrusion is questionable (Foard, 1971). To what extent does cell proliferation occur in the re-deetiolation phenomenon is to be established, and this then can also be compared to the sucrose-dependent leaf initiation in the dark. Elucidating how cell number and cell size are regulated using the 3 day dark protocol can help unravel other mechanisms of cell proliferation control and its transition to differentiation. Hypotheses of other mechanisms determining such transition include a cell size threshold, intrinsic memory of a cell of the number of divisions undergone, and the age of the leaf and/or cell.

6.4.5 **Ribosome biogenesis and translation capacity**

Growth of the leaf comprises consecutive cell division and expansion and both growth phases require protein synthesis. During the cell cycle, protein synthesis is required for cell cycle proteins that accumulate at specific phases. Thus, mRNA of these cell cycle genes needs to be translated by translation factors and ribosomes in order to synthesise more proteins. It is trivial that you must translate to divide, this fact has been described as an aphorism as 'ribosome makes protein makes cell' (Polymenis and Aramayo, 2015). Research in yeast (*Saccharomyces cerevisiae*) has elucidated the importance of this regulatory mechanism in cell proliferation. The yeast WHISKEY5 (Whi5) protein is functionally equivalent to RBR1 in modulating early cell cycle entry (Costanzo *et al.*, 2004; de Bruin *et al.*, 2004), known as the START point in yeast. Passing this START point is achieved in a ribosome number and translation capacity-dependent manner and both must be abundant to pass this checkpoint (Bernstein *et al.*, 2007). Here I used a single gene to assume ribosome biogenesis and translation capacity are induced by irradiation. It was clear from our earlier deetiolation work in *Arabidopsis* that ribosome biogenesis and translational capacity and cell cycle were upregulated in the transcriptomic analysis at 6 h post irradiation (Lopez-Juez *et al.*, 2008). Similarly in other plants a far-red to red light transfer increased ribosome levels by increasing proteins involved in ribosome synthesis (Reichler *et al.*, 2001). Reicher *et al.,* (2001) studied a well characterised protein involved in ribosome synthesis, NUCLEOLIN, and found that *NUCLEOLIN*

mRNA accumulated 6 h post irradiation. Moreover, because *NUCLEOLIN* mRNA preceded cell division (S phase at 9 h and M phase at 12 h) and is known to be regulated by phytochromes (Tong *et al.*, 1997) the authors concluded that light-induced *NUCLEOLIN* mRNA and cell proliferation are mediated by phytochromes. This was further supported by the observation that green light did upregulate *NULEOLIN* mRNA but not cell cycle genes (Reichler *et al.*, 2001). My findings suggest that ribosome biogenesis and translation capacity are correlated with cell cycle progression whereas in yeast repression of a specific combination of ribosomal proteins leads to cell cycle arrest at G1 or G2/M (Thapa *et al.*, 2013). Ribosome biogenesis and translation capacity may be directly regulated by light and precede cell cycle gene regulation during re-/deetiolation but in *Arabidopsis* this is still to be confirmed.

6.4.6 **Auxin and cytokinin interplay in the regulation of leaf growth**

Consistent with the deetiolation response (Lopez-Juez *et al.*, 2008) re-deetiolation involves a high auxin, low cytokinin, response in the dark that is reverse by light. Our hypothesis is that an overall high auxin response in the SAM represses leaf initiation in the dark and light induces changes in auxin flow so that this hormone is exported from the SAM and leaves initiate. The direction and mechanisms of changes in this flow are many and complex. Both auxin and cytokinin are synthesised in plants but at different locations, are involved in signal transduction and transcript expression. Transport of the two hormones differs; cytokinin diffuses readily but auxin is transported by transporter proteins, chemiosmosis and through plasmodesmata. Cross-talk of these two hormones remains ambiguous but a detailed and up-to-date summary can be found *here* (Schaller *et al.*, 2015; El-Showk *et al.*, 2013).

Cross-talk of hormone signalling pathways and energy status is less explored. My work did not examine the hormone reshuffling response when leaves initiate in the dark, because the SAM has direct contact with sucrose-containing medium, but this could be for future work. In support of the observations in the re-deetiolation hormonal response, auxin application to the tobacco meristem in the dark does not initiate leaf primordia but does promote growth of existing primordia and the study

also showed that cytokinin application in the dark did promote leaf initiation (Yoshida *et al.*, 2011). My data provide further evidence for the light-dependent cross talk of auxin and cytokinin in regulating primordia growth and allows this response to be tested in other organs. It would be useful to determine how comparable the hormonal response, amongst others, is to the high light transfer protocol (in leaves that have emerged as opposed to emerging leaves in high light).

6.5 Spatial boundaries in coordinating leaf growth

Spatial coordination of leaf growth during proliferation and differentiation is critical as plant cells are non-mobile compared to animal cells. Modifying E2FB levels changes cell proliferation, cell size and leaf curvature. Changes in leaf shape and curvature are a result of growth changes along the leaf axes. Leaf flatness is maintained by regulating growth of marginal and medial regions of the leaf (Nath *et al.*, 2003).

6.5.1 **Mobile *versus* non-mobile signals**

Auxin cannot initiate leaf growth in darkness but can promote growth of leaves that are present (Yoshida *et al.*, 2011). Morphologically the only partition in leaves already present in darkness and those that would emerge from the SAM in the dark is between leaf lamina and petiole, this is called the blade-petiole junction. The petiole elongates in the dark, observed in my results and initially reported by Roldan (Roldan *et al.*, 1999), as well as in low light conditions (Kalve *et al.*, 2014). In both conditions petiole extension leads to compromised leaf lamina. A rational hypothesis is that a mobile signal exists at the blade/petiole junction that promotes cell proliferation of the leaf lamina (Kazama *et al.*, 2010). The mobile signal is not truly mobile as it only promotes growth of the adjoining leaf lamina and does not relocate to initiate leaf primordia. It is plausible this signal is, to some extent, regulated by auxin where it promotes growth of existing leaf but is restricted and does not promote *de novo* leaf growth at the SAM, based on the findings of (Yoshida *et al.*, 2011). On the basis of my observations I speculate that an unknown signal, which is sensitive to energy status of a cell, regulates leaf initiation at the SAM but based on

the observation that chloroplast-containing leaf sectors acclimate to high light and those without chloroplasts do not (Tan *et al.*, 2008) one would suggest this signal is unable to be mobile in the same tissue. This explains why sucrose can initiate leaves at the SAM but within these new primordia and existing leaves further growth of the lamina does not occur.

6.5.2 **Plastid signalling and boundary maintenance**

Leaf abaxial/adaxial identity is regulated by gene expression patterns (see chapter 1). How abaxialisation and adaxialisation affect leaf growth is less explored. Abaxial and adaxial identity is also termed a 'boundary shift' regulated by *FILAMENTOUS FLOWER* (*FIL*) expression and MicroRNA165-166 (MiR165-166) activity (Tameshige *et al.*, 2013). In the initiating primordia *FIL* and MiR165-166 are expressed and sequentially repressed in an adaxial to abaxial 'shift'. This study (Tameshige *et al.*, 2013) is outlined here because a fast 'boundary shift' causes excess adaxialisation of mesophyll cells, a slow 'shift' causes excess abaxialisation, and both produce a narrow lamina when plastid function is inhibited. As mentioned above, retrograde signalling is important for correct cell proliferation and differentiation processes but is poorly understood. How abaxialisation and adaxialisation is altered in the high light-transfer protocol and whether or not it contributes to the double palisade layer is open to experimentation.

6.6 Contrast of regulatory mechanisms of root and shoot growth

6.6.1 **Proliferation to differentiation transition**

The SAM and root apical meristem (RAM) have been described in the introduction (chapter 1). The study of root and shoot in a systems biology approach distinguishes the root as a 1 dimensional (1D) model and the leaf as a 2D model. The RAM produces cells for a single axis although the plane of division can vary. Divisions may be anticlinal, to increase root length, periclinal, to increase cell layer and root thickness, and radial, increasing circumference. Some cell division is also involved in the formation of the root cap which is a protective structure.

The coordination of division *vs* differentiation is easily visualised in the root cells by their shape, size and position, as opposed to the need for the CYCB1;1::GUS reporter to indicate proliferation zones in the leaf. Elucidating mechanisms of how cells coordinate these growth phases in the leaf is difficult. Positioning is also important in the root and analysis of division and expansion can be based on calculating the rate at which cells flow past a particular (fixed) position, defined as 'cell flux' (Beemster and Baskin, 1998). To use a similar calculus method to study cell production (cells mm^{-1} h^{-1}) and division (cells $cell^{-1}$ h^{-1}) rates is not practical for a leaf that presents multi-directional growth. This poses the question how important is cell position in the leaf and how is it coordinated with leaf and cell age?

6.6.2 **Similarities and differences in auxin patterning**

The cross talk of auxin and cytokinin in early embryogenesis establishes the shoot-root axis (Su *et al.*, 2015). During post-embryonic development auxin induces meristem cell division and cytokinin promotes the switch from division to differentiation by inhibiting auxin signalling in roots; in the shoot cytokinin inhibits stem cell differentiation and auxin triggers primordium initiation by repressing cytokinin biosynthesis (Reinhardt *et al.*, 2003), for a detailed review see (Su *et al.*, 2011).

Despite differences in the antagonistic regulation of auxin and cytokinin in the root and shoot, details about the flow and concentration of auxin reveals similarities between root and leaf growth. Leaf primordium protrusion involves auxin movement by efflux transporters, PIN FORMED1 (PIN1), to the basal region of sub-epidermal cells. Therefore, PIN1 flows auxin to the centre of the leaf, defining the later developing midvein (Reinhardt *et al.*, 2003; Heisler *et al.*, 2005; Scarpella *et al.*, 2006).

An auxin maximum at the root tip is involved in the division around the quiescent centre (QC) with an interplay of ethylene (Ortega-Martínez *et al.*, 2007). Comparable to the auxin flow in the growing leaf towards the tip then to the centre, and eventually away into the stem, auxin flow in the root cap is bidirectional. Auxin flows downwards in the root towards the RAM, in the stele cells, but is removed by two mechanisms; 1) removal by cells adjacent to the stele cell at any position in the

root 2) removal by cortex and epidermal cells at the site of auxin accumulation in the root tip (Petrášek and Friml, 2009). In summary, auxin accumulation correlates with organ initiation in the shoot and root and removal of this auxin correlates with growing tips of the leaf, leaf adaxialisation (Qi *et al.*, 2014) and root tip growth (Tanaka *et al.*, 2006).

The presence of auxin minima is also an important feature in patterning development; in the leaf auxin minima patterns formation of the axillary meristem (Wang *et al.*, 2014b; Wang *et al.*, 2014a) and in the root is required for the transition zone (Veronica Grieneisen, manuscript in submission). Thus, transient low auxin has implications on morphogenesis. Amidst the similarities and differences in auxin patterning a clear difference is that, unlike the root, the shoot initiates other developmental organs with a transition in the SAM to the inflorescence meristem.

6.6.3 **Diverse cell shapes in the leaf**

Cell shape in the root is similar with cube and cyclindrical shapes. Most cells in the leaf have a similar shape but notably the leaf epidermis has three distinct cell shapes; guard cells, trichomes and pavement cells.

The 35S::HA-E2FB$^{\Delta RBR1}$/DPa lines occasionally displayed a phenotype of 3 cotyledons and new leaves. This occasional phenotype has been reported for the weak allelic mutations of *PINOID* (*PID*), *pid* (Treml *et al.*, 2005) (Benjamins *et al.*, 2001). Moreover, the epidermal cell shape in this line has lobes that are not as protruding as in the WT-Col, they are 'less lobed' (Fig. 3.11). It is plausible that changes in cell proliferation coincide with this change in cell shape. The less lobe phenotype of the *defective kernel1* mutant (*dek1-4*) in *Arabidopsis* is more pronounced compared to 35S::HA-E2FB$^{\Delta RBR1}$/DPa but shows no changes in ploidy, cell cycle gene expression or changes in epidermal cell size (Galletti *et al.*, 2015). Based on this finding it appears that cell wall mechanics directly influence lobedness as opposed to changes in E2FB levels. It is plausible that E2FB regulates an alternative pathway involved in pavement cell shape.

The Rho of Plant (ROP) proteins are part of the small GTPase family and regulate polarity, cytoskeletal dynamics and vesicle trafficking (Nagawa *et al.*, 2010).

Amongst the 11 *Arabidopsis* ROPs ROP2 and ROP6 are well documented for promoting lobe and indent formation, respectively, by acting on cortical microtubules and actin microfilaments (Fu *et al.*, 2002; Fu *et al.*, 2005; Fu *et al.*, 2009). How ROP and E2F pathways are coordinated to effect pavement cell shape is a potential field of study and may elucidate a novel mechanism of E2Fs in regulating development.

Kinematic analysis of leaf cells is frequently performed on the epidermal cell layer. The pavement cells in the epidermis maintain a jigsaw like shape along the anticlinal direction only (Jacques *et al.*, 2014). Despite the strict maintenance of this cellular pattern there remains lack of knowledge as to how this pattern has evolved for maintenance on a single axis of the same cell type (Jacques *et al.*, 2014).

6.7 Evolution of leaf growth.

Leaves grow to form very different shapes at maturity. Leaves may have serrations but are described as simple leaves as opposed to complex leaves that are made up of several leaflet units (Tsukaya, 2004). The serrations in *Arabidopsis* new leaves are partly patterned by the action of auxin (Bilsborough *et al.*, 2011). Of 3 homeobox genes involved in simple *vs* complex leaf shape 2 are lost in *Arabidopsis* in a study comparing *Cardamine hirsute* (member of the Brassicaceae family) (Vlad *et al.*, 2014). One of these genes, *REDUCED COMPLEXITY* (*RCO*), when expressed in *Arabidopsis* produces complex leaf shapes by restricting growth at leaf margins and consequently producing leaflets.

Additionally, growth is different even in leaves of similar shape. The developmental gradient, that is acropetal in *Arabidopsis,* is not a feature of all dicotyledonous plants. In contrast to *Arabidopsis* leaves proliferation can be greatest near the leaf tip in plants of the same or different species. This is attributed to a microRNA-transcription factor regulatory module and a complex evolution of leaf growth polarity along the proximal distal axis (Gupta and Nath, 2015). Using these different plants and experimenting with the 3 day dark re-deetiolation it would be possible to test the significance of a mobile signal at the blade petiole junction that acts as an anchor for the proliferation zone in *Arabidopsis*. A test on leaves with a different

developmental gradient pattern could also be done to observe if sucrose access at the SAM in the dark reproduces a similar response to *Arabidopsis* as this plant was used for my studies and the work of Roldan and colleagues (Roldan *et al.*, 1999).

6.8 Concluding remarks

My work shows that mechanisms of cell proliferation control can be separately studied by use of the 3 day dark protocol. The discussion emphasises that until now studying these responses has been difficult due to the cross talk and counter regulation. The 3 day dark re-deetiolation is a novel experimental approach to better understand leaf development. Work on the high light transfer response is incomplete but has potential to be used as an assay for understanding leaf development, as recently demonstrated (Kalve *et al.*, 2014). It is plausible that in the high light-promoted proliferation response of already emerged leaves the signature responses will be different to the re-/deetiolation. This is because light perception is not completely perturbed/absent and therefore leaves that emerge in high light may also not have identical signature responses, although of course some responses may be similar. Differences may be a matter of *de novo* leaf growth *vs* leaf being already present, but also of the absence and then presence of light in cell proliferation control.

Appendices

Appendix 2.1 Details of materials used

Relevant Section	Equipment mentioned	Brand/Details
2.1.1	Seed drying bags	-
2.1.1	Sieve	-
2.1.2	Laminar flow hood	Bassaire Model:
2.1.2	Vacuum	Polaris Instruments Ltd. Vacuuseed
2.1.2	Bleach	Kleen Off Original thick bleach
2.1.2	Rotator	Grant Bio
2.1.3	Phyto-agar	Duchefa Biochemie: Phyto agar
2.1.3	MES	Sigma Aldrich: MES hydrate
2.1.3	Murashige and Skoog	
2.1.3	Sucrose	
2.1.3	pH meter	Hanna instruments pH 210 Microprocessor pH meter
2.1.3	Square petri dishes	12.5cm x 12.5cm 1.5cm deep
2.1.3	Circular cell culture petri dishes	Cellstar: cell culture dishes 100 x 20 mm with vents
2.1.4	Laminar flow hood	Bassaire Model: A6HB
2.1.4	Micro-porous tape	3M Micropore™ 1.25cm width
2.1.5	Percival Scientific (I)	Percival scientific Model: CU-36L/5D Light bulb: GE Polylux XL_R F18W/840
2.1.5	Shelf and lighting (II)	Metal shelving Lighting: Fitzgerald Lighting Ltd Light Bulb: Philips TLD 58W/830
2.1.5	Percival Scientific (III)	Percival Scientific Model: I-36/4L Light bulb: GE Polylux XL_R F18W/840 Philips TLD 18W/840
2.1.5	Percival Scientific (IV)	Percival Scientific Model: I-30B3L Light bulb: Sylvania Stamdard F20W/33-640/RS cool white
2.1.5	LMS cooled incubator	LMS Ltd
2.2 2.5.6	Nikon stereo microscope	Nikon SMZ1500 Dig-cam DXM12

		NIS Freeware 2.10
2.2	Additional lighting source	Photonic PL2000
2.4.1 2.6.5 2.7.1	Microfine tweezers	Brand: Biologie (Number 5) Rustless, Dumoxel, Nun-magnetic
2.4.1	Petri dish	-
2.4.2	Plastic cuvettes	Brand: Sarstedt Length/Ømm 51/12
2.4.2	Filter	30µm non-sterile CellTrics®filters
2.5.1	Lactic acid	Sigma-Aldrich
2.5.2 2.6.6	Nikon Optiphot	Nikon Optiphot 2 Dig-cam DXM1200 NIS Elements AR
2.5.2 2.6.7	Graticule	SGI
2.6.2	X-gluc	5-bromo-4-chloro-3-indoly beta-D-glucuronide sodium salt Brand: Slater and Frith Ltd
2.6.3	Speed vac	Heto-DNA mini speed vac
2.6.3	37°C incubator	
2.6.6	Optiscan device	Prior-Optiscan II
2.7.1	Stereo microscope	SLS – Scientific Laboratory Supplies Pyser-SGI
2.7.1	RNAlater	Sigma Aldrich
2.7.2	Blue pestle	
2.7.4	Nanodrop	Nanodrop spectrophotometer ND-1000
2.7.5	Loading Dye	Bioline: 5x DNA Loading Buffer, Blue
2.7.5	Ladder	Bioline: Hyperladder I
2.7.5	Gel-electrophoresis Tank	Life Technologies™ GIBCO BRL Horizontal Gel Electrophoresis Apparatus
2.7.5	UV Gel Doc	UVP BioDoc-It™ System Or GENEFLASH Syngene Bio Imaging
2.7.9	Good grade water	Sigma Aldrich BPC grade Water-Mol. Bio. Reagent
2.7.9	Strip tubes (PCR)	Qiagen Strip tubes and caps 0.1ml 250 pack
2.7.9	Filter tips	Star Lab: Tip One

		Filtered tips
2.7.9	Laminar flow hood	Heraeus, HeraGuard.
2.9.1	Drill	BOSCH PSB450R 450W.BetonØ max 1.3mm
2.9.1	Fixative stand for drill	Wolfcraft brand
2.9.2	Bradfords Reagent	Bio-Rad
2.9.2	Cuvettes	-1cm light path
2.9.3	Gel cast platform	Amersham Biosciences Hoefer™ Dual Gel Caster
2.9.3	Ladder	Fermentas – prestained protein molecular weight marker, SM26619
2.9.4	P-RBR1 Ab	P-RBR1 Rabbit Ab Cell Signalling Technologies
2.9.4	Ponceau Stain	Ponceau S stain in 5% acetic acid Sigma Aldrich
2.9.5	HRP substrate	Millipore Immobilon Western Chemiluminescent HRP substrate
2.9.5	Cassette	Genetic Research Instrumentation Ltd
2.9.5	Film	Thermo scientific CL-XPosure ™Film Clear blue X-ray film

-= unknown, ordered in bulk from stores at Rhul, TW20 0EX

Appendix 2.2

Protocol for MES solution

25g MES hydrate (Sigma-Aldrich)
500ml distilled H_2O

Set pH to 5.8 using 1N KOH (pre-made buffer)

Autoclave at 110°C for 15 mins

Store at room temperature

Appendix 2.3

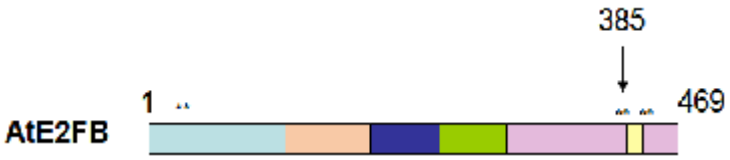

N-terminal part including cyclin binding motif

DNA-binding

Dimerization

Marked box

Transactivation domain

RB binding domain

* **CDK phosphorylation sites**

E2FB domain organisation: The E2FB$^{\Delta RBR1}$ is a truncated version of E2FB, 1-385. A shown, this lacks the RB binding domain (yellow) as well as part of the transactivation domain at the C-terminal end (purple, following yellow). At=Arabidopsis thaliana.

Appendix 2.4
Protocol details for sodium phosphate buffer, for CYCB1;1::GUS assay.

100mM sodium phosphate buffer

Phosphate Buffer (Sorensens)

Stock solutions (0.2M)

X		$Na_2HPO_4.\ 2H_2O$	3.561g Dibasic
	or	$Na_2HPO_4.\ 7H_2O$	5.365g
	or	$Na_2HPO_4.\ 12H_2O$	7.164g

distilled water to make 100ml

Y		$NaH_2PO_4.\ H_2O$	2.760gMonobasic
	or	$NaH_2PO_4.\ 2H_2O$	3.121g

distilled water to make 100ml

Prepare the 0.1M phosphate buffer by mixing xml of solution X with yml of solution Y depending on the acquired pH. Make the resulting solution up to 100ml with distilled water.

pH (at 25°C)	X ml	Y ml
6.8	24.5	25.5
7.0	30.5	19.5
7.2	36.0	14.0
7.4	40.5	9.4

Other pH values from 5.8 to 8.0 can be obtained but are not usually used with this buffer.
Adjust the osmolarity of the buffer by variation of the phosphate molarities or the addition of sucrose, glucose of NaCl. Other electrolytes such as Ca salts cannot be used as they will precipitate with the phosphate.

Appendix 2.5 - Table 2.5 Details of two different GUS assays

x-gluc solution based on:	Chemical Reagent	Calculations	Final Conc needed	ul needed Per 50ml
J Murray	**X-Gluc**	(0.3mg/ml x 50ml)/50mg/ml =0.3ml 0.3x1000=300ul	0.3mg/ml	**300**
	Potassium Ferricyanide	(0.005M x 50ml)/ 0.1M = 0.25ml x1000 = 250	0.5mM	**250**
	Potassium Ferrocyanide	As above	0.5mM	**250**
	Tween 20	((50mlx1000)/100) x 0.1 = 50ul	0.1%	**50**
	Sodium Phosphate Buffer	Make up to 50ml	100mM	**49150**
N Uchida	**X-Gluc**	(0.001M x 50ml) / 0.1M = 0.5ml 0.5 x 1000 = 500	1mM	**500**
	Potassium Ferricyanide	(0.005M x 50ml)/ 0.1M = 0.25ml x1000 = 250	0.5mM	**250**
	Potassium Ferrocyanide	As above	0.5mM	**250**
	Triton x-100	((50mlx1000)/100) x 1% = 500ul	0.1%	**500**
	EDTA	0.01M x 50ml / 0.5M = 1ml 1 x 1000 = 1000ul	10mM	**1000**
	DMSO	((50mlx1000)/100) x 1% = 500ul	0.1%	**500**
	Sodium Phosphate Buffer	Make up to 50ml	50mM	**47000**

Note: X-gluc can be dissolved in dimethyl-formamide and kept in the -20°C. Both potassium ferricyanide and potassium ferrocyanide must be made up fresh in H_2O or stored in -20°C and then be thawed prior to use.

Appendix 2.6
Table A2.6:Hoyer's Solution:

Hoyer's solution **Per 30ml Dist. Water**
100g choral hydrate
2.5g Arabic gum
15ml glycerol

Appendix 2.7 Fig A2.7 EDF *vs* stereo image of leaf
Extended Depth Focus image of ¼ of leaf

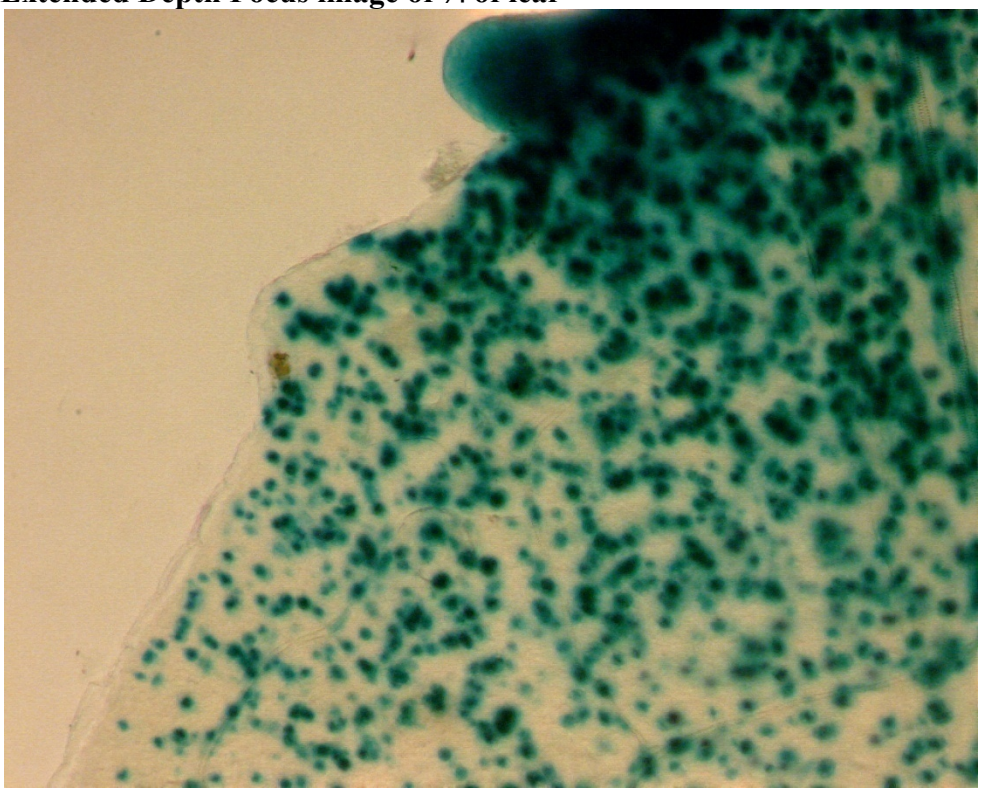

Stereo Microscope Image of whole leaf (used above)

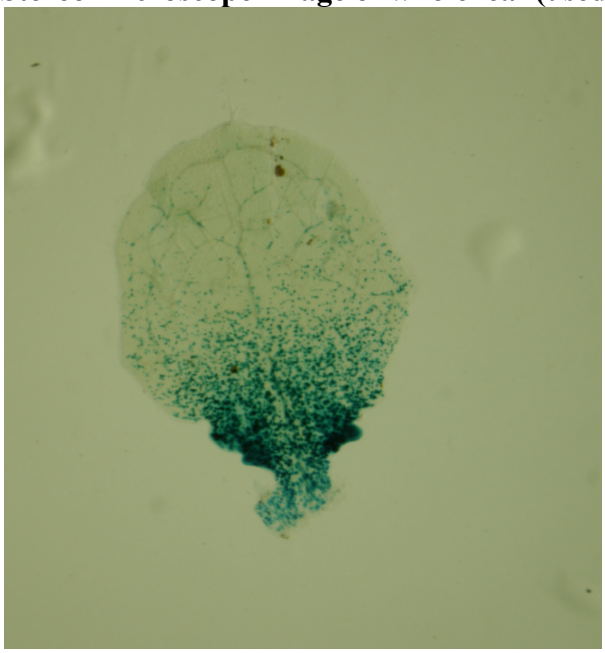

Appendix 2.8
Figure A2.8 RNA Gel for new leaves collected via RNAlater method, see section 2.7.1

Gel from Left to Right:
Hyperladder 1, Leaf samples A, B, C, D and E

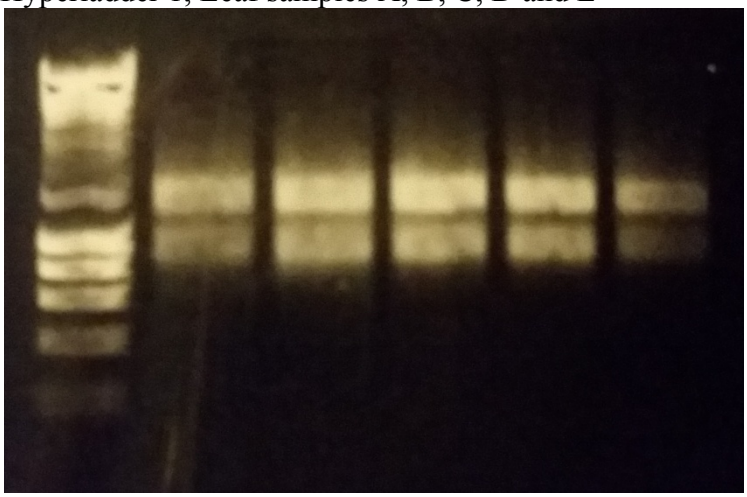

Appendix 2.9
Tables A2.9 Buffer compositions

TAE (1x)	
	Concentration (mM)
Tris (pH 7.6)	40
Acetic acid	20
EDTA (pH 8.0)	1

TBE (1x)	
	Concentration (mM)
Tris (pH 7.6)	89
Boric acid	89
EDTA (pH 8.0)	2

SDS sample buffer (x5)	
Dissolve all the below at 37°C shaking	
Tris (pH 6.8)	250 mM
SDS	10%
Glycerol	30%
DTT	5%
Some bromophenol blue	0.25M

Lacus Buffer (x5)	
	Concentration (mM)
Tris (pH 7.5)	25
$MgCl_2$	10
EGTA	15
NaCl	75
NaF	1
$NaVO_3$	0.5
3-Glycerol-phosphate	15
4-Nitrophenylphosphate (PNPP)	0.15
Tween 20	0.1%

TBS (10x)	
	Concentration (M)
Tris (pH 8.0)	0.5
NaCl	1.5

Transfer Buffer (1 L)

Tris base	6.06g	50 mM
Boric acid	3.09g	50mM

Edwards DNA extraction buffer			
	Initial concentration	**Working concentration**	**50 ml Prep:**
NaCl	5M	250mM	2.5ml
Tris pH7.5	1M	200mM	10 ml
EDTA	0.5M	250mM	2.5 ml
SDS	10%	0.5%	2.5 ml

TE DNA suspension buffer			
	Initial concentration	**Working concentration**	**50 ml Prep:**
EDTA	0.5M	10mM	2.5ml
Tris pH7.5	1M	50mM	1 ml

Appendix 2.10.
Tables A2.10: Solutions used for Western blot

Extraction buffer: 2000 µl	
Lacus Buffer	1900 µl
(1M) PNPP	20 µl
PIC	20 µl
0.1M PMSF	20 µl
Phos STOP	40 µl
DTT	2 µl

10 % Running Gel: 10 ml	
H_2O	4.0 ml
30% Acrylamide mix	3.3 ml
1.5M Tris pH8.8	2.5 ml
10% SDS	0.1 ml
10% APS	0.1 ml
TEMED	0.006 ml

Continued on next page

Stacking Gel: 5 ml	
H_2O	3.4 ml
30% Acrylamide mix	0.83 ml
1.0M Tris pH6.8	0.63 ml
10% SDS	0.05 ml
10% APS	0.05 ml
TEMED	0.005 ml

Appendix 2.11 Table A2.11-Primer sequences

Gene	AGI	Forward	Reverse
Chapter 3: Primers for PCR. Designed by Primer3. Ordered by Eurofins-MWG			
E2FB	Salk *e2fb-ko 959*	TTGGATTCCTTCCATTTGATG	GTGCCTTTACAGCTATCAGCG
Border primer	LBb1.3	Left Border: ATTTTGCCGATTTCGGAAC	
Chapter 3: Designed via Quantprime. Ordered by Eurofins-MWG			
E2FB	AT5G22220	AAGGCACCGCATGGAACAACTC	CCTCTGATAACCACCAGCCTCATC
CYCD3;1	AT4G34160	CCTCAACAAATGCCACCGTCTC	AGGTACCCGACAAATCTTGAATCG
CYCA2;3	AT1G15570	TCTTGGGAGATCAGCTTCTACAGC	GGCATAGAGGCAGCACAGTAAAGG
CDKB1;1	AT3G54180	CAACTGGTGTTGACATGTGGTCTG	TCAGTTGGTGTTCCTAGCAACCTG
RBR1	AT3G12280	GCCATCAACAACCGCTTGAACAAC	TCTGCGTCAAAGTTTAGCGTCCTC
UBQ10	AT4G05320	GGCCTTGTATAATCCCTGATGAATAAG	AAAGAGATAACAGGAACGGAAACATAGT
Chapter 3: Designed using Primer3 by previous Lab member, Safina Khan Ordered by Eurofins-MWG			
MCM3	AT5G46280	TGG GCAGCACATGAGGAC	CACTTTGTTATCTTGCAGTTTC
ORC1	AT4G14700	TCCCGAATCACAACAAACTC	CCACAATAATGGAGCGTTGA
Chapter 4: Designed by Quantprime. Ordered by Eurofins-MWG			
CYCD3;1, CDKB1;1, CYCA2;3, RBR1 and E2FB as above			
E2FA	AT2G36010	TAGATCGGGAGGAAGATGCTGTCG	TTGTCGCCTTTCTCTTTCGTGAAG
E2FC	AT1G47870	TGCCGTTATGACAGTTCTTTAGGG	AGTGTTCCATCCTCAGCTTCCTG
CYCA3;1	AT5G43080	GCAGCATAAGTTCAAGTGTGTAGC	AAACCGTAAGAGGCAGCTCTGG
ATL8	AT1G76410	AAGCTTCTCCGCCTTTCAACTCC	GTGCACAAAGAAGAACCGCAAGG
Chapter 4: Designed by Primer3. Ordered by Sigma-Aldrich			
E2FA, E2FB, E2FC and RBR1 as for chapter 3.			
CYCB1;1	AT4G37490	TCAGCAATGGAAGCAACAAG	AGCAGATTCAGTTCCGGTCA
H2A	AT1G51060	CAAATTGCTTGGAGATGTGA	GTCTTCAGCAGATGGCTTGG
KRP4	AT2G32710	TCGTGGTGATGGGTCTAGGT	GCCAAAGGTTGGATCTTTATTG

S6RP	AT4G31700	TTGAAGGAACAGCGTGACAG	GGTGACATCTTTGATTTGATTCTC
EBP	AT3G51800	GCCTGGCTCATGTCGTTTTG	TTCCTGAAGTGTATGTGAAGTGA
RNR2A	AT3G23580	TGCTATCGAGACCATTCCTTGT	GCCTCACAGCAAACGACATAG
bZIP1	AT5G49450	TGTCGACGATCAGAACGCAA	AGGACGCCATTGGTTGTAGA
TPS9	AT1G23870	CTGCACGGTGGGAAGAAAAC	CGTGTGCAATGAGGAGGATT
ARR5	AT3G48100	CAGCTAAAACGCGCAAAGA	CAAAAGAAGCCGTAATGTCTCA
AUX1	AT2G38120	TGCGTTTGTGGAGGGTTCTT	AGCTTAGCACGCATTTAAAGGG
EIN3	AT3G20770	ACAACAACAACAGCAGCAACA	TGTTGTGATCTGCAGTGTCGA
ABA2	AT1G52340	CGGAGGATGCATTTGTTGGT	CGCTACATCATCAACCGTCAGT
ACT2	AT3G18780	AAATCACAGCACTTGCACCA	TGAGGGAAGCAAGAATGGAA
UBQ10	AT4G05320	GGAGGATGGTCGTACTTTGG	TCCACTTCAAGGGTGATGGT
Gene	**AGI**	**Forward**	**Reverse**

Appendix 3.1: Shapiro-Wilk test and Q-Q plots for *e2fb-ko*

Result:	**WT-Col**	***E2fb-ko 959***
Mean:	2891.291	6399.853
Standard Deviation:	3367.161	5594.298
Variance:	11337771.97	31296171.8
Kurtosis:	2.553	-0.637
Calculated Shapiro-Wilk statistic W:	0.782824	0.904464
Calculated Shapiro-Wilk p-value:	<0.05	<0.05
Critical value of W (5% significance level):	0.947	0.947

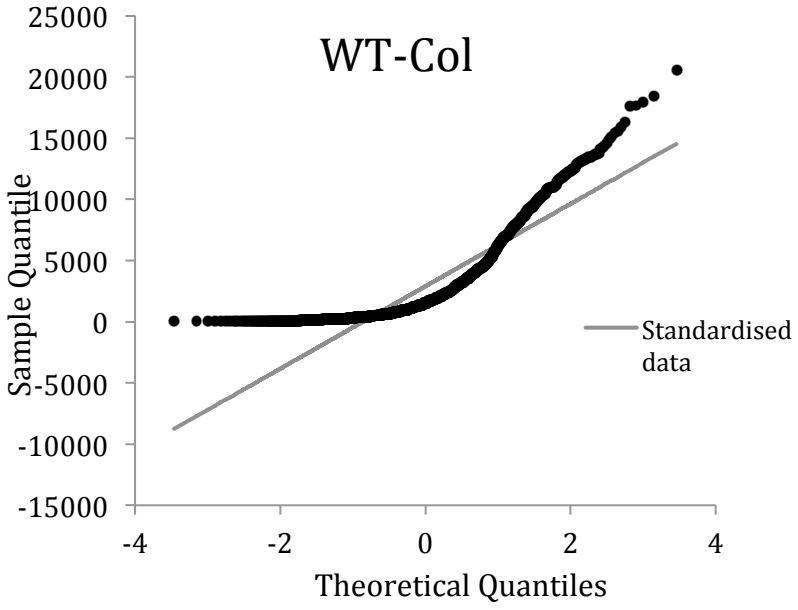

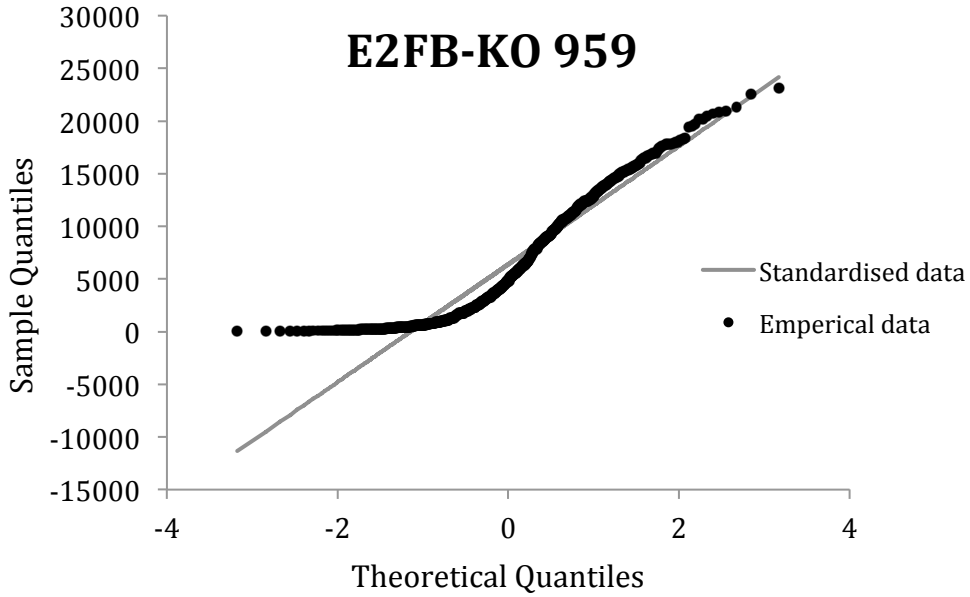

Appendix (Table) 3.2: 1Analysis of core cell cycle genes for putative E2F elements

Core cell cycle gene list from http://arabidopsis.org/browse/genefamily/cellcycle.jsp

AGRIS: http://arabidopsis.med.ohio-state.edu/AtcisDB/

PLACE: http://www.dna.affrc.go.jp/PLACE/signalscan.html
Promoter sequences from Agris were used for PLACE

(Borghi *et al.*, 2010):
Use of inducible RNAi line against *Arabidopsis RBR* to induce *RBR* expression levels at different developmental stages. Gene profiling was carried out after induction. (Notes have been made in the column where relevant). Putative E2F elements are based on supplemental material provided in the study.

Gene Family Name:	Protein Name:	Genomic Locus:	E2F element (Borghi *et al*, 2010) (out of 4 potential)	E2F element AGRIS	E2F element PLACE
Core Cell Cycle	CDKA;1	T21J18.20 AT3g48750	No	no	no
	CDKB1;1	F24B22.140 AT3g54180	YES 1/4	YES	YES
	CDKB1;2	T6A23.18 AT2g38620	no	no	no
	CDKB2;1	F14G6.14 AT1g76540	No (Up in *RBRi* line)	no	no
	CDKB2;2	F9H16.8 AT1g20930	YES 1/4	no	no
	CDKC;1	F18D22.40 AT5g10270	no	YES	YES
	CDKC;2	MXK3.19 AT5g64960	no	no	no
	CDKD;1	F25P22.11 AT1g73690	no	no	no
	CDKD;2	F4N21.12 AT1g66750	no	no	no
	CDKD;3	T10F20.5 AT1g18040	no	no	no
	CDKE;1	MBK5.8 AT5g63610	YES 1/4	no	yes
	CDKF;1	F25O24.8 AT4g28980	no	no	no
	CYCA1;1	T7O23.18 AT1g44110	YES 3/4 (Up in *RBRi* line)	no	no
	CYCA1;2	F2P24.10 AT1g77390	no (Up in *RBRi* line)	no	YES
	CYCA2;1	F18G18.15 AT5g25380	no	no	no
	CYCA2;2	F2I11.190 AT5g11300	no	no	no
	CYCA2;3	T16N11.8 AT1g15570	YES 1/4	no	no

	CYCA2;4	T16N11.8 AT1g80370	no (Strongly up in *RBRi* line)	no	no
	CYCA3;1	MMG4.10 AT5g43080	YES 2/4 (Up in *RBRi* line)	no	YES
	CYCA3;2	F8G22.8 AT1g47210	no	no	no
	CYCA3;3	F8G22.6 AT1g47220	no	no	no
	CYCA3;4	F8G22.5 AT1g47230	YES 1/4	no	no
	CYCB1;1	F6G17.140 AT4g37490	no	no	no
	CYCB1;2	K16F4.15 AT5g06150	no	no	YES
	CYCB1;3	F24K9.20 AT3g11520	no	no	YES
	CYCB1;4	F18A8.13 AT2g26760	YES 1/4	no	no
	CYCB2;1	T19E12.4 AT2g17620	YES 1/4	no	YES
	CYCB2;2	F8D20.130 AT4g35620	no	no	no
	CYCB2;3	F5M15.6 AT1g20610	no	no	no
	CYCB2;4	T23E18.24 AT1g76310	no	no	no
	CYCB3;1	F3O9.13 AT1g16330	YES 1/4	no	no
	CYCD1;1	F20P5.7 AT1g70210	no	no	YES
	CYCD2;1	F14M13.11 AT2g22490	YES 1/4	no	YES
	CYCD3;1	F28A23.80 AT4g34160	YES 3/4 (No change in *RBRi* line)	YES	YES
	CYCD3;2	K21H1.30 AT5g67260	no	no	YES
	CYCD3;3	F3A4.150 AT3g50070	no	no	YES
	CYCD4;1	MNA5.15 AT5g65420	no	no	no
	CYCD4;2	F12B17.210 AT5g10440	no	no	no
	CYCD5;1	F19F18.120 AT4g37630	no	no	YES
	CYCD6;1	F4C21.20 AT4g03270	YES 1/4 (Down in *RBRi* line)	no	no
	CYCD7;1	T7H20.160 AT5g02110	no	no	no
	CYCH;1	F15A18.80 AT5g27620	YES 1/4	no	no
	CKS1	T1E2.12 AT2g27960	no (No change in *RBRi* line)	no	YES
	CKS2	T1E2.11 AT2g27970	no (Up in *RBRi* line)	no	YES
	DEL1	T24C20.40 AT3g48160	No	no	no
	DEL2	F2G14.80	YES 1/4	no	YES

		AT5g14960			
	DEL3	T22N4.4 AT3g01330	YES 1/4	no	YES
	DPa	T1E22.4 AT5g02470	no	no	YES
	DPb	F12E4.160 AT5g03410	no	not found	
	E2Fa	F11F19.8 AT2g36010	no (Up in *RBRi* line)	YES	YES
	E2Fb	T6G21.10 AT5g22220	no (Up in *RBRi* line)	no	no (Zoltan Magyar analysis = Yes)
	E2Fc	T2E6.2 AT1g47870	YES 1/4 (Up in *RBRi* line)	no	YES
	KRP1	F26B6.8 AT2g23430	no	no	YES
	KRP2	T3A5.10 AT3g50630	no	no	no
	KRP3	K24G6.15 AT5g48820	no	no	no
	KRP4	F24L7.15 AT2g32710	no (Down in *RBRi* line)	no	YES
	KRP5	K7P8.10 AT3g24810	no	no	no
	KRP6	MVI11.5 AT3g19150	no	no	no
	KRP7	F14J22.14 AT1g49620	YES 1/4	no	no
	Rb	F28J15.11 AT3g12280	no	YES	YES
	WEE1	F22D16.3 AT1g02970	YES (Up in *RBRi* line)	no	no

Appendix (Figure) 3.3: Identifying E2FB protein levels in the E2FB-GFP lines

A)Western blot of 3 E2FB-GFP lines against an E2FB antibody. Two lines are high expressors (72/1 and 5891) where as line 93/14 is a medium (see 12 and 15 dag). RBR1 protein levels are also high suggesting E2FB overexpression positively regulated its negative regulator (RBR1).
B) Co-immunoprecipitation of high (72) and low (61) E2FB-GFP lines are extreme. GFP label is for co-immunoprecipitation of E2FB-GFP via a GFP antibody.

Images were kindly provided by Zoltan Magyar.

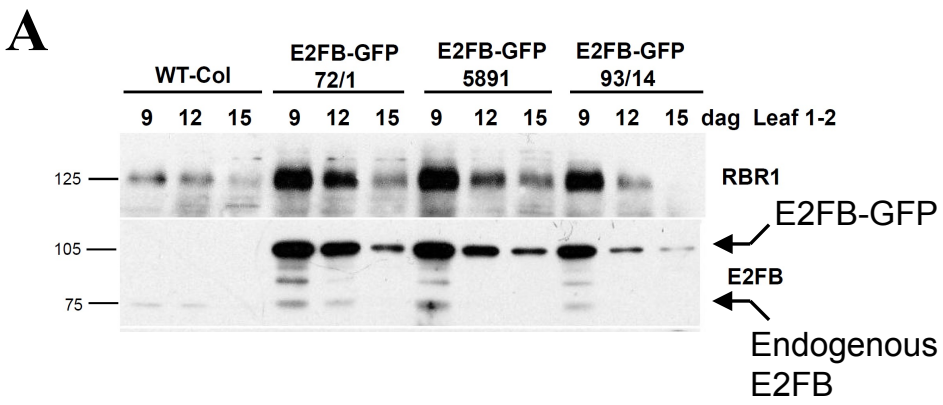

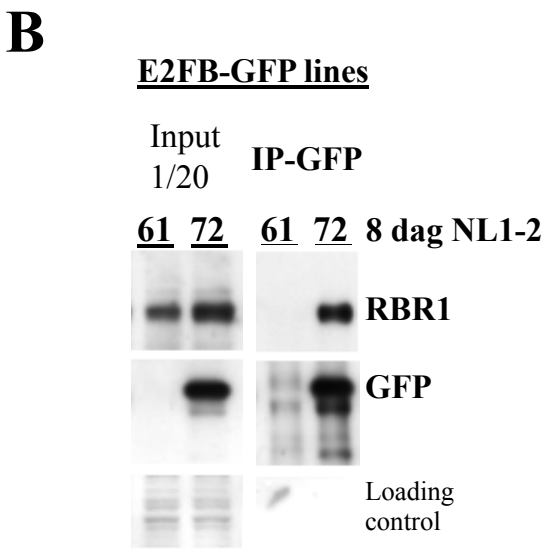

Appendix 3.4: Shapiro-Wilk test and Q-Q plots for 35S::HA-E2FB/DPa

Result:	WT-Col	35S::HA-E2FB/DPa
Mean:	2891.291	893.589
Standard Deviation:	3367.161	1346.89
Variance:	11337771.97	1814113
Kurtosis:	2.553	12.217
Calculated Shapiro-Wilk statistic W:	0.782824	0.626204
Calculated Shapiro-Wilk p-value:	<0.05	<0.05
Critical value of W (5% significance level):	0.947	0.947

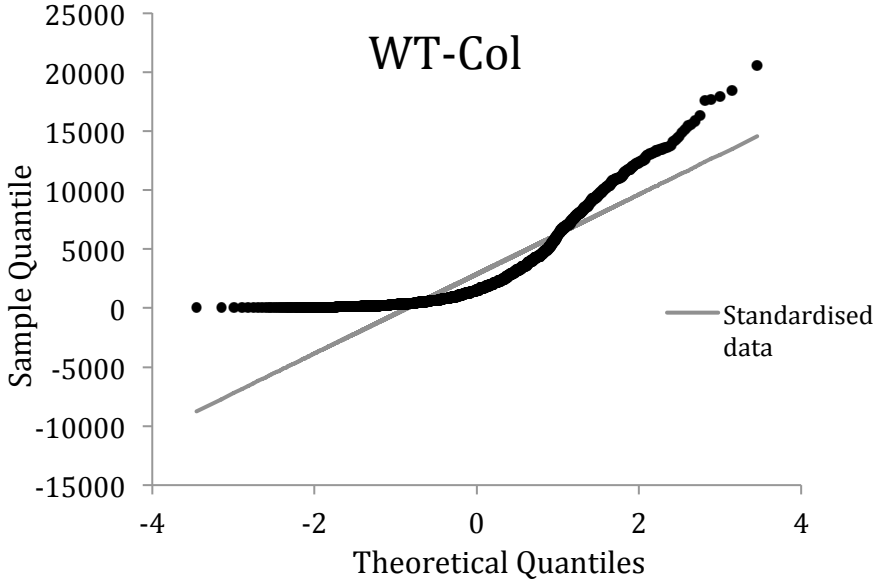

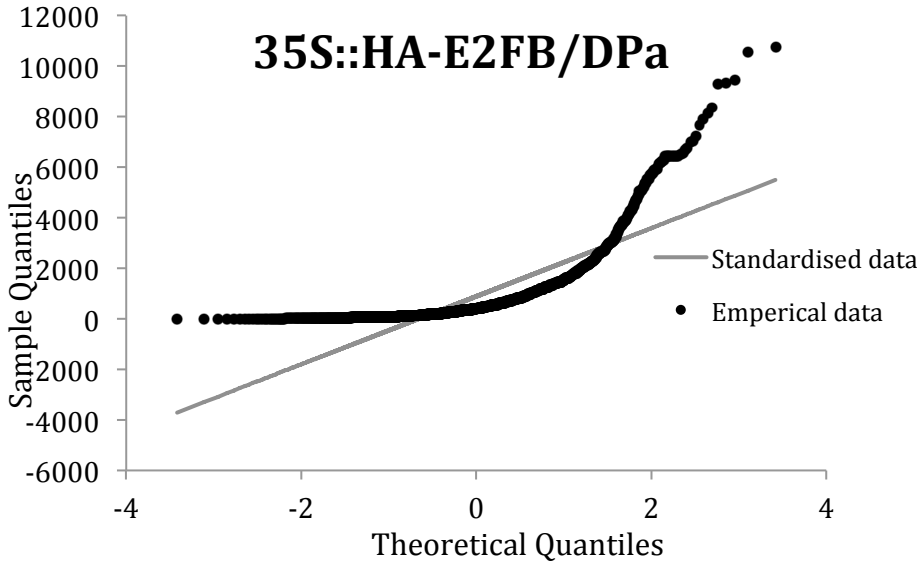

Appendix 3.5: Shapiro-Wilk test and Q-Q plots for *e2fb-ko*

Result:	**WT-Col**	***10/x/8***	***1/10***
Mean:	2891.291	2142.412	4105.424
Standard Deviation:	3367.161	2532.875	4888.233
Variance:	11337771.97	6415457.894	23894819.79
Kurtosis:	2.553	0.008	0.824
Calculated Shapiro-Wilk statistic W:	0.782824	0.8094	0.794368
Calculated Shapiro-Wilk p-value:	<0.05	<0.05	<0.05
Critical value of W (5% significance level):	0.947	0.947	0.947

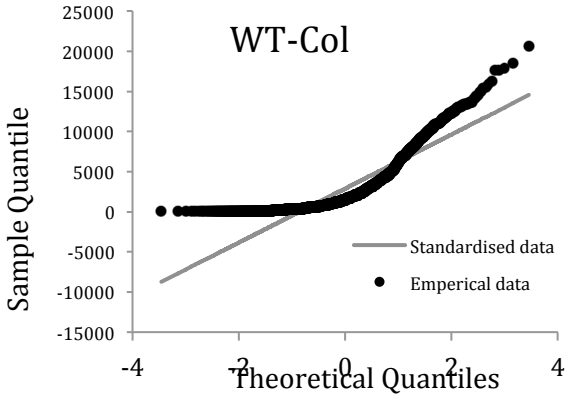

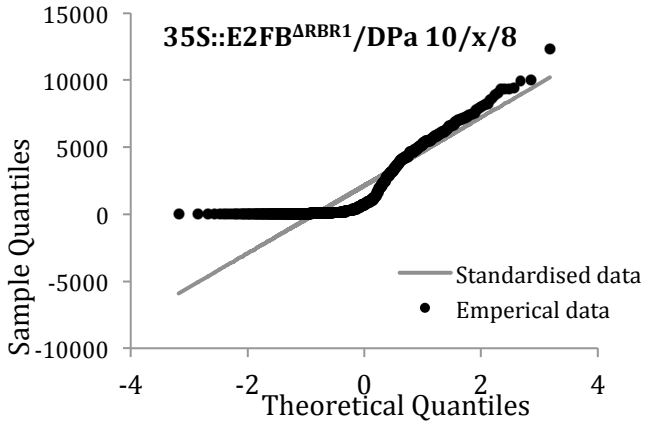

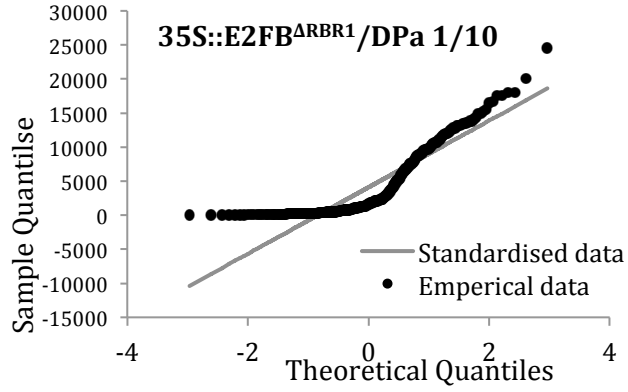

Appendix (Figure) 3.6: Use of the HA-Antibody for protein detection in the 35S::HA-E2FB/DPa line

The Western blot below shows excessive E2FB (HA-E2FB transgene and endogenous E2FB) in the 35S::HA-E2FB/DPa line. It also confirms overexpression of DPa and as a positive control CDKB1;1 is also up. Note how all proteins abundance bands dissipate over time, in the first new leaf pair.

This image was kindly provided by Zoltan Magyar.

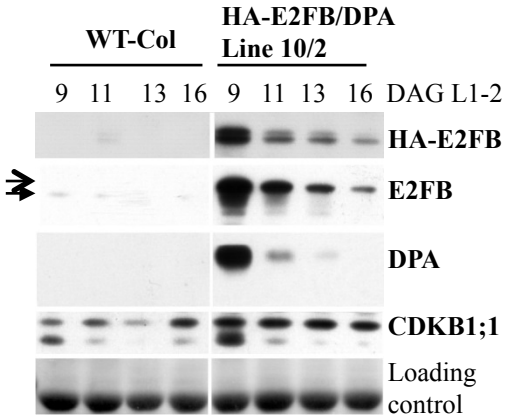

Appendix (Figure) 3.7: Trichomes in WT-Col and overexpressing E2FB lines are indifferent

No reduction in number of trichomes was observed in the constitutively expressed E2FB lines compared to the WT-Col.

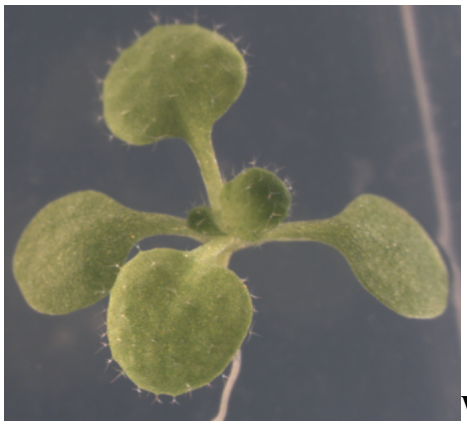

WT-Col

3S::HA-E2FB/DPa

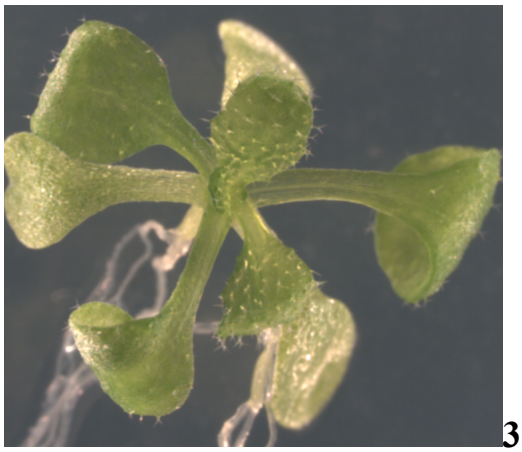

35S::HA-E2FB$^{\Delta RBR1}$/DPa

Appendix (Figure) 3.8: Tackling GUS assay problems

GUS staining can be problematic if not carried out accurately. These problems can be falsely reported as GUS staining for a specific promoter, here it is *CYCB1;1*. To note is the top left and middle left images (on left panel) showing diffusion at hydathodes (in a fairly young leaf) and darker staining at base of trichomes. Solutions are based on modifying the protocol (vacuum infiltration, two methods modified from two different references and vacuum timing).

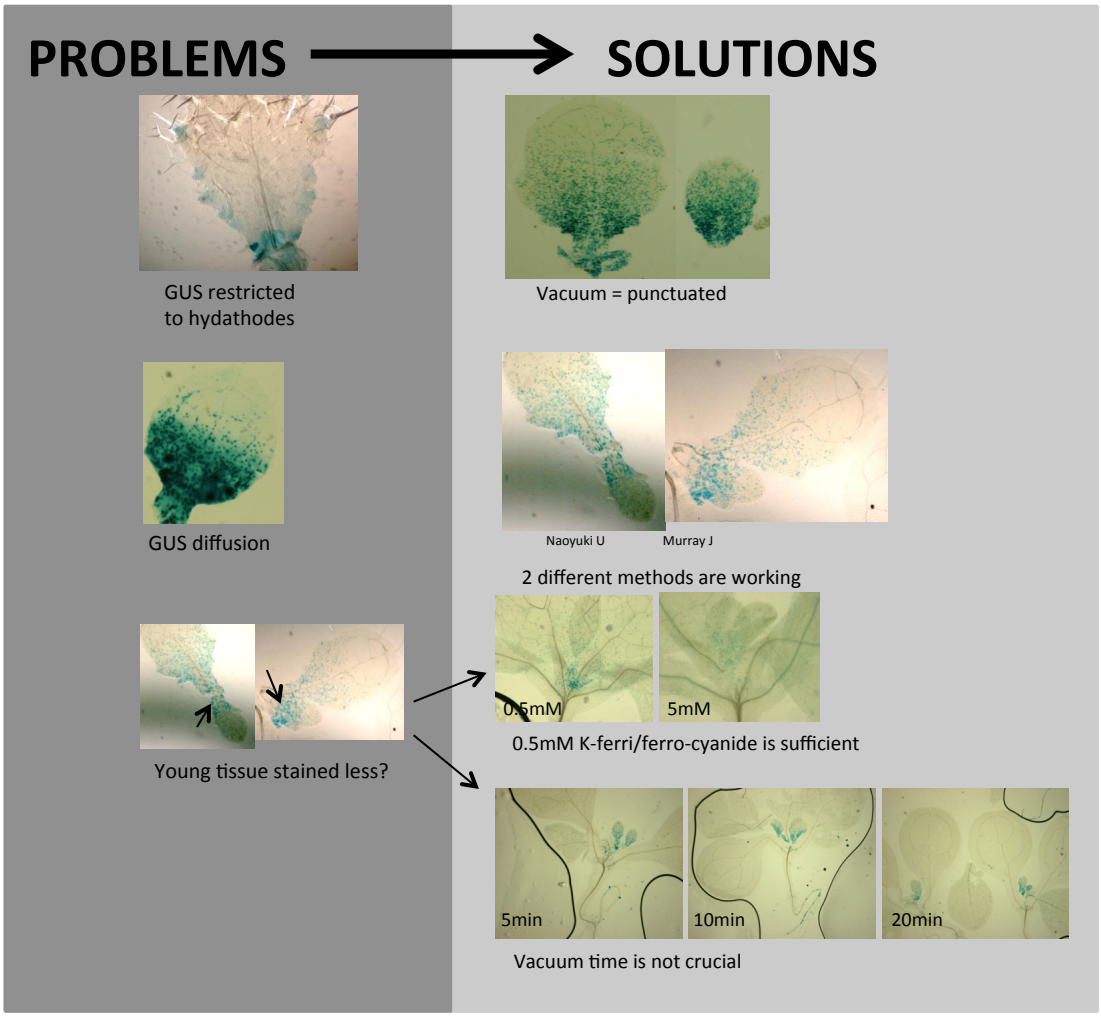

Appendix (Figure 4.1): An independent experiment on the diurnal behaviour of cell cycle gene transcripts

In reference to Q-RT-PCR data in Figs. 4.3-4.4. Based on the protocol of Gibon *et al.,* 2004 gene transcripts behaved as previously observed, text referenced on the left. Error bars show standard deviation between technical replicates. This experiment was conducted, and the results analysed, by Csaba Papdi.

Fig. 4.3B

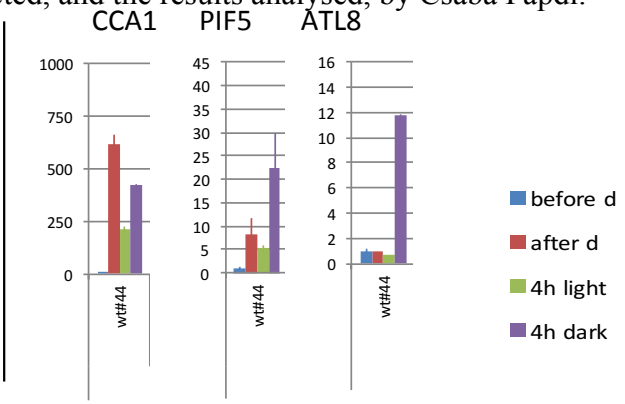

Fig. 4.3C

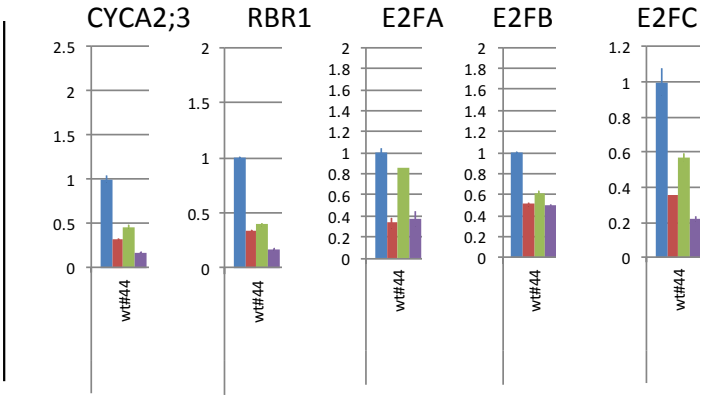

Fig. 4.4

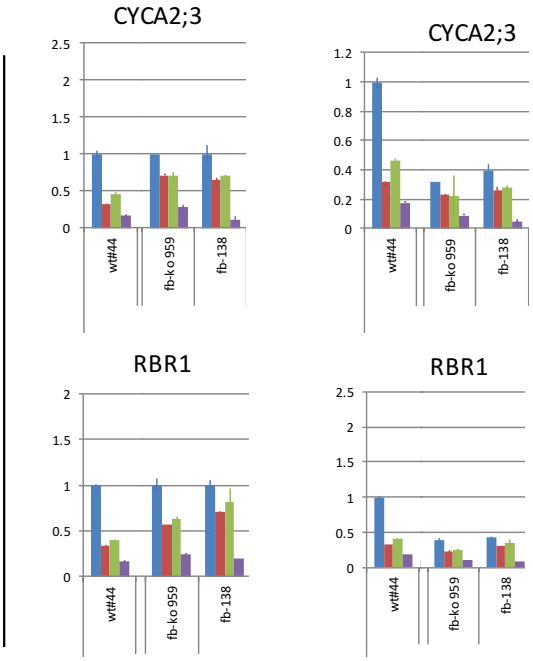

Appendix (Figure 5.1): Repeated Probing of Western blot with and without DCMU treatment in low light *vs* high light

The blot was reprobed on the same pool of biological replicates used in Fig. 5.4. This blot reprobing was performed by Csaba Papdi.

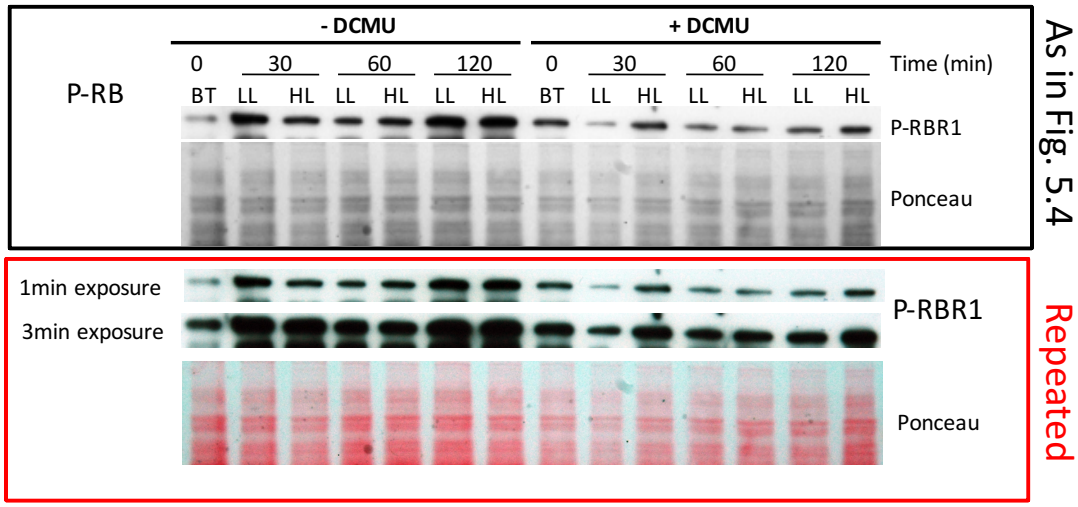

Appendix (Figure) 5.2: CYCB1;1::GUS quantitation of new leaves in low light to high light transfer

13 dag (days after germination) soil-grown seedlings under continuous low light (LL) (~60 µmol m^{-2} s^{-1}) were transferred to high light (HL) (~400 µmol m^{-2} s^{-1}) and the GUS assay carried out at 2, 6, 12, 24 and 48 hours (h) after transfer to HL. Measurement of the %GUS per leaf area was carried out using Image J software for new leaves. New leaves 1 and 2 are not shown as they showed no staining. NL 3 and 4 showed a higher %GUS in HL at 2h. (Asterisks mark statistical significance, where $p<0.05$, *t*-test).

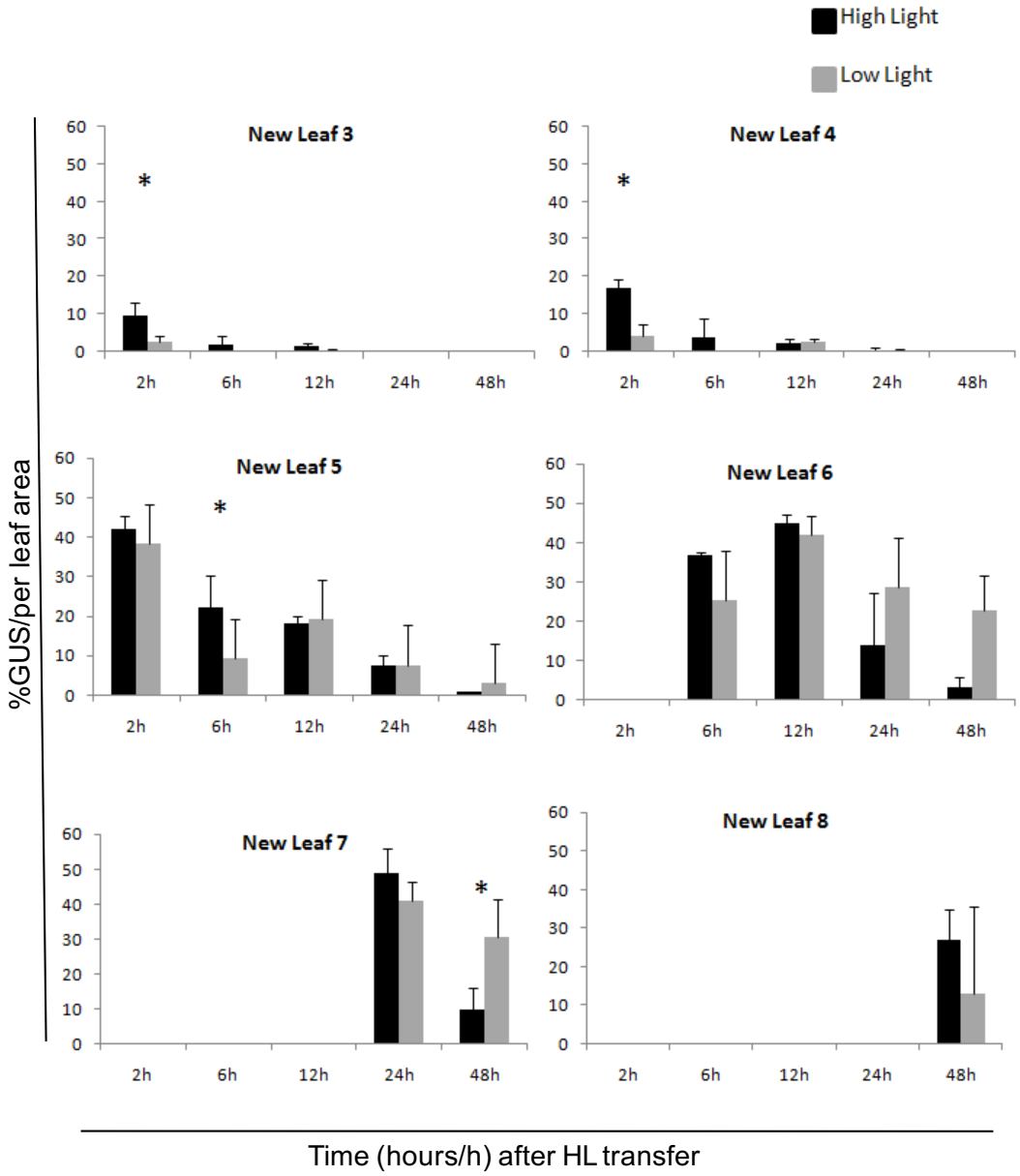

References

ABATE-SHEN, C. & SHEN, M. M. 2005. An unusual gene dosage effect of p27kip1 in a mouse model of prostate cancer. *Cell cycle,* 4**,** 426-428.

ABRASH, E. B., DAVIES, K. A. & BERGMANN, D. C. 2011. Generation of signaling specificity in Arabidopsis by spatially restricted buffering of ligand–receptor interactions. *The Plant Cell,* 23**,** 2864-2879.

ALCASABAS, A. A., DE CLARE, M. & OLIVER, S. G. 2013. Control analysis of the eukaryotic cell cycle using gene copy-number series in yeast tetraploids. *BMC genomics,* 14**,** 744.

ALLEN, J. F. 2003. Why chloroplasts and mitochondria contain genomes. *Comparative and Functional Genomics,* 4**,** 31-36.

ALONSO, J. M., HIRAYAMA, T., ROMAN, G., NOURIZADEH, S. & ECKER, J. R. 1999. EIN2, a bifunctional transducer of ethylene and stress responses in Arabidopsis. *Science,* 284**,** 2148-2152.

ANDERSON, J. M., CHOW, W. S. & PARK, Y.-I. 1995. The grand design of photosynthesis: acclimation of the photosynthetic apparatus to environmental cues. *Photosynthesis Research,* 46**,** 129-139.

ANDERSON, J. P., BADRUZSAUFARI, E., SCHENK, P. M., MANNERS, J. M., DESMOND, O. J., EHLERT, C., MACLEAN, D. J., EBERT, P. R. & KAZAN, K. 2004. Antagonistic interaction between abscisic acid and jasmonate-ethylene signaling pathways modulates defense gene expression and disease resistance in Arabidopsis. *The Plant Cell,* 16**,** 3460-3479.

ANDRIANKAJA, M., DHONDT, S., DE BODT, S., VANHAEREN, H., COPPENS, F., DE MILDE, L., MÜHLENBOCK, P., SKIRYCZ, A., GONZALEZ, N. & BEEMSTER, G. T. S. 2012. Exit from Proliferation during Leaf Development in< i> Arabidopsis thaliana</i>: A Not-So-Gradual Process. *Developmental cell*.

ARVIDSSON, S., KWASNIEWSKI, M., RIANO-PACHON, D. M. & MUELLER-ROEBER, B. 2008. QuantPrime--a flexible tool for reliable high-throughput primer design for quantitative PCR. *BMC bioinformatics,* 9**,** 465-2105-9-465.

ASL, L. K., DHONDT, S., BOUDOLF, V., BEEMSTER, G. T., BEECKMAN, T., INZÉ, D., GOVAERTS, W. & DE VEYLDER, L. 2011. Model-based analysis of Arabidopsis leaf epidermal cells reveals distinct division and expansion patterns for pavement and guard cells. *Plant physiology,* 156**,** 2172-2183.

BAENA-GONZÁLEZ, E., ROLLAND, F., THEVELEIN, J. M. & SHEEN, J. 2007. A central integrator of transcription networks in plant stress and energy signalling. *Nature,* 448**,** 938-942.

BAENA-GONZÁLEZ, E. & SHEEN, J. 2008. Convergent energy and stress signaling. *Trends in plant science,* 13**,** 474-482.

BARRANGOU, R., BIRMINGHAM, A., WIEMANN, S., BEIJERSBERGEN, R. L., HORNUNG, V. & VAN BRABANT SMITH, A. 2015. Advances in CRISPR-Cas9 genome engineering: lessons learned from RNA interference. *Nucleic acids research***,** gkv226.

BÄURLE, I. & LAUX, T. 2003. Apical meristems: the plant's fountain of youth. *Bioessays,* 25**,** 961-970.

BEEMSTER, G. T. & BASKIN, T. I. 1998. Analysis of cell division and elongation underlying the developmental acceleration of root growth in Arabidopsis thaliana. *Plant Physiology,* 116**,** 1515-1526.

BEEMSTER, G. T., DE VEYLDER, L., VERCRUYSSE, S., WEST, G., ROMBAUT, D., VAN HUMMELEN, P., GALICHET, A., GRUISSEM, W., INZE, D. & VUYLSTEKE, M. 2005. Genome-wide analysis of gene expression profiles associated with cell cycle transitions in growing organs of Arabidopsis. *Plant Physiology,* 138**,** 734-743.

BEEMSTER, G. T. S., FIORANI, F. & INZÉ, D. 2003. Cell cycle: the key to plant growth control? *Trends in plant science,* 8**,** 154-158.

BEN-SHLOMO, R. & KYRIACOU, C. P. Light Pulse Administered During the Circadian Dark Phase Alter Expression of Tumorigenesis Associated Transcripts in Mouse Brain. Recent Advances in Clinical Medicine (Anninos P, M Rossi, Pham TD, Falugi C, Bussing A, Koukkou M. Eds.), Proceedings of the International Conference on Oncology, University of Cambridge, UK, 2010. 331-336.

BENJAMINS, R., QUINT, A., WEIJERS, D., HOOYKAAS, P. & OFFRINGA, R. 2001. The PINOID protein kinase regulates organ development in Arabidopsis by enhancing polar auxin transport. *Development,* 128**,** 4057-4067.

BERCKMANS, B., VASSILEVA, V., SCHMID, S. P., MAES, S., PARIZOT, B., NARAMOTO, S., MAGYAR, Z., ALVIM KAMEI, C. L., KONCZ, C., BOGRE, L., PERSIAU, G., DE JAEGER, G., FRIML, J., SIMON, R., BEECKMAN, T. & DE VEYLDER, L. 2011. Auxin-dependent cell cycle reactivation through transcriptional regulation of Arabidopsis E2Fa by lateral organ boundary proteins. *The Plant Cell,* 23**,** 3671-3683.

BERNSTEIN, K. A., BLEICHERT, F., BEAN, J. M., CROSS, F. R. & BASERGA, S. J. 2007. Ribosome biogenesis is sensed at the Start cell cycle checkpoint. *Molecular biology of the cell,* 18**,** 953-964.

BEWLEY, J. D. & BLACK, M. 1978. The legacy of seed maturation. *Physiology and biochemistry of seeds in relation to germination.* Springer.

BIELER, J., CANNAVO, R., GUSTAFSON, K., GOBET, C., GATFIELD, D. & NAEF, F. 2014. Robust synchronization of coupled circadian and cell cycle oscillators in single mammalian cells. *Molecular systems biology,* 10**,** 739.

BILSBOROUGH, G. D., RUNIONS, A., BARKOULAS, M., JENKINS, H. W., HASSON, A., GALINHA, C., LAUFS, P., HAY, A., PRUSINKIEWICZ, P. & TSIANTIS, M. 2011. Model for the regulation of Arabidopsis thaliana leaf margin development. *Proceedings of the National Academy of Sciences,* 108**,** 3424-3429.

BLECKMANN, A., WEIDTKAMP-PETERS, S., SEIDEL, C. A. & SIMON, R. 2010. Stem cell signaling in Arabidopsis requires CRN to localize CLV2 to the plasma membrane. *Plant physiology,* 152**,** 166-176.

BLEECKER, A. B., ESTELLE, M. A., SOMERVILLE, C. & KENDE, H. 1988. Insensitivity to ethylene conferred by a dominant mutation in Arabidopsis thaliana. *Science,* 241**,** 1086-1089.

BLOMME, J., INZE, D. & GONZALEZ, N. 2014. The cell-cycle interactome: a source of growth regulators? *Journal of experimental botany,* 65**,** 2715-2730.

BOGRE, L., MAGYAR, Z. & LOPEZ-JUEZ, E. 2008. New clues to organ size control in plants. *Genome biology,* 9**,** 226.

BONIOTTI, M. B. & GRIFFITH, M. E. 2002. "Cross-talk" between cell division cycle and development in plants. *The Plant Cell,* 14**,** 11-16.

BORGHI, L., GUTZAT, R., FÜTTERER, J., LAIZET, Y. H., HENNIG, L. & GRUISSEM, W. 2010. Arabidopsis RETINOBLASTOMA-RELATED is required for stem cell maintenance, cell differentiation, and lateral organ production. *The Plant Cell,* 22**,** 1792-1811.

BOROWSKA-WYKRĘT, D., ELSNER, J., DE VEYLDER, L. & KWIATKOWSKA, D. 2013. Defects in leaf epidermis of Arabidopsis thaliana plants with CDKA; 1 activity reduced in the shoot apical meristem. *Protoplasma,* 250**,** 955-961.

BOUDOLF, V., BARROCO, R., ENGLER JDE, A., VERKEST, A., BEECKMAN, T., NAUDTS, M., INZE, D. & DE VEYLDER, L. 2004a. B1-type cyclin-dependent kinases are essential for the formation of stomatal complexes in Arabidopsis thaliana. *The Plant Cell,* 16**,** 945-955.

BOUDOLF, V., LAMMENS, T., BORUC, J., VAN LEENE, J., VAN DEN DAELE, H., MAES, S., VAN ISTERDAEL, G., RUSSINOVA, E., KONDOROSI, E., WITTERS, E., DE JAEGER, G., INZE, D. & DE VEYLDER, L. 2009. CDKB1;1 forms a functional complex with CYCA2;3 to suppress endocycle onset. *Plant Physiology,* 150**,** 1482-1493.

BOUDOLF, V., VLIEGHE, K., BEEMSTER, G. T., MAGYAR, Z., TORRES ACOSTA, J. A., MAES, S., VAN DER SCHUEREN, E., INZE, D. & DE VEYLDER, L. 2004b. The plant-specific cyclin-dependent kinase CDKB1;1 and transcription factor E2Fa-DPa control the balance of mitotically dividing and endoreduplicating cells in Arabidopsis. *The Plant Cell,* 16**,** 2683-2692.

BRAND, U., FLETCHER, J. C., HOBE, M., MEYEROWITZ, E. M. & SIMON, R. 2000. Dependence of stem cell fate in Arabidopsis on a feedback loop regulated by CLV3 activity. *Science (New York, N.Y.),* 289**,** 617-619.

BRAYBROOK, S. A. & KUHLEMEIER, C. 2010. How a plant builds leaves. *The Plant Cell,* 22**,** 1006-1018.

BREHM, A., MISKA, E. A., MCCANCE, D. J., REID, J. L., BANNISTER, A. J. & KOUZARIDES, T. 1998. Retinoblastoma protein recruits histone deacetylase to repress transcription. *Nature,* 391**,** 597-601.

BROWN, B. A., CLOIX, C., JIANG, G. H., KAISERLI, E., HERZYK, P., KLIEBENSTEIN, D. J. & JENKINS, G. I. 2005. A UV-B-specific signaling component orchestrates plant UV protection. *Proceedings of the National Academy of Sciences of the United States of America,* 102**,** 18225-18230.

BYRNE, M., TIMMERMANS, M., KIDNER, C. & MARTIENSSEN, R. 2001. Development of leaf shape. *Current opinion in plant biology,* 4**,** 38-43.

BYRNE, M. E., BARLEY, R., CURTIS, M., ARROYO, J. M., DUNHAM, M., HUDSON, A. & MARTIENSSEN, R. A. 2000. Asymmetric leaves1 mediates leaf patterning and stem cell function in Arabidopsis. *Nature,* 408**,** 967-971.

CABIB, E. & LELOIR, L. F. 1958. The biosynthesis of trehalose phosphate. *The Journal of biological chemistry,* 231**,** 259-275.

CASAL, J. J. 2013. Photoreceptor signaling networks in plant responses to shade. *Annual review of plant biology,* 64**,** 403-427.

CASPAR, T., HUBER, S. C. & SOMERVILLE, C. 1985. Alterations in Growth, Photosynthesis, and Respiration in a Starchless Mutant of Arabidopsis thaliana (L.) Deficient in Chloroplast Phosphoglucomutase Activity. *Plant Physiology,* 79**,** 11-17.

CASTELLANO, M. M., DEL POZO, J. C., RAMIREZ-PARRA, E., BROWN, S. & GUTIERREZ, C. 2001. Expression and stability of Arabidopsis CDC6 are associated with endoreplication. *The Plant Cell,* 13**,** 2671-2686.

CHATTERTON, N. J. & SILVIUS, J. E. 1979. Photosynthate partitioning into starch in soybean leaves I. Effects of photoperiod versus photosynthetic period duration. *Plant Physiology,* 64**,** 749-753.

CHAW, S.-M., CHANG, C.-C., CHEN, H.-L. & LI, W.-H. 2004. Dating the monocot–dicot divergence and the origin of core eudicots using whole chloroplast genomes. *Journal of molecular evolution,* 58**,** 424-441.

CHEN, M. 2008. Phytochrome nuclear body: an emerging model to study interphase nuclear dynamics and signaling. *Current opinion in plant biology,* 11**,** 503-508.

CHENG, W.-H., CHIANG, M.-H., HWANG, S.-G. & LIN, P.-C. 2009. Antagonism between abscisic acid and ethylene in Arabidopsis acts in parallel with the reciprocal regulation of their metabolism and signaling pathways. *Plant molecular biology,* 71**,** 61-80.

CHENG, W.-H., ENDO, A., ZHOU, L., PENNEY, J., CHEN, H.-C., ARROYO, A., LEON, P., NAMBARA, E., ASAMI, T. & SEO, M. 2002. A unique short-chain dehydrogenase/reductase in Arabidopsis glucose signaling and abscisic acid biosynthesis and functions. *The Plant Cell,* 14**,** 2723-2743.

CHITWOOD, D. H., HEADLAND, L. R., RANJAN, A., MARTINEZ, C. C., BRAYBROOK, S. A., KOENIG, D. P., KUHLEMEIER, C., SMITH, R. S. & SINHA, N. R. 2012. Leaf asymmetry as a developmental constraint imposed by auxin-dependent phyllotactic patterning. *The Plant Cell,* 24**,** 2318-2327.

CHORY, J., PETO, C., FEINBAUM, R., PRATT, L. & AUSUBEL, F. 1989. Arabidopsis thaliana mutant that develops as a light-grown plant in the absence of light. *Cell,* 58**,** 991-999.

CHORY, J., REINECKE, D., SIM, S., WASHBURN, T. & BRENNER, M. 1994. A Role for Cytokinins in De-Etiolation in Arabidopsis (det Mutants Have an Altered Response to Cytokinins). *Plant Physiology,* 104**,** 339-347.

COLÓN‐CARMONA, A., YOU, R., HAIMOVITCH‐GAL, T. & DOERNER, P. 1999. Spatio‐temporal analysis of mitotic activity with a labile cyclin–GUS fusion protein. *The Plant Journal,* 20**,** 503-508.

COOPER, G. M. & HAUSMAN, R. E. 2000. *The cell*, Sinauer Associates Sunderland.

COSGROVE, D. J. 2005. Growth of the plant cell wall. *Nature reviews molecular cell biology,* 6**,** 850-861.

COSTANZO, M., NISHIKAWA, J. L., TANG, X., MILLMAN, J. S., SCHUB, O., BREITKREUZ, K., DEWAR, D., RUPES, I., ANDREWS, B. & TYERS, M. 2004. CDK activity antagonizes Whi5, an inhibitor of G1/S transcription in yeast. *Cell,* 117**,** 899-913.

COUDREUSE, D. & NURSE, P. 2010. Driving the cell cycle with a minimal CDK control network. *Nature,* 468**,** 1074-1079.

DAUM, G., MEDZIHRADSZKY, A., SUZAKI, T. & LOHMANN, J. U. 2014. A mechanistic framework for noncell autonomous stem cell induction in Arabidopsis. *Proceedings of the National Academy of Sciences of the United States of America*.

DE BRUIN, R. A., MCDONALD, W. H., KALASHNIKOVA, T. I., YATES, J. & WITTENBERG, C. 2004. Cln3 activates G1-specific transcription via phosphorylation of the SBF bound repressor Whi5. *Cell,* 117**,** 887-898.

DE JAGER, S., MENGES, M., BAUER, U.-M. & MURRAY, J. 2001. Arabidopsis E2F1 binds a sequence present in the promoter of S-phase-regulated gene AtCDC6 and is a member of a multigene family with differential activities. *Plant molecular biology,* 47**,** 555-568.

DE REUILLE, P. B., BOHN-COURSEAU, I., LJUNG, K., MORIN, H., CARRARO, N., GODIN, C. & TRAAS, J. 2006. Computer simulations reveal properties of the cell-cell signaling network at the shoot apex in Arabidopsis. *Proceedings of the National Academy of Sciences of the United States of America,* 103**,** 1627-1632.

DE VEYLDER, L., BEECKMAN, T., BEEMSTER, G. T., KROLS, L., TERRAS, F., LANDRIEU, I., VAN DER SCHUEREN, E., MAES, S., NAUDTS, M. & INZE, D. 2001. Functional analysis of cyclin-dependent kinase inhibitors of Arabidopsis. *The Plant Cell,* 13**,** 1653-1668.

DE VEYLDER, L., BEECKMAN, T., BEEMSTER, G. T. S., DE ALMEIDA ENGLER, J., ORMENESE, S., MAES, S., NAUDTS, M., VAN DER SCHUEREN, E., JACQMARD, A. & ENGLER, G. 2002. Control of proliferation, endoreduplication and differentiation by the Arabidopsis E2Fa–DPa transcription factor. *The EMBO journal,* 21**,** 1360-1368.

DE VEYLDER, L., BEECKMAN, T. & INZÉ, D. 2007. The ins and outs of the plant cell cycle. *Nature Reviews Molecular Cell Biology,* 8**,** 655-665.

DEB, Y., MARTI, D., FRENZ, M., KUHLEMEIER, C. & REINHARDT, D. 2015. Phyllotaxis involves auxin drainage through leaf primordia. *Development,* 142**,** 1992-2001.

DEKENS, M. P. S., SANTORIELLO, C., VALLONE, D., GRASSI, G., WHITMORE, D. & FOULKES, N. S. 2003. Light regulates the cell cycle in zebrafish. *Current Biology,* 13**,** 2051-2057.

DEL POZO, J. C., BONIOTTI, M. B. & GUTIERREZ, C. 2002. Arabidopsis E2Fc functions in cell division and is degraded by the ubiquitin-SCFAtSKP2 pathway in response to light. *The Plant Cell,* 14**,** 3057-3071.

DENG, X. W., CASPAR, T. & QUAIL, P. H. 1991. cop1: a regulatory locus involved in light-controlled development and gene expression in Arabidopsis. *Genes & development,* 5**,** 1172-1182.

DENGLER, N. G. 1980. Comparative histological basis of sun and shade leaf dimorphism in Helianthus annuus. *Canadian Journal of Botany,* 58**,** 717-730.

DENGLER, N. G. & TSUKAYA, H. 2001. Leaf morphogenesis in dicotyledons: current issues. *International Journal of Plant Sciences,* 162**,** 459-464.

DESVOYES, B., DE MENDOZA, A., RUIZ-TRILLO, I. & GUTIERREZ, C. 2014. Novel roles of plant RETINOBLASTOMA-RELATED (RBR) protein in cell proliferation and asymmetric cell division. *Journal of experimental botany,* 65**,** 2657-2666.

DESVOYES, B., RAMIREZ-PARRA, E., XIE, Q., CHUA, N.-H. & GUTIERREZ, C. 2006. Cell type-specific role of the retinoblastoma/E2F pathway during Arabidopsis leaf development. *Plant physiology,* 140**,** 67-80.

DEVLIN, P. F., ROBSON, P. R., PATEL, S. R., GOOSEY, L., SHARROCK, R. A. & WHITELAM, G. C. 1999. Phytochrome D acts in the shade-avoidance syndrome in Arabidopsis by controlling elongation growth and flowering time. *Plant Physiology,* 119**,** 909-915.

DEWITTE, W., RIOU-KHAMLICHI, C., SCOFIELD, S., HEALY, J. M., JACQMARD, A., KILBY, N. J. & MURRAY, J. A. 2003. Altered cell cycle distribution, hyperplasia, and inhibited differentiation in Arabidopsis caused by the D-type cyclin CYCD3. *The Plant Cell,* 15**,** 79-92.

DEWITTE, W., SCOFIELD, S., ALCASABAS, A. A., MAUGHAN, S. C., MENGES, M., BRAUN, N., COLLINS, C., NIEUWLAND, J., PRINSEN, E., SUNDARESAN, V. & MURRAY, J. A. 2007. Arabidopsis CYCD3 D-type cyclins link cell proliferation and endocycles and are rate-limiting for cytokinin responses. *Proceedings of the National Academy of Sciences of the United States of America,* 104**,** 14537-14542.

DIAMOND, S., JUN, D., RUBIN, B. E. & GOLDEN, S. S. 2015. The circadian oscillator in Synechococcus elongatus controls metabolite partitioning during diurnal growth. *Proceedings of the National Academy of Sciences,* 112**,** E1916-E1925.

DIETRICH, K., WELTMEIER, F., EHLERT, A., WEISTE, C., STAHL, M., HARTER, K. & DROGE-LASER, W. 2011. Heterodimers of the Arabidopsis transcription factors bZIP1 and bZIP53 reprogram amino acid metabolism during low energy stress. *The Plant Cell,* 23**,** 381-395.

DODSWORTH, S. 2009. A diverse and intricate signalling network regulates stem cell fate in the shoot apical meristem. *Developmental biology,* 336**,** 1-9.

DONG, G., YANG, Q., WANG, Q., KIM, Y.-I., WOOD, T. L., OSTERYOUNG, K. W., VAN OUDENAARDEN, A. & GOLDEN, S. S. 2010. Elevated ATPase activity of KaiC applies a circadian checkpoint on cell division in Synechococcus elongatus. *Cell,* 140**,** 529-539.

DONNELLY, P. M., BONETTA, D., TSUKAYA, H., DENGLER, R. E. & DENGLER, N. G. 1999. Cell cycling and cell enlargement in developing leaves of Arabidopsis. *Developmental biology,* 215**,** 407-419.

DUEK, P. D. & FANKHAUSER, C. 2005. bHLH class transcription factors take centre stage in phytochrome signalling. *Trends in plant science,* 10**,** 51-54.

DUMAIS, J. & STEELE, C. R. 2000. New evidence for the role of mechanical forces in the shoot apical meristem. *Journal of Plant Growth Regulation,* 19**,** 7-18.

EASTMOND, P. J., VAN DIJKEN, A. J. H., SPIELMAN, M., KERR, A., TISSIER, A. F., DICKINSON, H. G., JONES, J. D. G., SMEEKENS, S. C. & GRAHAM, I. A. 2002. Trehalose‐6‐phosphate synthase 1, which catalyses the first step in trehalose synthesis, is essential for Arabidopsis embryo maturation. *The Plant Journal,* 29**,** 225-235.

EDWARDS, K., JOHNSTONE, C. & THOMPSON, C. 1991. A simple and rapid method for the preparation of plant genomic DNA for PCR analysis. *Nucleic acids research,* 19**,** 1349.

EL-SHOWK, S., RUONALA, R. & HELARIUTTA, Y. 2013. Crossing paths: cytokinin signalling and crosstalk. *Development,* 140**,** 1373-1383.

ELBEIN, A. D., PAN, Y. T., PASTUSZAK, I. & CARROLL, D. 2003. New insights on trehalose: a multifunctional molecule. *Glycobiology,* 13**,** 17R-27R.

FÀBREGAS, N., FORMOSA-JORDAN, P., CONFRARIA, A., SILIGATO, R., ALONSO, J. M., SWARUP, R., BENNETT, M. J., MÄHÖNEN, A. P., CAÑO-DELGADO, A. I. & IBAÑES, M. 2015. Auxin Influx Carriers Control Vascular Patterning

and Xylem Differentiation in Arabidopsis thaliana. *PLoS Genet,* 11**,** e1005183.

FANKHAUSER, C. & CHEN, M. 2008. Transposing phytochrome into the nucleus. *Trends in plant science,* 13**,** 596-601.

FERREIRA, P. C., HEMERLY, A. S., VILLARROEL, R., VAN MONTAGU, M. & INZE, D. 1991. The Arabidopsis functional homolog of the p34cdc2 protein kinase. *The Plant Cell,* 3**,** 531-540.

FLOYD, S. K. & BOWMAN, J. L. 2004. Gene regulation: ancient microRNA target sequences in plants. *Nature,* 428**,** 485-486.

FOARD, D. E. 1971. The initial protrusion of a leaf primordium can form without concurrent periclinal cell divisions. *Canadian Journal of Botany,* 49**,** 1601-1603.

FOLTA, K. M. & MARUHNICH, S. A. 2007. Green light: a signal to slow down or stop. *Journal of experimental botany,* 58**,** 3099-3111.

FONDY, B. R. & GEIGER, D. R. 1985. Diurnal changes in allocation of newly fixed carbon in exporting sugar beet leaves. *Plant Physiology,* 78**,** 753-757.

FOURNIER, C., DURAND, J., LJUTOVAC, S., SCHÄUFELE, R., GASTAL, F. & ANDRIEU, B. 2005. A functional–structural model of elongation of the grass leaf and its relationships with the phyllochron. *New Phytologist,* 166**,** 881-894.

FRANKLIN, K. A. & QUAIL, P. H. 2010. Phytochrome functions in Arabidopsis development. *Journal of experimental botany,* 61**,** 11-24.

FRIDLENDER, M., LEV-YADUN, S., BABUREK, I., ANGELIS, K. & LEVY, A. A. 1996. Cell divisions in cotyledons after germination: localization, time course and utilization for a mutagenesis assay. *Planta,* 199**,** 307-313.

FU, Y., GU, Y., ZHENG, Z., WASTENEYS, G. & YANG, Z. 2005. Arabidopsis interdigitating cell growth requires two antagonistic pathways with opposing action on cell morphogenesis. *Cell,* 120**,** 687-700.

FU, Y., LI, H. & YANG, Z. 2002. The ROP2 GTPase controls the formation of cortical fine F-actin and the early phase of directional cell expansion during Arabidopsis organogenesis. *The Plant Cell,* 14**,** 777-794.

FU, Y., XU, T., ZHU, L., WEN, M. & YANG, Z. 2009. A ROP GTPase signaling pathway controls cortical microtubule ordering and cell expansion in Arabidopsis. *Current Biology,* 19**,** 1827-1832.

FUNG, T. K. & POON, R. Y. A roller coaster ride with the mitotic cyclins. Seminars in cell & developmental biology, 2005. Elsevier, 335-342.

FURUYA, M. 1984. Cell division patterns in multicellular plants. *Annual review of plant physiology,* 35**,** 349-373.

GALLAGHER, J. N. 1979. Field studies of cereal leaf growth I. Initiation and expansion in relation to temperature and ontogeny. *Journal of experimental botany,* 30**,** 625-636.

GALLETTI, R., JOHNSON, K. L., SCOFIELD, S., SAN-BENTO, R., WATT, A. M., MURRAY, J. A. & INGRAM, G. C. 2015. DEFECTIVE KERNEL 1 promotes and maintains plant epidermal differentiation. *Development,* 142**,** 1978-1983.

GEELEN, D., ROYACKERS, K., VANSTRAELEN, M., DE BUS, M., INZÉ, D., VAN DIJCK, P., THEVELEIN, J. M. & LEYMAN, B. 2007. Trehalose-6-P synthase< i> At</i> TPS1 high molecular weight complexes in yeast and< i> Arabidopsis</i>. *Plant science,* 173**,** 426-437.

GEIGER, D. R. & SERVAITES, J. C. 1994. Diurnal regulation of photosynthetic carbon metabolism in C3 plants. *Annual review of plant biology,* 45**,** 235-256.

GENDREAU, E., TRAAS, J., DESNOS, T., GRANDJEAN, O., CABOCHE, M. & HOFTE, H. 1997. Cellular basis of hypocotyl growth in Arabidopsis thaliana. *Plant Physiology,* 114**,** 295-305.

GENSCHIK, P., MARROCCO, K., BACH, L., NOIR, S. & CRIQUI, M. C. 2014. Selective protein degradation: a rheostat to modulate cell-cycle phase transitions. *Journal of experimental botany,* 65**,** 2603-2615.

GIBON, Y., BLASING, O. E., PALACIOS-ROJAS, N., PANKOVIC, D., HENDRIKS, J. H., FISAHN, J., HOHNE, M., GUNTHER, M. & STITT, M. 2004. Adjustment of diurnal starch turnover to short days: depletion of sugar during the night leads to a temporary inhibition of carbohydrate utilization, accumulation of sugars and post-translational activation of ADP-glucose pyrophosphorylase in the following light period. *The Plant Journal : for cell and molecular biology,* 39**,** 847-862.

GIBON, Y., PYL, E. T., SULPICE, R., LUNN, J. E., HOEHNE, M., GUENTHER, M. & STITT, M. 2009. Adjustment of growth, starch turnover, protein content and central metabolism to a decrease of the carbon supply when Arabidopsis is grown in very short photoperiods. *Plant, Cell & Environment,* 32**,** 859-874.

GIEFFERS, C., PETERS, B. H., KRAMER, E. R., DOTTI, C. G. & PETERS, J.-M. 1999. Expression of the CDH1-associated form of the anaphase-promoting complex in postmitotic neurons. *Proceedings of the National Academy of Sciences,* 96**,** 11317-11322.

GONZALEZ, N., VANHAEREN, H. & INZÉ, D. 2012. Leaf size control: complex coordination of cell division and expansion. *Trends in plant science,* 17**,** 332-340.

GOTO, K. & JOHNSON, C. H. 1995. Is the cell division cycle gated by a circadian clock? The case of Chlamydomonas reinhardtii. *The Journal of cell biology,* 129**,** 1061-1069.

GRAF, A., SCHLERETH, A., STITT, M. & SMITH, A. M. 2010. Circadian control of carbohydrate availability for growth in Arabidopsis plants at night. *Proceedings of the National Academy of Sciences of the United States of America,* 107**,** 9458-9463.

GRAF, A. & SMITH, A. M. 2011. Starch and the clock: the dark side of plant productivity. *Trends in plant science,* 16**,** 169-175.

GRIENEISEN, V. A., XU, J., MARÉE, A. F., HOGEWEG, P. & SCHERES, B. 2007. Auxin transport is sufficient to generate a maximum and gradient guiding root growth. *Nature,* 449**,** 1008-1013.

GUO, M., THOMAS, J., COLLINS, G. & TIMMERMANS, M. C. 2008. Direct repression of KNOX loci by the ASYMMETRIC LEAVES1 complex of Arabidopsis. *The Plant Cell,* 20**,** 48-58.

GUPTA, M. D. & NATH, U. 2015. Divergence in patterns of leaf growth polarity is associated with the expression divergence of miR396. *The Plant Cell,* 27**,** 2785-2799.

GUSEMAN, J. M., LEE, J. S., BOGENSCHUTZ, N. L., PETERSON, K. M., VIRATA, R. E., XIE, B., KANAOKA, M. M., HONG, Z. & TORII, K. U. 2010. Dysregulation of cell-to-cell connectivity and stomatal patterning by loss-of-function

mutation in Arabidopsis chorus (glucan synthase-like 8). *Development,* 137**,** 1731-1741.

HARASHIMA, H., DISSMEYER, N. & SCHNITTGER, A. 2013. Cell cycle control across the eukaryotic kingdom. *Trends in cell biology,* 23**,** 345-356.

HAY, A. & TSIANTIS, M. 2010. KNOX genes: versatile regulators of plant development and diversity. *Development (Cambridge, England),* 137**,** 3153-3165.

HEISLER, M. G., OHNO, C., DAS, P., SIEBER, P., REDDY, G. V., LONG, J. A. & MEYEROWITZ, E. M. 2005. Patterns of Auxin Transport and Gene Expression during Primordium Development Revealed by Live Imaging of the< i> Arabidopsis</i> Inflorescence Meristem. *Current Biology,* 15**,** 1899-1911.

HEMERLY, A., ENGLER JDE, A., BERGOUNIOUX, C., VAN MONTAGU, M., ENGLER, G., INZE, D. & FERREIRA, P. 1995. Dominant negative mutants of the Cdc2 kinase uncouple cell division from iterative plant development. *The EMBO journal,* 14**,** 3925-3936.

HENRIQUES, R., MAGYAR, Z. & BÖGRE, L. 2013. S6K1 and E2FB are in mutually antagonistic regulatory links controlling cell growth and proliferation in. *Plant signaling & behavior,* 24367**,** 1.

HEYNEKE, E., LUSCHIN-EBENGREUTH, N., KRAJCER, I., WOLKINGER, V., MÜLLER, M. & ZECHMANN, B. 2013. Dynamic compartment specific changes in glutathione and ascorbate levels in Arabidopsis plants exposed to different light intensities. *BMC plant biology,* 13**,** 104.

HIRANO, H., HARASHIMA, H., SHINMYO, A. & SEKINE, M. 2008. Arabidopsis RETINOBLASTOMA-RELATED PROTEIN 1 is involved in G1 phase cell cycle arrest caused by sucrose starvation. *Plant molecular biology,* 66**,** 259-275.

HORIGUCHI, G., GONZALEZ, N., BEEMSTER, G. T. S., INZÉ, D. & TSUKAYA, H. 2009. Impact of segmental chromosomal duplications on leaf size in the grandifolia‐D mutants of Arabidopsis thaliana. *The Plant Journal,* 60**,** 122-133.

HORVATH, B. M., MAGYAR, Z., ZHANG, Y., HAMBURGER, A. W., BAKO, L., VISSER, R. G., BACHEM, C. W. & BOGRE, L. 2006. EBP1 regulates organ size through cell growth and proliferation in plants. *The EMBO journal,* 25**,** 4909-4920.

HUANG, M., ZHOU, Z. & ELLEDGE, S. J. 1998. The DNA replication and damage checkpoint pathways induce transcription by inhibition of the Crt1 repressor. *Cell,* 94**,** 595-605.

HUANG, X., OUYANG, X. & DENG, X. W. 2014. Beyond repression of photomorphogenesis: role switching of COP/DET/FUS in light signaling. *Current opinion in plant biology,* 21**,** 96-103.

HUBER, A., BODENMILLER, B., UOTILA, A., STAHL, M., WANKA, S., GERRITS, B., AEBERSOLD, R. & LOEWITH, R. 2009. Characterization of the rapamycin-sensitive phosphoproteome reveals that Sch9 is a central coordinator of protein synthesis. *Genes & development,* 23**,** 1929-1943.

HUMMEL, G. M., NAUMANN, M., SCHURR, U. & WALTER, A. 2007. Root growth dynamics of Nicotiana attenuata seedlings are affected by simulated herbivore attack. *Plant, Cell & Environment,* 30**,** 1326-1336.

HUMPLÍK, J. F., TUREČKOVÁ, V., FELLNER, M. & BERGOUGNOUX, V. 2015. Spatio-temporal changes in endogenous abscisic acid contents during etiolated growth and photomorphogenesis in tomato seedlings. *Plant signaling & behavior,* 10**,** e1039213.

HUQ, E., AL-SADY, B., HUDSON, M., KIM, C., APEL, K. & QUAIL, P. H. 2004. Phytochrome-interacting factor 1 is a critical bHLH regulator of chlorophyll biosynthesis. *Science (New York, N.Y.),* 305**,** 1937-1941.

HUYSMAN, M. J., FORTUNATO, A. E., MATTHIJS, M., COSTA, B. S., VANDERHAEGHEN, R., VAN DEN DAELE, H., SACHSE, M., INZE, D., BOWLER, C., KROTH, P. G., WILHELM, C., FALCIATORE, A., VYVERMAN, W. & DE VEYLDER, L. 2013. AUREOCHROME1a-mediated induction of the diatom-specific cyclin dsCYC2 controls the onset of cell division in diatoms (Phaeodactylum tricornutum). *The Plant Cell,* 25**,** 215-228.

ICHIHASHI, Y., KAWADE, K., USAMI, T., HORIGUCHI, G., TAKAHASHI, T. & TSUKAYA, H. 2011. Key proliferative activity in the junction between the leaf blade and leaf petiole of Arabidopsis. *Plant Physiology,* 157**,** 1151-1162.

IMAI, K. K., OHASHI, Y., TSUGE, T., YOSHIZUMI, T., MATSUI, M., OKA, A. & AOYAMA, T. 2006. The A-type cyclin CYCA2;3 is a key regulator of ploidy levels in Arabidopsis endoreduplication. *The Plant Cell,* 18**,** 382-396.

INAGAKI, S. & UMEDA, M. 2011. Cell-cycle control and plant development. *International review of cell and molecular biology,* 291**,** 227-261.

INZÉ, D. & DE VEYLDER, L. 2006. Cell cycle regulation in plant development 1. *Annu.Rev.Genet.,* 40**,** 77-105.

ITO, M. 1969. Light-induced synchrony of cell division in the protonema of the fern, Pteris vittata. *Planta,* 90**,** 22-31.

ITO, M., ARAKI, S., MATSUNAGA, S., ITOH, T., NISHIHAMA, R., MACHIDA, Y., DOONAN, J. H. & WATANABE, A. 2001. G2/M-phase-specific transcription during the plant cell cycle is mediated by c-Myb-like transcription factors. *The Plant Cell,* 13**,** 1891-1905.

JACQUES, E., VERBELEN, J.-P. & VISSENBERG, K. 2014. Review on shape formation in epidermal pavement cells of the Arabidopsis leaf. *Functional Plant Biology,* 41**,** 914-921.

JAMES, S. A. & BELL, D. T. 2000. Influence of light availability on leaf structure and growth of two Eucalyptus globulus ssp. globulus provenances. *Tree Physiology,* 20**,** 1007-1018.

JARILLO, J. A., GABRYS, H., CAPEL, J., ALONSO, J. M., ECKER, J. R. & CASHMORE, A. R. 2001. Phototropin-related NPL1 controls chloroplast relocation induced by blue light. *Nature,* 410**,** 952-954.

JASINSKI, S., RIOU-KHAMLICHI, C., ROCHE, O., PERENNES, C., BERGOUNIOUX, C. & GLAB, N. 2002. The CDK inhibitor NtKIS1a is involved in plant development, endoreduplication and restores normal development of cyclin D3; 1-overexpressing plants. *Journal of cell science,* 115**,** 973-982.

JIAO, Y., LAU, O. S. & DENG, X. W. 2007. Light-regulated transcriptional networks in higher plants. *Nature Reviews Genetics,* 8**,** 217-230.

JIAO, Y., YANG, H., MA, L., SUN, N., YU, H., LIU, T., GAO, Y., GU, H., CHEN, Z., WADA, M., GERSTEIN, M., ZHAO, H., QU, L. J. & DENG, X. W. 2003. A genome-wide analysis of blue-light regulation of Arabidopsis transcription factor gene

expression during seedling development. *Plant Physiology,* 133**,** 1480-1493.

JINEK, M., CHYLINSKI, K., FONFARA, I., HAUER, M., DOUDNA, J. A. & CHARPENTIER, E. 2012. A programmable dual-RNA–guided DNA endonuclease in adaptive bacterial immunity. *Science,* 337**,** 816-821.

JOSSE, E.-M. & HALLIDAY, K. J. 2008. Skotomorphogenesis: the dark side of light signalling. *Current Biology,* 18**,** R1144-R1146.

KAGAWA, T., SAKAI, T., SUETSUGU, N., OIKAWA, K., ISHIGURO, S., KATO, T., TABATA, S., OKADA, K. & WADA, M. 2001. Arabidopsis NPL1: a phototropin homolog controlling the chloroplast high-light avoidance response. *Science (New York, N.Y.),* 291**,** 2138-2141.

KAISERLI, E. & JENKINS, G. I. 2007. UV-B promotes rapid nuclear translocation of the Arabidopsis UV-B specific signaling component UVR8 and activates its function in the nucleus. *The Plant Cell,* 19**,** 2662-2673.

KALVE, S., FOTSCHKI, J., BEECKMAN, T., VISSENBERG, K. & BEEMSTER, G. T. 2014. Three-dimensional patterns of cell division and expansion throughout the development of Arabidopsis thaliana leaves. *Journal of experimental botany*.

KANG, J., MIZUKAMI, Y., WANG, H., FOWKE, L. & DENGLER, N. G. 2007. Modification of cell proliferation patterns alters leaf vein architecture in Arabidopsis thaliana. *Planta,* 226**,** 1207-1218.

KAZAMA, T., ICHIHASHI, Y., MURATA, S. & TSUKAYA, H. 2010. The mechanism of cell cycle arrest front progression explained by a KLUH/CYP78A5-dependent mobile growth factor in developing leaves of Arabidopsis thaliana. *Plant & Cell Physiology,* 51**,** 1046-1054.

KIM, G.-T., YANO, S., KOZUKA, T. & TSUKAYA, H. 2005. Photomorphogenesis of leaves: shade-avoidance and differentiation of sun and shade leaves. *Photochem.Photobiol.Sci.,* 4**,** 770-774.

KINOSHITA, T., DOI, M., SUETSUGU, N., KAGAWA, T., WADA, M. & SHIMAZAKI, K.-I. 2001. Phot1 and phot2 mediate blue light regulation of stomatal opening. *Nature,* 414**,** 656-660.

KIRCHER, S., GIL, P., KOZMA-BOGNAR, L., FEJES, E., SPETH, V., HUSSELSTEIN-MULLER, T., BAUER, D., ADAM, E., SCHAFER, E. & NAGY, F. 2002. Nucleocytoplasmic partitioning of the plant photoreceptors phytochrome A, B, C, D, and E is regulated differentially by light and exhibits a diurnal rhythm. *The Plant Cell,* 14**,** 1541-1555.

KIRCHER, S. & SCHOPFER, P. 2012. Photosynthetic sucrose acts as cotyledon-derived long-distance signal to control root growth during early seedling development in Arabidopsis. *Proceedings of the National Academy of Sciences,* 109**,** 11217-11221.

KOINI, M. A., ALVEY, L., ALLEN, T., TILLEY, C. A., HARBERD, N. P., WHITELAM, G. C. & FRANKLIN, K. A. 2009. High temperature-mediated adaptations in plant architecture require the bHLH transcription factor PIF4. *Current Biology,* 19**,** 408-413.

KOMAKI, S. & SUGIMOTO, K. 2012. Control of the plant cell cycle by developmental and environmental cues. *Plant & Cell Physiology,* 53**,** 953-964.

KONG, S. G., KINOSHITA, T., SHIMAZAKI, K. I., MOCHIZUKI, N., SUZUKI, T. & NAGATANI, A. 2007. The C‐terminal kinase fragment of Arabidopsis

phototropin 2 triggers constitutive phototropin responses. *The Plant Journal,* 51**,** 862-873.

KOORNNEEF, M., ROLFF, E. & SPRUIT, C. 1980. Genetic control of light-inhibited hypocotyl elongation in Arabidopsis thaliana (L.) Heynh. *Zeitschrift für Pflanzenphysiologie,* 100**,** 147-160.

KOROLEVA, O. A., TOMLINSON, M., PARINYAPONG, P., SAKVARELIDZE, L., LEADER, D., SHAW, P. & DOONAN, J. H. 2004. CycD1, a putative G1 cyclin from Antirrhinum majus, accelerates the cell cycle in cultured tobacco BY-2 cells by enhancing both G1/S entry and progression through S and G2 phases. *The Plant Cell,* 16**,** 2364-2379.

KOSUGI, S. & OHASHI, Y. 2002. E2Ls, E2F-like repressors of Arabidopsis that bind to E2F sites in a monomeric form. *Journal of Biological Chemistry,* 277**,** 16553-16558.

KOZUKA, T., HORIGUCHI, G., KIM, G. T., OHGISHI, M., SAKAI, T. & TSUKAYA, H. 2005. The different growth responses of the Arabidopsis thaliana leaf blade and the petiole during shade avoidance are regulated by photoreceptors and sugar. *Plant & Cell Physiology,* 46**,** 213-223.

KOZUKA, T., KONG, S. G., DOI, M., SHIMAZAKI, K. & NAGATANI, A. 2011. Tissue-autonomous promotion of palisade cell development by phototropin 2 in Arabidopsis. *The Plant Cell,* 23**,** 3684-3695.

KUWABARA, A. & GRUISSEM, W. 2014. Arabidopsis RETINOBLASTOMA-RELATED and Polycomb group proteins: cooperation during plant cell differentiation and development. *Journal of experimental botany,* 65**,** 2667-2676.

LAMMENS, T., LI, J., LEONE, G. & DE VEYLDER, L. 2009. Atypical E2Fs: new players in the E2F transcription factor family. *Trends in cell biology,* 19**,** 111-118.

LARSON, M. H., GILBERT, L. A., WANG, X., LIM, W. A., WEISSMAN, J. S. & QI, L. S. 2013. CRISPR interference (CRISPRi) for sequence-specific control of gene expression. *Nature protocols,* 8**,** 2180-2196.

LAU, O. S. & DENG, X. W. 2012. The photomorphogenic repressors COP1 and DET1: 20 years later. *Trends in plant science,* 17**,** 584-593.

LEIVAR, P., MONTE, E., OKA, Y., LIU, T., CARLE, C., CASTILLON, A., HUQ, E. & QUAIL, P. H. 2008. Multiple phytochrome-interacting bHLH transcription factors repress premature seedling photomorphogenesis in darkness. *Current Biology,* 18**,** 1815-1823.

LEIVAR, P. & QUAIL, P. H. 2011. PIFs: pivotal components in a cellular signaling hub. *Trends in plant science,* 16**,** 19-28.

LEÓN, P. & SHEEN, J. 2003. Sugar and hormone connections. *Trends in plant science,* 8**,** 110-116.

LEPISTO, A., KANGASJARVI, S., LUOMALA, E. M., BRADER, G., SIPARI, N., KERANEN, M., KEINANEN, M. & RINTAMAKI, E. 2009. Chloroplast NADPH-thioredoxin reductase interacts with photoperiodic development in Arabidopsis. *Plant Physiology,* 149**,** 1261-1276.

LEPISTO, A. & RINTAMAKI, E. 2012. Coordination of plastid and light signaling pathways upon development of Arabidopsis leaves under various photoperiods. *Molecular plant,* 5**,** 799-816.

LI, F.-W., MELKONIAN, M., ROTHFELS, C. J., VILLARREAL, J. C., STEVENSON, D. W., GRAHAM, S. W., WONG, G. K.-S., PRYER, K. M. & MATHEWS, S. 2015.

Phytochrome diversity in green plants and the origin of canonical plant phytochromes. *Nature communications,* 6.

LINDSEY, K. & TOPPING, J. F. 1993. Embryogenesis: a question of pattern. *Journal of experimental botany,* 44**,** 359-374.

LISCUM, E., HODGSON, D. W. & CAMPBELL, T. J. 2003. Blue light signaling through the cryptochromes and phototropins. So that's what the blues is all about. *Plant physiology,* 133**,** 1429-1436.

LIU, Y. & BASSHAM, D. C. 2010. TOR is a negative regulator of autophagy in Arabidopsis thaliana. *PLoS One,* 5**,** e11883.

LIU, Z., JIA, L., MAO, Y. & HE, Y. 2010. Classification and quantification of leaf curvature. *Journal of experimental botany,* 61**,** 2757-2767.

LOPEZ-JUEZ, E., BOWYER, J. R. & SAKAI, T. 2007. Distinct leaf developmental and gene expression responses to light quantity depend on blue-photoreceptor or plastid-derived signals, and can occur in the absence of phototropins. *Planta,* 227**,** 113-123.

LÓPEZ-JUEZ, E. & DEVLIN, P. F. 2008. Light and the control of plant growth. *Plant Growth Signaling.* Springer.

LOPEZ-JUEZ, E., DILLON, E., MAGYAR, Z., KHAN, S., HAZELDINE, S., DE JAGER, S. M., MURRAY, J. A., BEEMSTER, G. T., BOGRE, L. & SHANAHAN, H. 2008. Distinct light-initiated gene expression and cell cycle programs in the shoot apex and cotyledons of Arabidopsis. *The Plant Cell,* 20**,** 947-968.

LOPEZ-JUEZ, E., NAGATANI, A., TOMIZAWA, K., DEAK, M., KERN, R., KENDRICK, R. E. & FURUYA, M. 1992. The cucumber long hypocotyl mutant lacks a light-stable PHYB-like phytochrome. *The Plant Cell,* 4**,** 241-251.

LORRAIN, S., ALLEN, T., DUEK, P. D., WHITELAM, G. C. & FANKHAUSER, C. 2008. Phytochrome‐mediated inhibition of shade avoidance involves degradation of growth‐promoting bHLH transcription factors. *The Plant Journal,* 53**,** 312-323.

LU, P., PORAT, R., NADEAU, J. A. & O'NEILL, S. D. 1996. Identification of a meristem L1 layer-specific gene in Arabidopsis that is expressed during embryonic pattern formation and defines a new class of homeobox genes. *The Plant Cell,* 8**,** 2155-2168.

LU, Y., GEHAN, J. P. & SHARKEY, T. D. 2005. Daylength and circadian effects on starch degradation and maltose metabolism. *Plant Physiology,* 138**,** 2280-2291.

LUNN, J. E., DELORGE, I., FIGUEROA, C. M., VAN DIJCK, P. & STITT, M. 2014. Trehalose metabolism in plants. *The Plant Journal*.

LUO, R. X., POSTIGO, A. A. & DEAN, D. C. 1998. Rb interacts with histone deacetylase to repress transcription. *Cell,* 92**,** 463-473.

MA, L., GAO, Y., QU, L., CHEN, Z., LI, J., ZHAO, H. & DENG, X. W. 2002. Genomic evidence for COP1 as a repressor of light-regulated gene expression and development in Arabidopsis. *The Plant Cell,* 14**,** 2383-2398.

MA, L., LI, J., QU, L., HAGER, J., CHEN, Z., ZHAO, H. & DENG, X. W. 2001. Light control of Arabidopsis development entails coordinated regulation of genome expression and cellular pathways. *The Plant Cell,* 13**,** 2589-2607.

MACGREGOR, D. R., DEAK, K. I., INGRAM, P. A. & MALAMY, J. E. 2008. Root system architecture in Arabidopsis grown in culture is regulated by sucrose uptake in the aerial tissues. *The Plant Cell,* 20**,** 2643-2660.

MAGNAGHI-JAULIN, L., GROISMAN, R., NAGUIBNEVA, I., ROBIN, P., LORAIN, S., LE VILLAIN, J. P., TROALEN, F., TROUCHE, D. & HAREL-BELLAN, A. 1998. Retinoblastoma protein represses transcription by recruiting a histone deacetylase. *Nature,* 391**,** 601-605.

MAGYAR, Z. 2008. Keeping the balance between proliferation and differentiation by the E2F transcriptional regulatory network is central to plant growth and development. *In:* BOGRE, L. & AND BEEMSTER, G. T. (eds.) *Plant Growth Signalling; Plant Cell Monographs.* Berlin: Springer.

MAGYAR, Z., ATANASSOVA, A., DE VEYLDER, L., ROMBAUTS, S. & INZE, D. 2000. Characterization of two distinct DP-related genes from Arabidopsis thaliana. *FEBS letters,* 486**,** 79-87.

MAGYAR, Z., DE VEYLDER, L., ATANASSOVA, A., BAKÓ, L., INZÉ, D. & BÖGRE, L. 2005. The role of the Arabidopsis E2FB transcription factor in regulating auxin-dependent cell division. *The Plant Cell,* 17**,** 2527-2541.

MAGYAR, Z., HORVÁTH, B., KHAN, S., MOHAMMED, B., HENRIQUES, R., DE VEYLDER, L., BAKÓ, L., SCHERES, B. & BÖGRE, L. 2012. Arabidopsis E2FA stimulates proliferation and endocycle separately through RBR‐bound and RBR‐free complexes. *The EMBO journal,* 31**,** 1480-1493.

MAGYAR, Z., ITO, M., BINAROVÁ, P., MOHAMED, B. & BOGRE, L. 2013. Cell cycle modules in plants for entry into proliferation and for mitosis. *Plant Genome Diversity Volume 2.* Springer.

MALUMBRES, M., HARLOW, E., HUNT, T., HUNTER, T., LAHTI, J. M., MANNING, G., MORGAN, D. O., TSAI, L.-H. & WOLGEMUTH, D. J. 2009. Cyclin-dependent kinases: a family portrait. *Nature cell biology,* 11**,** 1275-1276.

MARICONTI, L., PELLEGRINI, B., CANTONI, R., STEVENS, R., BERGOUNIOUX, C., CELLA, R. & ALBANI, D. 2002. The E2F family of transcription factors from Arabidopsis thaliana. Novel and conserved components of the retinoblastoma/E2F pathway in plants. *The Journal of biological chemistry,* 277**,** 9911-9919.

MARROCCO, K., BERGDOLL, M., ACHARD, P., CRIQUI, M.-C. & GENSCHIK, P. 2010. Selective proteolysis sets the tempo of the cell cycle. *Current opinion in plant biology,* 13**,** 631-639.

MARTIN, D. E., SOULARD, A. & HALL, M. N. 2004. TOR regulates ribosomal protein gene expression via PKA and the Forkhead transcription factor FHL1. *Cell,* 119**,** 969-979.

MARTÍN-TRILLO, M. & CUBAS, P. 2010. TCP genes: a family snapshot ten years later. *Trends in plant science,* 15**,** 31-39.

MARTÍNEZ-GARCÍA, J. F., GALLEMÍ, M., MOLINA-CONTRERAS, M. J., LLORENTE, B., BEVILAQUA, M. R. & QUAIL, P. H. 2014. The shade avoidance syndrome in Arabidopsis: the antagonistic role of phytochrome A and B differentiates vegetation proximity and canopy shade. *PloS one,* 9**,** e109275.

MASUBELELE, N. H., DEWITTE, W., MENGES, M., MAUGHAN, S., COLLINS, C., HUNTLEY, R., NIEUWLAND, J., SCOFIELD, S. & MURRAY, J. A. 2005. D-type cyclins activate division in the root apex to promote seed germination in Arabidopsis. *Proceedings of the National Academy of Sciences of the United States of America,* 102**,** 15694-15699.

MATSUBARA, S., HURRY, V., DRUART, N., BENEDICT, C., JANZIK, I., CHAVARRÍA-KRAUSER, A., WALTER, A. & SCHURR, U. 2006. Nocturnal changes in leaf

growth of Populus deltoides are controlled by cytoplasmic growth. *Planta,* 223**,** 1315-1328.

MATT, P., SCHURR, U., KLEIN, D., KRAPP, A. & STITT, M. 1998. Growth of tobacco in short-day conditions leads to high starch, low sugars, altered diurnal changes in the Nia transcript and low nitrate reductase activity, and inhibition of amino acid synthesis. *Planta,* 207**,** 27-41.

MCCONNELL, J. R., EMERY, J., ESHED, Y., BAO, N., BOWMAN, J. & BARTON, M. K. 2001. Role of PHABULOSA and PHAVOLUTA in determining radial patterning in shoots. *Nature,* 411**,** 709-713.

MEIJER, M. & MURRAY, J. A. H. 2001. Cell cycle controls and the development of plant form. *Current opinion in plant biology,* 4**,** 44-49.

MENGES, M. & MURRAY, J. A. 2002. Synchronous Arabidopsis suspension cultures for analysis of cell‐cycle gene activity. *The Plant Journal,* 30**,** 203-212.

MENGES, M., SAMLAND, A. K., PLANCHAIS, S. & MURRAY, J. A. 2006. The D-type cyclin CYCD3;1 is limiting for the G1-to-S-phase transition in Arabidopsis. *The Plant Cell,* 18**,** 893-906.

MONTE, E., TEPPERMAN, J. M., AL-SADY, B., KACZOROWSKI, K. A., ALONSO, J. M., ECKER, J. R., LI, X., ZHANG, Y. & QUAIL, P. H. 2004. The phytochrome-interacting transcription factor, PIF3, acts early, selectively, and positively in light-induced chloroplast development. *Proceedings of the National Academy of Sciences of the United States of America,* 101**,** 16091-16098.

MOORE, B., ZHOU, L., ROLLAND, F., HALL, Q., CHENG, W. H., LIU, Y. X., HWANG, I., JONES, T. & SHEEN, J. 2003. Role of the Arabidopsis glucose sensor HXK1 in nutrient, light, and hormonal signaling. *Science (New York, N.Y.),* 300**,** 332-336.

MORGAN, D. O. 1997. Cyclin-dependent kinases: engines, clocks, and microprocessors. *Annual Review of Cell and Developmental Biology,* 13**,** 261-291.

MOULAGER, M., MONNIER, A., JESSON, B., BOUVET, R., MOSSER, J., SCHWARTZ, C., GARNIER, L., CORELLOU, F. & BOUGET, F. Y. 2007. Light-dependent regulation of cell division in Ostreococcus: evidence for a major transcriptional input. *Plant Physiology,* 144**,** 1360-1369.

MULLER, L. M., VON KORFF, M. & DAVIS, S. J. 2014. Connections between circadian clocks and carbon metabolism reveal species-specific effects on growth control. *Journal of experimental botany,* 65**,** 2915-2923.

NAGATANI, A. 2004. Light-regulated nuclear localization of phytochromes. *Current opinion in plant biology,* 7**,** 708-711.

NAGAWA, S., XU, T. & YANG, Z. 2010. RHO GTPase in plants: conservation and invention of regulators and effectors. *Small GTPases,* 1**,** 78-88.

NATH, U., CRAWFORD, B. C., CARPENTER, R. & COEN, E. 2003. Genetic control of surface curvature. *Science,* 299**,** 1404-1407.

NEJAD, E. S., ASKARI, H., HAMZELOU, S. & GHOLAMI, M. 2013. Regulation of core cell cycle genes by cis-regulatory elements in Arabidopsis thaliana. *Plant Knowl J,* 2**,** 69-75.

NELISSEN, H., GONZALEZ, N. & INZÉ, D. 2016. Leaf growth in dicots and monocots: so different yet so alike. *Current Opinion in Plant Biology,* 33**,** 72-76.

NISHIHAMA, R. & KOHCHI, T. 2013. Evolutionary insights into photoregulation of the cell cycle in the green lineage. *Current opinion in plant biology,* 16**,** 630-637.

NOWACK, M. K., HARASHIMA, H., DISSMEYER, N., ZHAO, X. A., BOUYER, D., WEIMER, A. K., DE WINTER, F., YANG, F. & SCHNITTGER, A. 2012. Genetic Framework of Cyclin-Dependent Kinase Function in< i> Arabidopsis</i>. *Developmental cell,* 22**,** 1030-1040.

O'HARA, L. E., PAUL, M. J. & WINGLER, A. 2013a. How do sugars regulate plant growth and development? New insight into the role of trehalose-6-phosphate. *Molecular plant,* 6**,** 261-274.

O'HARA, L. E., PAUL, M. J. & WINGLER, A. 2013b. How Do Sugars Regulate Plant Growth and Development? New Insight into the Role of Trehalose-6-Phosphate. *Molecular Plant,* 6.

OH, E., KIM, J., PARK, E., KIM, J. I., KANG, C. & CHOI, G. 2004. PIL5, a phytochrome-interacting basic helix-loop-helix protein, is a key negative regulator of seed germination in Arabidopsis thaliana. *The Plant Cell,* 16**,** 3045-3058.

OHGISHI, M., SAJI, K., OKADA, K. & SAKAI, T. 2004. Functional analysis of each blue light receptor, cry1, cry2, phot1, and phot2, by using combinatorial multiple mutants in Arabidopsis. *Proceedings of the National Academy of Sciences of the United States of America,* 101**,** 2223-2228.

ORAVECZ, A., BAUMANN, A., MATE, Z., BRZEZINSKA, A., MOLINIER, J., OAKELEY, E. J., ADAM, E., SCHAFER, E., NAGY, F. & ULM, R. 2006. CONSTITUTIVELY PHOTOMORPHOGENIC1 is required for the UV-B response in Arabidopsis. *The Plant Cell,* 18**,** 1975-1990.

ORTEGA-MARTÍNEZ, O., PERNAS, M., CAROL, R. J. & DOLAN, L. 2007. Ethylene modulates stem cell division in the Arabidopsis thaliana root. *Science,* 317**,** 507-510.

OSTERLUND, M. T., HARDTKE, C. S., WEI, N. & DENG, X. W. 2000. Targeted destabilization of HY5 during light-regulated development of Arabidopsis. *Nature,* 405**,** 462-466.

PAL, S. K., LIPUT, M., PIQUES, M., ISHIHARA, H., OBATA, T., MARTINS, M. C., SULPICE, R., VAN DONGEN, J. T., FERNIE, A. R., YADAV, U. P., LUNN, J. E., USADEL, B. & STITT, M. 2013. Diurnal changes of polysome loading track sucrose content in the rosette of wild-type arabidopsis and the starchless pgm mutant. *Plant Physiology,* 162**,** 1246-1265.

PAUL, M. J., PRIMAVESI, L. F., JHURREEA, D. & ZHANG, Y. 2008. Trehalose metabolism and signaling. *Annu.Rev.Plant Biol.,* 59**,** 417-441.

PERES, A., CHURCHMAN, M. L., HARIHARAN, S., HIMANEN, K., VERKEST, A., VANDEPOELE, K., MAGYAR, Z., HATZFELD, Y., VAN DER SCHUEREN, E., BEEMSTER, G. T., FRANKARD, V., LARKIN, J. C., INZE, D. & DE VEYLDER, L. 2007. Novel plant-specific cyclin-dependent kinase inhibitors induced by biotic and abiotic stresses. *The Journal of biological chemistry,* 282**,** 25588-25596.

PETRÁŠEK, J. & FRIML, J. 2009. Auxin transport routes in plant development. *Development,* 136**,** 2675-2688.

PEYRIC, E., MOORE, H. A. & WHITMORE, D. 2013. Circadian clock regulation of the cell cycle in the zebrafish intestine. *PloS one,* 8**,** e73209.

PFAFFL, M. W., HORGAN, G. W. & DEMPFLE, L. 2002. Relative expression software tool (REST©) for group-wise comparison and statistical analysis of relative expression results in real-time PCR. *Nucleic acids research,* 30**,** e36-e36.

PFEIFFER, A., JANOCHA, D., DONG, Y., MEDZIHRADSZKY, A., SCHÖNE, S., DAUM, G., SUZAKI, T., FORNER, J., LANGENECKER, T. & REMPEL, E. 2016. Integration of light and metabolic signals for stem cell activation at the shoot apical meristem. *Elife,* 5**,** e17023.

PHILIPPS, G., CLEMENT, B. & GIGOT, C. 1995. Molecular characterization and cell cycle-regulated expression of a cDNA clone from< i> Arabidopsis thaliana</i> homologous to the small subunit of ribonucleotide reductase. *FEBS letters,* 358**,** 67-70.

PLANCHAIS, S., SAMLAND, A. K. & MURRAY, J. A. H. 2004. Differential stability of Arabidopsis D‐type cyclins: CYCD3; 1 is a highly unstable protein degraded by a proteasome‐dependent mechanism. *The Plant Journal,* 38**,** 616-625.

POLYMENIS, M. & ARAMAYO, R. 2015. Translate to divide: control of the cell cycle by protein synthesis. *Microbial Cell,* 2**,** 94-104.

PONNU, J., WAHL, V. & SCHMID, M. 2011. Trehalose-6-phosphate: connecting plant metabolism and development. *Frontiers in plant science,* 2.

POORTER, H. & NAGEL, O. 2000. The role of biomass allocation in the growth response of plants to different levels of light, CO2, nutrients and water: a quantitative review. *Functional Plant Biology,* 27**,** 1191-1191.

QI, J., WANG, Y., YU, T., CUNHA, A., WU, B., VERNOUX, T., MEYEROWITZ, E. & JIAO, Y. 2014. Auxin depletion from leaf primordia contributes to organ patterning. *Proceedings of the National Academy of Sciences,* 111**,** 18769-18774.

QI, R. & JOHN, P. C. 2007. Expression of genomic AtCYCD2;1 in Arabidopsis induces cell division at smaller cell sizes: implications for the control of plant growth. *Plant Physiology,* 144**,** 1587-1597.

QIAO, J., LI, J., CHU, W. & LUO, M. 2013. PRDA1, a novel chloroplast nucleoid protein, is required for early chloroplast development and is involved in the regulation of plastid gene expression in Arabidopsis. *Plant and Cell Physiology,* 54**,** 2071-2084.

RAMIREZ‐PARRA, E., FRÜNDT, C. & GUTIERREZ, C. 2003. A genome‐wide identification of E2F‐regulated genes in Arabidopsis. *The Plant Journal,* 33**,** 801-811.

RAMON, M., DE SMET, I. V. E., VANDESTEENE, L., NAUDTS, M., LEYMAN, B., VAN DIJCK, P., ROLLAND, F., BEECKMAN, T. O. M. & THEVELEIN, J. M. 2009. Extensive expression regulation and lack of heterologous enzymatic activity of the Class II trehalose metabolism proteins from Arabidopsis thaliana. *Plant, Cell & Environment,* 32**,** 1015-1032.

RAMON, M., ROLLAND, F. & SHEEN, J. 2008. Sugar sensing and signaling. *The Arabidopsis Book*.

RAMON, M., RUELENS, P., LI, Y., SHEEN, J., GEUTEN, K. & ROLLAND, F. 2013. The hybrid Four‐CBS‐Domain KIN β γ subunit functions as the canonical γ subunit of the plant energy sensor SnRK1. *The Plant Journal,* 75**,** 11-25.

RASHOTTE, A. M., MASON, M. G., HUTCHISON, C. E., FERREIRA, F. J., SCHALLER, G. E. & KIEBER, J. J. 2006. A subset of Arabidopsis AP2 transcription

factors mediates cytokinin responses in concert with a two-component pathway. *Proceedings of the National Academy of Sciences,* 103**,** 11081-11085.

RAVEN, J. A. & ALLEN, J. F. 2003. Genomics and chloroplast evolution: what did cyanobacteria do for plants? *Genome biology,* 4**,** 1.

RAZ, V. & KOORNNEEF, M. 2001. Cell division activity during apical hook development. *Plant Physiology,* 125**,** 219-226.

REICHHELD, J. P., VERNOUX, T., LARDON, F., VAN MONTAGU, M. & INZÉ, D. 1999. Specific checkpoints regulate plant cell cycle progression in response to oxidative stress. *The Plant Journal,* 17**,** 647-656.

REICHLER, S. A., BALK, J., BROWN, M. E., WOODRUFF, K., CLARK, G. B. & ROUX, S. J. 2001. Light differentially regulates cell division and the mRNA abundance of pea nucleolin during de-etiolation. *Plant Physiology,* 125**,** 339-350.

REINHARDT, D., MANDEL, T. & KUHLEMEIER, C. 2000. Auxin regulates the initiation and radial position of plant lateral organs. *The Plant Cell,* 12**,** 507-518.

REINHARDT, D., PESCE, E.-R., STIEGER, P., MANDEL, T., BALTENSPERGER, K., BENNETT, M., TRAAS, J., FRIML, J. & KUHLEMEIER, C. 2003. Regulation of phyllotaxis by polar auxin transport. *Nature,* 426**,** 255-260.

REN, M., QIU, S., VENGLAT, P., XIANG, D., FENG, L., SELVARAJ, G. & DATLA, R. 2011. Target of rapamycin regulates development and ribosomal RNA expression through kinase domain in Arabidopsis. *Plant Physiology,* 155**,** 1367-1382.

REN, M., VENGLAT, P., QIU, S., FENG, L., CAO, Y., WANG, E., XIANG, D., WANG, J., ALEXANDER, D., CHALIVENDRA, S., LOGAN, D., MATTOO, A., SELVARAJ, G. & DATLA, R. 2012. Target of rapamycin signaling regulates metabolism, growth, and life span in Arabidopsis. *The Plant Cell,* 24**,** 4850-4874.

RIOU-KHAMLICHI, C., MENGES, M., HEALY, J. M. & MURRAY, J. A. 2000. Sugar control of the plant cell cycle: differential regulation of Arabidopsis D-type cyclin gene expression. *Molecular and cellular biology,* 20**,** 4513-4521.

RODRIGUEZ, R. E., DEBERNARDI, J. M. & PALATNIK, J. F. 2014. Morphogenesis of simple leaves: regulation of leaf size and shape. *Wiley Interdisciplinary Reviews: Developmental Biology,* 3**,** 41-57.

ROGGATZ, U., MCDONALD, A. J. S., STADENBERG, I. & SCHURR, U. 1999. Effects of nitrogen deprivation on cell division and expansion in leaves of Ricinus communis L. *Plant, Cell & Environment,* 22**,** 81-89.

ROLDAN, M., GOMEZ-MENA, C., RUIZ-GARCIA, L., SALINAS, J. & MARTINEZ-ZAPATER, J. M. 1999. Sucrose availability on the aerial part of the plant promotes morphogenesis and flowering of Arabidopsis in the dark. *The Plant Journal : for cell and molecular biology,* 20**,** 581-590.

RUST, M. J., GOLDEN, S. S. & O'SHEA, E. K. 2011. Light-driven changes in energy metabolism directly entrain the cyanobacterial circadian oscillator. *Science,* 331**,** 220-223.

SABLOWSKI, R. 2007. The dynamic plant stem cell niches. *Current opinion in plant biology,* 10**,** 639-644.

SABLOWSKI, R. & CARNIER DORNELAS, M. 2014. Interplay between cell growth and cell cycle in plants. *Journal of experimental botany,* 65**,** 2703-2714.

SAKAI, T., KAGAWA, T., KASAHARA, M., SWARTZ, T. E., CHRISTIE, J. M., BRIGGS, W. R., WADA, M. & OKADA, K. 2001. Arabidopsis nph1 and npl1: blue light receptors that mediate both phototropism and chloroplast relocation. *Proceedings of the National Academy of Sciences of the United States of America,* 98**,** 6969-6974.

SATINA, S., BLAKESLEE, A. F. & AVERY, A. G. 1940. Demonstration of the three germ layers in the shoot apex of Datura by means of induced polyploidy in periclinal chimeras. *American Journal of Botany***,** 895-905.

SATYANARAYANA, A. & KALDIS, P. 2009a. A dual role of Cdk2 in DNA damage response. *Cell division,* 4**,** 1.

SATYANARAYANA, A. & KALDIS, P. 2009b. Mammalian cell-cycle regulation: several Cdks, numerous cyclins and diverse compensatory mechanisms. *Oncogene,* 28**,** 2925-2939.

SCARPELLA, E., MARCOS, D., FRIML, J. & BERLETH, T. 2006. Control of leaf vascular patterning by polar auxin transport. *Genes & development,* 20**,** 1015-1027.

SCHALLER, G. E., BISHOPP, A. & KIEBER, J. J. 2015. The yin-yang of hormones: cytokinin and auxin interactions in plant development. *The Plant Cell,* 27**,** 44-63.

SCHEPETILNIKOV, M., DIMITROVA, M., MANCERA‐MARTÍNEZ, E., GELDREICH, A., KELLER, M. & RYABOVA, L. A. 2013. TOR and S6K1 promote translation reinitiation of uORF‐containing mRNAs via phosphorylation of eIF3h. *The EMBO journal,* 32**,** 1087-1102.

SCHLUEPMANN, H., BERKE, L. & SANCHEZ-PEREZ, G. F. 2012. Metabolism control over growth: a case for trehalose-6-phosphate in plants. *Journal of experimental botany,* 63**,** 3379-3390.

SCHNEIDER-POETSCH, T., JU, J., EYLER, D. E., DANG, Y., BHAT, S., MERRICK, W. C., GREEN, R., SHEN, B. & LIU, J. O. 2010. Inhibition of eukaryotic translation elongation by cycloheximide and lactimidomycin. *Nature chemical biology,* 6**,** 209-217.

SCHNITTGER, A., SCHOBINGER, U., BOUYER, D., WEINL, C., STIERHOF, Y. D. & HULSKAMP, M. 2002. Ectopic D-type cyclin expression induces not only DNA replication but also cell division in Arabidopsis trichomes. *Proceedings of the National Academy of Sciences of the United States of America,* 99**,** 6410-6415.

SCHOOF, H., LENHARD, M., HAECKER, A., MAYER, K. F. X., JÜRGENS, G. & LAUX, T. 2000. The Stem Cell Population of< i> Arabidopsis</i> Shoot Meristems Is Maintained by a Regulatory Loop between the< i> CLAVATA</i> and< i> WUSCHEL</i> Genes. *Cell,* 100**,** 635-644.

SCHRADER, A., WELTER, B., HULSKAMP, M., HOECKER, U. & UHRIG, J. F. 2013. MIDGET connects COP1‐dependent development with endoreduplication in Arabidopsis thaliana. *The Plant Journal,* 75**,** 67-79.

SCIALDONE, A., MUGFORD, S. T., FEIKE, D., SKEFFINGTON, A., BORRILL, P., GRAF, A., SMITH, A. M. & HOWARD, M. 2013. Arabidopsis plants perform arithmetic division to prevent starvation at night. *eLife,* 2**,** e00669.

SCOFIELD, S., JONES, A. & MURRAY, J. A. H. 2014. The plant cell cycle in context. *Journal of experimental botany,* 65**,** 2557-2562.

SEKINE, M., ITO, M., UEMUKAI, K., MAEDA, Y., NAKAGAMI, H. & SHINMYO, A. 1999. Isolation and characterization of the E2F-like gene in plants. *FEBS letters,* 460**,** 117-122.

SHANI, E., YANAI, O. & ORI, N. 2006. The role of hormones in shoot apical meristem function. *Current opinion in plant biology,* 9**,** 484-489.

SHEERIN, D. J., MENON, C., ZUR OVEN-KROCKHAUS, S., ENDERLE, B., ZHU, L., JOHNEN, P., SCHLEIFENBAUM, F., STIERHOF, Y.-D., HUQ, E. & HILTBRUNNER, A. 2015. Light-activated phytochrome A and B interact with members of the SPA family to promote photomorphogenesis in Arabidopsis by reorganizing the COP1/SPA complex. *The Plant Cell,* 27**,** 189-201.

SHEN, W.-H. 2001. The plant cell cycle: G1/S regulation. *Euphytica,* 118**,** 223-236.

SHEN, W.-H. & XU, L. 2009. Chromatin remodeling in stem cell maintenance in Arabidopsis thaliana. *Molecular plant,* 2**,** 600-609.

SHINOMURA, T., NAGATANI, A., HANZAWA, H., KUBOTA, M., WATANABE, M. & FURUYA, M. 1996. Action spectra for phytochrome A- and B-specific photoinduction of seed germination in Arabidopsis thaliana. *Proceedings of the National Academy of Sciences of the United States of America,* 93**,** 8129-8133.

SMALLE, J., HAEGMAN, M., KUREPA, J., VAN MONTAGU, M. & VAN DER STRAETEN, D. 1997. Ethylene can stimulate Arabidopsis hypocotyl elongation in the light. *Proceedings of the National Academy of Sciences,* 94**,** 2756-2761.

SMITH, A. M. & STITT, M. 2007. Coordination of carbon supply and plant growth. *Plant, Cell & Environment,* 30**,** 1126-1149.

SMITH, H. 1982. Light quality, photoperception, and plant strategy. *Annual review of plant physiology,* 33**,** 481-518.

SOMSSICH, M., BLECKMANN, A. & SIMON, R. 2016. Shared and distinct functions of the pseudokinase CORYNE (CRN) in shoot and root stem cell maintenance of Arabidopsis. *Journal of experimental botany***,** erw207.

SOZZANI, R., MAGGIO, C., VAROTTO, S., CANOVA, S., BERGOUNIOUX, C., ALBANI, D. & CELLA, R. 2006. Interplay between Arabidopsis activating factors E2Fb and E2Fa in cell cycle progression and development. *Plant physiology,* 140**,** 1355-1366.

SPADAFORA, N., PERROTTA, L., NIEUWLAND, J., ALBANI, D., BITONTI, M. B., HERBERT, R. J., DOONAN, J. H., MARCHBANK, A. M., SICILIANO, I., LENTZ GRONLUND, A., FRANCIS, D. & ROGERS, H. J. 2012. Gene dosage effect of WEE1 on growth and morphogenesis from arabidopsis hypocotyl explants. *Annals of botany,* 110**,** 1631-1639.

SPUDICH, J. L. & SAGER, R. 1980. Regulation of the Chlamydomonas cell cycle by light and dark. *The Journal of cell biology,* 85**,** 136-145.

SQUATRITO, M., MANCINO, M., DONZELLI, M., ARECES, L. B. & DRAETTA, G. F. 2004. EBP1 is a nucleolar growth-regulating protein that is part of pre-ribosomal ribonucleoprotein complexes. *Oncogene,* 23**,** 4454-4465.

SQUATRITO, M., MANCINO, M., SALA, L. & DRAETTA, G. F. 2006. Ebp1 is a dsRNA-binding protein associated with ribosomes that modulates eIF2α phosphorylation. *Biochemical and biophysical research communications,* 344**,** 859-868.

STEPANOVA, A. N., ROBERTSON-HOYT, J., YUN, J., BENAVENTE, L. M., XIE, D.-Y., DOLEŽAL, K., SCHLERETH, A., JÜRGENS, G. & ALONSO, J. M. 2008. TAA1-mediated auxin biosynthesis is essential for hormone crosstalk and plant development. *Cell,* 133**,** 177-191.

STIEGER, P. A., REINHARDT, D. & KUHLEMEIER, C. 2002. The auxin influx carrier is essential for correct leaf positioning. *The Plant Journal,* 32**,** 509-517.

STITT, M. & FEIL, R. 1999. Lateral root frequency decreases when nitrate accumulates in tobacco transformants with low nitrate reductase activity: consequences for the regulation of biomass partitioning between shoots and root1. *Plant and Soil,* 215**,** 143-153.

STITT, M., GIBON, Y., LUNN, J. E. & PIQUES, M. 2007. Multilevel genomics analysis of carbon signalling during low carbon availability: coordinating the supply and utilisation of carbon in a fluctuating environment. *Functional Plant Biology,* 34**,** 526-549.

STITT, M. & ZEEMAN, S. C. 2012. Starch turnover: pathways, regulation and role in growth. *Current opinion in plant biology,* 15**,** 282-292.

STREET, I. H., AMAN, S., ZUBO, Y., RAMZAN, A., WANG, X., SHAKEEL, S. N., KIEBER, J. J. & SCHALLER, G. E. 2015. Ethylene inhibits cell proliferation of the Arabidopsis root meristem. *Plant physiology,* 169**,** 338-350.

SU, Y.-H., LIU, Y.-B. & ZHANG, X.-S. 2011. Auxin–cytokinin interaction regulates meristem development. *Molecular plant,* 4**,** 616-625.

SU, Y. H., LIU, Y. B., BAI, B. & ZHANG, X. S. 2015. Establishment of embryonic shoot–root axis is involved in auxin and cytokinin response during Arabidopsis somatic embryogenesis. *Frontiers in plant science,* 5**,** 792.

SULLIVAN, M. & MORGAN, D. O. 2007. Finishing mitosis, one step at a time. *Nature Reviews Molecular Cell Biology,* 8**,** 894-903.

SUZUKI, G., YANAGAWA, Y., KWOK, S. F., MATSUI, M. & DENG, X. W. 2002. Arabidopsis COP10 is a ubiquitin-conjugating enzyme variant that acts together with COP1 and the COP9 signalosome in repressing photomorphogenesis. *Genes & development,* 16**,** 554-559.

SWARUP, R., PERRY, P., HAGENBEEK, D., VAN DER STRAETEN, D., BEEMSTER, G. T., SANDBERG, G., BHALERAO, R., LJUNG, K. & BENNETT, M. J. 2007. Ethylene upregulates auxin biosynthesis in Arabidopsis seedlings to enhance inhibition of root cell elongation. *The Plant Cell,* 19**,** 2186-2196.

TAMESHIGE, T., FUJITA, H., WATANABE, K., TOYOKURA, K., KONDO, M., TATEMATSU, K., MATSUMOTO, N., TSUGEKI, R., KAWAGUCHI, M. & NISHIMURA, M. 2013. Pattern dynamics in adaxial-abaxial specific gene expression are modulated by a plastid retrograde signal during Arabidopsis thaliana leaf development. *PLoS Genet,* 9**,** e1003655.

TAN, W., BÖGRE, L. & LÓPEZ-JUEZ, E. 2008. Light fluence rate and chloroplasts are sources of signals controlling mesophyll cell morphogenesis and division. *Cell biology international,* 32**,** 563-565.

TANAKA, H., DHONUKSHE, P., BREWER, P. & FRIML, J. 2006. Spatiotemporal asymmetric auxin distribution: a means to coordinate plant development. *Cellular and Molecular Life Sciences CMLS,* 63**,** 2738-2754.

TEPPERMAN, J. M., HUDSON, M. E., KHANNA, R., ZHU, T., CHANG, S. H., WANG, X. & QUAIL, P. H. 2004. Expression profiling of phyB mutant demonstrates substantial contribution of other phytochromes to red‐light‐regulated

gene expression during seedling de‐etiolation. *The Plant Journal,* 38**,** 725-739.

TEPPERMAN, J. M., HWANG, Y. S. & QUAIL, P. H. 2006. phyA dominates in transduction of red‐light signals to rapidly responding genes at the initiation of Arabidopsis seedling de‐etiolation. *The Plant Journal,* 48**,** 728-742.

TEPPERMAN, J. M., ZHU, T., CHANG, H. S., WANG, X. & QUAIL, P. H. 2001. Multiple transcription-factor genes are early targets of phytochrome A signaling. *Proceedings of the National Academy of Sciences of the United States of America,* 98**,** 9437-9442.

THAPA, M., BOMMAKANTI, A., SHAMSUZZAMAN, M., GREGORY, B., SAMSEL, L., ZENGEL, J. M. & LINDAHL, L. 2013. Repressed synthesis of ribosomal proteins generates protein-specific cell cycle and morphological phenotypes. *Molecular biology of the cell,* 24**,** 3620-3633.

THIMM, O., BLÄSING, O., GIBON, Y., NAGEL, A., MEYER, S., KRÜGER, P., SELBIG, J., MÜLLER, L. A., RHEE, S. Y. & STITT, M. 2004. mapman: a user‐driven tool to display genomics data sets onto diagrams of metabolic pathways and other biological processes. *The Plant Journal,* 37**,** 914-939.

TILNEY-BASSETT, R. A. 1986. *Plant chimeras*, Edward Arnold (Publishers) Ltd.

TO, J. P. C. & KIEBER, J. J. 2008. Cytokinin signaling: two-components and more. *Trends in plant science,* 13**,** 85-92.

TOLEDO-ORTIZ, G., HUQ, E. & QUAIL, P. H. 2003. The Arabidopsis basic/helix-loop-helix transcription factor family. *The Plant Cell,* 15**,** 1749-1770.

TONG, C.-G., REICHLER, S., BLUMENTHAL, S., BALK, J., HSIEH, H.-L. & ROUX, S. J. 1997. Light regulation of the abundance of mRNA encoding a nucleolin-like protein localized in the nucleoli of pea nuclei. *Plant physiology,* 114**,** 643-652.

TRAAS, J. & MONEGER, F. 2010. Systems biology of organ initiation at the shoot apex. *Plant Physiology,* 152**,** 420-427.

TREML, B. S., WINDERL, S., RADYKEWICZ, R., HERZ, M., SCHWEIZER, G., HUTZLER, P., GLAWISCHNIG, E. & RUIZ, R. A. T. 2005. The gene ENHANCER OF PINOID controls cotyledon development in the Arabidopsis embryo. *Development,* 132**,** 4063-4074.

TROJAN, A. & GABRYS, H. 1996. Chloroplast Distribution in Arabidopsis thaliana (L.) Depends on Light Conditions during Growth. *Plant Physiology,* 111**,** 419-425.

TRUERNIT, E., BAUBY, H., DUBREUCQ, B., GRANDJEAN, O., RUNIONS, J., BARTHÉLÉMY, J. & PALAUQUI, J.-C. 2008. High-resolution whole-mount imaging of three-dimensional tissue organization and gene expression enables the study of phloem development and structure in Arabidopsis. *The Plant Cell,* 20**,** 1494-1503.

TSUKAYA, H. 2002. Interpretation of mutants in leaf morphology: genetic evidence for a compensatory system in leaf morphogenesis that provides a new link between cell and organismal theories. *International review of cytology,* 217**,** 1-39.

TSUKAYA, H. 2003. Organ shape and size: a lesson from studies of leaf morphogenesis. *Current opinion in plant biology,* 6**,** 57-62.

TSUKAYA, H. 2004. Leaf shape: genetic controls and environmental factors. *International Journal of Developmental Biology,* 49**,** 547-555.

TSUKAYA, H. 2005. Leaf shape: genetic controls and environmental factors. *International Journal of Developmental Biology,* 49**,** 547.

TSUKAYA, H., SHODA, K., KIM, G.-T. & UCHIMIYA, H. 2000. Heteroblasty in Arabidopsis thaliana (L.) Heynh. *Planta,* 210**,** 536-542.

UCHIDA, N., TOWNSLEY, B., CHUNG, K. H. & SINHA, N. 2007. Regulation of SHOOT MERISTEMLESS genes via an upstream-conserved noncoding sequence coordinates leaf development. *Proceedings of the National Academy of Sciences of the United States of America,* 104**,** 15953-15958.

USADEL, B., BLASING, O. E., GIBON, Y., RETZLAFF, K., HOHNE, M., GUNTHER, M. & STITT, M. 2008. Global transcript levels respond to small changes of the carbon status during progressive exhaustion of carbohydrates in Arabidopsis rosettes. *Plant Physiology,* 146**,** 1834-1861.

VAN DE POEL, B. & VAN DER STRAETEN, D. 2015. 1-aminocyclopropane-1-carboxylic acid (ACC) in plants: more than just the precursor of ethylene! *" One Rotten Apple Spoils the Whole Barrel": The Plant Hormone Ethylene, the Small Molecule and its Complexity,* 5**,** 71.

VAN DEN HEUVEL, S. & DYSON, N. J. 2008. Conserved functions of the pRB and E2F families. *Nature reviews Molecular cell biology,* 9**,** 713-724.

VAN NORMAN, J. M., MURPHY, C. & SIEBURTH, L. E. 2011. BYPASS1: synthesis of the mobile root-derived signal requires active root growth and arrests early leaf development. *BMC plant biology,* 11**,** 28.

VAN VOLKENBURGH, E. & TAYLOR, G. 1996. Leaf growth physiology. *Biology of Populus and its implications for management and conservation***,** 283-299.

VANDENBUSSCHE, F., PETRASEK, J., ZADNIKOVA, P., HOYEROVA, K., PESEK, B., RAZ, V., SWARUP, R., BENNETT, M., ZAZIMALOVA, E., BENKOVA, E. & VAN DER STRAETEN, D. 2010. The auxin influx carriers AUX1 and LAX3 are involved in auxin-ethylene interactions during apical hook development in Arabidopsis thaliana seedlings. *Development (Cambridge, England),* 137**,** 597-606.

VANDENBUSSCHE, F., VERBELEN, J. P. & VAN DER STRAETEN, D. 2005. Of light and length: regulation of hypocotyl growth in Arabidopsis. *Bioessays,* 27**,** 275-284.

VANDEPOELE, K., VLIEGHE, K., FLORQUIN, K., HENNIG, L., BEEMSTER, G. T. S., GRUISSEM, W., VAN DE PEER, Y., INZÉ, D. & DE VEYLDER, L. 2005. Genome-wide identification of potential plant E2F target genes. *Plant Physiology,* 139**,** 316-328.

VAULOT, D., OLSON, R. J. & CHISHOLM, S. W. 1986. Light and dark control of the cell cycle in two marine phytoplankton species. *Experimental cell research,* 167**,** 38-52.

VERCRUYSSEN, L., TOGNETTI, V. B., GONZALEZ, N., VAN DINGENEN, J., DE MILDE, L., BIELACH, A., DE RYCKE, R., VAN BREUSEGEM, F. & INZE, D. 2015. GROWTH REGULATING FACTOR5 stimulates Arabidopsis chloroplast division, photosynthesis, and leaf longevity. *Plant Physiol,* 167**,** 817-32.

VLAD, D., KIERZKOWSKI, D., RAST, M. I., VUOLO, F., IOIO, R. D., GALINHA, C., GAN, X., HAJHEIDARI, M., HAY, A. & SMITH, R. S. 2014. Leaf shape evolution through duplication, regulatory diversification, and loss of a homeobox gene. *Science,* 343**,** 780-783.

VODERMAIER, H. C. 2004. APC/C and SCF: controlling each other and the cell cycle. *Current Biology,* 14**,** R787-R796.

VON ARNIM, A. G., OSTERLUND, M. T., KWOK, S. F. & DENG, X. W. 1997. Genetic and developmental control of nuclear accumulation of COP1, a repressor of photomorphogenesis in Arabidopsis. *Plant Physiology,* 114**,** 779-788.

WAITES, R. & HUDSON, A. 1995. phantastica: a gene required for dorsoventrality of leaves in Antirrhinum majus. *Development,* 121**,** 2143-2154.

WALTER, A., CHRIST, M. M., BARRON‐GAFFORD, G. A., GRIEVE, K. A., MURTHY, R. & RASCHER, U. 2005. The effect of elevated CO2 on diel leaf growth cycle, leaf carbohydrate content and canopy growth performance of Populus deltoides. *Global Change Biology,* 11**,** 1207-1219.

WALTER, A., FEIL, R. & SCHURR, U. 2003. Expansion dynamics, metabolite composition and substance transfer of the primary root growth zone of Zea mays L. grown in different external nutrient availabilities. *Plant, Cell & Environment,* 26**,** 1451-1466.

WALTER, A. & SCHURR, U. 2005. Dynamics of leaf and root growth: endogenous control versus environmental impact. *Annals of botany,* 95**,** 891-900.

WALTER, A., SILK, W. K. & SCHURR, U. 2009. Environmental effects on spatial and temporal patterns of leaf and root growth. *Annual review of plant biology,* 60**,** 279-304.

WANG, G., KONG, H., SUN, Y., ZHANG, X., ZHANG, W., ALTMAN, N., DEPAMPHILIS, C. W. & MA, H. 2004. Genome-wide analysis of the cyclin family in Arabidopsis and comparative phylogenetic analysis of plant cyclin-like proteins. *Plant Physiology,* 135**,** 1084-1099.

WANG, H., MA, L. G., LI, J. M., ZHAO, H. Y. & DENG, X. W. 2001. Direct interaction of Arabidopsis cryptochromes with COP1 in light control development. *Science (New York, N.Y.),* 294**,** 154-158.

WANG, H., ZHOU, Y., GILMER, S., WHITWILL, S. & FOWKE, L. C. 2000. Expression of the plant cyclin‐dependent kinase inhibitor ICK1 affects cell division, plant growth and morphology. *The Plant Journal,* 24**,** 613-623.

WANG, Q., KOHLEN, W., ROSSMANN, S., VERNOUX, T. & THERES, K. 2014a. Auxin depletion from the leaf axil conditions competence for axillary meristem formation in Arabidopsis and tomato. *The Plant Cell,* 26**,** 2068-2079.

WANG, X., XU, X. & CUI, J. 2015. The importance of blue light for leaf area expansion, development of photosynthetic apparatus, and chloroplast ultrastructure of Cucumis sativus grown under weak light. *Photosynthetica,* 53**,** 213-222.

WANG, Y., WANG, J., SHI, B., YU, T., QI, J., MEYEROWITZ, E. M. & JIAO, Y. 2014b. The stem cell niche in leaf axils is established by auxin and cytokinin in Arabidopsis. *The Plant Cell,* 26**,** 2055-2067.

WANG, Z.-Y. & TOBIN, E. M. 1998. Constitutive Expression of the< i> CIRCADIAN CLOCK ASSOCIATED 1</i>(< i> CCA1</i>) Gene Disrupts Circadian Rhythms and Suppresses Its Own Expression. *Cell,* 93**,** 1207-1217.

WEIMER, A. K., NOWACK, M. K., BOUYER, D., ZHAO, X., HARASHIMA, H., NASEER, S., DE WINTER, F., DISSMEYER, N., GELDNER, N. & SCHNITTGER, A. 2012. Retinoblastoma related1 regulates asymmetric cell divisions in Arabidopsis. *The Plant Cell,* 24**,** 4083-4095.

WESTON, E., THOROGOOD, K., VINTI, G. & LOPEZ-JUEZ, E. 2000. Light quantity controls leaf-cell and chloroplast development in Arabidopsis thaliana wild type and blue-light-perception mutants. *Planta,* 211**,** 807-815.

WHITELAM, G. C. & HALLIDAY, K. J. 2008. *Annual Plant Reviews, Light and Plant Development,* John Wiley & Sons.

WIESE, A., CHRIST, M. M., VIRNICH, O., SCHURR, U. & WALTER, A. 2007. Spatio‐temporal leaf growth patterns of Arabidopsis thaliana and evidence for sugar control of the diel leaf growth cycle. *New Phytologist,* 174**,** 752-761.

WOLF, S. & GREINER, S. 2012. Growth control by cell wall pectins. *Protoplasma,* 249**,** 169-175.

WOLLENBERG, A. C., STRASSER, B., CERDÁN, P. D. & AMASINO, R. M. 2008. Acceleration of flowering during shade avoidance in Arabidopsis alters the balance between FLOWERING LOCUS C-mediated repression and photoperiodic induction of flowering. *Plant physiology,* 148**,** 1681-1694.

WU, F., YU, L., CAO, W., MAO, Y., LIU, Z. & HE, Y. 2007. The N-terminal double-stranded RNA binding domains of Arabidopsis HYPONASTIC LEAVES1 are sufficient for pre-microRNA processing. *The Plant Cell,* 19**,** 914-925.

WU, G. & SPALDING, E. P. 2007. Separate functions for nuclear and cytoplasmic cryptochrome 1 during photomorphogenesis of Arabidopsis seedlings. *Proceedings of the National Academy of Sciences of the United States of America,* 104**,** 18813-18818.

WU, S.-H. 2014. Gene Expression Regulation in Photomorphogenesis from the Perspective of the Central Dogma. *Annual review of plant biology,* 65**,** 311-333.

WYRZYKOWSKA, J., PIEN, S., SHEN, W. H. & FLEMING, A. J. 2002. Manipulation of leaf shape by modulation of cell division. *Development (Cambridge, England),* 129**,** 957-964.

XIONG, Y., MCCORMACK, M., LI, L., HALL, Q., XIANG, C. & SHEEN, J. 2013. Glucose-TOR signalling reprograms the transcriptome and activates meristems. *Nature,* 496**,** 181-186.

XIONG, Y. & SHEEN, J. 2012. Rapamycin and glucose-target of rapamycin (TOR) protein signaling in plants. *The Journal of biological chemistry,* 287**,** 2836-2842.

XIONG, Y. & SHEEN, J. 2014. The role of target of rapamycin signaling networks in plant growth and metabolism. *Plant Physiology,* 164**,** 499-512.

YADAV, R. K., PERALES, M., GRUEL, J., GIRKE, T., JONSSON, H. & REDDY, G. V. 2011. WUSCHEL protein movement mediates stem cell homeostasis in the Arabidopsis shoot apex. *Genes & development,* 25**,** 2025-2030.

YAKIR, E., HILMAN, D., HASSIDIM, M. & GREEN, R. M. 2007. CIRCADIAN CLOCK ASSOCIATED1 transcript stability and the entrainment of the circadian clock in Arabidopsis. *Plant Physiology,* 145**,** 925-932.

YANAGAWA, Y., SULLIVAN, J. A., KOMATSU, S., GUSMAROLI, G., SUZUKI, G., YIN, J., ISHIBASHI, T., SAIJO, Y., RUBIO, V., KIMURA, S., WANG, J. & DENG, X. W. 2004. Arabidopsis COP10 forms a complex with DDB1 and DET1 in vivo and enhances the activity of ubiquitin conjugating enzymes. *Genes & development,* 18**,** 2172-2181.

YANG, H. Q., TANG, R. H. & CASHMORE, A. R. 2001. The signaling mechanism of Arabidopsis CRY1 involves direct interaction with COP1. *The Plant Cell,* 13**,** 2573-2587.

YANO, S. & TERASHIMA, I. 2001. Separate localization of light signal perception for sun or shade type chloroplast and palisade tissue differentiation in Chenopodium album. *Plant & Cell Physiology,* 42**,** 1303-1310.

YANO, S. & TERASHIMA, I. 2004. Developmental process of sun and shade leaves in Chenopodium album L. *Plant, Cell & Environment,* 27**,** 781-793.

YI, C. & DENG, X. W. 2005. COP1–from plant photomorphogenesis to mammalian tumorigenesis. *Trends in cell biology,* 15**,** 618-625.

YOSHIDA, S., MANDEL, T. & KUHLEMEIER, C. 2011. Stem cell activation by light guides plant organogenesis. *Genes & development,* 25**,** 1439-1450.

ZEEMAN, S. C., NORTHROP, F., SMITH, A. M. & REES, T. A. 1998. A starch‐accumulating mutant ofArabidopsis thalianadeficient in a chloroplastic starch‐hydrolysing enzyme. *The Plant Journal,* 15**,** 357-365.

ZHANG, H. S., POSTIGO, A. A. & DEAN, D. C. 1999. Active transcriptional repression by the Rb–E2F complex mediates G1 arrest triggered by p16 INK4a, TGFβ, and contact inhibition. *Cell,* 97**,** 53-61.

ZHANG, Q., VO, N. & GOODMAN, R. H. 2000. Histone binding protein RbAp48 interacts with a complex of CREB binding protein and phosphorylated CREB. *Molecular and cellular biology,* 20**,** 4970-4978.

ZHANG, Y., PRIMAVESI, L. F., JHURREEA, D., ANDRALOJC, P. J., MITCHELL, R. A., POWERS, S. J., SCHLUEPMANN, H., DELATTE, T., WINGLER, A. & PAUL, M. J. 2009. Inhibition of SNF1-related protein kinase1 activity and regulation of metabolic pathways by trehalose-6-phosphate. *Plant Physiology,* 149**,** 1860-1871.

ZHAO, X. A., HARASHIMA, H., DISSMEYER, N., PUSCH, S., WEIMER, A. K., BRAMSIEPE, J., BOUYER, D., RADEMACHER, S., NOWACK, M. K. & NOVAK, B. 2012. A general G1/S-phase cell-cycle control module in the flowering plant Arabidopsis thaliana. *PLoS genetics,* 8**,** e1002847.